

UNCLASSIFIED

AD NUMBER
ADB043539
NEW LIMITATION CHANGE
TO Approved for public release, distribution unlimited
FROM Distribution authorized to U.S. Gov't. agencies only; Test and Evaluation; Dec 1979. Other requests shall be referred to U.S. Army Armament Research and Development Weapons Systems Lab., Dover, NJ 07801.
AUTHORITY
USARDC ltr, 10 Apr 1984

THIS PAGE IS UNCLASSIFIED

AD B043539

AUTHORITY USAFDC Ltr 10 APR 84



② LEVEL III

AD

AD-E400 384

AD B043539

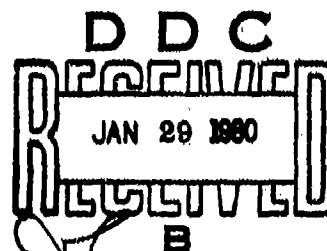
TECHNICAL REPORT ARLCD-TR-79030

FUZE GEAR-TRAIN ANALYSIS

G. G. LOWEN
CITY COLLEGE OF NEW YORK

F. R. TEPPER
ARRADCOM

DECEMBER 1979



US ARMY ARMAMENT RESEARCH AND DEVELOPMENT COMMAND
LARGE CALIBER
WEAPON SYSTEMS LABORATORY
DOVER, NEW JERSEY

DDC FILE COPY

Distribution limited to US Government agencies only because of test and evaluation, December 1979. Other requests for this document must be referred to Commander, ARRADCOM, ATTN: DRDAR-TSS, Dover, New Jersey 07801.

79 12 20 031
THIS DOCUMENT IS BEST QUALITY PRACTICABLE
THE COPY FURNISHED TO DDC CONTAINED A
SIGNIFICANT NUMBER OF PAGES WHICH DO NOT
REPRODUCE LEGIBLY.

The views, opinions, and/or findings contained in this report are those of the author(s) and should not be construed as an official Department of the Army position, policy or decision, unless so designated by other documentation.

Destroy this report when no longer needed. Do not return to the originator.

The citation in this report of the names of commercial firms or commercially available products or services does not constitute official endorsement or approval of such commercial firms, products, or services by the United States Government.

DISCLAIMER NOTICE

**THIS DOCUMENT IS BEST QUALITY
PRACTICABLE. THE COPY FURNISHED
TO DDC CONTAINED A SIGNIFICANT
NUMBER OF PAGES WHICH DO NOT
REPRODUCE LEGIBLY.**

UNCLASSIFIED

SECURITY CLASSIFICATION OF THIS PAGE (When Data Entered)

REPORT DOCUMENTATION PAGE		READ INSTRUCTIONS BEFORE COMPLETING FORM
1. REPORT NUMBER Technical Report ARLCD-TR-79030	2. GOVT ACQUISITION NO. (9) Technical report	3. RECIPIENT'S CATALOG NUMBER (1) Technical report
4. TITLE (and Subtitle) (6) Fuze Gear-Train Analysis		5. TYPE OF REPORT, PERIOD COVERED
7. AUTHOR(s) (10) G. G. Lowen, City College of New York F.R. Tepper, ARRADCOM		6. PERFORMING ORG. REPORT NUMBER
9. PERFORMING ORGANIZATION NAME AND ADDRESS Commander, ARRADCOM LCWSL (DRDAR-LCN) Dover, NJ 07801		8. CONTRACT OR GRANT NUMBER(s)
11. CONTROLLING OFFICE NAME AND ADDRESS Commander, ARRADCOM TSD, STINFO (DRDAR-TSS) Dover, NJ 07801		10. PROGRAM ELEMENT, PROJECT, TASK AREA & WORK UNIT NUMBERS
14. MONITORING AGENCY NAME & ADDRESS (if different from Controlling Office) (13) 481		12. REPORT DATE (11) December 1979
		13. NUMBER OF PAGES 478
		16. SECURITY CLASS. (of this report) Unclassified
15. DISTRIBUTION STATEMENT (of this Report) Distribution limited to U.S. Government agencies only because of test and evaluation, December 1979. Other requests for this document must be referred to Commander, ARRADCOM, ATTN: DRDAR-TSS, Dover, NJ 07801.		15a. DECLASSIFICATION/DOWNGRADING SCHEDULE
17. DISTRIBUTION STATEMENT (of the abstract entered in Block 20, if different from Report) (18) 5811		
18. SUPPLEMENTARY NOTES (19) NL E400 884		
19. KEY WORDS (Continue on reverse side if necessary and identify by block number) Clock gear Safing and arming Involute gear Timing Ogival gear Gear train		
20. A. SUMMARY (Continue on reverse side if necessary and identify by block number) This report documents the development of the tools needed to compare the efficiency of fuze-related gear trains designed to operate in a spin environment. Computer models have been developed for two and three pass step-up designs with clock (ogival) and involute tooth shapes. Using appropriate moment input-output relationships, the computer programs develop point and cycle efficiency for each type of gear train. Pivot friction partially caused by centrifugal force on the gear and pinion combinations during spin, and		

DDC

JAN 20 1980

B

DD FORM 1473, JAN 73 EDITION OF 1 NOV 65 IS OBSOLETE

UNCLASSIFIED

SECURITY CLASSIFICATION OF THIS PAGE (When Data Entered)

410 163

UNCLASSIFIED

SECURITY CLASSIFICATION OF THIS PAGE(When Data Entered)

20. Abstract (continued)

- tooth-to-tooth contact friction are considered. All models allow a variety of parameter variations.

UNCLASSIFIED

SECURITY CLASSIFICATION OF THIS PAGE(When Data Entered)

TABLE OF CONTENTS

	<u>Page No.</u>
Introduction	1
Point Efficiency and Cycle Efficiency	2
Description of Study	3
Appendixes	
A Step-up Gear Trains with Involute Teeth	A-1
B Design of Unequal Addendum Involute Gear Sets with Standard Center Distances	B-1
C Computer Models for Step-up Gear Trains with Involute Teeth	C-1
D Geometry of General Clock Gear Tooth	D-1
E Kinematics and Moment Input-Output Relationship for Single Step-up Gear Mesh with Clock Teeth	E-1
F Computer Models for Single Step-up Gear Mesh with Clock Teeth	F-1
G Kinematics of Two and Three Step-up Gear Trains with Clock Teeth	G-1
H Moment Input-Output Relationships for Two and Three Step-up Gear Trains with Teeth Operating in a Spin Environment	H-1
I Computer Models for Two and Three Step-up Gear Trains with Clock Teeth Operating in a Spin Environment	I-1

Distribution List

ACCESSION for	
NTIS	White Section <input type="checkbox"/>
DDC	Buff Section <input checked="" type="checkbox"/>
UNANNOUNCED	<input type="checkbox"/>
JUSTIFICATION	
BY	
DISTRIBUTION/AVAILABILITY CODES	
Dist. AVAIL. and/or SPECIAL	
B	23

LIST OF TABLES

<u>Table</u>	<u>Title</u>	<u>Page</u>
H-1	Possible Combinations of Phases for Three Pass Step-up Gear Train as Shown in Figure G-1	H-2
H-2	Possible Combinations of Phases for Two Pass Step-up Gear Train as Shown in Figure A-10	H-3

LIST OF FIGURES

<u>Figure</u>	<u>Title</u>	<u>Page</u>
A-1	Determination of Direction of Contact Friction Forces by Velocity Analysis	A-2
A-2	Free Body Diagrams of Pivot Shafts	A-5
A-3	Moments due to Friction Components Always Oppose Motion	A-7
A-4	Free Body Diagram for Single Step-Up Involute Gear Mesh	A-10
A-5	Basic Configuration for Involute Three Step-Up Gear Train in Spin Environment	A-19
A-6	Free Body Diagram of Pinion 4	A-21
A-7	Equilibrium of Gear and Pinion Set No.3	A-28
A-8	Free Body Diagram of Gear and Pinion Set No.2	A-35
A-9	Free Body Diagram of Gear No.1	A-42
A-10	Basic Configuration for Involute Two Step-Up Gear Train in Spin Environment	A-48
A-11	Free Body Diagram of Pinion No.3	A-49
A-12	Free Body Diagram of Gear and Pinion Set No.2	A-56
A-13	Free Body Diagram of Gear No.1	A-64
A-14	Pivot Hole Relationships	A-70

<u>Figure</u>	<u>Title</u>	<u>Page</u>
A-15	Involute Mesh Geometry	A-75
B-1	Relationship between Pinion Pitch Radius r_p , Rack Cutter Addendum A and Resulting Pinion Root Radius r_r	B-4
B-2	Minimum Root Radius r_{rm} for Rack Cutter with Sharp Corner	B-5
B-3	Rack Cutter with Corner Radius r_c (Effective Addendum of Cutter is Decreased)	B-6
D-1	Geometry of Ogival Tooth	D-2
E-1	Round on Round Phase of Contact (Gear Drives Pinion)	E-2
E-2	Round on Flat Phase of Contact (Gear Drives Pinion)	E-11
E-3	Sensing Geometry for Contact of Subsequent Tooth Mesh	E-19
E-4	Flat of Gear Contacts Round of Pinion	E-23
E-5	Free Body Diagram for Round on Round Phase	E-27
E-6	Free Body Diagram for Round on Flat Phase	E-34
G-1	Basic Configuration for Ogival Three Step-Up Gear Train in Spin Environment	G-2
G-2	Round on Round Phase for Mesh No.1	G-5
G-3	Round on Flat Phase for Mesh No.1	G-13
G-4	Round on Round Phase for Mesh No.2	G-24
G-5	Round on Flat Phase for Mesh No.2	G-31

<u>Figure</u>	<u>Title</u>	<u>Page</u>
H-1	Free Body Diagram of Pinion No.4 Mesh No.3: Round on Round	H-7
H-2	Free Body Diagram of Gear and Pinion No.3 Mesh No.3: Round on Round Mesh No.2: Round on Round	H-12
H-3	Free Body Diagram of Gear and Pinion No.2 Mesh No.2: Round on Round Mesh No.1: Round on Round	H-19
H-4	Free Body Diagram of Gear No.1 Mesh No.1: Round on Round	H-26
H-5	Free Body Diagram of Gear and Pinion No.2 Mesh No.2: Round on Round Mesh No.1: Round on Flat	H-32
H-6	Free Body Diagram of Gear No.1 Mesh No.1: Round on Flat	H-39
H-7	Free Body Diagram of Gear and Pinion No.3 Mesh No.3: Round on Round Mesh No.2: Round on Flat	H-45
H-8	Free Body Diagram of Gear and Pinion No.2 Mesh No.2: Round on Flat Mesh No.1: Round on Flat	H-52
H-9	Free Body Diagram of Gear and Pinion No.2 Mesh No.2: Round on Flat Mesh No.1: Round on Round	H-60

<u>Figure</u>	<u>Title</u>	<u>Page</u>
H-10	Free Body Diagram of Pinion No.4 Mesh No.3: Round on Flat	H-68
H-11	Free Body Diagram of Gear and Pinion No.3 Mesh No.3: Round on Flat Mesh No.2: Round On Flat	H-74
H-12	Free Body Diagram of Gear and Pinion No.3 Mesh No.3: Round on Flat Mesh No.2: Round on Round	H-83
H-13	Free Body Diagram of Pinion No.3 Mesh No.2: Round on Round	H-94
H-14	Free Body Diagram of Pinion No.3 Mesh No.2: Round on Flat	H-103

INTRODUCTION

This project provides the computer programs needed to compare the efficiency of fuze-related gear trains operating in a spin environment. Specifically, two and three pass step-up computer models with both involute and ogival (clock) tooth shapes were developed.

By using appropriate moment input-output relationships, the computer programs allow the determination of point and cycle efficiencies. Pivot friction, partly due to the centrifugal forces on the gear and pinion combinations, is considered in addition to tooth-to-tooth contact friction. The models derived allow a wide variety of parameter variations.

The main body of this report consists of nine appendixes, each of which contains a detailed analysis of each combination of tooth forms, the number of passes, and the spin environment. The derivation of moment relationships, pivot friction, gear tooth geometry, and the direct-contact mechanism kinematics are also included. The computer programs used are listed and instructions in their use and in interpreting the results are given.

The point efficiency ϵ_P is defined as

$$\epsilon_P = \frac{M_{OREF}}{M_{in}} \quad (1)$$

where M_{in} represents the instantaneous input moment to the gear train. M_{OREF} stands for the instantaneous equilibrant output moment M_o after it has been referred to the input shaft by way of the instantaneous angular velocity ratio

$$K_{RATIO} = \left| \frac{\dot{\psi}}{\dot{\phi}} \right|. \quad (2)$$

In the above,

$\dot{\psi}$ = instantaneous angular velocity of the output gear

$\dot{\phi}$ = instantaneous angular velocity of the input gear

Equation 1 then becomes

$$\epsilon_P = K_{RATIO} \frac{M_o}{M_{in}} \quad (3)$$

The cycle efficiency ϵ_C represents the ratio of the work available at the output shaft to that done by the input moment during one tooth cycle of the input gear. Thus,

$$\epsilon_C = \frac{\int M_o d\psi}{\int M_{in} d\phi} \quad (4)$$

The quantities $d\psi$ and $d\phi$ represent infinitesimal rotations of the output and input gears, respectively.

DESCRIPTION OF STUDY

Appendix A

Appendix A furnishes the background, as well as the derivations, for the moment input-output expressions for two and three pass step-up gear trains (where in each mesh the gear is the driver) with involute teeth and unity contact ratio.

Section 1 shows the development of a sign convention for the direction of the contact point friction force. It is based on the direction of the relative velocity between the contact points on the gear and pinion teeth. Section 2 discusses how to deal with the normal and friction forces at the gear and pinion pivots of single and multiple mesh trains. Section 3 shows the application of the above results to the moment input-output analysis of a single mesh. The frame is assumed stationary for this case, and the external loads are confined to the driving input moment and the equilibrating output moment.

The basic geometry of the three pass step-up gear train, mounted on a rotating fuze body, is formulated in section 4 for use in the moment input-output analysis. Force and moment equilibria of the individual component gears, which also account for the centrifugal forces, lead to the desired expression. Section 5 includes a similar derivation for a two pass step-up gear train with

involute teeth. In order to be able to continuously compute the moment relationships for these trains, a method for determining the simultaneous locations of the contact points of all the meshes had to be worked out. Such a method is given in section 6 together with certain angular relationships of the pivot locations on the model fuze body.

The kinematic relationships in involute gear trains are relatively simple compared to those in ogival trains because of the constant transmission ratio and the invariant direction of the line-of-action in each individual mesh.

Appendix B

To avoid the severe undercutting of pinions which generally is associated with step-up gear meshes, it is necessary to use non-standard involute gearing. Appendix B shows both the theory and the necessary steps for the design of unequal addendum gears and pinions of unity contact ratio. In addition, a numerical example is given.

Appendix C

This appendix contains four computer programs which make it possible to determine the point and cycle efficiencies of three gear combinations containing unequal addendum involute meshes with

unity contact ratio. In each case, the structure of the program is thoroughly discussed and a sample run is used to interpret the results. The names of these programs and their relationship to work described in the other appendixes are given below:

1. Program INVOL 1 : Design of unequal addendum involute gear and pinion set with unity contact ratio.

This program is based on the work in Appendix B. Five sample computations, which are used in other programs, are shown.

2. Program INVOL 2 : Point and cycle efficiencies for single pass involute step-up gear mesh with unity contact ratio.

This program is based on the work in section 3 of Appendix A.

3. Program INVOL 3 : Point and cycle efficiencies for three pass involute step-up gear train in spin environment. (All meshes have unity contact ratio).

This program is based on the work in sections 4 and 6 of Appendix A.

4. Program INVOL 4 : Point and cycle efficiencies for two pass involute step-up gear train in spin environment. (All meshes have unity contact ratio).

This program is based on the work in sections 5 and 6 of Appendix A.

Appendix D

This appendix describes the geometry of an ogival tooth in which each side of the tooth profile has a circular arc blending tangentially into a radial straight line flank. The basic tooth nomenclature is defined and methods for determining the required tooth parameters are given.

Appendix E

Section 1 of Appendix E gives all necessary kinematic derivations for a single step-up mesh with ogival teeth. The motion of an ogival mesh consists of two phases. On first contact, the circular arc portion of the driving gear tooth makes contact with the circular arc portion of the driven pinion tooth. Later in the cycle, and up to the point of final disengagement, the circular arc portion of the gear tooth contacts the straight line portion of the pinion tooth. These phases of motion were named "round on round" and "round on flat," respectively. Equivalent four-link mechanism models were used for both regimes to obtain expressions for the pinion output angles, for transition angles, for output angular velocities and for contact-point relative velocities. In addition, a sensing expression was developed which allows the computer determination of that position of a given mesh at which the subsequent mesh comes into engagement. (Because of the variable transmission ratio of ogival meshes, there is only one set of teeth in contact at any one time).

Section 2 of this appendix shows derivations of moment input-output expressions for both phases of contact of a single ogival mesh. Again, while pivot friction is considered in addition to contact friction, the frame is assumed to be stationary for this single mesh.

Appendix F

Two computer programs which deal with the kinematics and the moment input-output relationships of a single pass step-up gear mesh with clock teeth are given in this appendix. The structure of each of these programs is again discussed in detail and sample runs are used to explain their input and output parameters. The names of these programs and their relationships to work in other sections are given below:

1. Program CLOCK 1 : Kinematics of a single step-up gear mesh with clock teeth.

This program is based on work in Appendix D as well as on work in section 1 of Appendix E. In addition, it has been used to check the geometry of the ogival meshes which were used in programs CLOCK 2, CLOCK 3 and CLOCK 4 (See Appendix I for the latter two).

2. Program CLOCK 2 : Point and cycle efficiencies for single pass step-up gear mesh with clock teeth.

This program is based on work in section 2 of Appendix E.

Appendix G

When one considers the kinematic relationships of ogival meshes which are mounted on a fuse body as parts of two or three pass step-up trains, it becomes necessary to account for the relative positions of the individual meshes on the fuse body. Appendix G gives the appropriate derivations for each of the three meshes of a three-pass train. The model of the fuse body is identical with that used for involute step-up trains.

Appendix H

This appendix shows the derivations of moment input-output expressions for two and three pass step-up gear trains with ogival teeth which must operate in a spin environment.

Because of the increase in rotational speed associated with each tooth mesh, increasingly more sets of teeth will come into engagement in the second and third meshes as one set of teeth moves through one complete contact cycle in the first (i.e., the input) mesh. With two phases of motion for each mesh, there will be eight contact combinations in a three-pass train. Section 1 of Appendix H gives a derivation for the moment input-output expression of each of these eight cases.

Section 2 shows similar work for the four contact combinations which are associated with two pass step-up gear trains with ogival teeth.

Both analyses account for the effects of the centrifugal forces.

Appendix I

This appendix contains two computer programs which allow the determination of point and cycle efficiencies for two and three pass step-up gear meshes with clock teeth. As for other programs, the origins of their mathematical formulations are thoroughly discussed. In addition, their input and output parameters are explained with the help of a sample run. The names of these programs as well as their relationships to work in other appendixes are given below:

1. Program CLOCK 3 : Point and cycle efficiencies for three pass clock (ogival) step-up gear train in spin environment.

This program is based on work given in Appendix G as well as in section 1 of Appendix H. The general fuze geometry is that described in section 6 of Appendix A.

2. Program CLOCK 4 : Point and cycle efficiencies for two pass clock (ogival) step-up gear train in spin environment.

The kinematics of this program is again based on work given in Appendix G. The moment input-output relationships are from section 2 of Appendix H.

APPENDIX A

STEP-UP GEAR TRAINS WITH INVOLUTE TEETH

1. DIRECTION OF FRICTION FORCE AT TOOTH-TO-TOOTH CONTACT

Figure A-1 uses the base circle and the line-of-action configuration of an involute mesh, in which the gear drives the pinion, to determine the direction of the friction forces at contact point C before and after the contact point passes through pitch point P. Distance d represents the length of the line-of-action between base circle tangent points L and L'. The distance between contact point C and point L along the line-of-action is measured by length a.

Further:

- θ = actual (rolling) pressure angle
- R_b = gear base radius
- r_b = pinion base radius

The friction force of the pinion tooth on the gear tooth, for example, will have the direction of the relative velocity, \bar{V}_{C_p / C_g} , of the contact point on the pinion tooth, C_p , with respect to the coincident contact point on the gear tooth, C_g . (The friction force of the gear tooth on the pinion tooth has the opposite direction.) This relative velocity changes direction at the pitch point, where it becomes instantaneously zero.

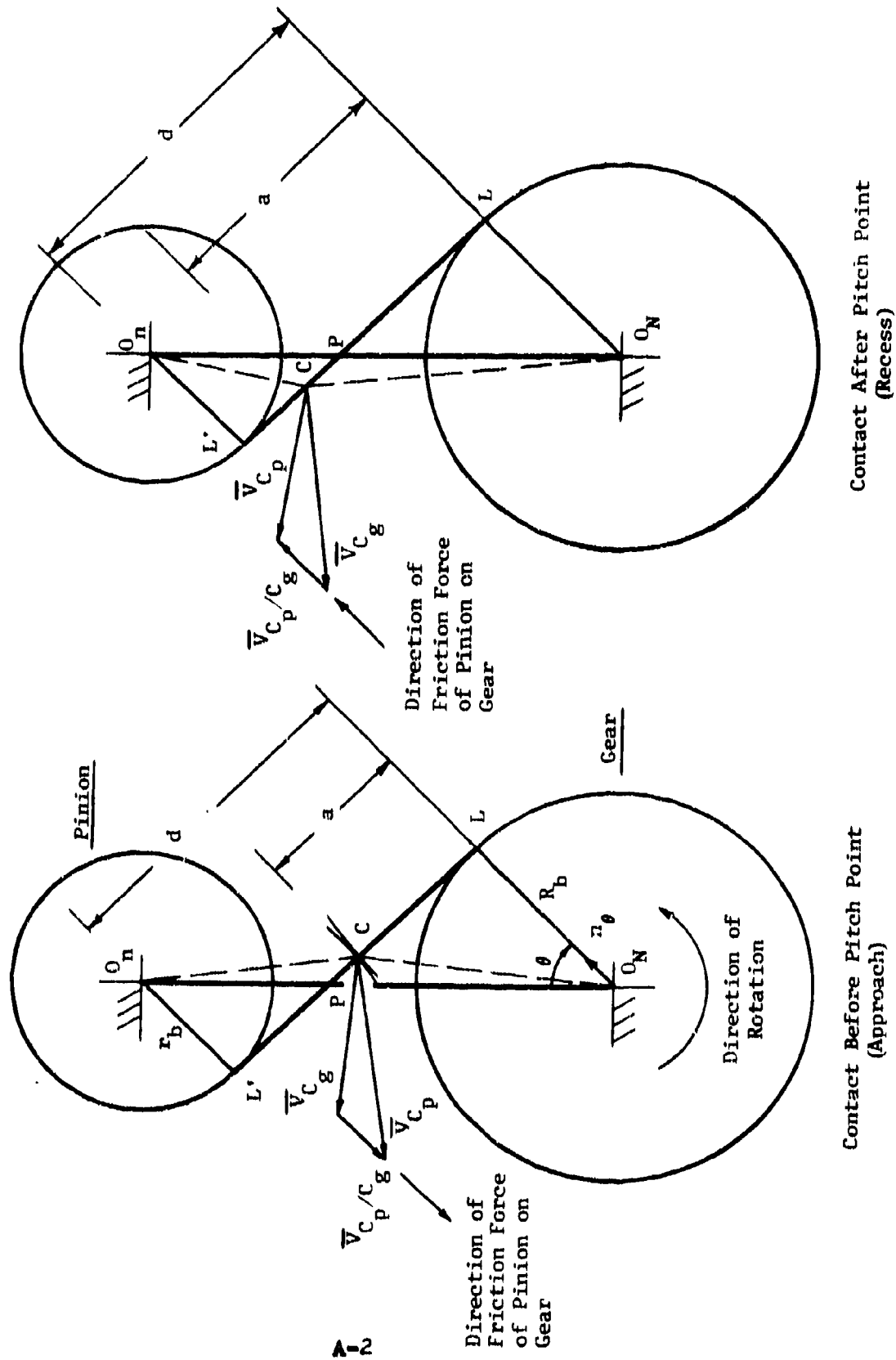


FIGURE A-1. DETERMINATION OF DIRECTION OF CONTACT FRICTION FORCES BY VELOCITY ANALYSIS

Figure A-1 shows contact before the pitch point (during approach). To obtain the direction of the relative velocity, V_{C_p/C_g} , by a graphical analysis, one makes use of the velocity equation

$$V_{C_p} = V_{C_p/C_g} + V_{C_g} \quad (A-1)$$

where V_{C_p} = velocity of point C_p on pinion tooth with direction normal to line $O_N - C$

V_{C_p/C_g} = relative velocity between point C_p and point C_g . The direction of this velocity is normal to the line of action.

V_{C_g} = velocity of point C_g on gear tooth with direction normal to line $O_N - C$. The magnitude of this velocity was arbitrarily chosen.

The graphical construction, according to Eq (A1), shows that V_{C_p/C_g} has the direction opposite to that of the unit vector \bar{N}_θ shown at point O_N . As stated earlier, this represents

the friction force on the gear tooth during approach.

Figure A-1b shows the same graphical analysis for contact during recess. Once the pitch point is passed, both the relative velocity, \bar{V}_{C_p/C_g} , and the friction force of the pinion on the gear have the direction of the positive unit vector \bar{n}_θ .

2. ASSUMPTIONS CONCERNING NORMAL AND FRICTION FORCES AT PIVOTS

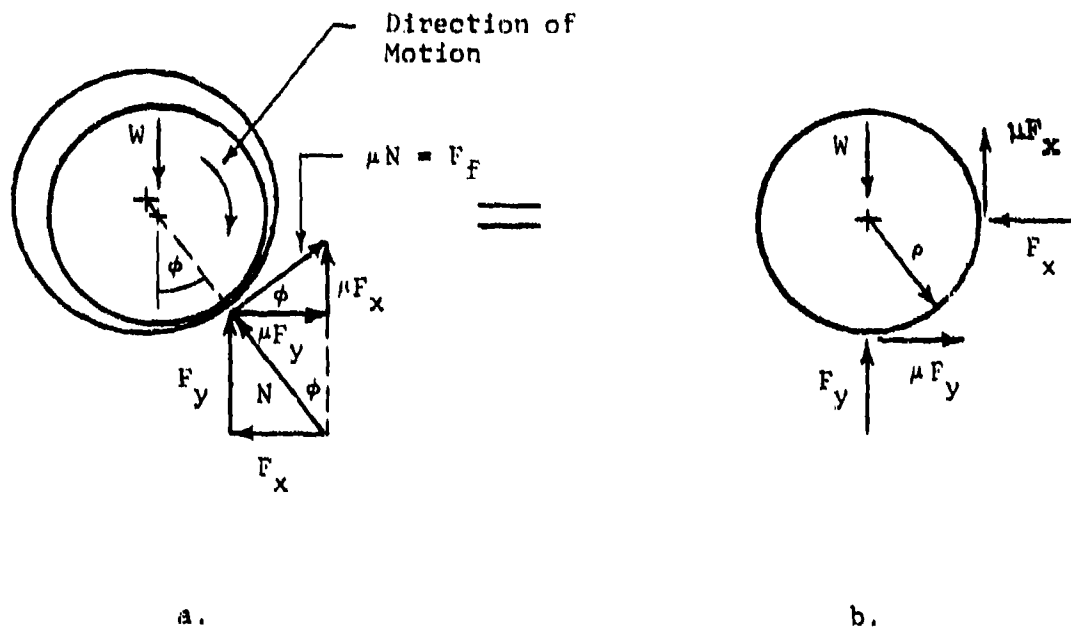


FIGURE A-2 FREE-BODY DIAGRAMS OF PIVOT SHAFTS

Figure A-2a shows a pivot shaft which is loaded by a known external force, W , and rotates in a clockwise direction. Due to friction between the shaft and the bearing, contact is made at an angle, $\phi = \tan^{-1} \mu$, where μ is the associated coefficient of friction. N is the normal contact

force. The friction force $F_f = \mu N$ opposes the clockwise rotation by creating a counterclockwise moment.

N may be resolved into the components F_x and F_y . The associated x and y components of the friction force are μF_y and μF_x , respectively.

The directions of the components of N and F_f are drawn in the same manner in Fig. A-2b in a somewhat more convenient representation. When the direction of the resultant external force, W , is not known, contact is possible anywhere on the periphery of the bearing and the components F_x and F_y of the normal contact force cannot be drawn with certainty in the free body diagram. The direction of the friction components must still oppose the motion.

Figure A-3 shows two general possibilities of drawing the free body diagram of a pivot which rotates in a clockwise direction. In either case, the moments of the friction components oppose the rotation while F_x and F_y may be positive or negative. Assume now, for example, that Fig. A-3a shows the wrong direction for F_x and that the solution of the applicable equilibrium equation will reverse the sign of F_x . This will automatically reverse the sign of the friction component μF_x also. Since contact is now made on the opposite

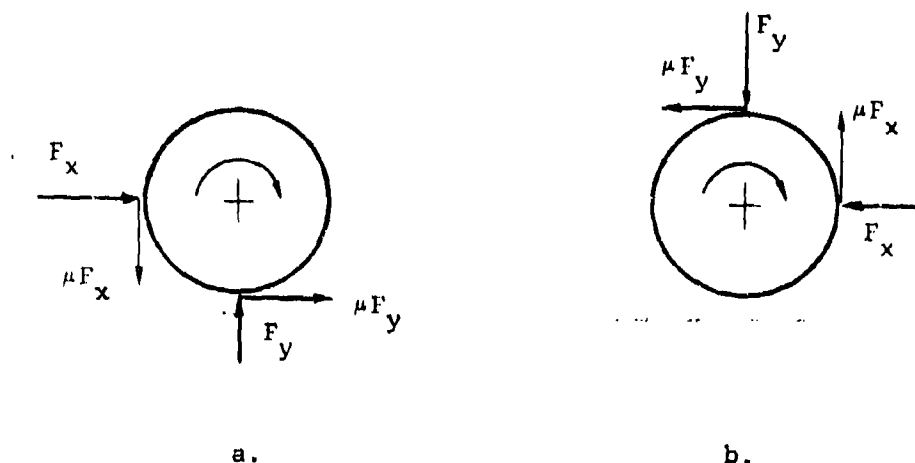


FIGURE A-3 MOMENTS DUE TO FRICTION COMPONENTS
ALWAYS OPPOSE MOTION

side of the pivot, the correct sign of the friction component is automatically assured.

The total friction moment then is expressed by

$$M_f = \pm \mu \rho \sqrt{F_x^2 + F_y^2} \quad (\text{A-2})$$

where ρ is the pivot radius. The sign of the above is chosen so that the rotation is opposed. In case F_x and F_y contain required terms that cannot be factored out of the square root of equation (A-2), the friction moment is conservatively overstated by the use of the absolute values of F_x and F_y .

$$M_f = \pm \mu p \left(|F_x| + |F_y| \right) \quad (A-3a)$$

If the expressions for F_x and F_y consist of sums of positive and negative terms, then F_x and F_y are presented as the sums of the absolute values of these terms. A conservative pivot friction moment becomes, similar to equation (A-3a),

$$M_f = \pm \mu p \left(\tilde{F}_x + \tilde{F}_y \right) \quad (A-3b)$$

The tildes represent the sums of the absolute values of the component terms.

3. MOMENT INPUT-OUTPUT RELATIONSHIP FOR SINGLE STEP-UP

GEAR MESH WITH INVOLUTE TEETH

Figure A-4 shows free body diagrams of the gear and the pinion of a single mesh where the gear is driven by a counterclockwise input moment M_{in} . It is desired to find the equilibrating output moment M_o .

a. UNIT VECTORS

The unit vector directed from point O_N to point L is given by

$$\bar{n}_\theta = \sin\theta\bar{i} + \cos\theta\bar{j} \quad (A-4)$$

where θ represents the actual pressure angle, regardless of tooth modification. The unit vector directed along the line of action from point L to point L' is given by

$$\bar{n}_{\theta T} = -\cos\theta\bar{i} + \sin\theta\bar{j} \quad (A-5)$$

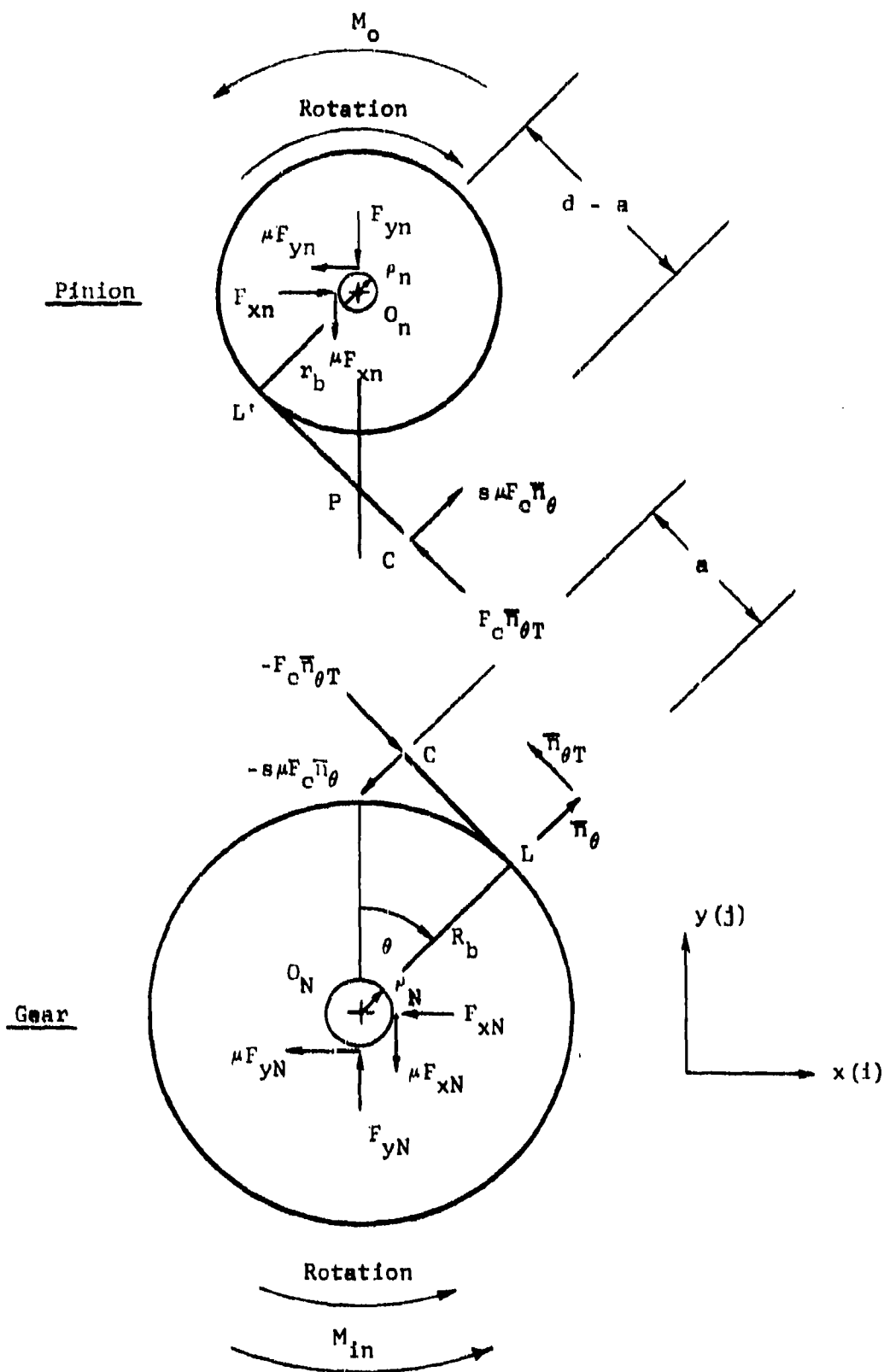


FIGURE A-4. FREE BODY DIAGRAM FOR SINGLE STEP-UP INVOLUTE GEAR MESH

5. NOMENCLATURE AND SIGNUM CONVENTION

F_{xN}, F_{yN} = x and y components of normal force acting on gear pivot

$\mu F_{xN}, \mu F_{yN}$ = friction force components acting on gear pivot. Directions chosen to result in friction moments which oppose motion. (See part 2).

F_{xn}, F_{yn} = x and y components of normal force acting on pinion pivot

$\mu F_{xn}, \mu F_{yn}$ = friction force components acting on pinion pivot

μ = coefficient of friction

F_c = normal contact force between gear and pinion.

The force of the pinion on the gear is $(-)F_c \bar{n}_{\theta T}$, while the normal force of the gear on the pinion becomes $F_c \bar{n}_{\theta T}$.

μF_c = tooth contact friction force. The analysis in Section 1 shows that the friction force of the pinion on the gear, before the pitch point, acts in the direction of $(-)\bar{n}_{\theta}$. Therefore

$-s\mu F_c \bar{n}_{\theta}$ = friction force on gear with

s = +1 for $a < \overline{LP}$ (approach) (A-6)

and

$$s = -1 \quad \text{for } a > \overline{LP} \quad (\text{recess}) \quad (\text{A-7})$$

while

$$s = 0 \quad \text{for } a = \overline{LP} \quad (\text{at pitch point}) \quad (\text{A-8})$$

Further,

ρ_N, ρ_n = gear and pinion pivot radii

R_b, r_b = gear and pinion base circle radii

c. FORCE ANALYSIS OF THE GEAR

By inspecting Figure A-4, one sees that force equilibrium of the gear is expressed by

$$-F_c \bar{n}_{\theta T} - \mu F_c \bar{n}_{\theta} - F_{xN} \bar{i} - \mu F_{xN} \bar{j} + F_{yN} \bar{j} - \mu F_{yN} \bar{i} = 0 \quad (A-9)$$

Similarly, moment equilibrium of the gear is given by

$$M_{in} \bar{k} - r_N \mu \sqrt{F_{xN}^2 + F_{yN}^2} \bar{k} + R_b \bar{n}_{\theta} \times (-) F_c \bar{n}_{\theta T} + (R_b \bar{n}_{\theta} + a \bar{n}_{\theta T}) \times (-) \mu F_c \bar{n}_{\theta} = 0 \quad (A-10)$$

Note the use of equation (A-2) to express the friction moment at the gear pivot.

With the help of equations (A-4) and (A-5) one may write equations (A-9) and (A-10) in scalar form. Thus,

$$F_c \cos \theta - \mu F_c \sin \theta - F_{xN} - \mu F_{yN} = 0 \quad (A-11)$$

$$-F_c \sin \theta - \mu F_c \cos \theta + F_{yN} - \mu F_{xN} = 0 \quad (A-12)$$

Equation (A-10) becomes

$$M_{in} - \rho_N \mu \sqrt{F_{xN}^2 + F_{yN}^2} - R_b F_c + \mu s a F_c = 0 \quad (A-13)$$

Simultaneous solution of equations (A-11) and (A-12) for

F_{xN} and F_{yN} gives

$$F_{xN} = F_c \frac{(1 - \mu^2 s) \cos \theta - \mu(1 + s) \sin \theta}{1 + \mu^2} \quad (A-14)$$

and

$$F_{yN} = F_c \frac{(1 - \mu^2 s) \sin \theta + \mu(1 + s) \cos \theta}{1 + \mu^2} \quad (A-15)$$

When the above expressions are substituted into the moment equation (A-13) and if one notes that s^2 always equals +1, the following expression for F_c is obtained:

$$F_c = \frac{M_{in}}{R_b + \mu(\rho_N - as)} \quad (A-16)$$

d. FORCE ANALYSIS OF THE PINION

Force equilibrium of the pinion is assured by

$$F_c \bar{n}_{\theta T} + \mu s F_c \bar{n}_\theta + F_{xn} \bar{i} - F_{yn} \bar{j} - \mu F_{xn} \bar{j} - \mu F_{yn} \bar{i} = 0, \quad (A-17)$$

while moment equilibrium is given by

$$M_o \bar{k} + \rho_n \mu \sqrt{F_{xn}^2 + F_{yn}^2} \bar{k} + [-r_b \bar{n}_\theta - (d - a) \bar{n}_{\theta T}] \times (F_c \bar{n}_{\theta T} + \mu s F_c \bar{n}_\theta) = 0 \quad (A-18)$$

In scalar form, the above become

$$-F_c \cos \theta + \mu s F_c \sin \theta + F_{xn} - \mu F_{yn} = 0 \quad (A-19)$$

$$F_c \sin \theta + \mu s F_c \cos \theta - \mu F_{xn} - F_{yn} = 0 \quad (A-20)$$

$$M_o + \mu \rho_n \sqrt{F_{xn}^2 + F_{yn}^2} - r_b F_c + \mu s (d - a) F_c = 0 \quad (A-21)$$

Equations (A-19) and (A-20) are now solved simultaneously for F_{xn} and F_{yn} . This gives

$$F_{xn} = F_c \frac{(1 + \mu^2 s) \cos \theta + \mu(1 - s) \sin \theta}{1 + \mu^2} \quad (A-22)$$

and

$$F_{yn} = F_c \frac{(1 + \mu^2 s) \sin \theta - \mu(1 - s) \cos \theta}{1 + \mu^2} \quad (A-23)$$

Equations (A-22) and (A-23) are then substituted into the moment equation (A-21). This furnishes the following expression for the normal contact force, F_c . (Again, s^2 always equals +1.):

$$F_c = \frac{M_o}{r_b - \mu [r_n + s(d - a)]} \quad (A-24)$$

e. MOMENT INPUT-OUTPUT RELATIONSHIP

The equilibrant moment, M_o , may be expressed as a function of the input moment, M_{in} , after equations (A-16) and (A-24) have been set equal to each other. Thus,

$$M_o = \frac{M_{in} \left\{ r_b - \mu \left[\rho_n + s(d - a) \right] \right\}}{R_b + \mu \left[\rho_N - sa \right]} \quad (A-25)$$

The input-output relationship may also then be expressed in terms of

$$M_o = M_{in} \frac{r_b}{R_b} E_2 \quad (A-26)$$

$$\text{where } E_2 = \frac{1 - \frac{\mu \left[\rho_n + s(d - a) \right]}{r_b}}{1 + \frac{\mu \left(\rho_N - sa \right)}{R_b}},$$

and represents the efficiency of moment transmission of a single step-up mesh with involute teeth.

4. MOMENT INPUT-OUTPUT RELATIONSHIP FOR THREE STEP-UP GEAR TRAIN IN SPIN ENVIRONMENT

Figure A-5 shows the basic configuration of the three step-up gear train for which the relationship between the equilibrant output moment M_{o4} , acting on pinion 4, and the input moment M_{in} , acting on gear 1, is to be found.

The body-fixed x-y coordinate system has its origin at the spin axis, C, of the fuze body, and its x-axis coincides with the line C- O_1 , where O_1 represents the pivot axis of the input gear-spin rotor combination. Points O_2 , O_3 and O_4 represent the pivot axes of gear and pinion no. 2, gear and pinion no. 3, and pinion no. 4, respectively. Further,

- R_1 = distance from the spin axis to the various pivot axes
- R_{b1} = base radii of gears
- r_{b1} = base radii of pinions
- β_1 = angle between positive x-axis and line of centers O_1 - O_2
- β_2 = angle between positive x-axis and line of centers O_2 - O_3
- β_3 = angle between positive x-axis and line of centers O_3 - O_4
- γ_1 = angle between positive x-axis and lines C- O_1

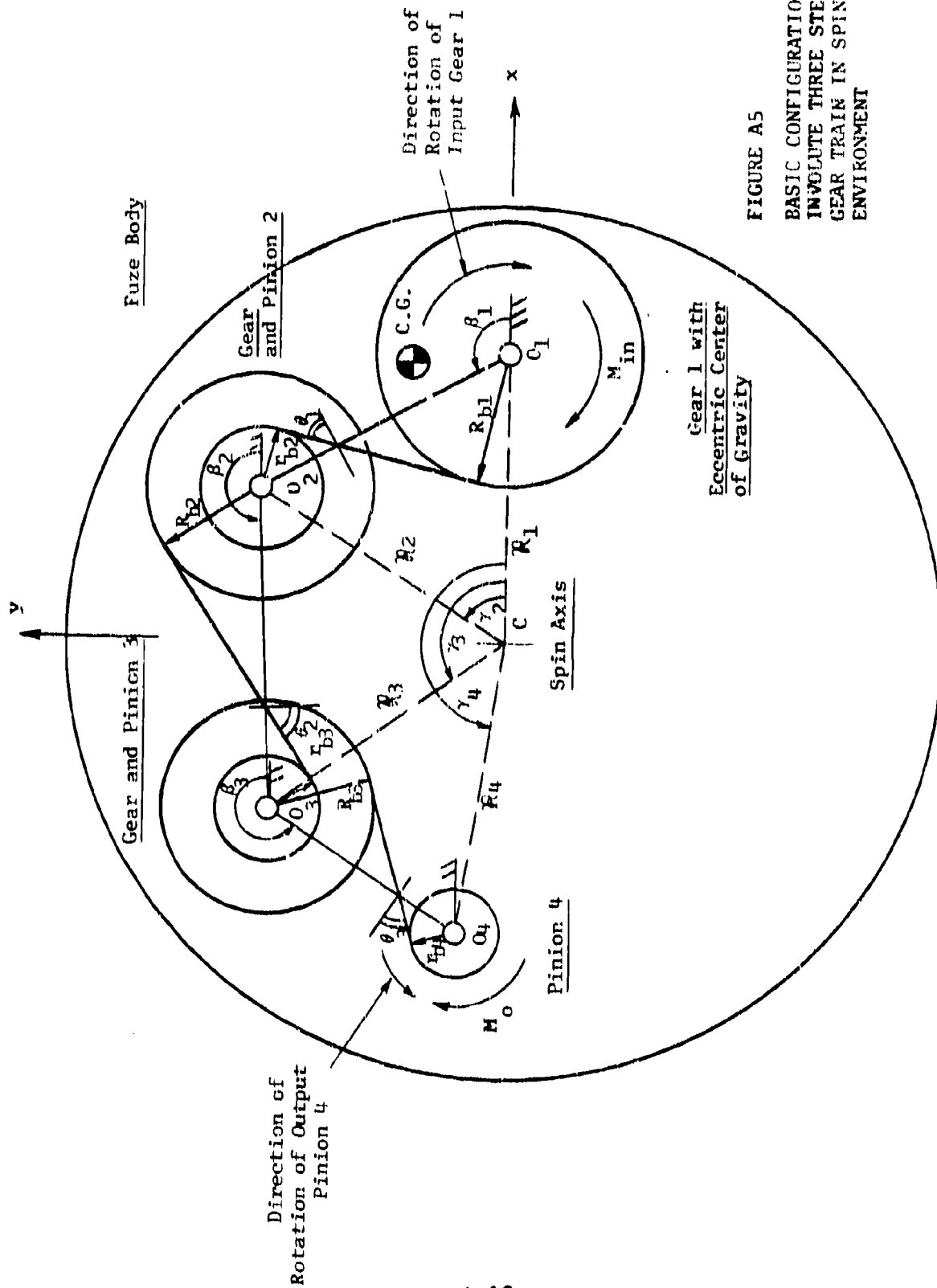


FIGURE A5

BASIC CONFIGURATION FOR
INVOLUTE THREE STEP-UP
GEAR TRAIN IN SPIN
ENVIRONMENT

- θ_1 = pressure angle of mesh between gear no. 1 and pinion no. 2
- θ_2 = pressure angle of mesh between gear no. 2 and pinion no. 3
- θ_3 = pressure angle of mesh between gear no. 3 and pinion no. 4

To obtain the moment input-output relationship of the total train, the input-output relationships of the individual components must first be obtained. The following equilibrium analyses include pivot as well as contact friction forces, in addition to loads due to the centrifugal forces on the individual components. The directions of the tooth-to-tooth friction forces are chosen according to the rules of Section 1 of this appendix, using an appropriate signum convention. The direction of the pivot friction forces is chosen according to Section 2 and, to avoid difficulties with the direction of the associated friction moment, equation (A-3b) will be used.

a. EQUILIBRIUM OF PINION 4

Figure A-6 shows a free body diagram of pinion 4. The contact between gear 3 and pinion 4 is shown before contact point C_3 has passed through pitch point P_3 . The unit vector \bar{n}_{34} is along the line-of-action in the direction of the contact force of the gear on the pinion.

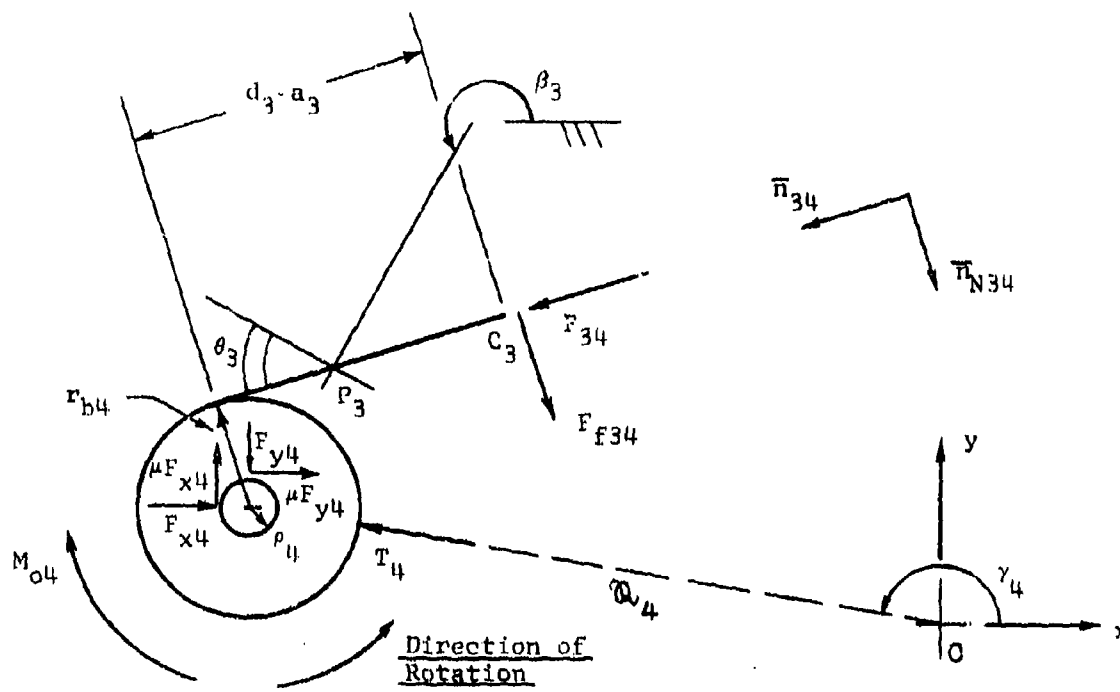


FIGURE A-6. FREE BODY DIAGRAM OF PINION 4

Thus,

$$\bar{n}_{34} = \sin(\beta_3 + \theta_3)\bar{i} - \cos(\beta_3 + \theta_3)\bar{j} \quad (A-27)$$

The unit vector normal to the line-of-action is given by

$$\bar{n}_{N34} = \cos(\beta_3 + \theta_3)\bar{i} + \sin(\beta_3 + \theta_3)\bar{j} \quad (A-28)$$

The contact force \bar{F}_{34} then becomes

$$\bar{F}_{34} = F_{34} \bar{n}_{34} \quad (A-29)$$

The friction force of gear 3 on pinion 4 is given by

$$\bar{F}_{f34} = \mu s_3 F_{34} \bar{n}_{N34} \quad (A-30)$$

where $s_3 = +1$, for contact before the pitch point

$s_3 = 0$, for contact at the pitch point

$s_3 = -1$, for contact after the pitch point

(See also Section 1.)

The normal forces on the pivot shaft are given by

$$\bar{F}_{x4} = F_{x4} \bar{I} \quad (A-31)$$

and

$$\bar{F}_{y4} = -F_{y4} \bar{J} \quad (A-32)$$

The associated pivot friction forces are given by $\mu F_{x4} \bar{J}$ and $\mu F_{y4} \bar{I}$ for the indicated direction of rotation. The centrifugal force T_4 on the pinion is represented by

$$\bar{T}_4 = T_4 (\cos \gamma_4 \bar{I} + \sin \gamma_4 \bar{J}) \quad (A-33)$$

where

$$T_4 = R_4 \omega^2 m_4 \quad (A-34a)$$

with

$$\omega = \text{spin angular velocity} \quad (A-34b)$$

and

$$m_4 = \text{mass of pinion 4} \quad (A-34c)$$

The force equilibrium equation is given by

$$\begin{aligned} F_{34} \bar{N}_{34} + \mu_s F_{34} \bar{N}_{34} + T_4 (\cos \gamma_4 \bar{I} + \sin \gamma_4 \bar{J}) + F_{x4} \bar{I} \\ + \mu F_{y4} \bar{I} + \mu F_{x4} \bar{J} - F_{y4} \bar{J} = 0 \end{aligned} \quad (A-35)$$

Moment equilibrium is given by the following expression, in which the pivot friction moment is expressed according to Equation (A-3b):

$$-M_{o4} - \rho_4^v (\tilde{F}_{x4} + \tilde{F}_{y4}) + r_{b4} F_{34} - \mu s_3 (d_3 - a_3) F_{34} = 0 \quad (A-36)$$

where ρ_4 represents the pivot radius. d_3 is the length of the line-of-action of the mesh from points of tangency to the base circles. a_3 is the distance on the line of action from the gear point of tangency to the contact point C_3 .

Equation (A-35) gives the following component equations:

$$F_{34} \sin(\beta_3 + \theta_3) + \mu s_3 F_{34} \cos(\beta_3 + \theta_3) + T_4 \cos \gamma_4 + F_{x4} + \mu F_{y4} = 0 \quad (A-37)$$

$$-F_{34} \cos(\beta_3 + \theta_3) + \mu s_3 F_{34} \sin(\beta_3 + \theta_3) + T_4 \sin \gamma_4 - F_{y4} + \mu F_{x4} = 0 \quad (A-38)$$

Simultaneous solution of the above for F_{x4} and F_{y4} results in

$$F_{x4} = \frac{1}{1 + \mu^2} \left\{ -T_4 [\cos \gamma_4 + \mu \sin \gamma_4] - F_{34} [(1 + \mu^2 s_3) \sin(\beta_3 + \theta_3) - \mu(1 - s_3) \cos(\beta_3 + \theta_3)] \right\} \quad (A-39)$$

and

$$F_{y4} = \frac{1}{1 + \mu^2} \left\{ T_4 [\sin \gamma_4 - \mu \cos \gamma_4] - F_{34} [(1 + \mu^2 s_3) \cos(\beta_3 + \theta_3) + \mu(1 - s_3) \sin(\beta_3 + \theta_3)] \right\} \quad (A-40)$$

To obtain conservative values for the pivot friction moment in equation (A-36) according to equation (A-3b), one substitutes the largest possible values for F_{x4} and F_{y4} . This is accomplished by making the signs of T_4 and F_{34} positive and by using the absolute values of their respective coefficients in Equations (A-39) and (A-40). Equation (A-36) then becomes

$$\begin{aligned} -M_{o4} &= \mu p_4 (T_4 A_1 + F_{34} A_2 + T_4 A_3 + F_{34} A_4) + r_{b4} F_{34} \\ &\quad - \mu s_3 (d_3 - s_3) F_{34} = 0 \end{aligned} \quad (A-41)$$

where

$$A_1 = \left| \frac{\sin \gamma_4 - \mu \cos \gamma_4}{1 + \mu^2} \right| \quad (A-42)$$

$$A_2 = \left| \frac{(1 + \mu^2 s_3) \cos(\beta_3 + \theta_3) + \mu(1 - s_3) \sin(\beta_3 + \theta_3)}{1 + \mu^2} \right| \quad (A-43)$$

$$A_3 = \left| \frac{\cos \gamma_4 + \mu \sin \gamma_4}{1 + \mu^2} \right| \quad (A-44)$$

$$A_4 = \left| \frac{(1 + \mu^2 s_3) \sin(\beta_3 + \theta_3) - \mu(1 - s_3) \cos(\beta_3 + \theta_3)}{1 + \mu^2} \right| \quad (A-45)$$

Finally equation (A-41) is solved for F_{34}

$$F_{34} = \frac{M_{o4}}{D_1} + \frac{T_4 C_1}{D_1} \quad (A-46)$$

where

$$C_1 = \mu \rho_4 (A_1 + A_3) \quad (A-47)$$

$$D_1 = r_{b4} - \mu [s_3 (d_3 - a_3) + \rho_4 (A_2 + A_4)] \quad (A-48)$$

b. EQUILIBRIUM OF GEAR AND PINION SET NO. 3

Figure A-7 shows the free body diagram of gear and pinion set no. 3. Contact point C_3 , between pinion 4 and gear 3, is, as shown previously in Figure A-6, before pitch point P_3 . The normal force, along the line-of-action, is given [see equation (A-29)] by

$$\bar{F}_{43} = -F_{34} \bar{n}_{34} \quad (A-49)$$

and the associated friction force \bar{F}_{f43} is given [see equation (A-30)] by

$$\bar{F}_{f43} = -s_3 \mu F_{34} \bar{n}_{34} \quad (A-50)$$

The unit vectors along (and perpendicular to) the line-of-action of gear 2 and pinion 3 are given by

$$\bar{n}_{23} = -\sin(\beta_2 - \theta_2) \bar{i} + \cos(\beta_2 - \theta_2) \bar{j} \quad (A-51)$$

and

$$\bar{n}_{N23} = -\cos(\beta_2 - \theta_2) \bar{i} - \sin(\beta_2 - \theta_2) \bar{j} \quad (A-52)$$

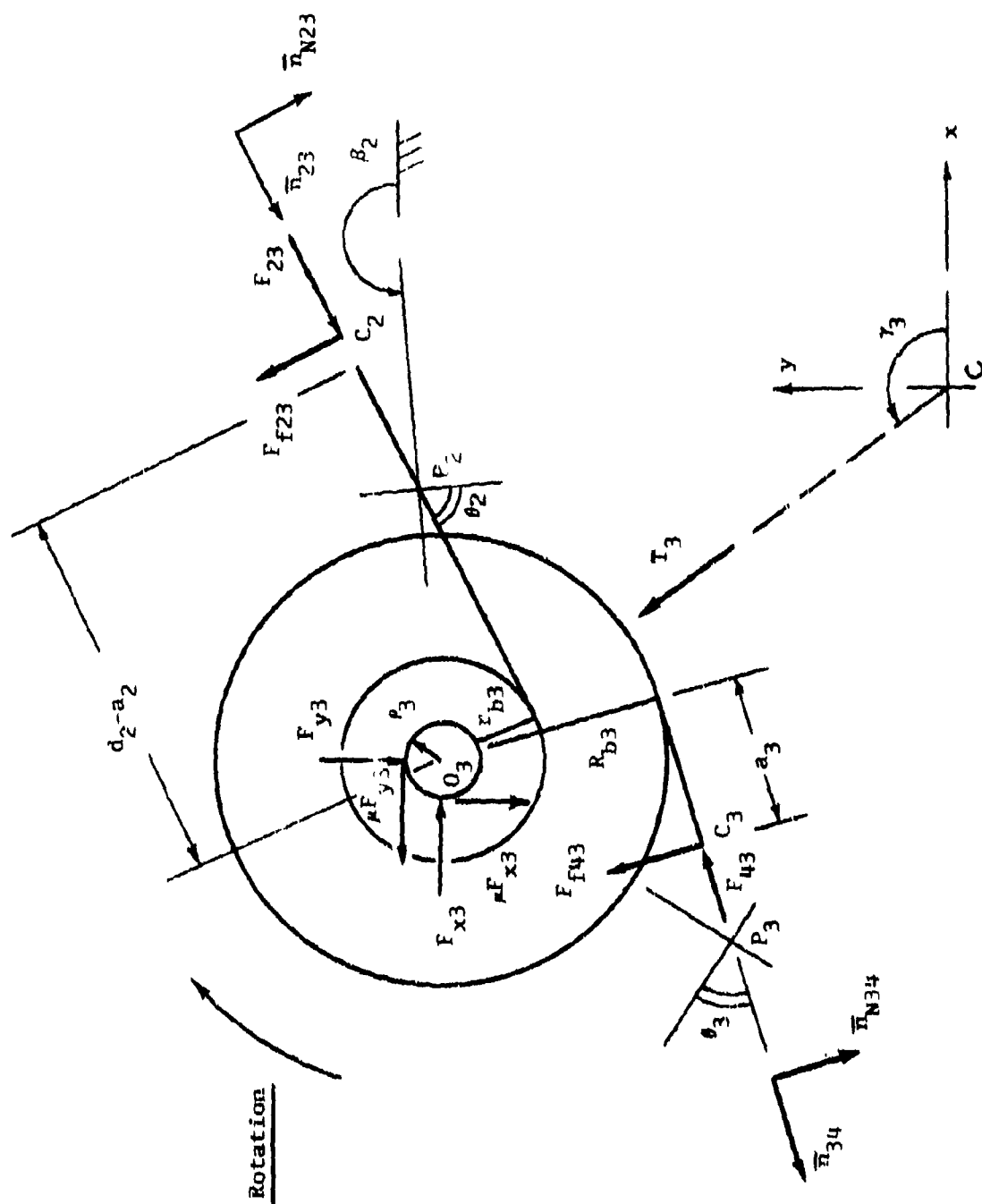


FIGURE A-7. EQUILIBRIUM OF GEAR AND PINION SET NO. 3

The contact point C_2 between gear 2 and pinion 3 is also shown before pitch point P_2 is passed.

The normal contact force between these teeth then becomes

$$\vec{F}_{23} = F_{23} \vec{n}_{23} \quad (A-53)$$

The associated friction force is given by

$$\vec{F}_{f23} = -\mu s_2 F_{23} \vec{n}_{23} \quad (A-54)$$

where $s_2 = +1$ for contact before pitch point P_2

$s_2 = 0$ for contact at pitch point P_2

$s_2 = -1$ for contact after pitch point P_2

The normal forces on the pivot shaft are given by

$$\vec{F}_{x3} = F_{x3} \vec{i} \quad (A-55)$$

and

$$\vec{F}_{y3} = -F_{y3} \vec{j} \quad (A-56)$$

The associated pivot friction forces are represented by $(-)\mu F_{y3} \vec{i}$

and $(-)\mu F_{x3}\bar{j}$ for the indicated direction of gear rotation.

The centrifugal force, \bar{T}_3 , on the assembly is given by

$$\bar{T}_3 = T_3(\cos\gamma_3\bar{i} + \sin\gamma_3\bar{j}) \quad (A-57)$$

where

$$T_3 = R_3\omega^2 m_3 \quad (A-58a)$$

with

$$m_3 = \text{mass of pinion and gear 3} \quad (A-58b)$$

Force equilibrium is given by

$$\begin{aligned} F_{23}\bar{n}_{23} - \mu s_2 F_{23}\bar{n}_{N23} - F_{34}\bar{n}_{34} - \mu s_3 F_{34}\bar{n}_{N34} + T_3(\cos\gamma_3\bar{i} + \sin\gamma_3\bar{j}) \\ + F_{x3}\bar{i} - \mu F_{y3}\bar{i} - F_{y3}\bar{j} - \mu F_{x3}\bar{j} = 0 \end{aligned} \quad (A-59)$$

Moment equilibrium requires

$$\begin{aligned} R_{b3}F_{34} - \mu s_3 a_3 F_{34} - r_{b3}F_{23} + \mu s_2(d_2 - a_2)F_{23} \\ + \mu p_3(\tilde{F}_{x3} + \tilde{F}_{y3}) = 0 \end{aligned} \quad (A-60)$$

Note the use of equation (A-3b) for the pivot friction moment.

p_3 represents the pivot radius and length d_2 is the length of the

line-of-action between the points of tangency to the base circles.

a_2 is the distance along the line-of-action from the gear point of tangency to the contact point C_2 .

The component form of equation (A-59) is represented by the following two expressions:

$$\begin{aligned} -F_{23}\sin(\beta_2 - \theta_2) + \mu s_2 F_{23}\cos(\beta_2 - \theta_2) - F_{34}\sin(\beta_3 + \theta_3) \\ - \mu s_3 F_{34}\cos(\beta_3 + \theta_3) + T_3\cos\gamma_3 + F_{x3} - \mu F_{y3} = 0 \end{aligned} \quad (A-61)$$

and

$$\begin{aligned} F_{23}\cos(\beta_2 - \theta_2) + \mu s_2 F_{23}\sin(\beta_2 - \theta_2) + F_{34}\cos(\beta_3 + \theta_3) \\ - \mu s_3 F_{34}\sin(\beta_3 + \theta_3) + T_3\sin\gamma_3 - F_{y3} - \mu F_{x3} \\ = 0 \end{aligned} \quad (A-62)$$

Simultaneous solution of the above for F_{x3} and F_{y3} leads to

$$\begin{aligned} F_{x3} = \frac{1}{1 + \mu^2} \left\{ F_{23} \left[(1 + \mu^2 s_2)\sin(\beta_2 - \theta_2) + \mu(1 - s_2)\cos(\beta_2 - \theta_2) \right] \right. \\ \left. + T_3 \left[\mu\sin\gamma_3 - \cos\gamma_3 \right] + F_{34} \left[(1 - \mu^2 s_3)\sin(\beta_3 + \theta_3) \right. \right. \\ \left. \left. + \mu(1 + s_3)\cos(\beta_3 + \theta_3) \right] \right\} \end{aligned} \quad (A-63)$$

and

$$F_{y3} = \frac{1}{1 + \mu^2} \left\{ F_{23} \left[(1 + \mu^2 a_2) \cos(\beta_2 - \theta_2) + \mu(a_2 - 1) \sin(\beta_2 - \theta_2) \right] \right. \\ \left. + T_3 \left[\sin \gamma_3 + \mu \cos \gamma_3 \right] + F_{34} \left[(1 - \mu^2 a_3) \cos(\beta_3 + \theta_3) \right. \right. \\ \left. \left. - \mu(a_3 + 1) \sin(\beta_3 + \theta_3) \right] \right\} \quad (A-64)$$

Now, equations (A-63) and (A-64) are substituted into the moment equation (A-60) with consideration of the pivot friction moment according to equation (A-3b). This gives

$$R_{b3} F_{34} - \mu a_3 a_3 F_{34} - r_{b3} F_{23} + \mu a_2 (d_2 - a_2) F_{23} \\ + \mu r_3 \left[F_{23} (A_5 + A_8) + T_3 (A_6 + A_9) + F_{34} (A_7 + A_{10}) \right] \\ = 0 \quad (A-65)$$

where

$$A_5 = \left| \frac{(1 + \mu^2 a_2) \cos(\beta_2 - \theta_2) + \mu(a_2 - 1) \sin(\beta_2 - \theta_2)}{1 + \mu^2} \right| \quad (A-66)$$

$$A_6 = \left| \frac{\sin \gamma_3 + \mu \cos \gamma_3}{1 + \mu^2} \right| \quad (A-67)$$

$$A_7 = \left| \frac{(1 - \mu^2 s_3) \cos(\beta_3 + \theta_3) - \mu(1 + s_3) \sin(\beta_3 + \theta_3)}{1 + \mu^2} \right| \quad (A-68)$$

$$A_8 = \left| \frac{(1 + \mu^2 s_2) \sin(\beta_2 - \theta_2) + \mu(1 - s_2) \cos(\beta_2 - \theta_2)}{1 + \mu^2} \right| \quad (A-69)$$

$$A_9 = \left| \frac{\mu s_1 \gamma_3 - \cos \gamma_3}{1 + \mu^2} \right| \quad (A-70)$$

$$A_{10} = \left| \frac{(1 - \mu^2 s_3) \sin(\beta_3 + \theta_3) + \mu(1 + s_3) \cos(\beta_3 + \theta_3)}{1 + \mu^2} \right| \quad (A-71)$$

Finally equation (A-65) is solved for F_{23}

$$F_{23} = \frac{F_{34} C_2 + T_3 C_3}{D_2} \quad (A-72)$$

where

$$C_2 = R_{b3} - \mu [s_3 a_3 - r_3 (A_7 + A_{10})] \quad (A-73)$$

$$C_3 = \mu r_3 (A_6 + A_9) \quad (A-74)$$

$$D_2 = r_{b3} - \mu [s_2 (d_2 - a_2) + r_3 (A_5 + A_8)] \quad (A-75)$$

c. EQUILIBRIUM OF GEAR AND PINION SET NO. 2

Figure A-8 shows the free body diagram of gear and pinion set no. 2. The contact point C_2 , between gear 2 and pinion 3, is again shown before the pitch point P_2 is passed. (See also Figure A-7.) The normal force, along the line-of-action, becomes with equation (A-72)

$$F_{32} = -F_{23}\bar{n}_{23} \quad (A-76)$$

The associated friction force, F_{f32} , is given by

$$F_{f32} = \mu_2 F_{23}\bar{n}_{N23} \quad (A-77)$$

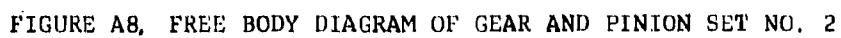
The unit vectors along (and perpendicular to) the line-of-action of gear 1 and pinion 2 are given by

$$\bar{n}_{12} = \sin(\beta_1 + \theta_1)\bar{I} - \cos(\beta_1 + \theta_1)\bar{J} \quad (A-78)$$

and

$$\bar{n}_{N12} = \cos(\beta_1 + \theta_1)\bar{I} + \sin(\beta_1 + \theta_1)\bar{J} \quad (A-79)$$

The contact point C_1 between gear 1 and pinion 2 is also shown before pitch point P_1 is passed.



The normal contact force between the teeth of this mesh becomes

$$\bar{F}_{12} = F_{12} \bar{n}_{12} , \quad (A-80)$$

while the associated friction force is given by
(See Section 1 of this Appendix.)

$$\bar{F}_{f12} = \mu s_1 F_{12} \bar{n}_{12} \quad (A-81)$$

where $s_1 = +1$ for contact before pitch point P_1

$s_1 = 0$ for contact at pitch point P_1

$s_1 = -1$ for contact after pitch point P_1

The normal forces on the pivot shaft are

$$\bar{F}_{x2} = -F_{x2} \bar{i} \quad (A-82)$$

and

$$\bar{F}_{y2} = -F_{y2} \bar{j} \quad (A-83)$$

The associated pivot friction forces are again chosen such that

their friction moments oppose the indicated rotation.

The centrifugal force, \bar{T}_2 , on this gear and pinion assembly is given by

$$\bar{T}_2 = T_2(\cos\gamma_2\bar{i} + \sin\gamma_2\bar{j}) \quad (A-84)$$

$$\text{where } T_2 = R_2\omega^2 m_2 \quad (A-85a)$$

with

$$m_2 = \text{mass of gear and pinion set no. 2} \quad (A-85b)$$

Force equilibrium is given by

$$\begin{aligned} & -F_{23}\bar{n}_{23} + \mu_{s2}F_{23}\bar{n}_{N23} + F_{12}\bar{n}_{12} + \mu_{s1}F_{12}\bar{n}_{N12} \\ & + T_2(\cos\gamma_2\bar{i} + \sin\gamma_2\bar{j}) - F_{x2}\bar{i} - F_{y2}\bar{j} + \mu_{Fy2}\bar{i} - \mu_{Fx2}\bar{j} \\ & = 0 \end{aligned} \quad (A-86)$$

Moment equilibrium is given by

$$\begin{aligned} & -R_{b2}F_{23} + \mu_{s2}a_2F_{23} + r_{b2}F_{12} - \mu_{s1}(d_1 - a_1)F_{12} \\ & - \mu_{p2}(\tilde{F}_{x2} + \tilde{F}_{y2}) = 0 \end{aligned} \quad (A-87)$$

Again, equation (A-3b) is used to account for the pivot friction moment. ρ_2 represents the pivot radius. d_1 is the length of the line-of-action between the points of tangency to the base circles, and a_1 is the distance from the point of tangency of the gear to the contact point C_1 .

The component form of equation (A-86) is given by

$$\begin{aligned} F_{23}\sin(\beta_2 - \theta_2) - \mu s_2 F_{23}\cos(\beta_2 - \theta_2) + F_{12}\sin(\beta_1 + \theta_1) \\ + \mu s_1 F_{12}\cos(\beta_1 + \theta_1) + T_2\cos\gamma_2 - F_{x2} + \mu F_{y2} \\ = 0 \end{aligned} \quad (A-88)$$

$$\begin{aligned} -F_{23}\cos(\beta_2 - \theta_2) - \mu s_2 F_{23}\sin(\beta_2 - \theta_2) - F_{12}\cos(\beta_1 + \theta_1) \\ + \mu s_1 F_{12}\sin(\beta_1 + \theta_1) + T_2\sin\gamma_2 - F_{y2} - \mu F_{x2} \\ = 0 \end{aligned} \quad (A-89)$$

Simultaneous solution of the above furnishes

$$\begin{aligned} F_{x2} = \frac{1}{1 + \mu^2} \left\{ -F_{12} \left[\mu(1 - s_1)\cos(\beta_1 + \theta_1) - (1 + \mu^2 s_1)\sin(\beta_1 + \theta_1) \right] \right. \\ \left. + T_2 \left[\mu\sin\gamma_2 + \cos\gamma_2 \right] \right. \\ \left. + F_{23} \left[(1 - \mu^2 s_2)\sin(\beta_2 - \theta_2) - \mu(1 + s_2)\cos(\beta_2 - \theta_2) \right] \right\} \end{aligned} \quad (A-90)$$

and

$$F_{y2} = \frac{1}{1 + \mu^2} \left\{ -F_{12} \left[\mu(1 - s_1) \sin(\beta_1 + \theta_1) + (1 + \mu^2 s_1) \cos(\beta_1 + \theta_1) \right] \right. \\ \left. + T_2 \left[\sin \gamma_2 - \mu \cos \gamma_2 \right] \right. \\ \left. + F_{23} \left[-\mu(1 + s_2) \sin(\beta_2 - \theta_2) - (1 - \mu^2 s_2) \cos(\beta_2 - \theta_2) \right] \right\} \quad (A-91)$$

Now, equations (A-90) and (A-91) are substituted into the moment equation (A-87). With consideration of the pivot friction moment according to equation (A-3b), this gives

$$-R_{b2} F_{23} + \mu s_2 a_2 F_{23} + r_{b2} F_{12} - \mu s_1 (d_1 - a_1) F_{12} \\ - \mu p_2 \left[F_{12} (A_{11} + A_{14}) + T_2 (A_{12} + A_{15}) + F_{23} (A_{13} + A_{16}) \right] \\ = 0 \quad (A-92)$$

In the above

$$A_{11} = \left| \frac{\mu(1 - s_1) \sin(\beta_1 + \theta_1) + (1 + \mu^2 s_1) \cos(\beta_1 + \theta_1)}{1 + \mu^2} \right| \quad (A-93)$$

$$A_{12} = \left| \frac{\sin \gamma_2 - \mu \cos \gamma_2}{1 + \mu^2} \right| \quad (A-94)$$

$$A_{13} = \left| \frac{\mu(1 + s_2)\sin(\beta_2 - \theta_2) + (1 - \mu^2 s_2)\cos(\beta_2 - \theta_2)}{1 + \mu^2} \right| \quad (\text{A-95})$$

$$A_{14} = \left| \frac{\mu(1 - s_1)\cos(\beta_1 + \theta_1) - (1 + \mu^2 s_1)\sin(\beta_1 + \theta_1)}{1 + \mu^2} \right| \quad (\text{A-96})$$

$$A_{15} = \left| \frac{\mu \sin \gamma_2 + \cos \gamma_2}{1 + \mu^2} \right| \quad (\text{A-97})$$

$$A_{16} = \left| \frac{(1 - \mu^2 s_2)\sin(\beta_2 - \theta_2) - \mu(1 + s_2)\cos(\beta_2 - \theta_2)}{1 + \mu^2} \right| \quad (\text{A-98})$$

Finally, equation (A-92) is solved for F_{12}

$$F_{12} = \frac{F_{23}C_4 + T_2C_5}{D_3} \quad (\text{A-99})$$

where

$$C_4 = R_{b2} - \mu \left[s_2 a_2 - p_2 (A_{13} + A_{16}) \right] \quad (\text{A-100})$$

$$C_5 = \mu p_2 (A_{12} + A_{15}) \quad (\text{A-101})$$

$$D_3 = r_{b2} - \mu \left[s_1 (d_1 - a_1) + p_2 (A_{11} + A_{14}) \right] \quad (\text{A-102})$$

d. EQUILIBRIUM OF GEAR NO. 1

Figure A-9 shows the free body diagram of gear no. 1, the input gear.

The contact point C_1 is identical with that shown in Figure A-8.

The normal force on gear no. 1 is given by (See equation (A-80).)

$$\bar{F}_{21} = -F_{12}\bar{n}_{12} \quad (A-103)$$

The associated friction force is

$$\bar{F}_{f21} = -\mu s_1 F_{12}\bar{n}_{12} \quad (A-104)$$

The normal forces on the pivot shaft are given by

$$\bar{F}_{x1} = -F_{x1}\bar{i} \quad (A-105)$$

and

$$\bar{F}_{y1} = F_{y1}\bar{j} \quad (A-106)$$

The associated pivot friction forces are chosen in such a direction that their moments oppose the indicated rotation.

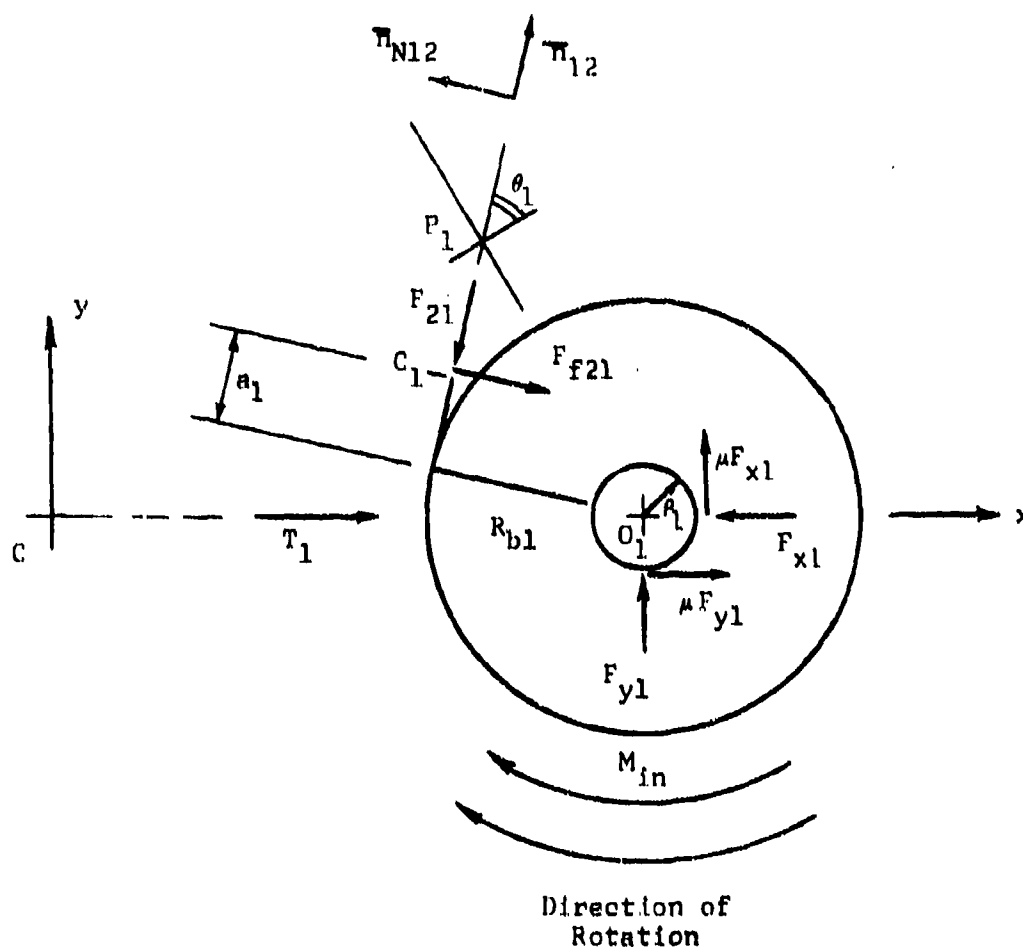


FIGURE A9. FREE BODY DIAGRAM OF GEAR 1

The centrifugal force \bar{T}_1 on gear 1 is given by

$$\bar{T}_1 = T_1 \bar{I} \quad (A-107)$$

where

$$T_1 = r_1 \omega^2 m_1 \quad (A-108a)$$

$$m_1 = \text{mass of gear 1} \quad (A-108b)$$

Force equilibrium is given by

$$-F_{12} \bar{H}_{12} - \mu s_1 F_{12} \bar{H}_{N12} + T_1 \bar{I} - F_{x1} \bar{I} + F_{y1} \bar{J} + \mu F_{y1} \bar{I} + \mu F_{x1} \bar{J} = 0 \quad (A-109)$$

Moment equilibrium is found from

$$R_{b1} F_{12} - \mu s_1 a_1 F_{12} - M_{in} + \mu p_1 (\tilde{F}_{x1} + \tilde{F}_{y1}) = 0 \quad (A-110)$$

The form of equation (A-3b) is again utilized to obtain the pivot friction moment. p_1 represents the pivot radius of gear 1.

The component form of equation (A-109) becomes

$$\begin{aligned} -F_{12}\sin(\beta_1 + \theta_1) - \mu s_1 F_{12}\cos(\beta_1 + \theta_1) - F_{x1} + \mu F_{y1} + T_1 \\ = 0 \end{aligned} \quad (A-111)$$

and

$$\begin{aligned} F_{12}\cos(\beta_1 + \theta_1) - \mu s_1 F_{12}\sin(\beta_1 + \theta_1) + F_{y1} + \mu F_{x1} \\ = 0 \end{aligned} \quad (A-112)$$

Simultaneous solution of equations (A-111) and (A-112) furnishes the forces on the pivot, i.e.,

$$F_{x1} = \frac{-F_{12}[(1 - \mu^2 s_1)\sin(\beta_1 + \theta_1) + \mu(1 + s_1)\cos(\beta_1 + \theta_1)] + T_1}{1 + \mu^2} \quad (A-113)$$

$$F_{y1} = \frac{F_{12}[\mu(1 + s_1)\sin(\beta_1 + \theta_1) - (1 - \mu^2 s_1)\cos(\beta_1 + \theta_1)] - \mu T_1}{1 + \mu^2} \quad (A-114)$$

Equations (A-113) and (A-114) are now substituted into the moment equation (A-110) in the following manner: (Again, the method of equation (A-3b) is applied.)

$$R_{b1}F_{12} - \mu s_1 a_1 F_{12} - M_{1n} + \mu p_1 [F_{12}(A_{17} + A_{19}) + T_1(A_{18} + A_{20})] = 0 \quad (A-115)$$

where

$$A_{17} = \left| \frac{(1 - \mu^2 s_1) \sin(\beta_1 + \theta_1) + \mu(1 + s_1) \cos(\beta_1 + \theta_1)}{1 + \mu^2} \right| \quad (A-116)$$

$$A_{18} = \left| \frac{1}{1 + \mu^2} \right| \quad (A-117)$$

$$A_{19} = \left| \frac{\mu(1 + s_1) \sin(\beta_1 + \theta_1) - (1 - \mu^2 s_1) \cos(\beta_1 + \theta_1)}{1 + \mu^2} \right| \quad (A-118)$$

$$A_{20} = \left| \frac{\mu}{1 + \mu^2} \right| \quad (A-119)$$

Finally, equation (A-115) is solved for F_{12}

$$F_{12} = \frac{M_{1n}}{D_4} - \frac{T_1 C_6}{D_4} \quad (A-120)$$

where

$$C_6 = \mu p_1 (A_{18} + A_{20}) \quad (A-121)$$

$$D_4 = R_{b1} - \mu [s_1 a_1 - p_1 (A_{17} + A_{19})] \quad (A-122)$$

e. INPUT-OUTPUT RELATIONSHIP

To obtain the input-output relationship for the complete gear train, equation (A-120) is now equated to equation (A-99).

This furnishes

$$F_{23} = \frac{D_3}{C_4 D_4} (M_{in} - T_1 C_6) - T_2 \frac{C_5}{C_4} \quad (A-123)$$

Further, the above is equated to equation (A-72). This results in the following expression for F_{34}

$$F_{34} = \frac{D_2 D_3}{C_1 C_4 D_4} (M_{in} - T_1 C_6) - T_2 \frac{C_5 D_2}{C_2 C_4} - T_3 \frac{C_3}{C_2} \quad (A-124)$$

Finally, equation (A-124) is equated to equation (A-46).

This establishes the input-output relationship

$$M_{o4} = \frac{D_1 D_2 D_3}{C_2 C_4 D_4} (M_{in} - T_1 C_6) - T_2 \frac{C_5 D_1 D_2}{C_2 C_4} - T_3 \frac{C_3 D_1}{C_2} - T_4 C_1 \quad (A-125)$$

5. MOMENT INPUT-OUTPUT RELATIONSHIP FOR INVOLUTE TWO STEP-UP
GEAR TRAIN IN SPIN ENVIRONMENT

Figure A-10 shows the basic configuration of a two step-up gear train with involute teeth for which the relationship between the equilibrant output moment, M_{o3} , acting on pinion 3, and the input moment, M_{in} , acting on gear 1 is to be found. All nomenclature is identical with that used in Section 4 in connection with the three step-up gear train.

Again, the general relationship between input and output is found by assembling the input-output relationships of the individual component gears.

a. EQUILIBRIUM OF PINION 3

Figure A-11 shows the free body diagram of pinion 3. The contact point C_2 between gear 2 and pinion 3 is shown before the pitch point P_2 is passed.

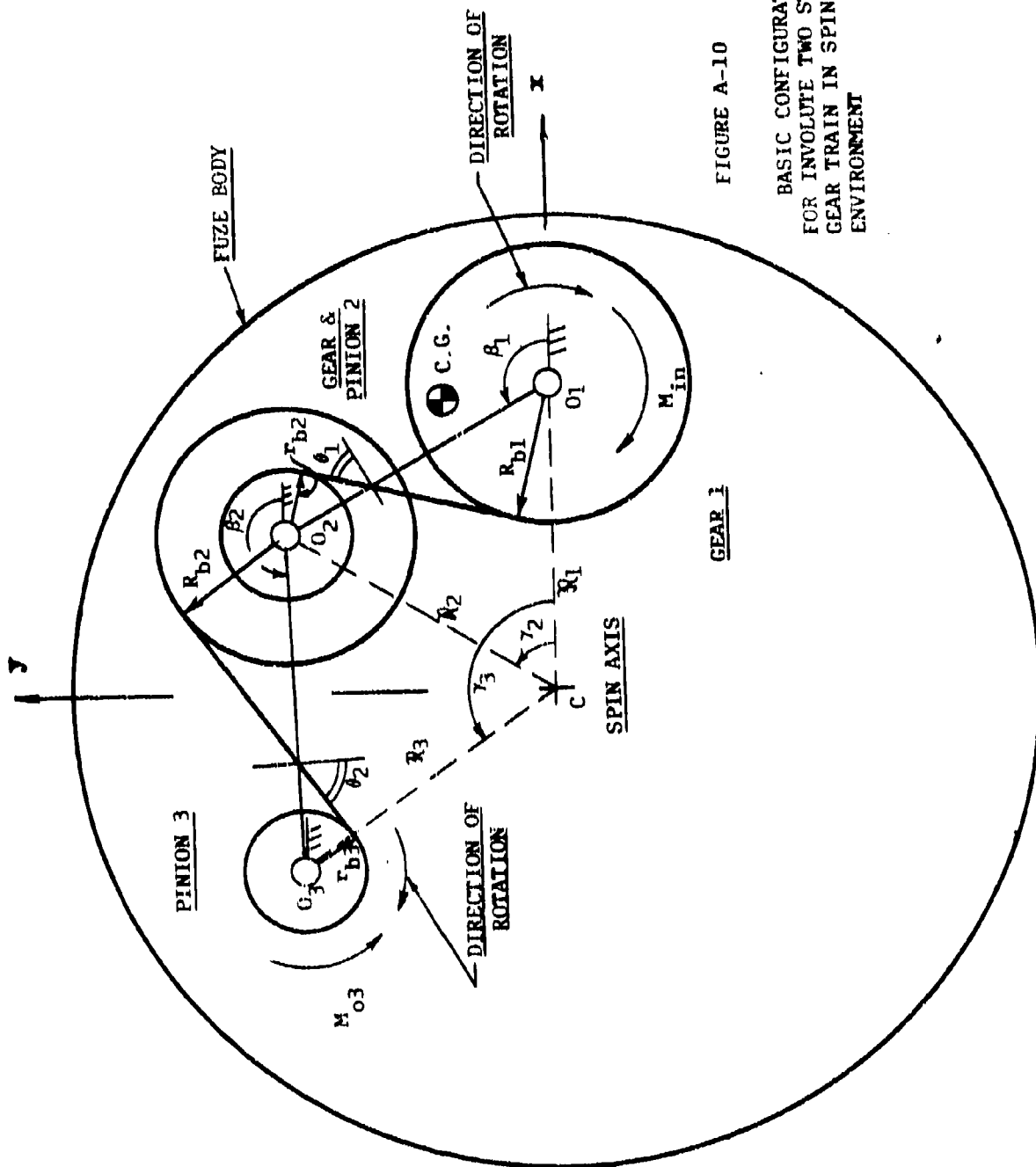


FIGURE A-10

BASIC CONFIGURATION
FOR INVOLUTE TWO STEP-UP
GEAR TRAIN IN SPIN
ENVIRONMENT

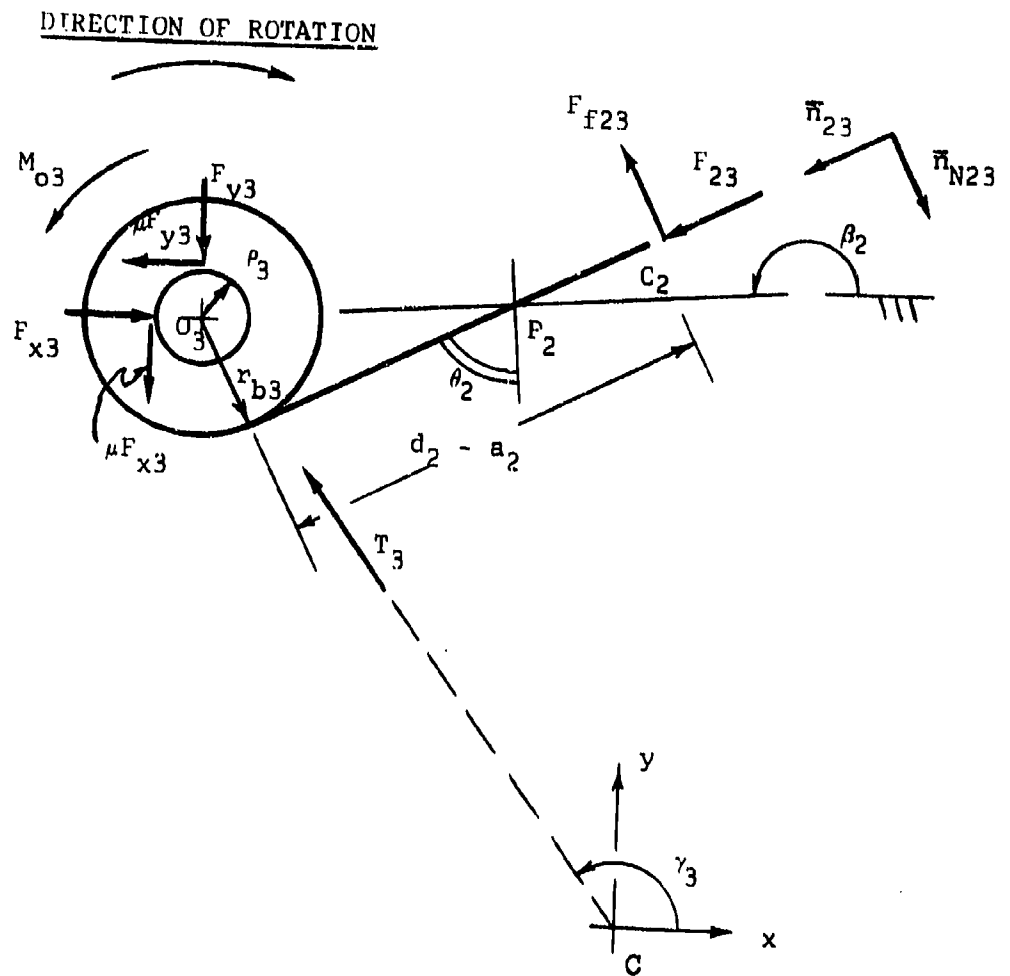


FIGURE A-11 FREE BODY DIAGRAM OF PINION 3

As in equation (A-53), the normal force between the teeth of gear 2 and pinion 3 is given by

$$\bar{F}_{23} = F_{23} \bar{n}_{23} \quad (A-126)$$

The associated friction force is given by equation (A-54), i.e.,

$$\bar{F}_{f23} = -\mu s_2 F_{23} \bar{n}_{N23} \quad (A-127)$$

where $s_2 = +1$, for contact before pitch point P_2

$s_2 = 0$, for contact at pitch point P_2

$s_2 = -1$, for contact after pitch point P_2

The unit vectors in equations (A-126) and (A-127) were defined by equations (A-51) and (A-52), respectively. The normal forces on the pivot shaft are given by

$$\bar{F}_{x3} = F_{x3} \bar{i} \quad (A-128)$$

and

$$\bar{F}_{y3} = -F_{y3} \bar{j} \quad (A-129)$$

The pivot friction forces become $(-)\mu F_{y3}\bar{i}$ and $(-)\mu F_{x3}\bar{j}$ for the indicated direction of rotation.

As in equation (A-57), the centrifugal force on the pinion is given by

$$\bar{T}_3 = T_3(\cos\gamma_3\bar{i} + \sin\gamma_3\bar{j}) \quad (A-130)$$

where

$$T_3 = R_3\omega^2 m_3 \quad (A-131)$$

with

$$m_3 = \text{mass of pinion 3} \quad (A-132)$$

Force equilibrium is given by

$$\begin{aligned} F_{23}\bar{n}_{23} - \mu s_2 F_{23}\bar{n}_{23} + T_3(\cos\gamma_3\bar{i} + \sin\gamma_3\bar{j}) + F_{x3}\bar{i} \\ - \mu F_{y3}\bar{i} - F_{y3}\bar{j} - \mu F_{x3}\bar{j} = 0 \end{aligned} \quad (A-133)$$

Moment equilibrium is obtained from

$$M_{o3} - r_{b3}F_{23} + \mu s_2(d_2 - s_2)F_{23} + \mu^3_3(\tilde{F}_{x3} + \tilde{F}_{y3}) = 0 \quad (A-134)$$

Note the use of equation (A-3b) for the pivot friction moment.

r_3 represents the pivot radius. d_2 is the length of the line of action between the points of tangency to the base circles of pinion 3 and gear 2. a_2 is the distance along the line-of-action from the gear point of tangency to contact point C_2 .

The x and y components of equation (A-133) are given by

$$-F_{23}\sin(\beta_2 - \theta_2) + \mu s_3 F_{23}\cos(\beta_2 - \theta_2) + T_3\cos\gamma_3 + F_{x3} - \mu F_{y3} = 0, \quad (A-135)$$

and

$$F_{23}\cos(\beta_2 - \theta_2) + \mu s_3 F_{23}\sin(\beta_2 - \theta_2) + T_3\sin\gamma_3 - F_{y3} - \mu F_{x3} = 0 \quad (A-136)$$

Simultaneous solution of these expressions for F_{x3} and F_{y3} yields

$$F_{x3} = \frac{1}{1 + \mu^2} \left\{ F_{23} \left[(1 + \mu^2 s_2)\sin(\beta_2 - \theta_2) + \mu(1 - s_2)\cos(\beta_2 - \theta_2) \right] + T_3 \left[\mu\sin\gamma_3 - \cos\gamma_3 \right] \right\} \quad (A-137)$$

and

$$F_{y3} = \frac{1}{1 + \mu^2} \left\{ F_{23} \left[(1 + \mu^2 s_2) \cos(\beta_2 - \theta_2) + \mu(s_2 - 1) \sin(\beta_2 - \theta_2) \right] + T_3 \left[\sin \gamma_3 + \mu \cos \gamma_3 \right] \right\} \quad (A-138)$$

Now, equations (A-137) and (A-138) are substituted into the moment equation (A-134), with the pivot friction moment given according to the formulation of equation (A-3b):

$$M_{o3} - r_{b3} F_{23} + \mu s_2 (d_2 - s_2 F_{23}) + \mu P_3 \left[F_{23} (A_1 + A_3) + T_3 (A_2 + A_4) \right] = 0 \quad (A-139)$$

where

$$A_1 = \left| \frac{(1 + \mu^2 s_2) \cos(\beta_2 - \theta_2) + \mu(s_2 - 1) \sin(\beta_2 - \theta_2)}{1 + \mu^2} \right| \quad (A-140)$$

$$A_2 = \left| \frac{\sin \gamma_3 + \mu \cos \gamma_3}{1 + \mu^2} \right| \quad (A-141)$$

$$A_3 = \left| \frac{(1 + \mu^2 s_2) \sin(\beta_2 - \theta_2) + \mu(1 - s_2) \cos(\beta_2 - \theta_2)}{1 + \mu^2} \right| \quad (A-142)$$

$$A_4 = \left| \frac{\mu \sin \gamma_3 - \cos \gamma_3}{1 + \mu^2} \right| \quad (A-143)$$

Finally, equation (A-139) is solved for F_{23}

$$F_{23} = \frac{M_{o3}}{D_1} + T_3 \frac{C_1}{D_1} \quad (A-144)$$

where

$$C_1 = \mu p_3 (A_2 + A_4) \quad (A-145)$$

$$D_1 = r_{b3} - \mu \left[a_2 (d_2 - a_2) + p_3 (A_1 + A_3) \right] \quad (A-146)$$

b. EQUILIBRIUM OF GEAR AND PINION SET NO. 2

Figure A-12 shows the free body diagram of gear and pinion set no. 2. The contact point, C_2 , between gear 2 and pinion 3 is again shown before the pitch point, P_2 . With equation (A-126), the normal force between the teeth of this mesh becomes

$$\bar{F}_{32} = -F_{23}\bar{n}_{23} \quad (A-147)$$

The associated friction force is the negative of equation (A-127), i.e.,

$$\bar{F}_{f32} = \mu s_2 F_{23}\bar{n}_{23} \quad (A-148)$$

Similar to equation (A-80), the normal force between gear 1 and pinion 2 is given by

$$\bar{F}_{12} = F_{12}\bar{n}_{12} \quad (A-149)$$

(See equation (A-78) for the definition of unit vector \bar{n}_{12} .)

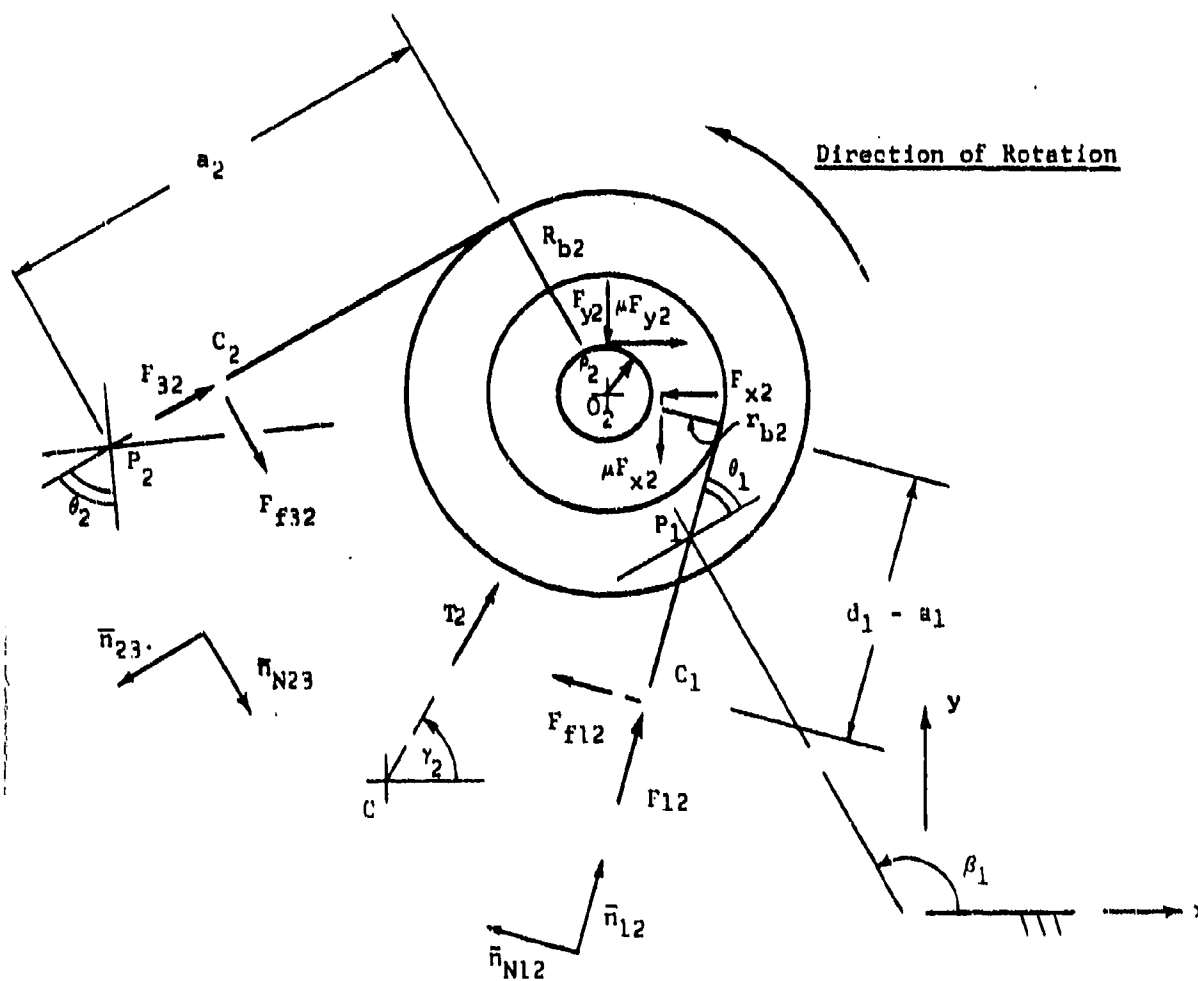


FIGURE A-12 FREE BODY DIAGRAM OF GEAR AND PINION SET NO. 2

Figure A-12 shows the contact point C_1 before the pitch point P_1 is passed.

The associated friction force is given by

$$\vec{F}_{f12} = \mu s_1 F_{12} \vec{H}_{N12} \quad (A-150)$$

where $s_1 = +1$, for contact before pitch point P_1

$s_1 = 0$, for contact at pitch point P_1

$s_1 = -1$, for contact after pitch point P_1

The unit vector \vec{H}_{N12} is given by equation (A-79).

The normal forces on the pivot shaft are given by

$$F_{x2} = -F_{x2} \vec{i} \quad (A-151)$$

and

$$F_{y2} = -F_{y2} \vec{j} \quad (A-152)$$

The associated friction forces $\mu F_{y2} \vec{i}$ and $(-)\mu F_{x2} \vec{j}$ were chosen so that their moments oppose the indicated rotation.

The centrifugal force on this gear and pinion assembly is expressed by

$$\bar{T}_2 = T_2(\cos\gamma_2\bar{i} + \sin\gamma_2\bar{j}) \quad (A-153)$$

$$\text{where } T_2 = \mathcal{Q}_2\omega^2 m_2 \quad (A-154)$$

$$m_2 = \text{mass of gear and pinion set no. 2} \quad (A-155)$$

Force equilibrium is given by

$$\begin{aligned} -F_{23}\bar{n}_{23} + \mu s_2 F_{23}\bar{n}_{N23} + F_{12}\bar{n}_{12} + \mu s_1 F_{12}\bar{n}_{N12} \\ + T_2(\cos\gamma_2\bar{i} + \sin\gamma_2\bar{j}) - F_{x2}\bar{i} + \mu F_{y2}\bar{i} - F_{y2}\bar{j} - \mu F_{x2}\bar{j} \\ = 0 \end{aligned} \quad (A-156)$$

Moment equilibrium is given by

$$\begin{aligned} -R_{b2}F_{23} + \mu s_2 a_2 F_{23} + r_{b2}F_{12} - \mu s_1(d_1 - a_1)F_{12} \\ - \mu p_2(\tilde{F}_{x2} + \tilde{F}_{y2}) = 0 \end{aligned} \quad (A-157)$$

Again, equation (A-3b) is used to obtain a conservative pivot friction moment. p_2 represents the pivot radius. d_1 and a_1 are similar to the previously used distances along the lines of action of the other meshes.

The component form of equation (A-156) becomes

$$F_{23}\sin(\beta_2 - \theta_2) - \mu s_2 F_{23}\cos(\beta_2 - \theta_2) + F_{12}\sin(\beta_1 + \theta_1) + \mu s_1 F_{12}\cos(\beta_1 + \theta_1) + T_2\cos\gamma_2 - F_{x2} + \mu F_{y2} = 0 \quad (A-158)$$

and

$$-F_{23}\cos(\beta_2 - \theta_2) - \mu s_2 F_{23}\sin(\beta_2 - \theta_2) - F_{12}\cos(\beta_1 + \theta_1) + \mu s_1 F_{12}\sin(\beta_1 + \theta_1) + T_2\sin\gamma_2 - F_{y2} - \mu F_{x2} = 0 \quad (A-159)$$

Simultaneous solution of the above expressions for F_{x2} and F_{y2} gives

$$F_{x2} = \frac{1}{1 + \mu^2} \left\{ -F_{12} \left[\mu(1 - s_1)\cos(\beta_1 + \theta_1) - (1 + \mu^2 s_1)\sin(\beta_1 + \theta_1) \right] + T_2 \left[\mu\sin\gamma_2 + \cos\gamma_2 \right] + F_{23} \left[(1 - \mu^2 s_2)\sin(\beta_2 - \theta_2) - \mu(1 + s_2)\cos(\beta_2 - \theta_2) \right] \right\} \quad (A-160)$$

$$F_{y2} = \frac{1}{1 + \mu^2} \left\{ -F_{12} \left[\mu(1 - s_1) \sin(\beta_1 + \theta_1) + (1 + \mu^2 s_1) \cos(\beta_1 + \theta_1) \right] \right. \\
+ T_2 \left[\sin \gamma_2 - \mu \cos \gamma_2 \right] \\
+ F_{23} \left[-\mu(1 + s_2) \sin(\beta_2 - \theta_2) - (1 - \mu^2 s_2) \cos(\beta_2 - \theta_2) \right] \left. \right\}$$

(A-161)

Now equations (A-160) and (A-161) are substituted into the moment equation (A-157) with the pivot friction moment formulated again according to equation (A-3b):

$$-R_{b2}F_{23} + \mu s_2 a_2 F_{23} + r_{b2}F_{12} - \mu s_1 (d_1 - a_1)F_{12} - \mu P_2 \left[F_{12}(A_5 + A_8) + T_2(A_6 + A_9) + F_{23}(A_7 + A_{10}) \right] = 0 \quad (A-162)$$

where

$$A_5 = \left| \frac{\mu(1 - s_1)\sin(\beta_1 + \theta_1) + (1 + \mu^2 s_1)\cos(\beta_1 + \theta_1)}{1 + \mu^2} \right| \quad (A-163)$$

$$A_6 = \left| \frac{s_1 \gamma_2 - \mu \cos \gamma_2}{1 + \mu^2} \right| \quad (A-164)$$

$$A_7 = \left| \frac{\mu(1 + s_2)\sin(\beta_2 - \theta_2) + (1 - \mu^2 s_2)\cos(\beta_2 - \theta_2)}{1 + \mu^2} \right| \quad (A-165)$$

$$A_8 = \left| \frac{\mu(1 - s_1)\cos(\beta_1 + \theta_1) - (1 + \mu^2 s_1)\sin(\beta_1 + \theta_1)}{1 + \mu^2} \right| \quad (A-166)$$

$$A_9 = \left| \frac{\mu s_1 \gamma_2 + \cos \gamma_2}{1 + \mu^2} \right| \quad (A-167)$$

$$A_{10} = \left| \frac{(1 - \mu^2 s_2) \sin(\beta_2 - \theta_2) - \mu(1 + s_2) \cos(\beta_2 - \theta_2)}{1 + \mu^2} \right| \quad (A-168)$$

Finally equation (A-162) is solved for F_{12}

$$F_{12} = \frac{F_2 C_2}{D_2} + \frac{T_2 C_3}{D_2} \quad (A-169)$$

where

$$C_2 = R_{b2} - \mu [s_2 s_2 - r_2 (A_7 + A_{10})] \quad (A-170)$$

$$C_3 = \mu r_2 (A_6 + A_9) \quad (A-171)$$

$$D_2 = r_{b2} - \mu [s_1 (d_1 - u_1) + r_2 (A_5 + A_8)] \quad (A-172)$$

c. EQUILIBRIUM OF GEAR NO. 1

Figure A-13 shows the free body diagram of gear no. 1, the input gear.

The contact point, C_1 , corresponds to that shown in Figure A-12.

According to equation (A-149), the normal contact force between pinion 2 and gear 1 becomes

$$\bar{F}_{21} = -F_{12}\bar{n}_{12} \quad (A-173)$$

The associated friction force is the negative of equation (A-150), i.e.,

$$\bar{F}_{f21} = -\mu_{S1}F_{12}\bar{n}_{N12} \quad (A-174)$$

The normal forces on the pivot shaft are given by

$$\bar{F}_{x1} = -F_{x1}\bar{i} \quad (A-175)$$

and

$$\bar{F}_{y1} = F_{y1}\bar{j} \quad (A-176)$$

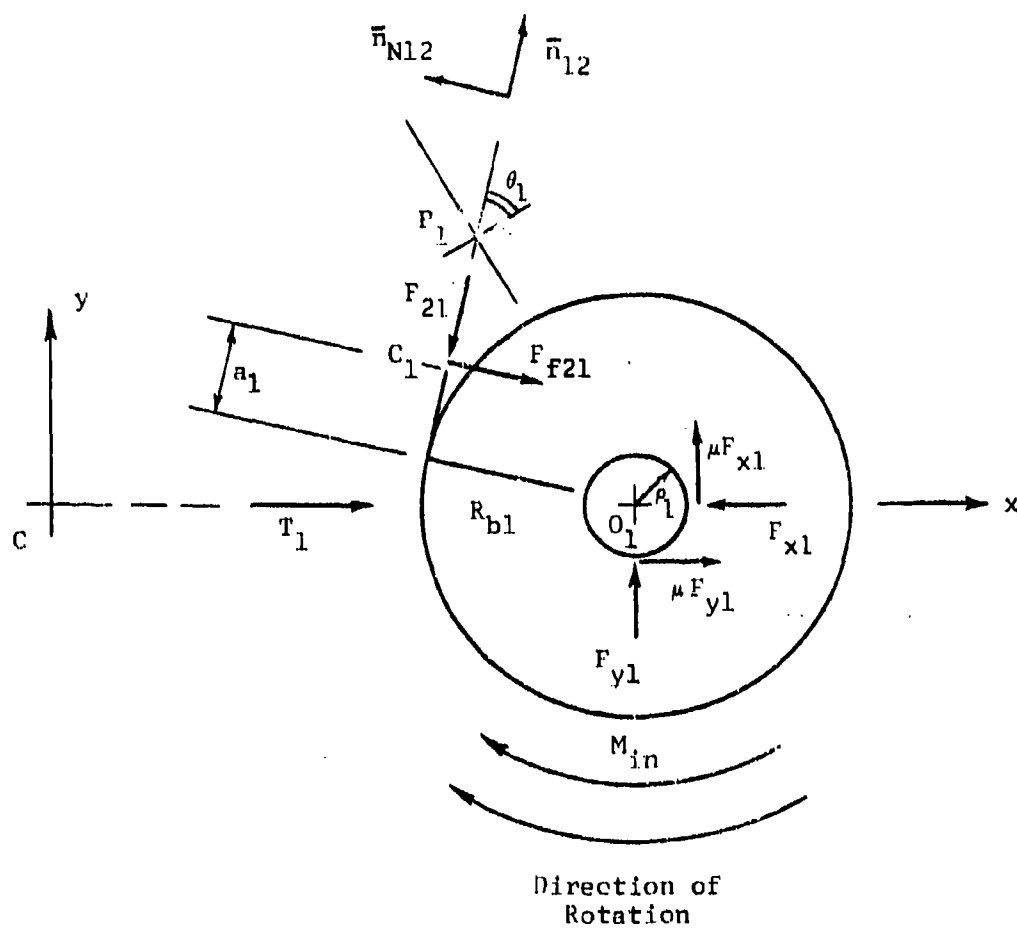


FIGURE A-13. FREE BODY DIAGRAM OF GEAR 1

The associated friction forces $\mu F_{y1}\bar{i}$ and $\mu F_{x1}\bar{j}$ were chosen with such directions that their moments oppose rotation due to input moment M_{in} .

Centrifugal force \bar{T}_1 on gear 1 is given by

$$\bar{T}_1 = T_1\bar{i} \quad (A-177)$$

where, as with equation (A-107)

$$T_1 = R_1 \omega^2 m_1 \quad (A-178)$$

and

$$m_1 = \text{mass of gear 1} \quad (A-179)$$

Force equilibrium of gear 1 is given by

$$\begin{aligned} -F_{12}\bar{n}_{12} - \mu s_1 F_{12}\bar{n}_{N12} + T_1\bar{i} - F_{x1}\bar{i} + F_{y1}\bar{j} + \mu F_{y1}\bar{i} \\ + \mu F_{x1}\bar{j} = 0 \end{aligned} \quad (A-180)$$

Moment equilibrium is given by

$$R_{b1}F_{12} - \mu s_1 a_1 F_{12} - M_{in} + \mu p_1 (\hat{F}_{x1} + \hat{F}_{y1}) = 0 \quad (A-181)$$

Note that equations (A-180) and (A-181) have the same forms as equations (A-109) and (A-110).

The force component expressions are the same as given by equations (A-111) and (A-112), and their simultaneous solution for the pivot forces is identical to that given by equations (A-113) and (A-114), i.e.,

$$F_{x1} = \frac{-F_{12} \left[(1 - \mu^2 s_1) \sin(\beta_1 + \theta_1) + \mu(1 + s_1) \cos(\beta_1 + \theta_1) \right] + T_1}{1 + \mu^2} \quad (\text{A-182})$$

and

$$F_{y1} = \frac{F_{12} \left[\mu(1 + s_1) \sin(\beta_1 + \theta_1) - (1 - \mu^2 s_1) \cos(\beta_1 + \theta_1) \right] - \mu T_1}{1 + \mu^2} \quad (\text{A-183})$$

Equations (A-182) and (A-183) are now substituted into equation (A-181) according to the method of equation (A-3b)

$$\begin{aligned} R_{b1} F_{12} - \mu s_1 s_1 F_{12} - M_{1n} + \mu \rho_1 \left[F_{12} (A_{11} + A_{13}) + T_1 (A_{12} + A_{14}) \right] \\ = 0 \end{aligned} \quad (\text{A-184})$$

where

$$A_{11} = \left| \frac{(1 - \mu^2 s_1) \sin(\beta_1 + \theta_1) + \mu(1 + s_1) \cos(\beta_1 + \theta_1)}{1 + \mu^2} \right| \quad (A-185)$$

$$A_{12} = \left| \frac{1}{1 + \mu^2} \right| \quad (A-186)$$

$$A_{13} = \left| \frac{\mu(1 + s_1) \sin(\beta_1 + \theta_1) - (1 - \mu^2 s_1) \cos(\beta_1 + \theta_1)}{1 + \mu^2} \right| \quad (A-187)$$

$$A_{14} = \left| \frac{\mu}{1 + \mu^2} \right| \quad (A-188)$$

Finally, equation (A-184) is solved for F_{12}

$$F_{12} = \frac{M_{1n}}{D_3} - \frac{T_1 C_4}{D_3} \quad (A-189)$$

where

$$C_4 = \mu \rho_1 (A_{12} + A_{14}) \quad (A-190)$$

$$D_3 = R_{b1} - \mu [s_1 a_1 - \rho_1 (A_{11} + A_{13})] \quad (A-191)$$

d. INPUT-OUTPUT RELATIONSHIP

To obtain the input-output relationship for the complete gear train, equation (A-189) is now set equal to equation (A-169). This furnishes

$$F_{23} = \frac{D_2}{C_2 D_3} [M_{1n} - T_1 C_4] - T_2 \frac{C_3}{C_2} \quad (A-192)$$

The above is then set equal to equation (A-144). This results in the input-output moment relationship

$$M_{o3} = \frac{D_1 D_2}{C_2 D_3} [M_{1n} - T_1 C_4] - T_2 \frac{C_3 D_1}{C_2} - T_3 C_1 \quad (A-193)$$

6. AUXILIARY GEOMETRIC AND KINEMATIC EXPRESSIONS FOR TWO AND THREE STEP-UP GEAR TRAINS WITH INVOLUTE TEETH

a. NOMENCLATURE FOR INVOLUTE GEAR TEETH

R_{pi}, r_{pi} = pitch radii of gear and pinion of i^{th} gear and pinion set

R_{bi}, r_{bi} = base radii of gear and pinion of i^{th} gear and pinion set

R_{oi}, r_{oi} = outside radii of gear and pinion of i^{th} gear and pinion set

θ_j = effective pressure angle of j^{th} mesh

R_i = distance from spin axis to pivot of i^{th} gear and pinion set

b. ANGULAR RELATIONSHIPS BETWEEN PIVOT HOLES

Figure A-14 shows the angular relationships between the lines connecting the pivot holes as well as the spin center. (See also Figures A-5 and A-10.) The following serves to determine the angles γ_1 and β_1 for certain combinations of gears and pinions as well as spin radii R_1 .

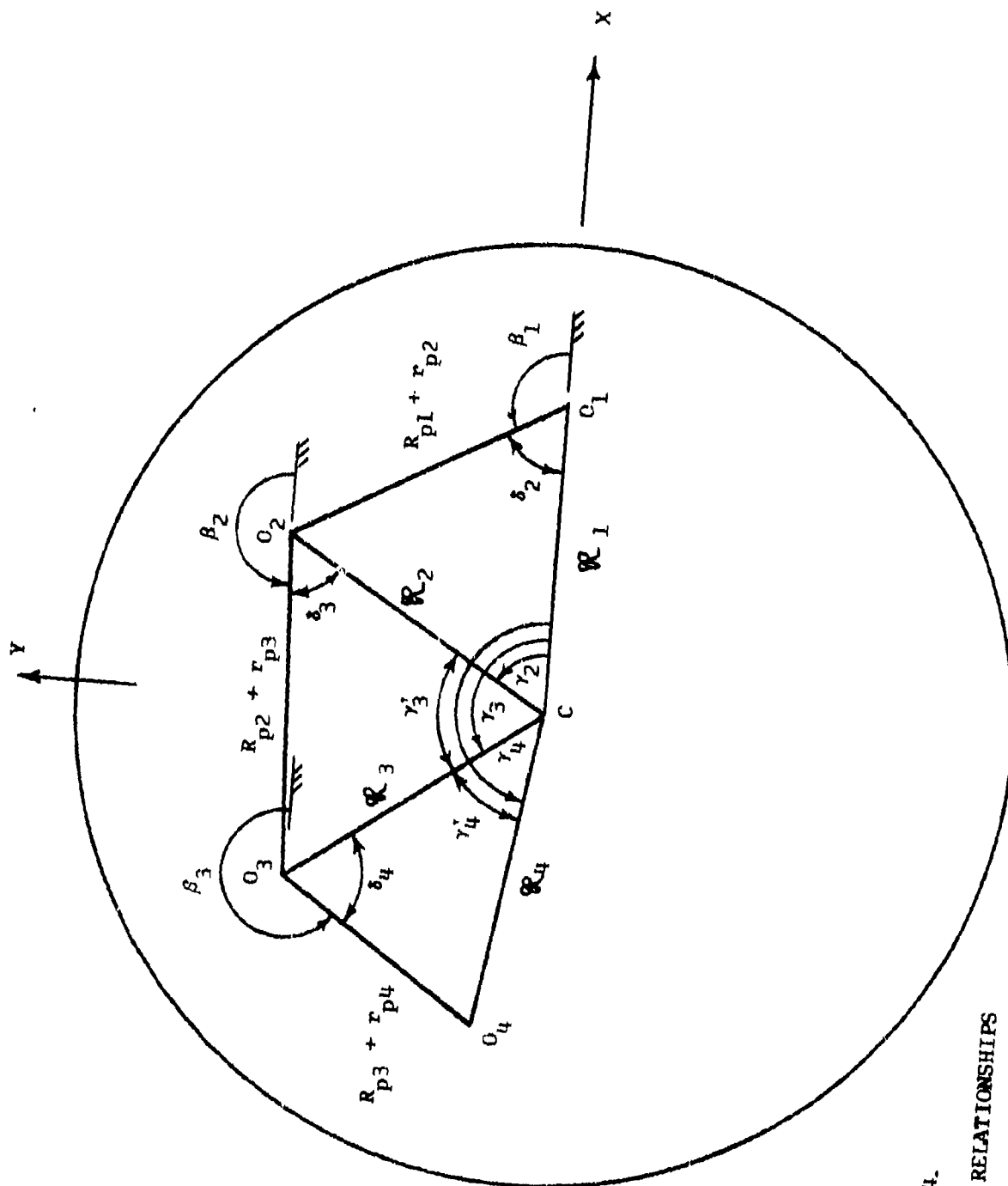


FIGURE A-14.
PIVOT HOLE RELATIONSHIPS

ANGLE γ_1

From

$$(R_{p1} + r_{p2})^2 = R_1^2 + R_2^2 - 2R_1R_2\cos\gamma_2$$

one obtains

$$\gamma_2 = \cos^{-1} \left[\frac{R_1^2 + R_2^2 - (R_{p1} + r_{p2})^2}{2R_1R_2} \right] \quad (\text{A-194})$$

Similarly, from

$$\gamma_3' = \cos^{-1} \left[\frac{R_2^2 + R_3^2 - (R_{p2} + r_{p3})^2}{2R_2R_3} \right]$$

one obtains

$$\gamma_3 = \gamma_2 + \gamma_3' \quad (\text{A-195})$$

Also with

$$\gamma_4' = \cos^{-1} \left[\frac{R_3^2 + R_4^2 - (R_{p3} + r_{p4})^2}{2R_3R_4} \right]$$

one obtains

$$\gamma_4 = \gamma_3 + \gamma_4' \quad (A-196)$$

ANGLES δ_1

Since

$$R_2^2 = (R_{p1} + r_{p2})^2 + R_1^2 - 2(R_{p1} + r_{p2})R_1 \cos \delta_2$$

$$\delta_2 = \cos^{-1} \left[\frac{(R_{p1} + r_{p2})^2 + R_1^2 - R_2^2}{2R_1(R_{p1} + r_{p2})} \right] \quad (A-197)$$

Similarly,

$$\delta_3 = \cos^{-1} \left[\frac{(R_{p2} + r_{p3})^2 + R_2^2 - R_3^2}{2R_2(R_{p2} + r_{p3})} \right] \quad (A-198)$$

and

$$\delta_4 = \cos^{-1} \left[\frac{(R_{p3} + r_{p4})^2 + R_3^2 - R_4^2}{2R_3(R_{p3} + r_{p4})} \right] \quad (A-199)$$

ANGLES β_1

With Equation (A-197)

$$\beta_1 = \pi - \delta_2 \quad (A-200)$$

Further, with Equations (A-194) and (A-198)

$$\beta_2 = \gamma_2 + (\pi - \delta_3) \quad (A-201)$$

Finally, with Equations (A-195) and (A-199)

$$\beta_3 = \gamma_3 + (\pi - \delta_4) \quad (A-202)$$

c. DETERMINATION OF CONTACT POINT C FOR VARIOUS MESHES

Figure A-15 shows the points of interest along the line of action of an involute gear which drives an involute pinion.

Points L and L' are the points of tangency to the base circles of radius R_b and r_b , respectively, and the distance $d = LL'$. Initial contact is made at point M, where the line of action intersects the pinion addendum circle of radius r_o . Final contact corresponds to point N. Here the line of action intersects the gear addendum circle of radius R_o .

The position of the instantaneous contact point C with respect to point L, i.e., the length, a , is expressed with the help of instantaneous angle α which has its origin at the line O_1L . Then,

$$a = LC = R_b \alpha$$

(A-203)

A computer procedure for the determination of instantaneous angle α of any mesh must first find the associated initial and final angles of contact α_{in} and α_{fin} . In addition, it must contain a method for incrementing angle α . The following shows such a procedure for each of the meshes of a two pass and a three pass step-up gear train, together with a means of obtaining the signs of the signum terms.

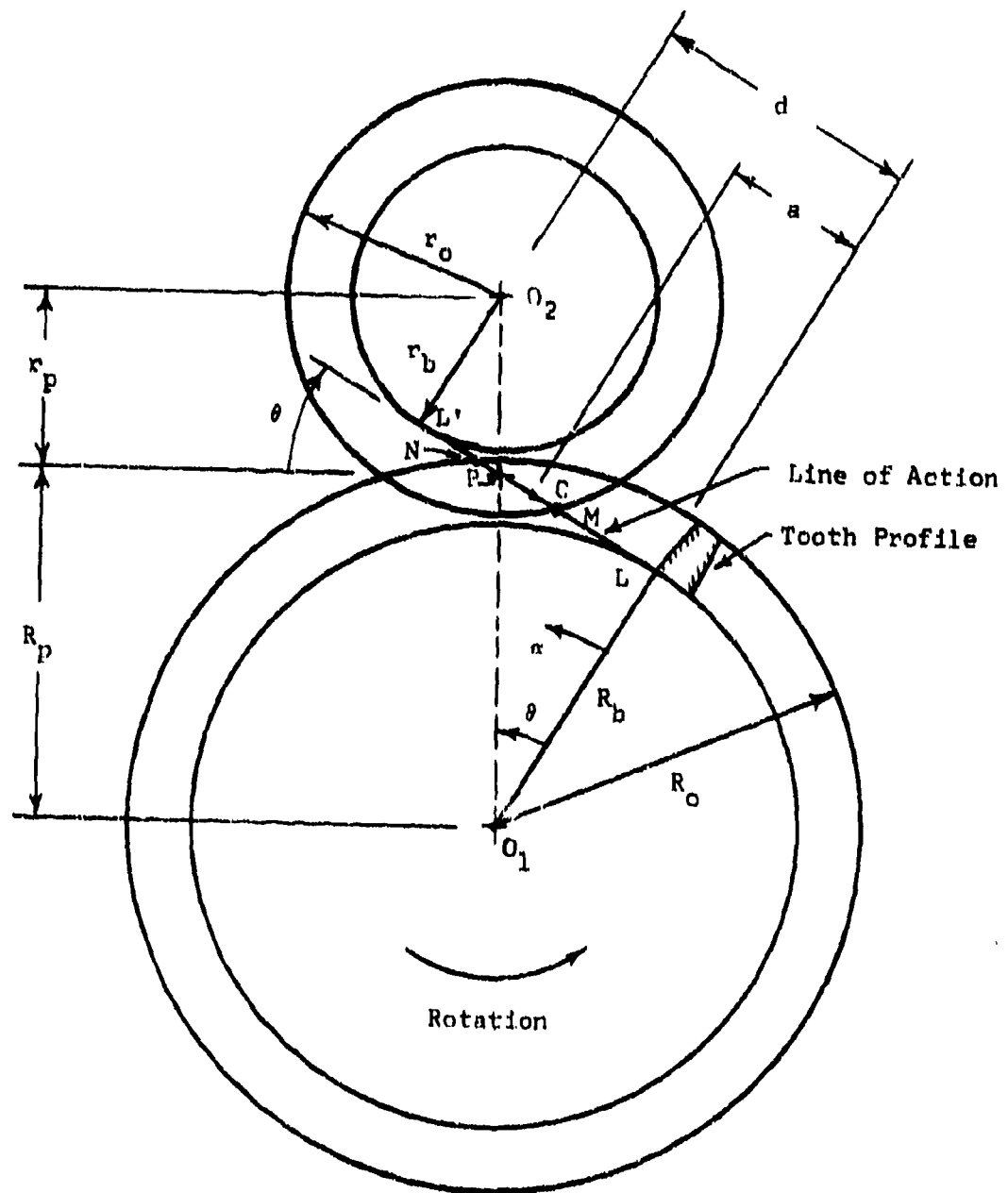


FIGURE A-15.
INVOLUTE MESH GEOMETRY

1.) MESH OF GEAR 1 AND PINION 2

The total length, $d_1 = LL'$, is given by

$$d_1 = (R_{b1} + r_{b1}) \tan \theta_1 \quad (A-204)$$

The initial angle of contact, α_{1IN} , is obtained from

$$\alpha_{1in} = \frac{ML}{R_{b1}} = \frac{(R_{b1} + r_{b2}) \tan \theta_1 - \sqrt{r_{o2}^2 - r_{b2}^2}}{R_{b1}} \quad (A-205)$$

Similarly, the final angle of contact, α_{1FIN} , is given by

$$\alpha_{1fin} = \frac{\sqrt{R_{o1}^2 - R_{b1}^2}}{R_{b1}} \quad (A-206)$$

The magnitude of the increment $\Delta\alpha_1$ depends on whether one deals with a two step-up or a three step-up gear train.

Assuming that a two step-up train is involved and that one wishes to compute the length a_2 of mesh 2 K_2 times after the first contact, the angular increment, $\Delta\alpha_{22}$, has the magnitude

$$\Delta \alpha_{22} = \frac{\alpha_{2fin} - \alpha_{2in}}{K_2} \quad (A-207)$$

(The second subscript refers to a two step-up configuration.)

Because of the transmission ratio between gear sets 1 and 2, the associated angular increment of gear 1 will be smaller than $\Delta \alpha_{22}$, i.e.,

$$\Delta \alpha_{12} = \Delta \alpha_{22} \frac{r_{b2}}{R_{b1}} \quad (A-208)$$

The instantaneous angle, α_1 , will then be given by

$$\alpha_1 = \alpha_{1in} + j_{12} \Delta \alpha_{12} \quad (A-209)$$

and, the instantaneous distance, a_1 , becomes

$$a_1 = R_{b1} (\alpha_{1in} + j_{12} \Delta \alpha_{12}) \quad (A-210)$$

In the above, j_{12} represents the number of times the angle α_1 has been incremented. While the total number of increments depends on the length of contact, the incrementing of α_1 comes to an end when $\alpha_1 \geq \alpha_{1fin}$. This also corresponds to a complete mechanism

cycle. Since mesh 2 goes through R_{b1}/r_{b2} times as many cycles as mesh no. 1, the angle α_2 has to be re-initialized to α_{2in} when $\alpha_1 \geq \alpha_{2fin}$, i.e., after K_2 increments. (For simplicity it is assumed that the motion starts when all meshes are at their initial contact angles, α_{in} .)

When a three step-up gear train is involved, one must make sure that enough computations are made for mesh 3. Assuming that K_3 increments are to be made, one obtains

$$\Delta \alpha_{33} = \frac{\alpha_{3fin} - \alpha_{3in}}{K_3} \quad (A-211)$$

The associated angular increments for meshes 2 and 1 then become

$$\Delta \alpha_{23} = \Delta \alpha_{33} \frac{r_{b3}}{R_{b2}} \quad (A-212)$$

and

$$\Delta \alpha_{13} = \Delta \alpha_{33} \frac{r_{b3}}{R_{b2}} \times \frac{r_{b2}}{R_{b1}} \quad (A-213)$$

For this case the instantaneous distance a_1 becomes

$$a_1 = R_{b1} (\alpha_{1in} + j_{13} \Delta \alpha_{13}) \quad (A-214)$$

j_{13} stands for the number of times α_1 has been incremented at any given instant. This incrementing again ends when $\alpha_1 \geq \alpha_{1fin}$. Meshes 2 and 3 are re-initialized to α_{2in} and α_{3in} as often as is necessary to complete one cycle for mesh no. 1.

The sign of s_1 is best obtained from the fact that at pitch point P_1

$$\alpha_{1p} = \frac{LP}{R_{b1}} = \frac{R_{b1} \tan \theta_1}{R_{b1}} = \tan \theta_1 \quad (A-215)$$

then for

$$\begin{aligned} \alpha_1 < \tan \theta_1 : s_1 &= +1 \\ \alpha_1 &= \tan \theta_1 : s_1 &= 0 \\ \alpha_1 > \tan \theta_1 : s_1 &= -1 \end{aligned} \quad (A-216)$$

2.) MESH OF GEAR 2 AND PINION 3

Similar to the previous section.

$$d_2 = (R_{b2} + r_{b3}) \tan \theta_2 \quad (A-217)$$

$$\alpha_{2in} = \frac{(R_{b2} + r_{b3}) \tan \theta_2 - \sqrt{r_{o3}^2 - r_{b3}^2}}{R_{b2}} \quad (A-218)$$

$$\alpha_{2fin} = \frac{\sqrt{R_{o2}^2 - R_{b2}^2}}{R_{b2}} \quad (A-219)$$

For a two step-up gear train, the instantaneous length, a_2 , becomes

$$a_2 = R_{b2}(\alpha_{2in} + j_{22} \Delta \alpha_{22}) \quad (A-220)$$

where $\Delta \alpha_{22}$ is given by Equation (A-207) and

$$j_{22} = 1, 2, \dots, K_2.$$

When $\alpha_2 \geq \alpha_{2fin}$ it must be re-initialized to α_{2in} until mesh no. 1 has completed its full cycle.

For a three step-up gear train, the length, a_2 , becomes

$$a_2 = R_{b2}(\alpha_{21n} + j_{23}\Delta\alpha_{23}) \quad (A-221)$$

with $\Delta\alpha_{23}$ given by Equation (A-212). j_{23} stands for the number of times α_2 has been incremented and again depends on the length of contact. Re-initialization follows the same rule as given above.

The sign of s_2 is obtained as follows: (See Equation (A-215).)

For

$$\begin{aligned} \alpha_2 < \tan\theta_2 : s_2 &= +1 \\ \alpha_2 = \tan\theta_2 : s_2 &= 0 \\ \alpha_2 > \tan\theta_2 : s_2 &= -1 \end{aligned} \quad (A-222)$$

3.) MESH OF GEAR 3 AND PINION 4

Again, in the same vein as in Section 1,

$$d_3 = (R_{b3} + r_{b4}) \tan \theta_3 \quad (A-223)$$

$$a_{3in} = \frac{(R_{b3} + r_{b4}) \tan \theta_3 - \sqrt{r_{o4}^2 - r_{b4}^2}}{R_{b3}} \quad (A-224)$$

$$a_{3fin} = \frac{\sqrt{R_{o3}^2 - R_{b3}^2}}{R_{b3}} \quad (A-225)$$

The instantaneous length, a_3 , is given by

$$a_3 = R_{b3}(a_{3in} + j_{33} \Delta a_{33}) \quad (A-226)$$

where Δa_{33} is given by Equation (A-211) and $j_{33} = 1, 2, \dots, K_3$.

Whenever $a_3 \geq a_{3fin}$ it must be re-initialized until mesh no. 1

completed its full cycle.

The sign of s_3 is again obtained with the help of an expression

Equation (A-215):

$$a_3 < \tan \theta_3 : s_3 = +1$$

$$a_3 = \tan \theta_3 : s_3 = 0$$

$$a_3 > \tan \theta_3 : s_3 = -1$$

(A-227)

APPENDIX B

DESIGN OF UNEQUAL ADDENDUM INVOLUTE GEAR SETS WITH STANDARD CENTER DISTANCES

One of the ways of preventing undercutting in pinions with small numbers of teeth, which must mesh with gears of unequal and larger numbers of teeth, is to decrease the pinion dedendum together with the gear addendum by the necessary amount. To maintain standard working depth for such a mesh, the addendum of the pinion as well as the dedendum of the gear are increased by the same amount. (This, of course, presupposes that the gear is not undercut by this modification.) This can be accomplished without any change in the standard base and pitch radii or the associated standard center distance by "withdrawing" the hob during the cutting of the pinion and feeding it "deeper" when the gear is cut. In this way the pinion, which has its outside radius increased by the hob withdrawal distance, will have a larger than standard circular tooth thickness at its standard pitch circle. The outside radius of the gear is decreased by the same amount. Because the cutter is fed to full depth, the gear tooth thickness at the standard pitch circle will be less than standard.

The following gives the design steps for this type of gearing and illustrates them by way of an example.

1. STANDARD GEAR NOMENCLATURE

N = number of teeth of gear

n = number of teeth of pinion

θ = pressure angle

$P_d = \frac{N}{2R_p} = \frac{n}{2r_p}$ = diametral pitch

P_{cs} = standard circular pitch at pitch circle, where also

$$P_{cs} = \frac{\pi}{P_d}$$

R_p, r_p = pitch radii of gear and pinion, respectively

R_b = $R_p \cos \theta$, base circle radius of gear

r_b = $r_p \cos \theta$, base circle radius of pinion

$T_{cs}, t_{cs} = \frac{P_{cs}}{2}$, circular tooth thickness of gear and pinion,
respectively, at standard pitch circles

$\frac{1}{P_d}$ = standard gear addendum

$\frac{1.157}{P_d}$ = standard gear dedendum

2. DETERMINATION OF HOB WITHDRAWAL DISTANCE C

Figure B-1 indicates the relationship between the pinion pitch radius, r_p , its root radius, r_r , and the rack cutter addendum A . The root radius is formed by the addendum line of the cutter tooth, so that

$$r_r = r_p - A \quad (B-1)$$

In order to avoid undercutting, the addendum line of a sharp cornered cutter must not pass below point L, the tangent point of the line of action and the base circle (see Figure B-2).

The minimum root radius, r_{rm} , becomes for this case

$$r_{rm} = r_b \cos \theta = r_p \cos^2 \theta \quad (B-2)$$

When the rack tooth corner is rounded off with a radius r_c , as shown in Figure B-3, the effective addendum line of the cutter tooth moves up the distance $r_c(1 - \sin \theta)$. To avoid undercutting with this type of cutter, the effective addendum line must not pass the base circle below point L in Figure B-2. This allows a reduction of the minimum allowable root radius to

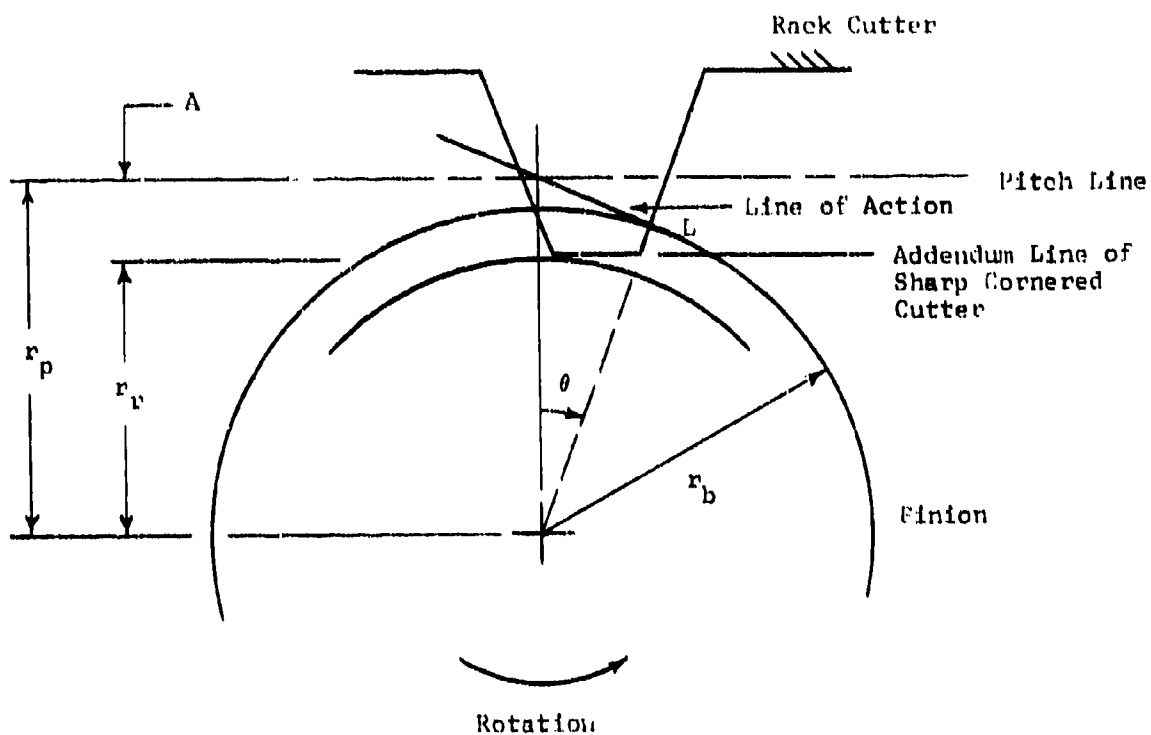


FIGURE B-1

RELATIONSHIP BETWEEN PINION PITCH RADIUS, r_p , RACK CUTTER ADDENDUM A AND RESULTING PINION ROOT RADIUS, r_r

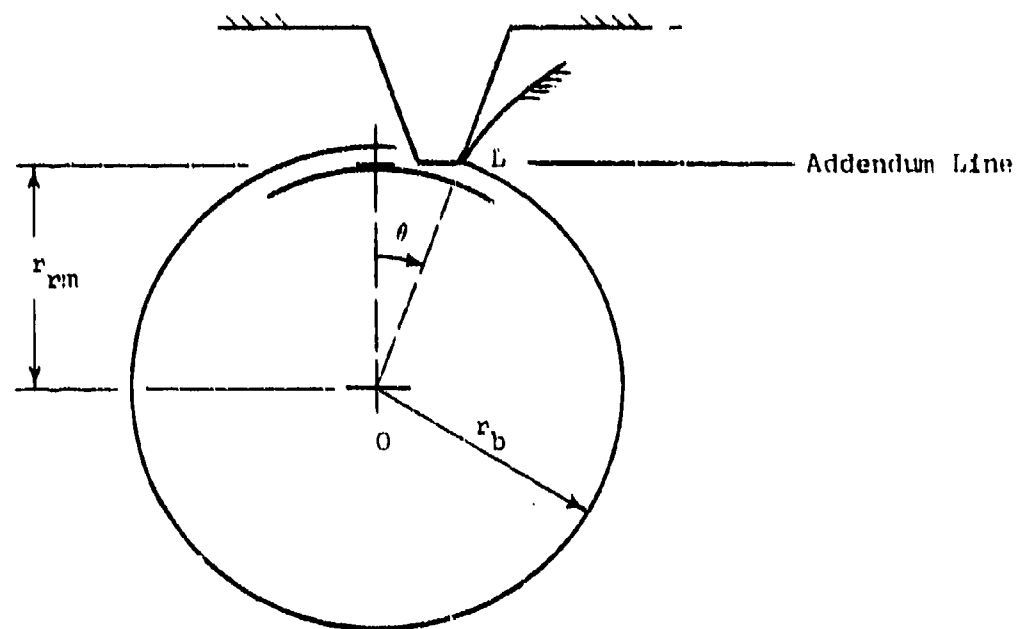


FIGURE B-2

MINIMUM ROOT RADIUS, r_{min} , FOR RACK CUTTER WITH SHARP CORNER

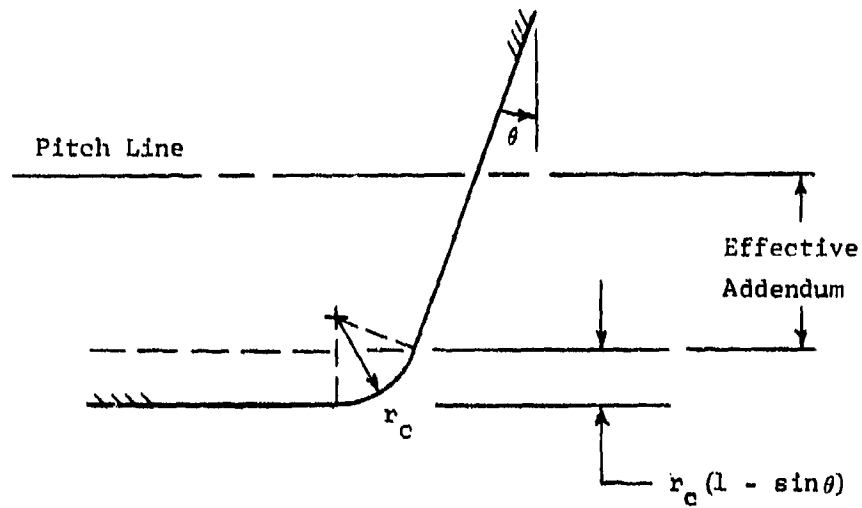


FIGURE B-3

RACK CUTTER WITH CORNER RADIUS, r_c (EFFECTIVE ADDENDUM OF CUTTER IS DECREASED)

$$r_{rmc} = r_p \cos^2 \theta - r_c (1 - \sin \theta) \quad (B-3)$$

By common usage the corner radius may either be

$$r_c = .1 t_s = \frac{.05 \pi}{P_d}, \quad (B-4)$$

or it is chosen such that the second term in Equation (B-3) becomes

$$r_c (1 - \sin \theta) \approx \frac{.157}{P_d} \quad (B-5)$$

(This makes for an effective cutter addendum of $1/P_d$.)

Hob withdrawal becomes necessary if the root radius, obtained by setting the cutter to standard depth, is smaller than the minimum given by Equation (B-3). Thus, the hob withdrawal C is obtained from Equations (B-1) and (B-3), i.e.,

$$C = r_{rmc} - r_r \quad (B-6)$$

With the cutter addendum $A = 1.157/P_d$, and using the expression of Equation (B-4) for the rack corner radius, Equation (B-6) becomes

$$C = \frac{1}{P_d} (1 + .157 \sin \theta) - r_p \sin^2 \theta \quad (B-7)$$

If Equation (B-5) is used, with the same definition of the cutter addendum, one obtains for C

$$C = \frac{1}{P_d} - r_p \sin^2 \theta \quad (B-7)$$

3. OUTSIDE RADII OF PINION AND GEAR BLANKS

The outside radius of the pinion blank becomes

$$r_o = r_p + \frac{1}{P_d} + C \quad (B-8)$$

The outside radius of the gear blank becomes

$$R_o = R_p + \frac{1}{P_d} - C \quad (B-9)$$

4. TOOTH THICKNESS AT PITCH CIRCLES OF PINION AND GEAR

Since the thickness of the hobtooth at the pinion pitch circle will be reduced by the amount $2C\tan\theta$, due to the withdrawal C , the circular thickness of the pinion tooth at this location will be increased by this amount, i.e.,

$$t_c = t_{cs} + 2C\tan\theta \quad (B-10)$$

The gear tooth thickness will be decreased to

$$T_c = T_{cs} - 2C\tan\theta \quad (B-11)$$

at its pitch circle.

5. TOOTH THICKNESS AT OUTSIDE AND BASE RADII BY INVOLUTOMETRY

The circular tooth thickness at an arbitrary radius of an involute tooth may be obtained if the tooth thickness, radius, and pressure angle of any other location, such as the pitch circle, are known together with the pressure angle at the arbitrary radius. [See Equation (5-5), pg. 80, E. Buckingham: Analytical Mechanics of Gears, McGraw-Hill Book Co., Inc. New York, 1949.]

Accordingly, the circular tooth thickness, t_o , at the outside radius of the pinion, may be obtained from

$$t_o = t_c \frac{r_o}{r_p} - 2r_o(\text{INV}\theta_{OP} - \text{INV}\theta) \quad (\text{B-12})$$

where

$\text{INV}\theta = \tan\theta - \theta$, the involute function corresponding to the pressure angle θ

θ = pressure angle of mesh. This is also the pressure angle at the pitch circle.

$\theta_{OP} = \cos^{-1} \frac{r_b}{r_o}$, the pressure angle associated with the outside radius of the pinion

Similarly, the circular tooth thickness, T_o , at the outside radius of the gear is obtained from:

$$T_o = T_c \frac{R_o}{R_p} - 2R_o(\text{INV}\theta_{OG} - \text{INV}\theta) \quad (\text{B-13})$$

where

$$\theta_{OG} = \cos^{-1} \frac{R_b}{R_o}, \text{ the pressure angle associated with the outside radius of the gear}$$

The tooth thickness at the base circle radius of the modified pinion is given by

$$t_b = t_c \cos \theta + 2r_p \text{INV} \theta \quad (\text{B-14})$$

This becomes for the gear

$$T_b = T_c \cos \theta + 2R_g \text{INV} \theta \quad (\text{B-15})$$

(The above is only of theoretical interest in case the inter-tooth space is not cut below the base circle radius.)

6. EXPRESSIONS FOR CONTACT RATIO AND PINION OUTSIDE RADIUS FOR

UNITY CONTACT RATIO

The expression for contact ratio [Equation 4-19, pg. 72, E. Buckingham: Analytical Mechanics of Gears] is given by

$$m_p = \frac{\sqrt{R_o^2 - R_b^2} + \sqrt{r_o^2 - r_b^2} - (R_b + r_b)\tan\theta}{p_{cs}\cos\theta} \quad (B-16)$$

If the contact ratio of a certain mesh is larger than unity, and one wishes to reduce it to unity by reducing the outside radius of the pinion, one may find this new pinion outside radius with the help of

$$r_o' = \sqrt{r_b^2 + \left[p_{cs}\cos\theta + (R_b + r_b)\tan\theta - \sqrt{R_o^2 - R_b^2} \right]^2} \quad (B-17)$$

7. EXAMPLE

Design a pinion and a gear with the following specifications:

$$P_d = 44, \quad N = 42, \quad n = 8, \quad \theta = 20^\circ$$

This gives

$$R_p = .47727 \text{ in. (1.212 cm)} \quad r_p = .09091 \text{ in. (.231 cm)}$$

$$R_b = R_p \cos 20^\circ = .44848 \text{ in. (1.139 cm)} \quad r_b = .08542 \text{ in. (.217 cm)}$$

$$P_{cs} = \frac{\pi}{44} = .07140 \text{ in. (.181 cm)} \quad T_{cs} = t_{cs} = .03570 \text{ in. (.091 cm)}$$

According to Equation (B-7), the hob withdrawal C is computed as

$$C = \frac{1}{44} - .09091 \sin^2 20^\circ = .012093 \text{ in. (.031 cm)}$$

Then, according to Equations (B-8) and (B-9)

$$r_o = .09091 + .022727 + .012093 = .12573 \text{ in. (.319 cm)}$$

$$R_o = .47727 + .022727 - .012093 = .48790 \text{ in. (1.239 cm)}$$

The new tooth thickness at the pitch radii is found with the help of Equations (B-10) and (B-11)

$$t_c = .03570 + 2(.012093)\tan 20^\circ = .04450 \text{ in. } (.113 \text{ cm})$$

$$T_c = .03570 - 2(.012093)\tan 20^\circ = .02689 \text{ in. } (.068 \text{ cm})$$

For the purposes of the present analysis, the pinion outside radius is now reduced to obtain a contact ratio of unity. With Equation (B-17)

$$r_o' = .110 \text{ in. } (.279 \text{ cm}) \text{ This is essentially the unmodified pinion radius of } .113 \text{ in. } (.287 \text{ cm}).$$

Now compute the circular tooth thickness at the outside radii r_o' and R_o using the following data in Equations (B-12) and (B-13):

$$\phi = 20^\circ \qquad \text{INV } 20^\circ = .01490$$

$$\theta_{OP} = \cos^{-1} \frac{.08542}{.110} = 39.0509^\circ \qquad \text{INV } 39.0509^\circ = .12969$$

$$\theta_{OG} = \cos^{-1} \frac{.44848}{.48790} = 23.1889^\circ \qquad \text{INV } 23.1889^\circ = .02365$$

Then

$$t_o = .04450 \left(\frac{.110}{.09091} \right) - 2(.110)(.12969 - .0149) = .02860 \text{ in. (.073 cm)}$$

and

$$T_o = .02689 \left(\frac{.4879}{.47727} \right) - 2(.4879)(.02365 - .0149) = .01896 \text{ in. (.048 cm)}$$

These are sufficient to allow for rounding off the teeth.

Finally, check that the gear is not undercut. The actual root radius of the gear is

$$R_o = \frac{2.157}{P_d} = .4879 - .04902 = .4389 \text{ in. (1.115 cm)}$$

The minimum permissible root radius without undercutting, according to Equations (B-3) and (B-4), is computed from

$$\begin{aligned} R_{rm} &= R_p \cos^2 \theta - \frac{.05\pi}{P_d} (1 - \sin \theta) = .47727(.883) - .0023 \\ &= .419 \text{ in. (1.064 cm)} \end{aligned}$$

Thus, the gear is not undercut.

APPENDIX C

COMPUTER MODELS FOR STEP-UP GEAR TRAINS WITH INVOLUTE TEETH

The present appendix contains descriptions, listings, and sample outputs of the following involute gear-train-related computer programs:

1. Program INVOL 1 : Design of unequal addendum involute gear and pinion set with unity contact ratio.
2. Program INVOL 2 : Point and cycle efficiencies for single pass involute step-up gear mesh with unity contact ratio.
3. Program INVOL 3 : Point and cycle efficiencies for three pass involute step-up gear train in spin environment. (All meshes have unity contact ratio).
4. Program INVOL 4 : Point and cycle efficiencies for two pass involute step-up gear train in spin environment. (All meshes have unity contact ratio).

The relevant background, the input parameters, the manner of the computations and the form of the output of each program are discussed in detail. The program proper forms the last part of each section.

1. Program INVOL 1: Design of Unequal Addendum Involute Gear
and Pinion Set with Unity Contact Ratio.

The program INVOL 1 is based on Appendix B which shows the design equations for unequal addendum involute gear sets with standard center distances.

The nomenclature of the program is chosen to coincide as much as possible with that of Appendix B.

a. Input Parameters (See also Program INVOL 1, below)

The following parameters represent the input data of the program:

PSUBD	-	P_d	, the diametral pitch
NG	-	N_G	, the number of teeth of the gear
NP	-	N_P	, the number of teeth of the pinion
THETAD	-	θ	, the pressure angle of the mesh as well as of the hob (in degrees)
ISTOP	-		arbitrary single-digit integer for multiple data sets. Must be zero for last set of data.

b. Computations

The program computes the following quantities (where not otherwise indicated, consult Section 1 of Appendix B for nomenclature):

CAPRP	-	R_p
RP	-	r_p
CAPRB	-	R_b
RB	-	r_b

PSUBC	-	p_c
TSTAND	-	t_{cs}
C	-	hob withdrawal distance. See eq (B-7)
RO	-	r_o , See eq (B-8). This is the original pinion blank radius.
CAPRO	-	R_o , see eq (B-9)
TC	-	t_o , see eq (B-10)
CAPTC	-	T_o , see eq (B-11)
TB	-	t_b , see eq (B-14). Note also the computation of the involute function at the end of the program.
CAPTB	-	T_b , see eq (B-15)
ROFIN	-	r'_o , see eq (B-17). This is the pinion outside radius for unity contact ratio.
THETOG	-	θ_{OG} , according to expression associated with eq (B-13)
THETOP	-	θ_{OP} , according to expression associated with eq (B-12)
CAPTO	-	T_o , see eq (B-13)
TO	-	t_o , see eq (B-12). Computed with ROFIN.
CRATIO	-	m_p , see eq (B-16). This is the original contact ratio ,which uses the unmodified pinion blank radius RO.
CRFIN	-	represents the contact ratio when computed with the final pinion blank radius ROFIN.
ROOT	-	actual root radius of pinion
CAPROOT	-	actual root radius of gear
CAPRMIN	-	R_{rm} , see equations (B-3) and (B-4)

c. Output of Program

The output of the program is best explained by means of the first sample computations which are shown at the end of the program. This example is identical with that given in section 7 of Appendix B. The output lists the following:

I. The input parameters, PSUBD, NG, NP, and pressure angle, THETAD, are printed out.

II. The above is followed by computational results for

CAPRP

RP

CAPRB

TSTAND

C

CAPRO

RO, this is the original pinion blank radius before the unity contact ratio modification.

CRATIO, note that for the given case, this original contact ratio equals 1.3

ROFIN, the pinion outside radius which corresponds to unity contact ratio

CRFIN, this, of course, has to be unity because of the use of ROFIN. This computation serves as a check.

CAPTC, this tooth thickness, as well as the following one, is useful for strength computations

TC

THEOGD, this pressure angle, as well as the following one, corresponds to the final outside radii of the gear and pinion, respectively, and is needed for the computations of the tooth thicknesses at the outside radii

THEOPD

CAPTO, this tooth thickness at the outside radius of the gear, as well as the following one for the pinion, must be sufficiently large to allow for the presence of a tip radius

TO

CAPTB

TB

CAPROOT

ROOT

CAPRMIN

The values of the last five parameters are to some extent interconnected. First, it is important to see whether the gear is undercut. This does not occur as long as CAPROOT is larger than CAPRMIN, i.e., the actual root radius is larger than the minimum allowable one. The gear tooth thickness at the base circle is of interest for strength purposes. Since, for the given case, CAPRB = .44849 in. (1.139 cm) and CAPROOT = .4388 in. (1.115 cm) the base circle lies above the root circle, and the greatest cross-section of the tooth is approximately equal to CAPTB. TB is called the theoretical

pinion tooth thickness at the base circle since it is possible that the base circle lies below the minimum allowable root circle of the pinion. In such a case, the actual tooth may be weaker than indicated by this dimension. For the present case, $RB = .08543$ in. (.217 cm) and $ROOT = .07671$ in. (.195 cm), and therefore, the base circle, which lies above the root circle, gives a good indication of the actual tooth cross-section at the root.

Program INVOL 1

This program contains five different sets of gears. This will be of use in programs INVOL 2, INVOL 3 and INVOL 4.

FUNCTION INV 74/74 - OPT=1 PAGE 1

09/05/78 14.23.16

FTN 4.6-420

REAL FUNCTION INV(META)
INV = JAN(META) - JAN(META)
RETURN
END

```

55 / FORMAT(0H08 WITHDRAWAL DISTANCE (C) =F8.5)
    WRITE(6,8)CAPROD,H0
    8 FORMAT(0GEAR BLANK RADIUS (CAPRO) =F9.5,3X,0ORIGINAL PINION 0LA
    INK RADIUS (RO) =F9.5)
    WRITE(6,9)CRATIO
    9 FORMAT(0ORIGINAL CONTACT RATIO (CRATIO) =F6.3)
    60 WRITE(6,10)ROFIN
    10 FORMAT(0PINION OUTSIDE RADIUS FOR UNITY CONTACT RATIO (ROFIN) =F
    IF(9.5)
    WRITE(6,11)CRFIN
    11 FORMAT(0FINAL CONTACT RATIO (CRFIN) =F6.3)
    65 WRITE(6,12)CAPTC,TC
    12 FORMAT(0GEAR TOOTH THICKNESS AT PITCH CIRCLE (CAPTC) =F9.5,3X,
    1PINION TOOTH THICKNESS AT PITCH CIRCLE (TC) =F8.5)
    WRITE(6,13)THEOD,THEOD
    13 FORMAT(0GEAR PRESSURE ANGLE AT OUTSIDE RADIUS (THEOD) =F9.5,
    13X,0PINION PRESSURE ANGLE AT FINAL OUTSIDE RADIUS (THEOD) =F
    IF(9.5)
    WRITE(6,14)CAPTO,T0
    14 FORMAT(0GEAR TOOTH THICKNESS AT OUTSIDE RADIUS (CAPTO) =F8.5,
    13X,0PINION TOOTH THICKNESS AT FINAL OUTSIDE RADIUS (T0) =F8.5)
    WRITE(6,15)CAPTB,B
    15 FORMAT(0GEAR TOOTH THICKNESS AT BASE CIRCLE (CAPTB) =F8.5,3X,
    1THEORETICAL PINION TOOTH THICKNESS AT BASE CIRCLE (TB) =F8.5)
    WRITE(6,16)CAPROOT,CAPRMIN
    16 FORMAT(0RADIUS OF ROOT CIRCLE OF GEAR (CAPROOT) =F8.5,3X,
    1MINIMUM ALLOWABLE RADIUS OF ROOT CIRCLE OF GEAR (CAPRMIN) =F8.5
    2)
    IF(CAPROOT .GE. CAPRMIN)WRITE(6,17)
    IF(CAPROOT .LT. CAPRMIN)WRITE(6,18)
    17 FORMAT(0THE GEAR IS NOT UNDERCUT*)
    18 FORMAT(0THE GEAR IS UNDERCUT*)
    WRITE(6,19)ROOT
    19 FORMAT(0RADIUS OF ROOT CIRCLE OF PINION (ROOT) =F8.5)
    IF(1STOP .EQ. 0)GO TO 9999
    GO TO 1
    9999 STOP
    END

```

DIAMETRIC PITCH (PSUDO) = 44.00

GEAR NUMBER OF TEETH (NO) = 42

PINION NUMBER OF TEETH (NP) = 8

PRESSURE ANGLE (DEG) = 20.00

GEAR PITCH RADIUS (CPMP) = .07727 PINION PITCH RADIUS (RP) = .09051

GEAR BASE RADIUS (CPMB) = .08889 PINION BASE RADIUS (RPB) = .08543

STANDARD TOOTH THICKNESS AT PITCH RADIUS (STAND) = .03570

MIN WITHDRAWAL DISTANCE (IC) = .01209

GEAR BLANK RADIUS (CPMOT) = .08741 ORIGINAL PINION BLANK RADIUS (MOT) = .12573

ORIGINAL CONTACT RATIO (CPATIO) = 1.342

PINION OUTSIDE RADIUS FOR UNITY CONTACT RATIO (TOPIN) = .11000

FINAL CONTACT RATIO (CPFIN) = 1.098

GEAR TOOTH THICKNESS AT HIGH CIRCLE (CPHIC) = .02498 PINION TOOTH THICKNESS AT PINION CIRCLE (IC) = .04450

GEAR PRESSURE ANGLE AT OUTSIDE RADIUS (THEOGOT) = 23.18094 PINION PRESSURE ANGLE AT FINAL OUTSIDE RADIUS (THEOPH) = 39.85893

GEAR TOOTH THICKNESS AT OUTSIDE RADIUS (CPOT) = .01994 PINION TOOTH THICKNESS AT FINAL OUTSIDE RADIUS (IOT) = .02868

GEAR TOOTH THICKNESS AT BASE CIRCLE (CPBOT) = .03264 THEORETICAL PINION TOOTH THICKNESS AT BASE CIRCLE (IB) = .04437

RADIUS OF ROOT CIRCLE OF GEAR (CPMROOT) = .03805 MINIMUM ALLOWABLE RADIUS OF ROOT CIRCLE OF GEAR (CAPRMIN) = .41909

THE GEAR IS NOT UNDERCUT

RADIUS OF ROOT CIRCLE OF PINION (MOPH) = .07571

DIAMETRAL PITCH (INCH) = 65.00
GEAR NUMBER OF PITCH (NO) = 27
PITCH NUMBER OF PITCH (NO) = 9
PRESSURE ANGLE (T-P-A) = 20.00
GEAR PITCH RADIUS (CAPM) = .20769 PINION PITCH RADIUS (RP) = .06923
GEAR BASE RADIUS (CBM) = .19317 PINION BASE RADIUS (RB) = .06586
STANDARD TOOTH THICKNESS AT PITCH RADIUS (STAND) = .02417
ADD ADDITIONAL DISTANCE (C) = .00729
GEAR BASE RADIUS (CBM) = .21579 ORIGINAL PINION BASE RADIUS (RO) = .09199
ORIGINAL CONTACT RATIO (C-RATIO) = 1.371
PINION OUTSIDE RADIUS FOR UNIT CONTACT RATIO (ROF1) = .09099
PINION CONTACT RATIO (C-RATIO) = 1.000
GEAR TOOTH THICKNESS AT PITCH CIRCLE (CAP1C) = .01666 PINION TOOTH THICKNESS AT PINION CIRCLE (IC1) = .02067
GEAR PRESSURE ANGLE AT OUTSIDE RADIUS (THEOG1) = 25.25337 PINION PRESSURE ANGLE AT FINAL OUTSIDE RADIUS (THEOP1) = 36.85942
GEAR TOOTH THICKNESS AT OUTSIDE RADIUS (CAP1O) = .01267 PINION TOOTH THICKNESS AT FINAL OUTSIDE RADIUS (IC1) = .02024
GEAR TOOTH THICKNESS AT BASE CIRCLE (CBM1) = .02754 THEORETICAL PINION TOOTH THICKNESS AT BASE CIRCLE (IB1) = .02963
RADIUS OF ROOT CIRCLE OF GEAR (CBM001) = .18261 MINIMUM ALLOWABLE RADIUS OF ROOT CIRCLE OF GEAR (CBMMIN) = .18181
THE GEAR IS NOT INTERFERED
RADIUS OF ROOT CIRCLE OF PINION (R001) = .05472

GEOMETRICAL PITCH (PSUMOT) = 77.80

GEAR NUMBER OF PITCH (NPT) = 27

PITCH NUMBER OF PITCH (NPT) = 9

PRESSURE ANGLE (THETA) = 20.00

GEAR PITCH RADIUS (CARPT) = .17532 PINION PITCH RADIUS (RPT) = .05944

GEAR BASE RADIUS (CARBT) = .10479 PINION BASE RADIUS (RBT) = .05492

STANDARD TOOTH THICKNESS AT PITCH RADIUS (TSAND) = .02940

NON WITRORIAL DISTANCE (C) = .00015

GEAR BLANK RADIUS (CARBO) = .10210 ORBITAL PINION BLANK RADIUS (RBO) = .01750

ORIGINAL CONTACT RATIO (CRATIO) = 1.371

PINION OUTSIDE RADIUS FOR UNITY CONTACT RATIO (ROUFTN) = .04020

FINAL CONTACT RATIO (CARFIN) = 1.980

GEAR TOOTH THICKNESS AT PITCH CIRCLE (CARPT) = .01592 PINION TOOTH THICKNESS AT PITCH CIRCLE (RPT) = .02488

GEAR PRESSURE ANGLE AT OUTSIDE RADIUS (THCBOU) = 25.25382 PINION PRESSURE ANGLE AT FINAL OUTSIDE RADIUS (THCPOU) = 36.45992

GEAR TOOTH THICKNESS AT OUTSIDE RADIUS (CARPTO) = .01076 PINION TOOTH THICKNESS AT FINAL OUTSIDE RADIUS (RPTO) = .01710

GEAR TOOTH THICKNESS AT BASE CIRCLE (CARBTB) = .01907 THEORETICAL PINION TOOTH THICKNESS AT BASE CIRCLE (RBTB) = .02501

RADIUS OF ROOT CIRCLE OF GEAR (CARPOCT) = .10415 MINIMUM ALLOWABLE RADIUS OF ROOT CIRCLE OF GEAR (CARMIN) = .15347

THE GEAR IS NOT DIVERGENT

RADIUS OF ROOT CIRCLE OF PINION (RPOCT) = .04957

DIAMETRAL PITCH (PCURD) = 44.00

GEAR NUMBER OF TEETH (NG) = 56

PINION NUMBER OF TEETH (NP) = 8

PRESSURE ANGLE (PETA) = 20.00

GEAR PITCH RADIUS (CAPMP) = .63636 PINION PITCH RADIUS (AP) = .09091

GEAR BASE RADIUS (CAPMB) = .59799 PINION BASE RADIUS (BP) = .08943

STANDARD TOOTH THICKNESS AT PITCH RADIUS (STAND) = .03570

MOD WITHORAL DISTANCE (CI) = .01209

GEAR BLANK RADIUS (CAPMD) = .04700 ORIGINAL PINION BLANK RADIUS (RO) = .12573

ORIGINAL CONTACT RATIO (CRATIO) = 1.349

PINION OUTSIDE RADIUS FOR UNITY CONTACT RATIO (ROFIM) = .10970

FINAL CONTACT RATIO (CNFIN) = 1.000

GEAR TOOTH THICKNESS AT PITCH CIRCLE (CAPIC) = .02690 PINION TOOTH THICKNESS AT PITCH CIRCLE (TC) = .04450

GEAR PRESSURE ANGLE AT OUTSIDE RADIUS (TMEOG) = 22.00055 PINION PRESSURE ANGLE AT FINAL OUTSIDE RADIUS (TMEOP) = 30.85337

GEAR TOOTH THICKNESS AT OUTSIDE RADIUS (CAPID) = .01901 PINION TOOTH THICKNESS AT FINAL OUTSIDE RADIUS (TO) = .02901

GEAR TOOTH THICKNESS AT BASE CIRCLE (CAPTB) = .04310 THEORETICAL PINION TOOTH THICKNESS AT BASE CIRCLE (TB) = .04437

RADIUS OF ROOT CIRCLE OF GEAR (CAPROO) = .59798 MINIMUM ALLOWABLE RADIUS OF ROOT CIRCLE OF GEAR (CAPRMIN) = .55957

THE GEAR IS NOT UNDERSTRESS

RADIUS OF ROOT CIRCLE OF PINION (ROOT) = .07671

DIAMETRAL PITCH (PCURD) = 65.00
 GEAR NUMBER OF TEETH (NG) = 56
 PINION NUMBER OF TEETH (NP) = 8
 PRESSURE ANGLE (THETA) = 20.00
 GEAR PITCH RADIUS (CAPHP) = .43877 PINION PITCH RADIUS (RP) = .06154
 GEAR BASE RADIUS (CAPRB) = .40479 PINION BASE RADIUS (RBB) = .05783
 STANDARD TOOTH THICKNESS AT PITCH RADIUS (ISTAND) = .02417
 MIN WITHDRAWAL DISTANCE (C) = .00819
 GEAR BLANK RADIUS (CAPG0) = .43797 ORIGINAL PINION BLANK RADIUS (RO) = .08511
 ORIGINAL CONTACT RATIO (CRATIO) = 1.349
 PINION OUTSIDE RADIUS FOR UNITY CONTACT RATIO (ROFIM) = .07426
 FINAL CONTACT RATIO (CFMIN) = 1.008
 GEAR TOOTH THICKNESS AT PITCH CIRCLE (CAPIC) = .01821 PINION TOOTH THICKNESS AT PITCH CIRCLE (IC) = .03012
 GEAR PRESSURE ANGLE AT OUTSIDE RADIUS (THEOP) = 22.44463 PINION PRESSURE ANGLE AT FINAL OUTSIDE RADIUS (THEOPD) = 30.85337
 GEAR TOOTH THICKNESS AT OUTSIDE RADIUS (CAPLO) = .01287 PINION TOOTH THICKNESS AT FINAL OUTSIDE RADIUS (TO) = .01464
 GEAR TOOTH THICKNESS AT BASE CIRCLE (CAPTB) = .02918 THEORETICAL PINION TOOTH THICKNESS AT BASE CIRCLE (TB) = .03003
 RADIUS OF ROOT CIRCLE OF GEAR (CAPROOT) = .49478 MINIMUM ALLOWABLE RADIUS OF ROOT CIRCLE OF GEAR (CAPRMIN) = .37879
 THE GEAR IS NOT UNDER CUT
 RADIUS OF ROOT CIRCLE OF PINION (ROOTI) = .06192

2. Program INVOL 2: Point and Cycle Efficiencies for Single
Pass Involute Step-Up Gear Mesh With
Unity Contact Ratio

The program INVOL 2 is based on section 3 of Appendix A, which gives the moment input-output relationship for a single step-up gear mesh with involute teeth. The mesh has unity contact ratio. Again, the nomenclature of the program is chosen to coincide as much as possible with that of the original derivation. The contact geometry is adapted from section 6c of Appendix A.

a. Input Parameters (See also program in section d below)

The following parameters represent the input data of the program. Most of these are taken from the results of INVOL 1 since the moment expressions are for unity contact ratio only.

CAPRP = R_p , the pitch radius of the gear

RP = r_p , the pitch radius of the pinion

CAPRO = R_o , the outside radius of the gear

ROFIN = R_o' , see eq. (B-17). This is the pinion outside radius
for unity contact ratio.

RHOCAPN = ρ_N , the pivot radius of the gear

RHON = ρ_N , the pivot radius of the pinion

MU = μ , the coefficient of friction at both pivots as well as
at the gear and pinion contact point

K, range divisor, i.e., it represents the number of times the
output moment and the efficiency are computed between
initial and final contact of the gear and the pinion

ISTOP, arbitrary single digit for multiple data sets. It must be zero for the last set of data.

b. Computations

Both point and cycle efficiencies are based on eq. (A-25).
With the help of eq. (3), the point
efficiency becomes

$$\epsilon_p = \frac{\{r_b - \mu [r_n + s(d-a)]\}}{\{R_b + \mu [r_N - sa]\}} \frac{\dot{\psi}}{\dot{\phi}} \quad (C-1)$$

Since the angular velocity is constant for involute gears, and may be expressed in terms of the base circle radii R_b and r_b ,

$$K_{ratio} = \frac{\dot{\psi}}{\dot{\phi}} = \frac{R_b}{r_b} \quad (C-2)$$

Therefore,

$$\epsilon_p = E_2 \quad (\text{POINTEF}) \quad (C-3)$$

as given by eq. (A-26).

The cycle efficiency expression is based on eq. (4). If one replaces both integrals by summations, one obtains

$$\epsilon_c = \frac{\sum M_o \Delta\psi}{\sum M_{in} \Delta\phi} \quad (C-4)$$

where $\Delta\phi$ and $\Delta\psi$ now represent incremental changes in the input and output angles, respectively. The input moment is constant

over the total interval. Also

$$\Sigma \Delta \varphi = \alpha_{FIN} - \alpha_{IN} \quad (C-5)$$

(See eqs. (A205) and (A206).)

The increment $\Delta \psi$ is also constant and may therefore be taken outside the summation sign. It is expressed with the help of $\Delta \varphi$

$$\Delta \psi = \Delta \alpha = \frac{\alpha_{FIN} - \alpha_{IN}}{K} = \text{DELALPH} \quad (C-6)$$

(This is an adaptation of eq. (A-207) to the single step-up mesh.)

With the above

$$\Delta \psi = K_{\text{ratio}} \Delta \alpha \quad (C-7)$$

Substitution into eq. (C-4) gives

$$\epsilon_o = \frac{K_{\text{ratio}} \Delta \alpha \Sigma M_o}{M_{in} (\alpha_{FIN} - \alpha_{IN})} \quad (C-8)$$

Since

$$\epsilon_p = K_{\text{ratio}} \frac{M_o}{M_{in}} \quad (C-9)$$

one obtains for the cycle efficiency

$$\epsilon_o = \frac{\Delta \alpha \Sigma \epsilon_p}{(\alpha_{FIN} - \alpha_{IN})} \quad (\text{CYCLEFF}) \quad (C-10)$$

To arrive at expressions for both POINTEF and CYCLEFF in the program, the following other important computations are necessary:

ALPHIN = α_{IN} , see eq. (A-205)

ALPHFIN = α_{FIN} , see eq. (A-206)

D = d, see eq. (A-204)

A = a, see eq. (A-203)

The signum value s is obtained according to eqs. (A-215) and (A-216), which are alternate ways of expressing eqs. (A-6) to (A-8).

c. Output of Program (see Program INVOL 2, below)

The output of the program is best explained by means of the single sample computation which is shown at the end of the program. This example uses the data of the first sample output of INVOL 1. The output lists the following:

I. Input Parameters

The input parameters CAPRP, RP, CAPRO, RO and THETAD are reproduced. In addition, the following dimensions, which were selected from a practical viewpoint, are shown:

RHOCAPN = ρ_M = .060 in. (.152 cm)

RHON = ρ_n = .030 in. (.076 cm)

MU = μ = .2

K = 25 (no substantial changes in cycle efficiency were encountered for larger values of K)

II. Computed Values

The point efficiency is listed as a function of the angle α , while the cycle efficiency is computed for the interval from α_{IN} to α_{FIN} . The signum parameter, s , is listed for checking purposes.

Program INVOL 2

C-21

GEAR PITCH RADIUS (CAPRO) = .47727 PINION PITCH RADIUS (RP) = .09001
 GEAR OUTSIDE RADIUS (CARPO) = .49791 PINION OUTSIDE RADIUS FOR UNITY CONTACT RATIO (RPSM) = .11000
 PRESSURE ANGLE IN DEGREES (TMEAN) = 20.00
 GEAR PIVOT RADIUS (RMOCDM) = .040 PINION PIVOT RADIUS (RMOCM) = .030
 COEFFICIENT OF FRICTION (MU) = .20
 DANCE DIVISOR (K) = 25

ALPHAD = 15.07	S = 1.0	POINTEF = .7905
ALPHAD = 16.32	S = 1.0	POINTEF = .7979
ALPHAD = 16.66	S = 1.0	POINTEF = .8054
ALPHAD = 17.00	S = 1.0	POINTEF = .8129
ALPHAD = 17.34	S = 1.0	POINTEF = .8204
ALPHAD = 17.69	S = 1.0	POINTEF = .8279
ALPHAD = 18.03	S = 1.0	POINTEF = .8355
ALPHAD = 18.37	S = 1.0	POINTEF = .8430
ALPHAD = 18.72	S = 1.0	POINTEF = .8506
ALPHAD = 19.06	S = 1.0	POINTEF = .8582
ALPHAD = 19.40	S = 1.0	POINTEF = .8658
ALPHAD = 19.75	S = 1.0	POINTEF = .8735
ALPHAD = 20.09	S = 1.0	POINTEF = .8811
ALPHAD = 20.43	S = 1.0	POINTEF = .8888
ALPHAD = 20.77	S = 1.0	POINTEF = .8965
ALPHAD = 21.12	S = 1.0	POINTEF = .9047
ALPHAD = 21.46	S = 1.0	POINTEF = .9000
ALPHAD = 21.80	S = 1.0	POINTEF = .8933
ALPHAD = 22.15	S = 1.0	POINTEF = .8866
ALPHAD = 22.49	S = 1.0	POINTEF = .8800
ALPHAD = 22.83	S = 1.0	POINTEF = .8734
ALPHAD = 23.17	S = 1.0	POINTEF = .8667
ALPHAD = 23.52	S = 1.0	POINTEF = .8601
ALPHAD = 23.86	S = 1.0	POINTEF = .8535
ALPHAD = 24.20	S = 1.0	POINTEF = .8470

CYCLE EFFICIENCY = .8566

3. Program INVOL 3: Point and Cycle Efficiencies for Three
Pass Involute Step-Up Gear Train in
Spin Environment (All Meshes Have Unity
Contact Ratio)

The program INVOL 3 is based on section 4 of Appendix A, which derives the moment input-output relationship for a three pass step-up gear train operating in a spin environment. Again, all meshes have unity contact ratio. As previously, the nomenclature of the program is chosen to coincide as closely as possible with that of the original derivations. The expressions for the contact geometry and other auxiliary geometric terms may be found in section 6 of Appendix A.

a. Input Parameters (see Program INVOL 3, below)

The following parameters represent the input data for the program. Those which involve gear dimensions only must be obtained from the results of INVOL 1 since the moment expressions are derived for unity contact ratio only.

MU = μ , the coefficient of friction at all pivots and at
all tooth contact points

RPM, revolutions per minute of the fuze body

CAPRP1 = R_{p1}

CAPRP2 = R_{p2}

CAPRP3 = R_{p3}

RP2 = r_{p2}

RP3 = r_{p3}

RP4 = r_{p4}

$$\text{THETA1} = \theta_1$$

$$\text{THETA2} = \theta_2$$

$$\text{THETA3} = \theta_3$$

ISTOP, arbitrary single digit integer for multiple data set.

It must be zero for last set of data.

$$R1 = R_1$$

$$R2 = R_2$$

$$R3 = R_3$$

$$R4 = R_4$$

$$\text{RHO1} = \rho_1$$

$$\text{RHO2} = \rho_2$$

$$\text{RHO3} = \rho_3$$

$$\text{RHO4} = \rho_4$$

$$\text{CAPRB1} = R_{b1}$$

$$\text{CAPRB2} = R_{b2}$$

$$\text{CAPRB3} = R_{b3}$$

$$\text{RB2} = r_{b2}$$

$$\text{RB3} = r_{b3}$$

$$\text{RB4} = r_{b4}$$

$$\text{CAFR01} = R_{o1}$$

$$\text{CAFR02} = R_{o2}$$

$$\text{CAFR03} = R_{o3}$$

$$\text{RO2} = r'_{o2}$$

$$\text{RO3} = r'_{o3}$$

$$\text{RO4} = r'_{o4}$$

$$M1 = m_1, \quad \text{mass of input gear 1}$$

$$M2 = m_2, \quad \text{mass of gear and pinion 2}$$

$M_3 = m_3$, mass of gear and pinion 3
 $M_4 = m_4$, mass of pinion 4
 $MD = md^2$, the "mass-distance" product contained in the expression
 for the input moment M_{in}
 $K = K_3$, the range divisor which is associated with gear 3,
 the driving gear of the last mesh (see eq. (A-211))

b. Computations (see COMMENT cards in program)

I. Computation of MIN, GAMMAS and BETAS

To start with, the program computes the input moment

$$MIN = M_{in} = md^2 \omega^2 \quad (C-11)$$

Subsequently, the angles γ_2 , γ_3 , γ_4 and β_1 , β_2 , β_3 are established according to the expressions given in section 6b of Appendix A.

II. Determination of Gear Train Constants

The determination of the gear train constants consists of the following:

$RATIO = K_{ratio}$, (see eq. (2)). Since the angular velocity
 is constant, this parameter may be expressed
 in terms of the applicable base radii, i.e.,

$$\frac{R_{b1} \times R_{b2} \times R_{b3}}{r_{b2} \times r_{b3} \times r_{b4}}$$

$TEST1$, $TEST2$ and $TEST3$ represent the tangent functions of
 the mesh pressure angles, which are used in conjunction with the
 values of the signum functions, s .

D1, D2 and D3 are given by eqs. (A-204), (A-217) and (A-223), respectively, and represent the distances between the points of tangency to the base circles along the lines-of-action of the three meshes.

MTOT = 0 represents the initialization of the sum of the output moments. This is used for the determination of the cycle efficiency.

III. Determination of Initial and Final Values of ALPHAS. Initialization of ALPHAS and Centrifugal Forces

The determination of the initial and final angles of rotation is accomplished with the help of subroutine ALPHA, at the end of the program, which makes use of eqs. (A-205), (A-206), (A-218), (A-219), (A-224) and (A-225). Thus, the initial values of the individual angles of rotation, ALPHA1, ALPHA2 and ALPHA3 are represented by AL1IN, AL2IN and AL3IN, while the final angles are given by AL1FIN, AL2FIN and AL3FIN.

The angular increments of gears 3, 2 and 1, i.e., DELAL3, DELAL2 and DELAL1, are determined with the help of eqs. (A-211) - (A-213), respectively.

The centrifugal forces, which act on the pivots of the various gear and/or pinion assemblies, are obtained by way of eqs. (A-33), (A-57), (A-84) and (A-107).

IV. Point and Cycle Efficiencies (See "output moment" in program)

Both point and cycle efficiencies are based on eq. (A-125) for the output moment $MO4 = M_{O4}$.

The point efficiency is computed directly in the manner of eq. (3), i.e.,

$$\eta_p = K_{ratio} \frac{M_{o4}}{M_{in}} = \text{POINTEFF} \quad (\text{C-12})$$

The cycle efficiency is treated in the manner of eq. (C-8), i.e.,

$$\eta_p = \frac{K_{ratio} \Delta \alpha_1 \Sigma M_{o4}}{M_{in} (\alpha_{1FIN} - \alpha_{1IN})} = \text{CYCLEEFF} \quad (\text{C-13})$$

The program gives the summation as

$$MTOT = \Sigma M_{o4} \quad (\text{C-14})$$

V. Gear Train Motion Model

The simulation of the gear train motion, which is necessary for the computation of both POINTEFF and CYCLEEFF, is found in a loop which starts with statement label no. 14 (card no. 116) and ends with card no. 199. As discussed earlier, the motions of the individual driving gears are initialized at their respective angles, AL1IN, AL2IN and AL3IN. (This starting of the total train is arbitrary and is done only for convenience. There is an infinite number of other starting combinations each of which produces a different starting point efficiency.) The position of each mesh is subsequently incremented by the appropriate DELAL1, DELAL2 or DELAL3. When the angle ALPHA1 reaches the magnitude AL1FIN, CYCLEEFF is determined, and the computation is ended. Since meshes 2 and 3 go through numerous cycles while mesh 1 goes through one cycle, they have

to be reset to their initial angles of rotation once their respective final angles have been reached. This is accomplished by the conditional statements on cards 116 and 117.

The values of the signum functions s_1 , s_2 and s_3 are determined continuously according to eqs. (A-216), (A-222) and (A-227).

The instantaneous positions of the contact $A_1 = a_1$, $A_2 = a_2$, and $A_3 = a_3$ are determined for each of the meshes by an appropriate adaptation of eq. (A-203). (See also eqs. (A-214), (A-220) and (A-226).)

The determination of the instantaneous output moment, $M_{O4} = M_{O4}$, requires the continuous computation of the variable quantities A_1 to A_{20} , C_1 to C_6 and D_1 to D_4 , which are given originally in conjunction with the various equilibrium conditions in section 4 of Appendix A. The program uses the following nomenclature for these variables:

AA1 to AA20
CC1 to CC6
DD1 to DD4

c. Output (see Program INVOL 3, below)

Again, the output of the program is best explained by means of the sample computation which is shown at the end of the program. This example uses the gear data of the first three sample computations of program INVOL 1. The output lists the following:

I. Input Parameters

Mesh No. 1

$$\text{CAPRP1} = R_{p1} = .47727 \text{ in. } (.212 \text{ cm})$$

$$\text{CAPRB1} = R_{b1} = .44849 \text{ in. } (.139 \text{ cm})$$

$$\text{CAPRO1} = R_{o1} = .48791 \text{ in. } (.239 \text{ cm})$$

$$\text{RP2} = r_{p2} = .09091 \text{ in. } (.231 \text{ cm})$$

$$\text{RB2} = r_{b2} = .08543 \text{ in. } (.217 \text{ cm})$$

$$\text{RO2} = r'_{o2} = .11000 \text{ in. } (.279 \text{ cm}) \text{ (This is an ROFIN as given by INVOL 1.)}$$

Also,

$$\text{THETA1} = \theta_1 = 20^\circ$$

Mesh No. 2

$$\text{CAPRP2} = R_{p2} = .20769 \text{ in. } (.527 \text{ cm})$$

$$\text{CAPRB2} = R_{b2} = .19517 \text{ in. } (.496 \text{ cm})$$

$$\text{CAPRO2} = R_{o2} = .21579 \text{ in. } (.548 \text{ cm})$$

$$\text{RP3} = r_{p3} = .06923 \text{ in. } (.176 \text{ cm})$$

$$\text{RB3} = r_{b3} = .06506 \text{ in. } (.165 \text{ cm})$$

$$\text{RO3} = r'_{o3} = .08089 \text{ in. } (.205 \text{ cm})$$

Also,

$$\text{THETA2} = \theta_2 = 20^\circ$$

Mesh No. 3

$$\text{CAPRP3} = R_{p3} = .17532 \text{ in. } (.445 \text{ cm})$$

$$\text{CAPRB3} = R_{b3} = .16475 \text{ in. } (.418 \text{ cm})$$

$$\text{CAPRO3} = R_{o3} = .18216 \text{ in. } (.463 \text{ cm})$$

$$\text{RP4} = r_{p4} = .05844 \text{ in. } (.148 \text{ cm})$$

$$\text{RB4} = r_{b4} = .05492 \text{ in. } (.139 \text{ cm})$$

$$\text{RO4} = r'_{o4} = .06828 \text{ in. } (.173 \text{ cm})$$

Also,

$$\text{THETA3} = \theta_3 = 20^\circ$$

In addition,

$$\text{MU} = \mu = .2$$

$$\text{RPM} = 1000$$

$$\text{M1} = m_1 = .51079 \times 10^{-4} \text{ lb-sec}^2/\text{in.} \quad (8.943 \text{ g})$$

$$\text{M2} = m_2 = .17413 \times 10^{-4} \text{ lb-sec}^2/\text{in.} \quad (3.049 \text{ g})$$

$$\text{M3} = m_3 = .69788 \times 10^{-5} \text{ lb-sec}^2/\text{in.} \quad (1.222 \text{ g})$$

$$\text{M4} = m_4 = .7745 \times 10^{-6} \text{ lb-sec}^2/\text{in.} \quad (0.136 \text{ g})$$

$$\text{R1} = R_1 = .75 \text{ in.} \quad (1.905 \text{ cm})$$

$$\text{R2} = R_2 = .75 \text{ in.} \quad (1.905 \text{ cm})$$

$$\text{R3} = R_3 = .75 \text{ in.} \quad (1.905 \text{ cm})$$

$$\text{R4} = R_4 = .75 \text{ in.} \quad (1.905 \text{ cm})$$

$$\text{RHO1} = \rho_1 = .060 \text{ in.} \quad (.152 \text{ cm})$$

$$\text{RHO2} = \rho_2 = .030 \text{ in.} \quad (.076 \text{ cm})$$

$$\text{RHO3} = \rho_3 = .025 \text{ in.} \quad (.064 \text{ cm})$$

$$\text{RHO4} = \rho_4 = .020 \text{ in.} \quad (.051 \text{ cm})$$

$$\text{MD} = m d^2 = .15 \times 10^{-4} \text{ lb-sec}^2 \text{ in.} \quad (16.944 \text{ g-cm}^2)$$

$$\text{K} = 25$$

II. Computed Values

The point efficiency is given as a function of the angle α_1 , together with the signum parameters s_1 , s_2 and s_3 (given for checking purposes). The cycle efficiency is shown at the end of the output. In addition, the input moment, MIN, is printed out.

Program INVOL 3

C-32

```

1      PROGRAM INVOL3(INPUT,OUTPUT,TAPES=INPUT,TAPE6=OUTPUT)
C
C POINT AND CYCLE EFFICIENCIES FOR THREE PASS INVOLUTE STEP-UP
C IN SPIN ENVIRONMENT (ALL MESHERS HAVE UNITY CONTACT RATIO)
C
C      REAL MIN,MU,M1,M2,M3,M4,M03,M04,MTOT,MD
C
C      READ AND WRITE INPUT DATA
C
10     READ(5,1)MU,RPM,CAPRP1,CAPRP2,CAPRP3,RP2,RP3,RP4,THETA1,
1      THETA2,THETA3,ISTOP
      READ(5,2)R1,R2,R3,R4
      READ(5,3)RH01,RH02,RH03,RH04
      READ(5,4)CAPR01,CAPR02,CAPR03,R02,R03,R04
      READ(5,5)CAPR01,CAPR02,CAPR03,R02,R03,R04
      READ(5,6)M1,M2,M3,M4
      READ(5,7)MD,K
      PI = 3.14159
      OMEGA = RPM*2.3PI/60.
      OM2 = OMEGA*OMEGA
1      FORMAT(F16.3,F10.078F10.573F10.47I1)
2      FORMAT(4F10.4)
3      FORMAT(4F10.4)
4      FORMAT(6F10.5)
5      FORMAT(6F10.5)
6      FORMAT(4E10.2)
7      FORMAT(E10.2/I3)
C
C COMPUTATION OF MIN, GAMMAS AND BETAS
C
      MIN = MD*OM2
      GAMMA2 = ACOS((R1*R1 + R2*R2 - (CAPRP1*RP2)*(CAPRP1*RP2)))/
1      (2.*R1*R2))
      GAMMA3P = ACOS((R2*R2 + R3*R3 - (CAPRP2*RP3)*(CAPRP2*RP3)))/
1      (2.*R2*R3))
      GAMMA3 = GAMMA2 + GAMMA3P
      GAMMA4P = ACOS((R3*R3 + R4*R4 - (CAPRP3*RP4)*(CAPRP3*RP4)))/
1      (2.*R3*R4))
      GAMMA4 = GAMMA3 + GAMMA4P
      DELTA2 = ACOS(((CAPRP1*RP2)*(CAPRP1*RP2) + R1*R1 - R2*R2)/
1      (2.*R1*(CAPRP1 + RP2)))
      DELTA3 = ACOS(((CAPRP2*RP3)*(CAPRP2*RP3) + R2*R2 - R3*R3)/
1      (2.*R2*(CAPRP2 + RP3)))
      DELTA4 = ACOS(((CAPRP3*RP4)*(CAPRP3*RP4) + R3*R3 - R4*R4)/
1      (2.*R3*(CAPRP3 + RP4)))
      BETAI = PI - DELTA2
      BETAI2 = GAMMA2 + PI - DELTA3
      BETAI3 = GAMMA3 + PI - DELTA4
      WRITE(6,8)MIN,MU,RPM,CAPRP1,CAPRP2,CAPRP3,RP2,RP3,RP4,THETA1,
1      THETA2,THETA3
      WRITE(6,9)R1,R2,R3,R4,M1,M2,M3,M4
      WRITE(6,10)RH01,RH02,RH03,RH04
      WRITE(6,11)CAPR01,CAPR02,CAPR03,R02,R03,R04

```

55 WRITE(6,12)CAPR01,CAPR02,CAPR03,M02,R03,R04
WRITE(6,13)M0,X

60 R FORMAT(10.5X,M0,X) = F12.5,3X,M0,X = F6.3,3X,PPM = F6.0//
14X,CAPR01 = F8.5,3X,CAPR02 = F6.5,3X,CAPR03 = F8.5//6X,
2RR2 = F8.5,3X,RR3 = F.5 X,RR4 = F8.5//6X,
3*THETA1 = F6.3,3X,THETA2 = F.3,3X,THETA3 = F9.3//
9 FORMAT(6X,R01 = F7.5,3X,R02 = F7.5,3X,R03 = F7.5,3X,R04 = F7.5
1//6X,M) = F15.5,3X,M0 = F15.5,3X,M03 = F15.5,3X,
2M4 = F15.5//
10 FORMAT(6X,RM01 = F7.5,3X,RM02 = F7.5,3X,RM03 = F7.5,3X,
1RM04 = F7.5//

65 11 FORMAT(6X,CAPR01 = F7.5,3X,CAPR02 = F7.5,3X,CAPR03 = F7.5,
13X,RR2 = F7.5,3X,RR3 = F7.5,3X,RR4 = F7.5//
12 FORMAT(6X,CAPR01 = F7.5,3X,CAPR02 = F7.5,3X,CAPR03 = F7.5,3X
1,R02 = F7.5,3X,R03 = F7.5,3X,R04 = F7.5//
13 FORMAT(6X,M0 = F10.3//6X,ORANGE DIVISOR = F14//)

70 C CONVERSION TO RADIAN

C Z = PI/180.

C THETA1 = THETA1*Z

C THETA2 = THETA2*Z

C THETA3 = THETA3*Z

C DETERMINATION OF GEAR TRAIN CONSTANTS

80 RATIO = CAPR03/CAPR02/CAPR01/(R02*R03*RR4)

C TEST1 = TAN(THETA1)

C TEST2 = TAN(THETA2)

C TEST3 = TAN(THETA3)

85 D1 = (CAPR01 + R02)*TAN(THETA1)

C D2 = (CAPR02 + R03)*TAN(THETA2)

C D3 = (CAPR03 + R04)*TAN(THETA3)

C MTGT = 0.

C DETERMINATION OF INITIAL AND FINAL VALUES OF ALPHAS

90 CALL ALPHA(CAPR01,R02,THETA1,CAPR01,P02,AL1IN,AL1FIN)

C CALL ALPHA(CAPR02,R03,THETA2,CAPR02,P03,AL2IN,AL2FIN)

C CALL ALPHA(CAPR03,R04,THETA3,CAPR03,P04,AL3IN,AL3FIN)

95 DELAL3 = (AL3FIN - AL3IN)/K

C DELAL2 = DELAL3*R03/CAPR02

C DELAL1 = DELAL2*R02/CAPR01

C INITIALIZATION OF ALPHAS

100 ALPHA1 = AL1IN

C ALPHA2 = AL2IN

C ALPHA3 = AL3IN

C CENTRIFUGAL FORCE

C

T1 = H1*Z1*OM2

T2 = H2*Z2*OM2

T3 = H3*Z3*OM2

T4 = H4*Z4*OM2

DENOM = 1. + MU*RU

C UPDATE VALUES OF ALPHA3

14 I1 ALPHA2 =GT H2*F13*ALPHA2 = ALZIN

IF (ALPHA3 .GT. ALZIN) ALPHA3 = ALZIN

C TEST TO DETERMINE IF CONTACT POINT IS IN APPROACH OR RECESS

12 I1 APPROACH, S = 1.

IF RECESS, S = -1.

C AT PITCH POINT, S = 0.

IF (ALPHA1 .EQ. TEST1) S1 = 1.

IF (ALPHA2 .EQ. TEST2) S2 = 1.

IF (ALPHA3 .EQ. TEST3) S3 = 1.

IF (ALPHA1 .GT. TEST1) S1 = -1.

IF (ALPHA2 .GT. TEST2) S2 = -1.

IF (ALPHA3 .GT. TEST3) S3 = -1.

IF (ALPHA1 .LT. TEST1) S1 = 0.

IF (ALPHA2 .LT. TEST2) S2 = 0.

IF (ALPHA3 .LT. TEST3) S3 = 0.

C DETERMINATION OF INPUT FOR MOMENT EXPRESSIONS

A1 = ALPHA1*CAPR81

A2 = ALPHA2*CAPR82

A3 = ALPHA3*CAPR83

A41 = ABS((SIN(GAMMA4) - MU* $\cos(\text{GAMMA4})$)/DENOM)A42 = ABS((1. - S3* μ)* $\cos(\text{BETA3} - \text{THETA3})$ + MU*(1. - S3))* $\sin(\text{BETA3} - \text{THETA3})$)/DENOMA43 = ABS(($\cos(\text{GAMMA4})$ + MU* $\sin(\text{GAMMA4})$)/DENOM)A44 = ABS((1. - S3* μ)* $\sin(\text{BETA3} - \text{THETA3})$ - MU*(1. - S3))* $\cos(\text{BETA3} - \text{THETA3})$)/DENOMA45 = ABS((1. - MU* μ)* $\cos(\text{BETA2} - \text{THETA2})$ - MU*(S2 - 1.))* $\sin(\text{BETA2} - \text{THETA2})$)/DENOMA46 = ABS((SIN(GAMMA3) + MU* $\cos(\text{GAMMA3})$)/DENOM)A47 = ABS((1. - MU* μ)* $\cos(\text{BETA3} - \text{THETA3})$ - MU*(1. - S3))* $\sin(\text{BETA3} - \text{THETA3})$)/DENOMA48 = ABS((1. - MU* μ)* $\sin(\text{BETA2} - \text{THETA2})$ + MU*(1. - S2))* $\cos(\text{BETA2} - \text{THETA2})$)/DENOMA49 = ABS((MU* $\sin(\text{GAMMA3})$ - $\cos(\text{GAMMA3})$)/DENOM)A50 = ABS((1. - MU* μ)* $\sin(\text{BETA3} - \text{THETA3})$ + MU*(1. - S3))* $\cos(\text{BETA3} - \text{THETA3})$)/DENOMA51 = ABS((MU*(1. - S1)* $\sin(\text{BETA1} - \text{THETA1})$ + (1. - S1)* μ)* μ)/DENOMA52 = ABS(($\sin(\text{GAMMA2})$ - MU* $\cos(\text{GAMMA2})$)/DENOM)A53 = ABS((MU*(1. - S2)* $\sin(\text{BETA2} - \text{THETA2})$ + (1. - S2)* μ)* μ)/DENOMA54 = ABS((1. - MU* μ)* $\sin(\text{BETA2} - \text{THETA2})$ + MU*(S2 - 1.))* $\cos(\text{BETA2} - \text{THETA2})$)/DENOM

```

160 AA14 = ABS((MU*(1.-S1)*COS(RFTAL*THETA1) - (1.-MU)*MU*S1)
      1* SIN(BETAL*THETA1))/DENOM)
      AA15 = ABS((MU*SIN(GAMMA2) + COS(GAMMA2))/DENOM)
      AA16 = ABS((1.-MU)*MU*S1*SIN(BETA2-THETA2) - MU*(1.-S2)
      1* COS(RFTA2-THETA2))/DENOM)
      AA17 = ABS((1.-MU)*MU*S1*SIN(BETA1*THETA1) + MU*(1.-S1)
      1* COS(RFTA1*THETA1))/DENOM)
      AA18 = ABS(1./DENOM)
      AA19 = ABS((MU*(1.-S1)*SIN(BETAL*THETA1) - (1.-MU)*MU*S1)
      1* COS(RFTA1*THETA1))/DENOM)
      AA20 = ABS(MU/DENOM)
      DD1 = RPA - MU*(S3*(D3-A3) + RHO4*(A2-AA4))
      DD2 = -MU*(RHO3*(AA5-AA4) + S2*(D2-A2)) + PR3
      DD3 = PR2 - MU*(S1*(D1-A1) + RHO2*(AA1-AA14))
      DD4 = CAPR81 - MU*(S1*A1 - RHO1*(AA17-AA19))
      CC1 = MU*RHO2*(AA1-AA3)
      CC2 = CAPR83 - MU*(S3*A3 - RHO3*(AA7-AA10))
      CC3 = MU*RHO3*(A3-AA9)
      CC4 = CAPR82 - MU*(S2*A2 - RHO2*(A13-AA16))
      CC5 = MU*RHO2*(AA12-AA15)
      CC6 = MU*RHO1*(AA18-AA20)

170 C OUTPUT MOMENT
      C
      C
      ALPHA10 = ALPHA1*129./PI
      W04 = D01*D02*D03/((CC2-CC4)*D04*(MIN-T1*CC6) - T2*CC5*D01*D02)
      1/(CC2*CC4) - T3*CC3*D01/CC2 - T4*CC1
      POINTEF = RATIO*W04/M14
      WRITE(6,15) ALPHA10,S1,S2,S3,POINTEF
185 15 FORMAT(1X,F10.4,ALPHA1 = F4.2,6 (DEG),3F5.1,3X,E52 = F5.1,
      13X,E53 = F5.1,3X,POINT EFFICIENCY = F7.5)
      MTOT = MTOT + W04

190 C ADVANCE GEAR TRAIN TO NEXT POS. FROM
      C
      C
      ALPHA1 = ALPHA1 + DELA1
      IF (ALPHA1 .GT. ALIFIN) GO TO 16
      ALPHA2 = ALPHA2 + DELA2
      ALPHA3 = ALPHA3 + DELA3
      GO TO 14
200 14 CYCLEFF = RATIO*DELA1*MTOT/(MIN*(ALIFIN-AL1IN))
      WRITE(6,17) CYCLEFF
      17 FORMAT(1X,F8.5,CYCLE EFFICIENCY = F5.3)
      IF (ISTOP .NE. 0) GO TO 100
      STOP
205 END

```

SUBROUTINE ALPHA 76/76 OPT=1

FTM 4.6-428

99/96/78 18.01.15

PAGE

1

```
1      SUBROUTINE ALPHA(CAPR8,RR,THETA,CAPRO,RO,ALIN,ALFIN)
C      THIS SUBROUTINE COMPUTES THE INITIAL AND FINAL VALUES OF ALPHAS
C
5      ALIN = ((CAPR8 + RR)*TAN(THETA) - SQRT(DO*RO - RR*RR))/CAPR8
      ALFIN = SQRT(CAPRO*CAPRO - CAPR8*CAPR8)/CAPR8
      RETURN
      END
```

C-37

WIS = -16442.00 MU = .200 MM = 1000.

CAP001 = .47727 CAP002 = -20760 CAP003 = -17532

BP2 = .00001 BP3 = .00023 BP4 = .05444

INETAI = 40.000 INETIA2 = 20.000 INETIA3 = 20.000

R1 = .75000 R2 = .75000 R3 = .75000 R4 = .75000

M1 = .210700-04 M2 = .12-13-04 M3 = .69700E-05 M4 = .77454E-06

RM01 = .00000 RM02 = .03000 RM03 = .02500 RM04 = .02000

CAP001 = .64009 CAP002 = .19517 CAP003 = .10475 RM3 = .00500 RM4 = .05497

CAP001 = .00701 CAP002 = .21570 CAP003 = .10216 RM2 = .11000 RM3 = .00000 RM4 = .00020

MB = .150E-04

WAGE DIVISOR = 25

ALPHA1 = 15.97 (DEG)	S1 = 1.0	S2 = 1.0	S3 = 1.0	POINT EFFICIENCY = .37062
ALPHA1 = 16.01 (DEG)	S1 = 1.0	S2 = 1.0	S3 = 1.0	POINT EFFICIENCY = .37597
ALPHA1 = 16.04 (DEG)	S1 = 1.0	S2 = 1.0	S3 = 1.0	POINT EFFICIENCY = .38117
ALPHA1 = 16.08 (DEG)	S1 = 1.0	S2 = 1.0	S3 = 1.0	POINT EFFICIENCY = .38642
ALPHA1 = 16.11 (DEG)	S1 = 1.0	S2 = 1.0	S3 = 1.0	POINT EFFICIENCY = .39172
ALPHA1 = 16.14 (DEG)	S1 = 1.0	S2 = 1.0	S3 = 1.0	POINT EFFICIENCY = .39707
ALPHA1 = 16.19 (DEG)	S1 = 1.0	S2 = 1.0	S3 = 1.0	POINT EFFICIENCY = .40247
ALPHA1 = 16.21 (DEG)	S1 = 1.0	S2 = 1.0	S3 = 1.0	POINT EFFICIENCY = .40791
ALPHA1 = 16.26 (DEG)	S1 = 1.0	S2 = 1.0	S3 = 1.0	POINT EFFICIENCY = .41301
ALPHA1 = 16.29 (DEG)	S1 = 1.0	S2 = 1.0	S3 = 1.0	POINT EFFICIENCY = .41896
ALPHA1 = 16.31 (DEG)	S1 = 1.0	S2 = 1.0	S3 = 1.0	POINT EFFICIENCY = .42456
ALPHA1 = 16.35 (DEG)	S1 = 1.0	S2 = 1.0	S3 = 1.0	POINT EFFICIENCY = .43021
ALPHA1 = 16.34 (DEG)	S1 = 1.0	S2 = 1.0	S3 = 1.0	POINT EFFICIENCY = .43591
ALPHA1 = 16.51 (DEG)	S1 = 1.0	S2 = 1.0	S3 = 1.0	POINT EFFICIENCY = .44166
ALPHA1 = 16.55 (DEG)	S1 = 1.0	S2 = 1.0	S3 = 1.0	POINT EFFICIENCY = .44695
ALPHA1 = 16.64 (DEG)	S1 = 1.0	S2 = 1.0	S3 = 1.0	POINT EFFICIENCY = .45252
ALPHA1 = 16.52 (DEG)	S1 = 1.0	S2 = 1.0	S3 = 1.0	POINT EFFICIENCY = .45809
ALPHA1 = 16.55 (DEG)	S1 = 1.0	S2 = 1.0	S3 = 1.0	POINT EFFICIENCY = .46464
ALPHA1 = 16.58 (DEG)	S1 = 1.0	S2 = 1.0	S3 = 1.0	POINT EFFICIENCY = .47018
ALPHA1 = 16.62 (DEG)	S1 = 1.0	S2 = 1.0	S3 = 1.0	POINT EFFICIENCY = .47572
ALPHA1 = 16.65 (DEG)	S1 = 1.0	S2 = 1.0	S3 = 1.0	POINT EFFICIENCY = .48121
ALPHA1 = 16.75 (DEG)	S1 = 1.0	S2 = 1.0	S3 = 1.0	POINT EFFICIENCY = .48669
ALPHA1 = 16.70 (DEG)	S1 = 1.0	S2 = 1.0	S3 = 1.0	POINT EFFICIENCY = .49215
ALPHA1 = 16.72 (DEG)	S1 = 1.0	S2 = 1.0	S3 = 1.0	POINT EFFICIENCY = .49760
ALPHA1 = 16.85 (DEG)	S1 = 1.0	S2 = 1.0	S3 = 1.0	POINT EFFICIENCY = .50305
ALPHA1 = 16.89 (DEG)	S1 = 1.0	S2 = 1.0	S3 = 1.0	POINT EFFICIENCY = .50853
ALPHA1 = 16.92 (DEG)	S1 = 1.0	S2 = 1.0	S3 = 1.0	POINT EFFICIENCY = .51406
ALPHA1 = 16.96 (DEG)	S1 = 1.0	S2 = 1.0	S3 = 1.0	POINT EFFICIENCY = .51964
ALPHA1 = 16.99 (DEG)	S1 = 1.0	S2 = 1.0	S3 = 1.0	POINT EFFICIENCY = .52508
ALPHA1 = 17.02 (DEG)	S1 = 1.0	S2 = 1.0	S3 = 1.0	POINT EFFICIENCY = .53046
ALPHA1 = 17.06 (DEG)	S1 = 1.0	S2 = 1.0	S3 = 1.0	POINT EFFICIENCY = .53576
ALPHA1 = 17.09 (DEG)	S1 = 1.0	S2 = 1.0	S3 = 1.0	POINT EFFICIENCY = .54106
ALPHA1 = 17.12 (DEG)	S1 = 1.0	S2 = 1.0	S3 = 1.0	POINT EFFICIENCY = .54636
ALPHA1 = 17.15 (DEG)	S1 = 1.0	S2 = 1.0	S3 = 1.0	POINT EFFICIENCY = .55166
ALPHA1 = 17.19 (DEG)	S1 = 1.0	S2 = 1.0	S3 = 1.0	POINT EFFICIENCY = .55696
ALPHA1 = 17.23 (DEG)	S1 = 1.0	S2 = 1.0	S3 = 1.0	POINT EFFICIENCY = .56226
ALPHA1 = 17.26 (DEG)	S1 = 1.0	S2 = 1.0	S3 = 1.0	POINT EFFICIENCY = .56756
ALPHA1 = 17.29 (DEG)	S1 = 1.0	S2 = 1.0	S3 = 1.0	POINT EFFICIENCY = .57286
ALPHA1 = 17.33 (DEG)	S1 = 1.0	S2 = 1.0	S3 = 1.0	POINT EFFICIENCY = .57816

[illegible]

ALPHA1 = 24.07 (DEG)	S1 = -1.0	S2 = 1.0	S3 = 1.0	POINT EFFICIENCY = .65544
ALPHA1 = 24.10 (DEG)	S1 = -1.0	S2 = 1.0	S3 = 1.0	POINT EFFICIENCY = .65544
ALPHA1 = 24.13 (DEG)	S1 = -1.0	S2 = 1.0	S3 = 1.0	POINT EFFICIENCY = .65528
ALPHA1 = 24.17 (DEG)	S1 = -1.0	S2 = 1.0	S3 = 1.0	POINT EFFICIENCY = .65528
ALPHA1 = 24.20 (DEG)	S1 = -1.0	S2 = 1.0	S3 = 1.0	POINT EFFICIENCY = .65528
ALPHA1 = 24.24 (DEG)	S1 = -1.0	S2 = 1.0	S3 = 1.0	POINT EFFICIENCY = .65528
ALPHA1 = 24.27 (DEG)	S1 = -1.0	S2 = 1.0	S3 = 1.0	POINT EFFICIENCY = .65528
ALPHA1 = 24.30 (DEG)	S1 = -1.0	S2 = 1.0	S3 = 1.0	POINT EFFICIENCY = .65528
ALPHA1 = 24.34 (DEG)	S1 = -1.0	S2 = 1.0	S3 = 1.0	POINT EFFICIENCY = .65528
ALPHA1 = 24.37 (DEG)	S1 = -1.0	S2 = 1.0	S3 = 1.0	POINT EFFICIENCY = .65528
ALPHA1 = 24.40 (DEG)	S1 = -1.0	S2 = 1.0	S3 = 1.0	POINT EFFICIENCY = .65528
ALPHA1 = 24.44 (DEG)	S1 = -1.0	S2 = 1.0	S3 = 1.0	POINT EFFICIENCY = .65528
ALPHA1 = 24.47 (DEG)	S1 = -1.0	S2 = 1.0	S3 = 1.0	POINT EFFICIENCY = .65528
ALPHA1 = 24.51 (DEG)	S1 = -1.0	S2 = 1.0	S3 = 1.0	POINT EFFICIENCY = .65528
ALPHA1 = 24.54 (DEG)	S1 = -1.0	S2 = 1.0	S3 = 1.0	POINT EFFICIENCY = .65528

CYCLE EFFICIENCY = .641

4. Program INVOL 4: Point and Cycle Efficiencies for Two
Pass Involute Step-Up Gear Train in
Spin Environment (All Meshes Have
Unity Contact Ratio)

The program INVOL 4 is based on section 5 of Appendix A, which derives the moment input-output relationship for a two pass step-up gear train, operating in a spin environment. Here again, all meshes have unity contact ratio. INVOL 4 is very similar to INVOL 3 in its construction. Again, the expressions for the contact geometry and other auxiliary geometric terms may be found in section 6 of Appendix A.

a. Input Parameters (see Program INVOL 4, below)

The following parameters represent the input data for the program. Those which involve gear dimensions only must be obtained from the results of INVOL 1 since the moment expressions are again derived for unity contact ratio only.

MU = μ , coefficient of friction at all pivots and at all
tooth contact points

RPM, revolutions per minute of the fuze body

CAPRP1 = R_{p1}

CAPRP2 = R_{p2}

RF2 = r_{p2}

RP3 = r_{p3}

THETA1 = θ_1

THETA2 = θ_2

ISTOP, arbitrary single digit integer for multiple data sets.

It must be zero for last set of data.

$$R1 = R_1$$

$$R2 = R_2$$

$$R3 = R_3$$

$$RHO1 = \rho_1$$

$$RHO2 = \rho_2$$

$$RHO3 = \rho_3$$

$$CAPRB1 = R_{b1}$$

$$CAPRB2 = R_{b2}$$

$$RB2 = r_{b2}$$

$$RB3 = r_{b3}$$

$$CAPRO1 = R_{o1}$$

$$CAPRO2 = R_{o2}$$

$$RO2 = r'_{o2}$$

$$RO3 = r'_{o3}$$

$$M1 = m_1, \text{ mass of input gear 1}$$

$$M2 = m_2, \text{ mass of gear and pinion 2}$$

$$M3 = m_3, \text{ mass of pinion 3}$$

$$MD = md^2, \text{ "mass-distance" product contained in the following expression for the input moment } M_{in}$$

$$K = K_2, \text{ the range divisor which is associated with gear 2, the driving gear of the last mesh for this case (see eq. (A-207))}$$

b. Computations (see COMMENT cards in program)

I. Computation of MIN, Gammas and Betas

To start with, the program computes the input moment

$$MIN = M_{in} = m d \omega^2 \quad (C-15)$$

The program computes the angles γ_2 , γ_3 and β_1 , β_2 according to the expressions given in section 6b of Appendix A.

II. Determination of the Gear Train Constants

The determination of the gear train constants consists of the following:

RATIO = K_{ratio} (see eq. (2)). Since the angular velocity is constant, this parameter may be expressed in terms of the applicable base radii, i.e.,

$$\frac{R_{b1} \times R_{b2}}{r_{b2} \times r_{b3}}$$

TEST1 and TEST2 represent the tangent functions of the mesh pressure angles, which are used in conjunction with the values of the signum functions s .

D1, and D2 are given by eqs. (A-204) and (A-217), respectively, and represent the distances between the points of tangency to the base circles along the lines-of-action of the two meshes.

MTOT = 0 represents the initialization of the sum of the output moments. This is used for the determination of the cycle efficiency.

III. Determination of Initial and Final Values of ALPHAS.

Initialization of ALPHAS and Centrifugal Forces

The determination of the initial and final angles of rotation is accomplished with the help of subroutine ALPHA, at the end of the program, which makes use of eqs. (A-205), (A-206) as well as (A-218) and (A-219). Thus, the initial values of the individual angles of rotation, ALPHA1 and ALPHA2, are represented by AL1IN and AL2IN, respectively, while the final ones are given by AL1FIN and AL2FIN.

The angular increments of gears 2 and 1, i.e., DELAL2 and DELAL1, are determined with the help of eqs. (A-207) and (A-208), respectively.

The centrifugal forces, which act on the pivots of the various gear and/or pinion assemblies, are obtained by way of eqs. (A-131), (A-154) and (A-178).

IV. Point and Cycle Efficiencies (See "output moment" in program)

Both point and cycle efficiencies are based on eq. (A-193) for the output moment $M_{O3} = M_{O3}$.

The point efficiency is computed directly in the manner of eq. (3), i.e.,

$$\eta_p = K_{ratio} \frac{M_{O3}}{M_{in}} = \text{POINTEF} \quad (\text{C-16})$$

The cycle efficiency is treated in the manner of eq. (C-13), i.e.,

$$\epsilon_o = \frac{K_{ratio} \Delta \alpha_1 \Sigma M_{o3}}{M_{in} (\alpha_{1FIN} - \alpha_{1IN})} = CYCLEFF \quad (C-17)$$

The program gives the summation as

$$MTOT = \Sigma M_{o3} \quad (C-18)$$

V. Gear Train Motion Model

The simulation of the gear train motion, which is necessary for the computation of both POINTEF and CYCLEFF, is found in a loop which begins with statement label no. 14 (card no. 98) and ends with card no. 161.

As discussed earlier, the motions of the individual driving gears are initialized at their respective angles, $AL1IN$ and $AL2IN$. (This starting of the total train is arbitrary and is done only for convenience. There is an infinite number of other starting combinations, each of which produces a different starting point efficiency.) The position of each mesh is subsequently incremented by the appropriate $DELAL1$ or $DELAL2$. When the angle $ALPHA1$ reaches the magnitude $AL1FIN$, $CYCLEFF$ is determined, and the computation is ended. Since mesh 2 goes through a number of cycles while mesh 1 goes through one cycle, mesh 2 has to be reset to its starting position, $AL2IN$, once the angle $AL2FIN$ has been reached. This is accomplished by the conditional statement on card no. 98.

The values of the signum functions s_1 and s_2 are determined continuously according to eqs. (A-216) and (A-222).

The instantaneous positions of the contact, $A1 = a_1$ and $A2 = a_2$, are determined for each of the meshes by appropriate

adaptations of eq. (A-203). (See also eqn. (A-214) and (A-220).)

The determination of the instantaneous output moment, $M_{O3} = M_{O3}$, requires the continuous computation of the variable quantities A_1 to A_{14} , C_1 to C_4 and D_1 to D_3 , which are given originally in conjunction with the various equilibrium conditions in section 5 of Appendix A. The program uses the following nomenclature for these variables:

AA1 to AA14

CC1 to CC4

DD1 to DD3

c. Output (see Program INVOL 4, below)

The output of the program is again best explained with the help of the sample computation shown at the end of the program. This example uses the gear data of the fourth and fifth sample computations of program INVOL 1. The output lists the following:

I. Input Parameters

Mesh No. 1

CAPRP1 = R_{p1} = .63636 in. (1.616 cm)

CAPRB1 = R_{b1} = .59799 in. (1.519 cm)

CAPRO1 = R_{o1} = .64700 in. (1.643 cm)

RP2 = r_{p2} = .09091 in. (0.231 cm)

RB2 = r_{b2} = .08543 in. (0.217 cm)

RO2 = r'_{o2} = .1097 in. (0.279 cm) (This is a ROFIN as given by INVOL 1.)

Also

THETA1 = θ_1 = 20°

Mesh No. 2

$$\text{CAPRP2} = R_{p2} = .43077 \text{ in. (1.094 cm)}$$

$$\text{CAPRB2} = R_{b2} = .40479 \text{ in. (1.028 cm)}$$

$$\text{CAPRO2} = R_{o2} = .43977 \text{ in. (1.117 cm)}$$

$$\text{RP3} = r_{p3} = .06154 \text{ in. (0.156 cm)}$$

$$\text{RB3} = r_{b3} = .05783 \text{ in. (0.147 cm)}$$

$$\text{RO3} = r_{o3} = .07426 \text{ in. (0.189 cm)}$$

Also

$$\text{THETA2} = \theta_2 = 20^\circ$$

In addition,

$$\text{MU} = \mu = .2$$

$$\text{RPM} = 1000$$

$$\text{M1} = m_1 = .51079 \times 10^{-4} \text{ lb-sec}^2/\text{in. (8.943 g)}$$

$$\text{M2} = m_2 = .17413 \times 10^{-4} \text{ lb-sec}^2/\text{in. (3.049 g)}$$

$$\text{M3} = m_3 = .69788 \times 10^{-5} \text{ lb-sec}^2/\text{in. (1.222 g)}$$

$$\text{R1} = R_1 = .75 \text{ in. (1.905 cm)}$$

$$\text{R2} = R_2 = .75 \text{ in. (1.905 cm)}$$

$$\text{R3} = R_3 = .75 \text{ in. (1.905 cm)}$$

$$\text{RHO1} = \rho_1 = .060 \text{ in. (0.152 cm)}$$

$$\text{RHO2} = \rho_2 = .030 \text{ in. (0.076 cm)}$$

$$\text{RHO3} = \rho_3 = .025 \text{ in. (0.064 cm)}$$

$$\text{MD} = md^2 = .15 \times 10^{-4} \text{ lb-sec}^2 \text{ in. (16.944 g-cm}^2\text{)}$$

$$\text{K} = 25$$

II. Computed Values

The point efficiency is given as a function of the angle α_1 , together with the signum parameters s_1 and s_2 (given for checking purposes). The cycle efficiency is shown at the end of the output. In addition, the input moment, MIN, is printed out.

Program INVOL 4

C-51


```

55      11 FORMAT(6X,'CAPR81 =',F7.5,'X',CAPR82 =',F7.5,'X',R82 =',F7.5,'X',
      1,R83 =',F7.5/')
      12 FORMAT(6X,'CAPR01 =',F7.5,'X',CAPR02 =',F7.5,'X',R02 =',F7.5,'X',
      1,R03 =',F7.5/')
      13 FORMAT(6X,'WD =',E10.3,'/6X,'RANGE DIVISOR =',I4,'/')

60      C
      C CONVERSION TO RADIAN
      2 = PI/180.
      THETA1 = THETA1*2
      THETA2 = THETA2*2

65      C
      C DETERMINATION OF GEAR TRAIN CONSTANTS
      C
      RATIO = (CAPR02*CAPR81)/(R02*R03)
      TEST1 = TAN(THETA1)
      TEST2 = TAN(THETA2)
      D1 = (CAPR81 + R02)*TAN(THETA1)
      D2 = (CAPR82 + R03)*TAN(THETA2)
      MTOT = 0.

70      C
      C DETERMINATION OF INITIAL AND FINAL VALUES OF ALPHAS
      C
      CALL ALPHA(CAPR81,R02,THETA1,CAPR01,R02,AL1IN,AL1FIN)
      CALL ALPHA(CAPR82,R03,THETA2,CAPR02,R03,AL2IN,AL2FIN)

      DELAL2 = (AL2FIN - AL2IN)/K
      DELAL1 = DELAL2*R02/CAPR81

80      C
      C INITIALIZATION OF ALPHAS
      C
      ALPHA1 = AL1IN
      ALPHA2 = AL2IN

85      C
      C CENTRIFUGAL FORCES
      C
      T1 = M1*R1*OM2
      T2 = M2*R2*OM2
      T3 = M3*R3*OM2

90      C
      C DEMON = 1. + MU*RUJ

95      C
      C UPDATE VALUES OF ALPHAS
      C
      14 IF (ALPHA2 .GT. AL2FIN) ALPHA2 = AL2FIN

100      C
      C TEST TO DETERMINE IF CONTACT POINT IS IN APPROACH OR RECESS
      C
      IF APPROACH, S = 1.
      IF RECESS, S = -1.
      C
      C AT PITCH POINT, S = 0.

105      C
      C IF (ALPHA1 .LT. TEST1) S1 = 1.
      C IF (ALPHA2 .LT. TEST2) S2 = 1.

```

```

110 IF (ALPHA1 .GT. TEST1) S1 = -1.
    IF (ALPHA2 .GT. TEST2) S2 = -1.
    IF (ALPHA1 .EQ. TEST1) S1 = 0.
    IF (ALPHA2 .EQ. TEST2) S2 = 0.
C
C DETERMINATION OF INPUT FOR MOMENT EXPRESSIONS
C
    A1 = ALPHA1 * CAPR01
    A2 = ALPHA2 * CAPR02
    A3 = ABS((1. - MU * MU * S2) * COS(BETA2 - THETA2) + MU * (S2 - 1.) *
    SIN(BETA2 - THETA2)) / DENOM
    A4 = ABS((S1 * SIN(GAMMA3) + MU * COS(GAMMA3)) / DENOM)
    A5 = ABS((1. - MU * MU * S2) * SIN(BETA2 - THETA2) + MU * (1. - S2) * COS(BETA2
    - THETA2)) / DENOM
    A6 = ABS((MU * SIN(GAMMA3) - COS(GAMMA3)) / DENOM)
    A7 = ABS((MU * (1. - S1) * SIN(BETA1 - THETA1) + (1. - S1) * MU * MU *
    COS(BETA1 - THETA1)) / DENOM)
    A8 = ABS((S1 * SIN(GAMMA2) - MU * COS(GAMMA2)) / DENOM)
    A9 = ABS((MU * (1. - S2) * SIN(BETA2 - THETA2) + (1. - MU * MU * S2) *
    COS(BETA2 - THETA2)) / DENOM)
    A10 = ABS((MU * (1. - S1) * COS(BETA1 - THETA1) - (1. - MU * MU * S1) *
    SIN(BETA1 - THETA1)) / DENOM)
    A11 = ABS((MU * SIN(GAMMA2) + COS(GAMMA2)) / DENOM)
    A12 = ABS((1. - MU * MU * S2) * SIN(BETA2 - THETA2) - MU * (1. - S2) *
    COS(BETA2 - THETA2)) / DENOM
    A13 = ABS((1. - MU * MU * S1) * SIN(BETA1 - THETA1) + MU * (1. - S1) *
    COS(BETA1 - THETA1)) / DENOM
    A14 = MU / DENOM
    CC1 = MU * R03 * (AA2 * AA4)
    CC2 = MU * R02 - MU * (S2 * A2 - P * Q2 * (AA7 - AA10))
    CC3 = MU * R02 * (AA6 * AA9)
    CC4 = MU * R01 * (AA12 * AA14)
    D01 = R03 - MU * (S2 * (Q2 - A2) * R03 + (AA1 * AA3))
    D02 = R02 - MU * (S1 * (Q1 - A1) * R02 + (AA5 * AA8))
    D03 = CAPR01 - MU * (S1 * A1 - R01 * (AA11 * AA13))
    ALPHA10 = ALPHA1 / Z
C
C OUTPUT MOMENT
C
    M03 = (D01 * D02) / (CC2 * D03) * (MIN - TI * CC4) - I2 * CC3 * D01 / CC2 - I3 * CC1
    POINTEE = Z * ATIG * M03 / MIN
    WRITE(6,15) ALPHA10, S1, S2, POINTEE
15 FORMAT(81.0, ALPHA1 =, F6.2, 3X, S1 =, F5.1, 3X, S2 =, F5.1, 3X,
    1 * POINT EFFICIENCY =, F7.5)
    MTOT = MTOT + M03
C
C ADVANCE GEAR TRAIN 10 NEXT POSITION
C
    ALPHA1 = ALPHA1 + DELTA1
    IF (ALPHA1 .GT. ALFIN) GO TO 16

```

PROGRAM INVDL4 74/74 QP1=1

PAGE 4

09/05/70 14.49.21

FTN 4.6-420

160

ALPHA2 = ALPHA2 * DELAL1 * CAPRB1 / R52
GO TO 14

16 CYCLEFF = (RATIO * DELAL1 * MTOT) / (WIN * (AL1 * FIN - AL1 * IN1))
WRITE(6,17) CYCLEFF

165

17 FORMAT(99.6X, 'CYCLE EFFICIENCY =', F5.3)
IF (J .NE. 0) GO TO 100
STOP
END

0-55

09/05/78 16.49.21

FIN 4.6428

SUBROUTINE ALPHA 74/74 OP1=1

```
1 SUBROUTINE ALPHA(CAPRB, RB, THETA, CAPRO, RO, ALIN, ALFIN)
C
C THIS SUBROUTINE COMPUTES THE INITIAL AND FINAL VALUES OF ALPHAS
C
5 ALIN = ((CAPRB + RB)*TAN(THETA) - SQRT(RO*RO - RB*RB))/CAPRB
ALFIN = SQRT(CAPRB*CAPRO - CAPRB*CAPRB)/CAPRB
RETURN
END
```

MIN = .12440E+08 MU = .288 GMM = 1888.

CAPR01 = .64636 CAPR02 = .43077

RP2 = .89901 RP3 = .96154

THETA1 = 28.838 THETA2 = 28.888

R1 = .75888 R2 = .75888 R3 = .75888

R1 = .51870E-04 R2 = .17413E-04 R3 = .69780E-05

R401 = .86888 R402 = .83888 R403 = .62588

CAPR01 = .50799 CAPR02 = .48478 R404 = .88543 R405 = .65783

CAPR01 = .54788 CAPR02 = .43797 R402 = .18978 R403 = .87426

MO = .158E-04

RA00E DIVISOR = 25

ALPHA1 = 17.24	S1 = 1.0	S2 = 1.0	POINT EFFICIENCY = .41855
ALPHA1 = 17.24	S1 = 1.0	S2 = 1.0	POINT EFFICIENCY = .41634
ALPHA1 = 17.31	S1 = 1.0	S2 = 1.0	POINT EFFICIENCY = .42267
ALPHA1 = 17.35	S1 = 1.0	S2 = 1.0	POINT EFFICIENCY = .42784
ALPHA1 = 17.39	S1 = 1.0	S2 = 1.0	POINT EFFICIENCY = .43360
ALPHA1 = 17.42	S1 = 1.0	S2 = 1.0	POINT EFFICIENCY = .43952
ALPHA1 = 17.46	S1 = 1.0	S2 = 1.0	POINT EFFICIENCY = .44539
ALPHA1 = 17.50	S1 = 1.0	S2 = 1.0	POINT EFFICIENCY = .45128
ALPHA1 = 17.53	S1 = 1.0	S2 = 1.0	POINT EFFICIENCY = .45720
ALPHA1 = 17.57	S1 = 1.0	S2 = 1.0	POINT EFFICIENCY = .46314
ALPHA1 = 17.61	S1 = 1.0	S2 = 1.0	POINT EFFICIENCY = .46918
ALPHA1 = 17.64	S1 = 1.0	S2 = 1.0	POINT EFFICIENCY = .47529
ALPHA1 = 17.68	S1 = 1.0	S2 = 1.0	POINT EFFICIENCY = .48140
ALPHA1 = 17.72	S1 = 1.0	S2 = 1.0	POINT EFFICIENCY = .48754
ALPHA1 = 17.75	S1 = 1.0	S2 = 1.0	POINT EFFICIENCY = .49321
ALPHA1 = 17.79	S1 = 1.0	S2 = 1.0	POINT EFFICIENCY = .49884
ALPHA1 = 17.83	S1 = 1.0	S2 = 1.0	POINT EFFICIENCY = .50455
ALPHA1 = 17.86	S1 = 1.0	S2 = 1.0	POINT EFFICIENCY = .51034
ALPHA1 = 17.90	S1 = 1.0	S2 = 1.0	POINT EFFICIENCY = .51620
ALPHA1 = 17.94	S1 = 1.0	S2 = 1.0	POINT EFFICIENCY = .52214
ALPHA1 = 17.97	S1 = 1.0	S2 = 1.0	POINT EFFICIENCY = .52814
ALPHA1 = 18.01	S1 = 1.0	S2 = 1.0	POINT EFFICIENCY = .53420
ALPHA1 = 18.05	S1 = 1.0	S2 = 1.0	POINT EFFICIENCY = .54034
ALPHA1 = 18.09	S1 = 1.0	S2 = 1.0	POINT EFFICIENCY = .54654
ALPHA1 = 18.12	S1 = 1.0	S2 = 1.0	POINT EFFICIENCY = .55280
ALPHA1 = 18.16	S1 = 1.0	S2 = 1.0	POINT EFFICIENCY = .55914
ALPHA1 = 18.19	S1 = 1.0	S2 = 1.0	POINT EFFICIENCY = .56554
ALPHA1 = 18.23	S1 = 1.0	S2 = 1.0	POINT EFFICIENCY = .57200
ALPHA1 = 18.27	S1 = 1.0	S2 = 1.0	POINT EFFICIENCY = .57854
ALPHA1 = 18.31	S1 = 1.0	S2 = 1.0	POINT EFFICIENCY = .58514
ALPHA1 = 18.34	S1 = 1.0	S2 = 1.0	POINT EFFICIENCY = .59184
ALPHA1 = 18.38	S1 = 1.0	S2 = 1.0	POINT EFFICIENCY = .59864
ALPHA1 = 18.42	S1 = 1.0	S2 = 1.0	POINT EFFICIENCY = .60554
ALPHA1 = 18.45	S1 = 1.0	S2 = 1.0	POINT EFFICIENCY = .61254
ALPHA1 = 18.49	S1 = 1.0	S2 = 1.0	POINT EFFICIENCY = .61964
ALPHA1 = 18.53	S1 = 1.0	S2 = 1.0	POINT EFFICIENCY = .62684
ALPHA1 = 18.56	S1 = 1.0	S2 = 1.0	POINT EFFICIENCY = .63414
ALPHA1 = 18.60	S1 = 1.0	S2 = 1.0	POINT EFFICIENCY = .64154
ALPHA1 = 18.64	S1 = 1.0	S2 = 1.0	POINT EFFICIENCY = .64904
ALPHA1 = 18.67	S1 = 1.0	S2 = 1.0	POINT EFFICIENCY = .65664
ALPHA1 = 18.71	S1 = 1.0	S2 = 1.0	POINT EFFICIENCY = .66434

ALP001	18.72	51	1.0	52	1.0	POINT EFFICIENCY = .53565
ALP002	18.74	51	1.0	52	1.0	POINT EFFICIENCY = .53161
ALP003	18.82	51	1.0	52	1.0	POINT EFFICIENCY = .52777
ALP004	18.86	51	1.0	52	1.0	POINT EFFICIENCY = .52392
ALP005	18.89	51	1.0	52	1.0	POINT EFFICIENCY = .52007
ALP006	18.93	51	1.0	52	1.0	POINT EFFICIENCY = .51621
ALP007	18.97	51	1.0	52	1.0	POINT EFFICIENCY = .51234
ALP008	19.00	51	1.0	52	1.0	POINT EFFICIENCY = .50847
ALP009	19.04	51	1.0	52	1.0	POINT EFFICIENCY = .50460
ALP010	19.09	51	1.0	52	1.0	POINT EFFICIENCY = .50072
ALP011	19.11	51	1.0	52	1.0	POINT EFFICIENCY = .49689
ALP012	19.15	51	1.0	52	1.0	POINT EFFICIENCY = .49303
ALP013	19.19	51	1.0	52	1.0	POINT EFFICIENCY = .48917
ALP014	19.22	51	1.0	52	1.0	POINT EFFICIENCY = .48531
ALP015	19.26	51	1.0	52	1.0	POINT EFFICIENCY = .48145
ALP016	19.30	51	1.0	52	1.0	POINT EFFICIENCY = .47758
ALP017	19.33	51	1.0	52	1.0	POINT EFFICIENCY = .47372
ALP018	19.37	51	1.0	52	1.0	POINT EFFICIENCY = .46985
ALP019	19.41	51	1.0	52	1.0	POINT EFFICIENCY = .46598
ALP020	19.44	51	1.0	52	1.0	POINT EFFICIENCY = .46212
ALP021	19.48	51	1.0	52	1.0	POINT EFFICIENCY = .45825
ALP022	19.52	51	1.0	52	1.0	POINT EFFICIENCY = .45438
ALP023	19.56	51	1.0	52	1.0	POINT EFFICIENCY = .45051
ALP024	19.59	51	1.0	52	1.0	POINT EFFICIENCY = .44664
ALP025	19.63	51	1.0	52	1.0	POINT EFFICIENCY = .44277
ALP026	19.66	51	1.0	52	1.0	POINT EFFICIENCY = .43890
ALP027	19.70	51	1.0	52	1.0	POINT EFFICIENCY = .43503
ALP028	19.74	51	1.0	52	1.0	POINT EFFICIENCY = .43116
ALP029	19.77	51	1.0	52	1.0	POINT EFFICIENCY = .42729
ALP030	19.81	51	1.0	52	1.0	POINT EFFICIENCY = .42342
ALP031	19.85	51	1.0	52	1.0	POINT EFFICIENCY = .41955
ALP032	19.89	51	1.0	52	1.0	POINT EFFICIENCY = .41568
ALP033	19.92	51	1.0	52	1.0	POINT EFFICIENCY = .41181
ALP034	19.96	51	1.0	52	1.0	POINT EFFICIENCY = .40794
ALP035	19.99	51	1.0	52	1.0	POINT EFFICIENCY = .40407
ALP036	20.03	51	1.0	52	1.0	POINT EFFICIENCY = .40020
ALP037	20.06	51	1.0	52	1.0	POINT EFFICIENCY = .39633
ALP038	20.10	51	1.0	52	1.0	POINT EFFICIENCY = .39246
ALP039	20.14	51	1.0	52	1.0	POINT EFFICIENCY = .38859
ALP040	20.17	51	1.0	52	1.0	POINT EFFICIENCY = .38472
ALP041	20.21	51	1.0	52	1.0	POINT EFFICIENCY = .38085
ALP042	20.25	51	1.0	52	1.0	POINT EFFICIENCY = .37698
ALP043	20.29	51	1.0	52	1.0	POINT EFFICIENCY = .37311
ALP044	20.33	51	1.0	52	1.0	POINT EFFICIENCY = .36924
ALP045	20.37	51	1.0	52	1.0	POINT EFFICIENCY = .36537
ALP046	20.41	51	1.0	52	1.0	POINT EFFICIENCY = .36150
ALP047	20.45	51	1.0	52	1.0	POINT EFFICIENCY = .35763
ALP048	20.49	51	1.0	52	1.0	POINT EFFICIENCY = .35376
ALP049	20.53	51	1.0	52	1.0	POINT EFFICIENCY = .34989
ALP050	20.57	51	1.0	52	1.0	POINT EFFICIENCY = .34602
ALP051	20.61	51	1.0	52	1.0	POINT EFFICIENCY = .34215
ALP052	20.65	51	1.0	52	1.0	POINT EFFICIENCY = .33828
ALP053	20.69	51	1.0	52	1.0	POINT EFFICIENCY = .33441
ALP054	20.73	51	1.0	52	1.0	POINT EFFICIENCY = .33054
ALP055	20.77	51	1.0	52	1.0	POINT EFFICIENCY = .32667
ALP056	20.81	51	1.0	52	1.0	POINT EFFICIENCY = .32280
ALP057	20.85	51	1.0	52	1.0	POINT EFFICIENCY = .31893
ALP058	20.89	51	1.0	52	1.0	POINT EFFICIENCY = .31506
ALP059	20.93	51	1.0	52	1.0	POINT EFFICIENCY = .31119
ALP060	20.97	51	1.0	52	1.0	POINT EFFICIENCY = .30732
ALP061	21.01	51	1.0	52	1.0	POINT EFFICIENCY = .30345
ALP062	21.05	51	1.0	52	1.0	POINT EFFICIENCY = .29958
ALP063	21.09	51	1.0	52	1.0	POINT EFFICIENCY = .29571
ALP064	21.13	51	1.0	52	1.0	POINT EFFICIENCY = .29184
ALP065	21.17	51	1.0	52	1.0	POINT EFFICIENCY = .28797
ALP066	21.21	51	1.0	52	1.0	POINT EFFICIENCY = .28410
ALP067	21.25	51	1.0	52	1.0	POINT EFFICIENCY = .28023
ALP068	21.29	51	1.0	52	1.0	POINT EFFICIENCY = .27636
ALP069	21.33	51	1.0	52	1.0	POINT EFFICIENCY = .27249
ALP070	21.37	51	1.0	52	1.0	POINT EFFICIENCY = .26862
ALP071	21.41	51	1.0	52	1.0	POINT EFFICIENCY = .26475
ALP072	21.45	51	1.0	52	1.0	POINT EFFICIENCY = .26088
ALP073	21.49	51	1.0	52	1.0	POINT EFFICIENCY = .25701
ALP074	21.53	51	1.0	52	1.0	POINT EFFICIENCY = .25314
ALP075	21.57	51	1.0	52	1.0	POINT EFFICIENCY = .24927
ALP076	21.61	51	1.0	52	1.0	POINT EFFICIENCY = .24540
ALP077	21.65	51	1.0	52	1.0	POINT EFFICIENCY = .24153
ALP078	21.69	51	1.0	52	1.0	POINT EFFICIENCY = .23766
ALP079	21.73	51	1.0	52	1.0	POINT EFFICIENCY = .23379
ALP080	21.77	51	1.0	52	1.0	POINT EFFICIENCY = .22992
ALP081	21.81	51	1.0	52	1.0	POINT EFFICIENCY = .22605
ALP082	21.85	51	1.0	52	1.0	POINT EFFICIENCY = .22218
ALP083	21.89	51	1.0	52	1.0	POINT EFFICIENCY = .21831
ALP084	21.93	51	1.0	52	1.0	POINT EFFICIENCY = .21444
ALP085	21.97	51	1.0	52	1.0	POINT EFFICIENCY = .21057
ALP086	22.01	51	1.0	52	1.0	POINT EFFICIENCY = .20670
ALP087	22.05	51	1.0	52	1.0	POINT EFFICIENCY = .20283
ALP088	22.09	51	1.0	52	1.0	POINT EFFICIENCY = .19896
ALP089	22.13	51	1.0	52	1.0	POINT EFFICIENCY = .19509
ALP090	22.17	51	1.0	52	1.0	POINT EFFICIENCY = .19122
ALP091	22.21	51	1.0	52	1.0	POINT EFFICIENCY = .18735
ALP092	22.25	51	1.0	52	1.0	POINT EFFICIENCY = .18348
ALP093	22.29	51	1.0	52	1.0	POINT EFFICIENCY = .17961
ALP094	22.33	51	1.0	52	1.0	POINT EFFICIENCY = .17574
ALP095	22.37	51	1.0	52	1.0	POINT EFFICIENCY = .17187
ALP096	22.41	51	1.0	52	1.0	POINT EFFICIENCY = .16800
ALP097	22.45	51	1.0	52	1.0	POINT EFFICIENCY = .16413
ALP098	22.49	51	1.0	52	1.0	POINT EFFICIENCY = .16026
ALP099	22.53	51	1.0	52	1.0	POINT EFFICIENCY = .15639
ALP100	22.57	51	1.0	52	1.0	POINT EFFICIENCY = .15252

U

ALPHA1 = 23.63 S1 = -1.0 SC = -1.0 POINT EFFICIENCY = .53423
ALPHA2 = 23.63 S2 = -1.0 POINT EFFICIENCY = .53423
CYCLE EFFICIENCY = .513

APPENDIX D
GEOMETRY OF GENERAL CLOCK GEAR TOOTH

The general ogival tooth of thickness t and outside radius r_o consists of a circular arc of radius ρ which blends tangentially into a radial tooth flank, as shown in Figure D-1 (only one center of curvature is indicated). The center of curvature, C , is located at a distance a from the center of the gear or pinion. Frequently this distance a equals the pitch radius r_p . The tooth geometry may either be described with the help of the parameters t , ρ and a , or with the combination t , ρ and r_o . Both approaches are shown below.

1. TOOTH GEOMETRY WITH HELP OF PARAMETERS t , ρ AND a

C_x and C_y represent the coordinates of the center of curvature C . C_x is defined by

$$C_x = \rho - \frac{t}{2} \quad (D-1)$$

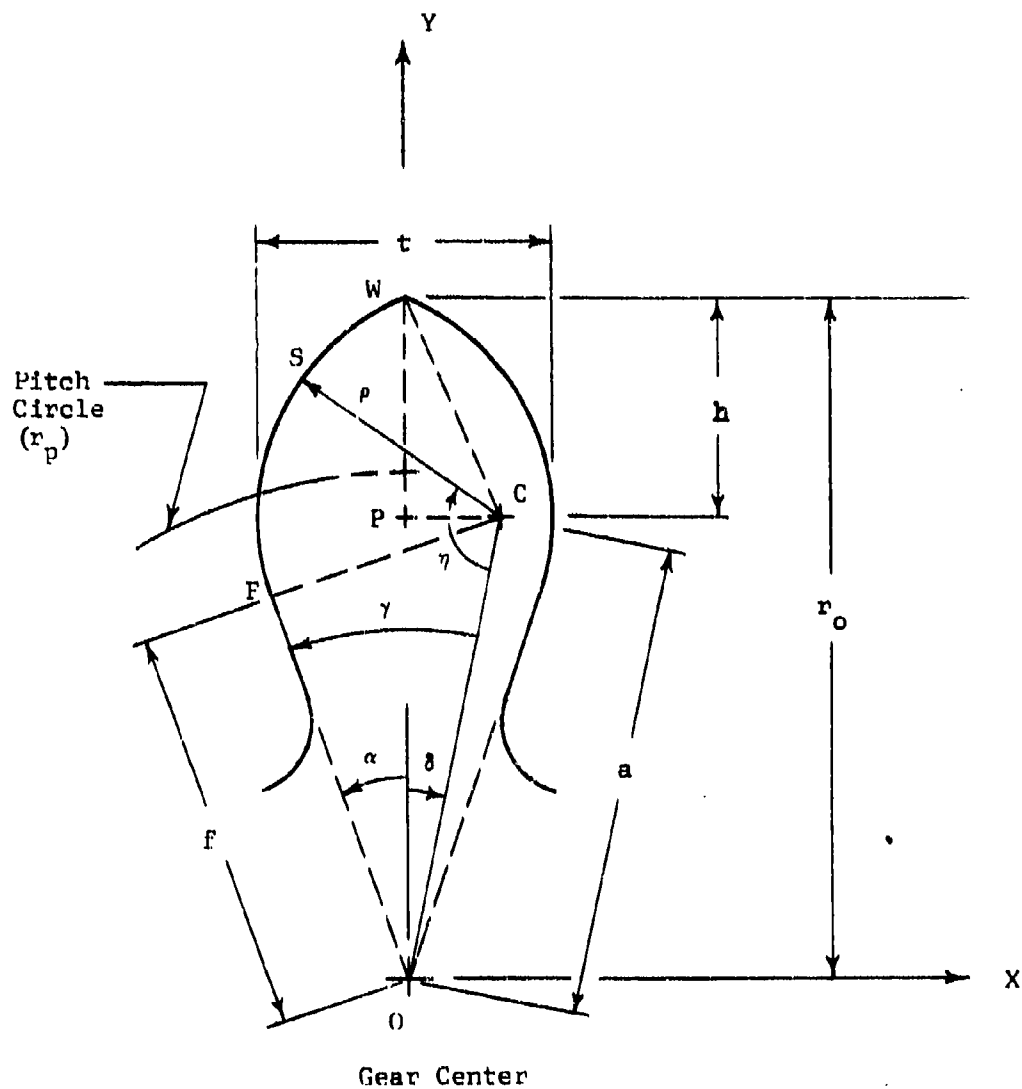


FIGURE D-1

GEOMETRY OF OGIVAL TOOTH (ONLY ONE CENTER OF CURVATURE SHOWN)

The angle δ is given by

$$\delta = \sin^{-1} \frac{C_x}{a} \quad (D-2)$$

With the above,

$$C_y = a \cos \delta \quad (D-3)$$

Further, the outside radius r_o may be computed from

$$r_o = C_y + \sqrt{\rho^2 - C_x^2} \quad (D-4)$$

The angle γ is obtained from

$$\gamma = \sin^{-1} \frac{\rho}{a}, \quad (D-5)$$

and the flank angle α from

$$\alpha = \gamma - \delta \quad (D-6)$$

The distance, f , from the center of rotation, O , to the blend point, F , of the flank of the tooth, is given by

$$f = a \cos \gamma \quad (D-7)$$

The angle γ defines the tooth contact point S on the ogival, i.e., circular, portion of the tooth with the lines OC and CS . The minimum and maximum angles γ_{\min} and γ_{\max} are, respectively,

$$\gamma_{\min} = \frac{\pi}{2} - \gamma \quad (D-8)$$

and

$$\gamma_{\max} = \sin^{-1} \frac{r_o \sin \delta}{\rho} \quad (D-9)$$

(This angle extends into the second quadrant)

2. TOOTH GEOMETRY FROM PARAMETERS ρ , t AND r_o

If the outside radius, r_o , is given, distance a must be computed. The length, C_x , is still given by Equation (D-1), while

$$a = \sqrt{(r_o - h)^2 + C_x^2} \quad (D-10)$$

where, according to Figure D-1,

$$h = \sqrt{\rho^2 - C_x^2} \quad (D-11)$$

All other quantities of interest remain as before, i.e.,

$$\delta = \sin^{-1} \frac{C_x}{a} \quad \text{See Equation (D-2)}$$

$$\gamma = \sin^{-1} \frac{\rho}{a} \quad \text{See Equation (D-5)}$$

$$\alpha = \gamma - \delta \quad \text{See Equation (D-6)}$$

$$f = a \cos \gamma \quad \text{See Equation (D-7)}$$

$$\eta_{\min} = \frac{\pi}{2} - \gamma \quad \text{See Equation (D-8)}$$

$$\eta_{\max} = \sin^{-1} \frac{r_o \sin \delta}{\rho} \quad \text{See Equation (D-9)}$$

APPENDIX E

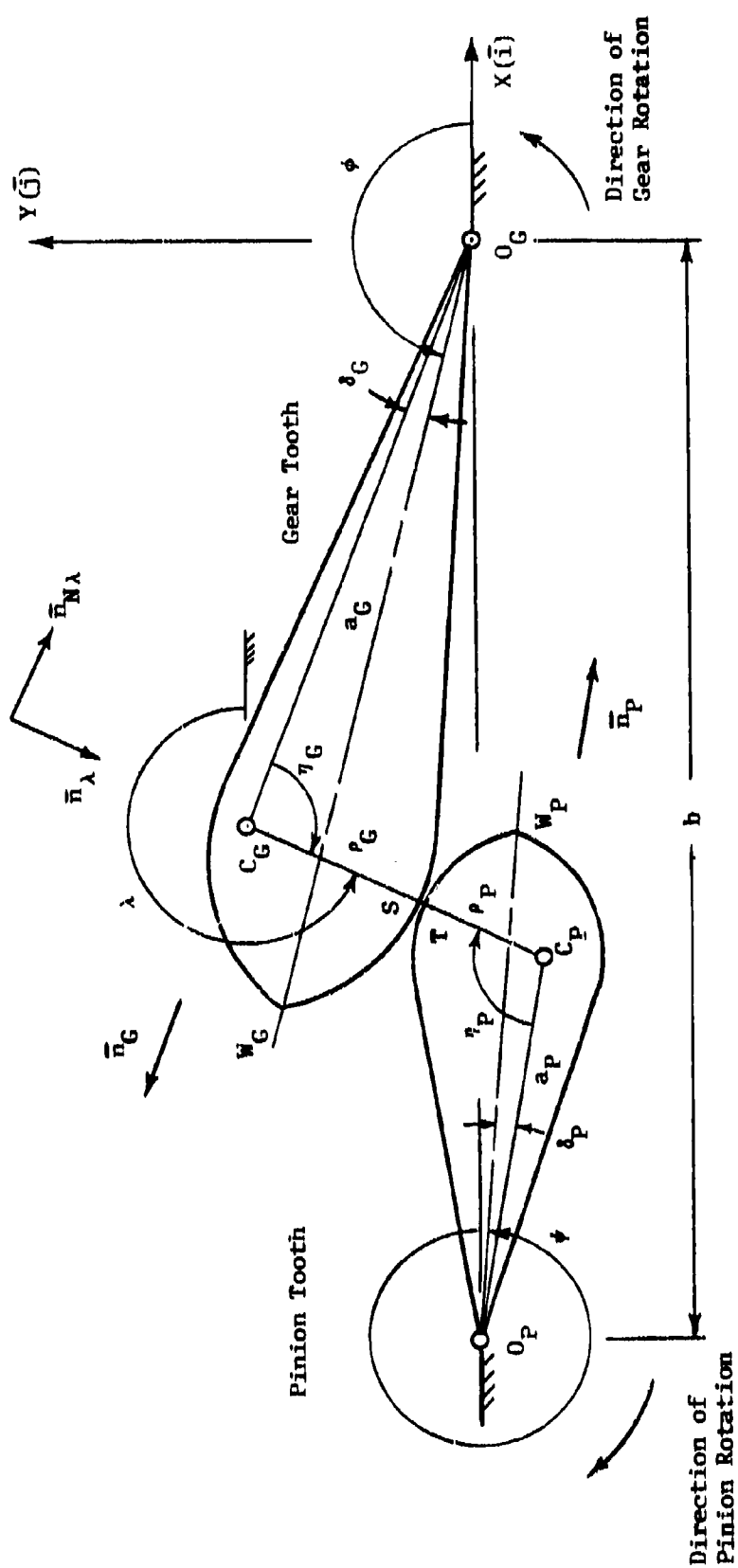
KINEMATICS AND MOMENT INPUT-OUTPUT RELATIONSHIP FOR SINGLE STEP-UP GEAR MESH WITH CLOCK TEETH

This appendix shows the kinematics of a single step-up gear mesh with ogival teeth and derives the moment input-output relationship. Both contact and pivot friction are included.

1. KINEMATICS OF AN OGIVE MESH

Figure E-1 indicates the condition of initial contact in ogival meshes when the circular arc portion of the gear tooth drives the circular arc portion of the pinion tooth.¹ This type of direct contact will be called "round on round". As the motion progresses, the circular arc of the gear tooth moves into contact with the straight flank of the pinion tooth (Figure E-2). During this "round on flat" phase, distance g at first decreases and then increases again. Before round on round contact can again occur for a given mesh, i.e., g has become equal to f_p again, the subsequent mesh comes into engagement with round on round contact. (See below.)

¹See section b-VII of this appendix for a check that indicates whether the initial contact is round on round or whether possibly the round portion of the pinion touches the flat portion of the gear.



E-2

FIGURE E-1

ROUND ON ROUND PHASE OF CONTACT (GEAR DRIVES PINION)

The kinematics of both round on round and round on flat phases will be given first. Further it will be shown how to determine those gear angles, ϕ , at which the regime changes from round on round to round on flat, and at which contact is taken over by the subsequent set of teeth. Since the ratio of angular velocities between gear and pinion varies with contact point, and the pinion moves faster for a given gear speed for round on round than for round on flat, the original set of teeth disengages as soon as the subsequent one makes contact. Thus, the contact ratio is unity for this type of gearing.

The gear tooth nomenclature given in Appendix D is used throughout. The additional subscripts G and P refer to gear and pinion, respectively.

a. ROUND ON ROUND PHASE OF MOTION

Figure E-1 shows the input angle ϕ as the angle between the x-axis and the center line, $O_G W_G$, of the gear tooth. The output angle, ψ , is the angle between the x-axis and the centerline $O_P W_P$. During this phase of motion, the line connecting the centers of curvature C_G and C_P is of constant length $L = \rho_G + \rho_P$ and passes

through the instantaneous contact points S on the gear and T on the pinion. Because of this constant length one may obtain both the output angle ψ and the "coupler" angle λ from the equivalent four-bar linkage $O_G-C_G-C_P-O_P$, with ground pivot distance b .

I. UNIT VECTORS AND ANGLES η_G AND η_P

The unit vectors associated with round on round phase are given now.

In direction O_G-C_G

$$\bar{n}_G = \cos(\phi - \delta_G)\bar{I} + \sin(\phi - \delta_G)\bar{J} \quad (E-1)$$

In direction C_G-C_P

$$\bar{n}_\lambda = \cos\lambda\bar{I} + \sin\lambda\bar{J} \quad (E-2)$$

The unit vector normal to \bar{n}_λ (in the right hand sense) becomes

$$\bar{n}_{N\lambda} = -\sin\lambda\bar{I} + \cos\lambda\bar{J} \quad (E-3)$$

In direction O_P-C_P .

$$\bar{n}_p = \cos(\psi - \delta_p)\bar{i} + \sin(\psi - \delta_p)\bar{j} \quad (E-4)$$

$$\text{Since } \lambda - (\phi - \delta_g) = \pi - \eta_g$$

$$\eta_g = \pi + \phi - \lambda - \delta_g \quad (E-5)$$

The angle η_p is obtained from

$$\eta_p = (\psi - \delta_p) - \lambda \quad \text{for } \psi - \delta_p > 90^\circ \quad (E-6a)$$

and

$$\eta_p = 2\pi + (\psi - \delta_p) - \lambda \quad \text{for } \psi - \delta_p < 90^\circ \quad (E-6b)$$

The above values for η_g and η_p are only good for the round on round phase of the motion. For the round on flat phase the angle η_{GF} of the gear, may be of interest. (See Figure E-2).

This angle is given by:

$$\eta_{GF} = (\phi - \delta_g) - (\psi + \alpha_p) + \frac{3\pi}{2} \quad \text{for } \psi + \alpha_p > 90^\circ \quad (E-6c)$$

and

$$\eta_{GF} = (\phi - \delta_g) - (\psi + \alpha_p) - \frac{\pi}{2} \quad \text{for } \psi + \alpha_p < 90^\circ \quad (E-6d)$$

[Pinion flank in
4th quadrant]

[Pinion flank in
first quadrant]

II. DETERMINATION OF OUTPUT ANGLE ψ AND "COUPLER" ANGLE λ

The loop equation of the equivalent four-bar linkage is given by

$$a_G \bar{n}_G + (\rho_G + \rho_P) \bar{n}_\lambda - a_P \bar{n}_P + b \bar{i} = 0 \quad (E-7)$$

With appropriate substitutions for the unit vectors, according to Equations (E-1), (E-2), and (E-4), one obtains the following component equation

$$a_G \cos(\phi - \delta_G) + L \cos \lambda + b - a_P \cos(\psi - \delta_P) = 0 \quad (E-8)$$

$$a_G \sin(\phi - \delta_G) + L \sin \lambda - a_P \sin(\psi - \delta_P) = 0 \quad (E-9)$$

where

$$L = \rho_G + \rho_P \quad (E-10)$$

To eliminate λ , let

$$\sin^2 \lambda + \cos^2 \lambda = 1 \quad (E-11)$$

Substitution of expressions for $\sin\lambda$ and $\cos\lambda$ from Equations (E-9) and (E-8), respectively, leads to

$$A_R \sin\psi + B_R \cos\psi = C_R \quad (E-12)$$

where

$$A_R = \sin(\phi - \delta_G) + \cos(\phi - \delta_G) \tan\delta_P + \frac{b}{a_G} \tan\delta_P$$

$$B_R = \cos(\phi - \delta_G) + \frac{b}{a_G} - \sin(\phi - \delta_G) \tan\delta_P$$

$$C_R = \frac{a_P^2 + a_G^2 + b^2 - L^2}{2a_P a_G \cos\delta_P} + \frac{b \cos(\phi - \delta_G)}{a_P \cos\delta_P}$$

Equation(E-12) is solved for ψ by a method similar to the one given on pg. 296 of R. S. Hartenberg and J. Denavit; Kinematic Synthesis of Linkages, McGraw-Hill Book Co., New York, 1964. Thus,

$$\psi = 2 \tan^{-1} \frac{A_R \pm \sqrt{A_R^2 + B_R^2 - C_R^2}}{B_R + C_R} \quad (E-13)$$

The correct sign in Equation (E-13) must be found from the geometric conditions of the equivalent four-bar linkage.

The "coupler" angle λ may now be determined either from Equation (E-8) or from Equation (E-9), i.e.,

$$\lambda = \cos^{-1} \left[\frac{a_P \cos(\psi - \delta_P) - a_G \cos(\phi - \delta_G) - b}{L} \right] \quad (E-14)$$

or

$$\lambda = \sin^{-1} \left[\frac{a_P \sin(\psi - \delta_P) - a_G \sin(\phi - \delta_G)}{L} \right] \quad (E-15)$$

III. DETERMINATION OF OUTPUT PINION ANGULAR VELOCITY $\dot{\psi}$

Differentiation of Equation (E-12) with respect to time leads to

$$\dot{\psi} = \dot{\phi} \left[\frac{A_{RD} \sin \psi + B_{RD} \cos \psi - C_{RD}}{A_R \cos \psi - B_R \sin \psi} \right] \quad (E-16)$$

where A_R and B_R are given with Equation (E-12), and where

$$A_{RD} = \tan \delta_P \sin(\phi - \delta_G) - \cos(\phi - \delta_G)$$

$$B_{RD} = \sin(\phi - \delta_G) + \tan \delta_P \cos(\phi - \delta_G)$$

$$C_{RD} = \frac{b}{a_P \cos \delta_P} \sin(\phi - \delta_G)$$

E-8

IV. RELATIVE VELOCITY AT CONTACT POINT BETWEEN GEAR AND PINION

With point S on the gear and point T on the pinion, as shown by Figure E-1, the relative velocity between gear and pinion at the contact point is given by

$$\mathbf{V}_{S/T} = \mathbf{V}_{S/O_G} - \mathbf{V}_{T/O_P} \quad (\text{E-17})$$

This relative velocity is tangent to the contacting surfaces and can therefore be expressed in terms of the unit vector $\bar{n}_{N\lambda}$ (see Figure E-1). Then, the above becomes

$$\mathbf{V}_{S/T} = \left[(\mathbf{V}_{S/O_G} \cdot \bar{n}_{N\lambda}) - (\mathbf{V}_{T/O_P} \cdot \bar{n}_{N\lambda}) \right] \bar{n}_{N\lambda} \quad (\text{E-18})$$

or

$$\mathbf{V}_{S/T} = \left\{ \left[\dot{\phi} \bar{k} \times (a_G \bar{n}_G + r_G \bar{n}_\lambda) \right] \cdot \bar{n}_{N\lambda} - \left[\dot{\psi} \bar{k} \times (a_P \bar{n}_P - r_P \bar{n}_\lambda) \right] \cdot \bar{n}_{N\lambda} \right\} \bar{n}_{N\lambda} \quad (\text{E-19})$$

Appropriate substitution of unit vectors and simplification results in

$$\mathbf{V}_{S/T} = \left\{ \dot{\phi} \left[a_G \cos(\phi - \theta_G - \lambda) + r_G \right] - \dot{\psi} \left[a_P \cos(\psi - \theta_P - \lambda) - r_P \right] \right\} \bar{n}_{N\lambda} \quad (\text{E-20})$$

b. ROUND ON FLAT PHASE OF MOTION

Figure E-2 gives the details of the round on flat contact between the driving gear and the driven pinion. The input angle ϕ and the output angle ψ are again defined counter-clockwise between the x-axis and the respective tooth center lines $O_G W_G$ and $O_P W_P$. Since contact is always made on the straight radial flank of the pinion, the line SC_G of the gear is always normal to the flank of the pinion. The contact point is at a distance g from the pinion center, O_P , and this distance is always smaller than, or equal to the distance f_P (which is defined by Equation (D-7) in Appendix D). Again, the subscripts G and P are used for gear and pinion tooth parameters, respectively.

I. UNIT VECTORS

As before, the unit vector in direction $O_G C_G$ is given by

$$\bar{n}_G = \cos(\phi - \delta_G)\bar{i} + \sin(\phi - \delta_G)\bar{j} \quad (E-21)$$

The unit vector in direction $O_P T$, along the flank of the pinion is given by

$$\bar{n}_F = \cos(\psi + \alpha_P)\bar{i} + \sin(\psi + \alpha_P)\bar{j} \quad (E-22)$$

The unit vector in direction SC_G is normal to \bar{n}_F in the right hand sense

$$\bar{n}_{NF} = -\sin(\psi + \alpha_P)\bar{i} + \cos(\psi + \alpha_P)\bar{j} \quad (E-23)$$

II. DETERMINATION OF OUTPUT ANGLE ψ AND DISTANCE g

The vector equation for the mechanism loop $O_G-C_G-S-T-O_P$, which forms the basis of the desired solution, has the following form:

$$a_G\bar{n}_G - \rho_G\bar{n}_{NF} - g\bar{n}_F + b\bar{i} = 0 \quad (E-24)$$

Substitution of Equations (E-21) to (E-23) furnishes the component equations

$$a_G\cos(\phi - \delta_G) + \rho_G\sin(\psi + \alpha_P) - g\cos(\psi + \alpha_P) + b = 0 \quad (E25)$$

$$a_G\sin(\phi - \delta_G) - \rho_G\cos(\psi + \alpha_P) - g\sin(\psi + \alpha_P) = 0 \quad (E26)$$

From Equation (E-26) one obtains for g

$$g = \frac{a_G \sin(\phi - \delta_G) - \rho_G \cos(\psi + \alpha_P)}{\sin(\psi + \alpha_P)} \quad (\text{E-27})$$

This expression for g is now substituted into Equation (E-25).

Rearrangement and simplification lead to

$$A_F \sin \psi + B_F \cos \psi = C_F \quad (\text{E-28})$$

where

$$A_F = b \cos \alpha_P + a_G \cos(\phi - \delta_G - \alpha_P)$$

$$B_F = b \sin \alpha_P - a_G \sin(\phi - \delta_G - \alpha_P)$$

$$C_F = -\rho_G$$

The solution of Equation (E-28) for ψ is obtained in the same way as that of Equation (E-13), i.e.,

$$\psi = 2 \tan^{-1} \frac{A_F \pm \sqrt{A_F^2 + B_F^2 - C_F^2}}{B_F + C_F} \quad (\text{E-29})$$

The correct sign in Equation (E-29) depends on the geometric conditions of the mechanism position as in all four-bar linkage solutions of this type.

III. DETERMINATION OF PINION ANGULAR VELOCITY $\dot{\psi}$

Differentiation of Equation (E-28) with respect to time gives

$$\dot{\psi} = \dot{\phi} \left[\frac{A_{FD} \sin \psi + B_{FD} \cos \psi}{A_F \cos \psi - B_F \sin \psi} \right] \quad (E-30)$$

where A_F and B_F are given with Equation (E-28) and where

$$A_{FD} = a_G \sin(\phi - \delta_G - \alpha_P)$$

$$B_{FD} = a_G \cos(\phi - \delta_G - \alpha_P)$$

IV. RELATIVE VELOCITY AT CONTACT POINT BETWEEN GEAR AND PINION

As for round on round contact, the relative velocity between point S on the gear tooth and point T on the pinion tooth is tangent to the contacting surfaces. In this case it will have the direction of unit vector \bar{H}_F (see Figure E-2).

Then,

$$\bar{V}_{S/T} = \bar{V}_{S/O_G} - \bar{V}_{T/O_P} = \left[(\bar{V}_{S/O_G} \cdot \bar{n}_F) - (\bar{V}_{T/O_P} \cdot \bar{n}_F) \right] \bar{n}_F \quad (E-31)$$

Since, because of the radial flank of the pinion, the velocity of the contact point T is normal to unit vector \bar{n}_F .

$$\bar{V}_{T/O_P} \cdot \bar{n}_F = 0 \quad (E-32)$$

Therefore,

$$\bar{V}_{S/T} = \left[\bar{V}_{S/O_G} \cdot \bar{n}_F \right] \bar{n}_F \quad (E-33)$$

or

$$\bar{V}_{S/T} = \left\{ \left[\dot{\phi} \bar{k} \times (a_G \bar{n}_P - r_G \bar{n}_{NF}) \right] \cdot \bar{n}_F \right\} \bar{n}_F \quad (E-34)$$

Appropriate substitution of unit vectors gives:

$$\bar{V}_{S/T} = \dot{\phi} \left[r_G + a_G \sin(\psi - \phi + \alpha_P + \delta_G) \right] \bar{n}_F \quad (E-35)$$

V. DETERMINATION OF TRANSITION ANGLES FROM ROUND ON ROUND TO
ROUND ON FLAT MOTION

The transition angles ϕ_T and ψ_T , which occur when the round on flat phase follows the round on round one, may be determined with the help of the modified component equations (E-25) and (E-26), i.e., one lets $\phi = \phi_T$, $\psi = \psi_T$ and $g = f_P$. This results in

$$a_G \cos(\phi_T - \delta_G) + \rho_G \sin(\psi_T + \alpha_P) - f_P \cos(\psi_T + \alpha_P) + b = 0 \quad (E-36)$$

and

$$a_G \sin(\phi_T - \delta_G) - \rho_G \cos(\psi_T + \alpha_P) - f_P \sin(\psi_T + \alpha_P) = 0 \quad (E-37)$$

From the above,

$$\cos(\phi_T - \delta_G) = \frac{1}{a_G} [f_P \cos(\psi_T + \alpha_P) - b - \rho_G \sin(\psi_T + \alpha_P)] \quad (E-38)$$

and

$$\sin(\phi_T - \delta_G) = \frac{1}{a_G} [f_P \sin(\psi_T + \alpha_P) + \rho_G \cos(\psi_T + \alpha_P)] \quad (E-39)$$

The angle ψ_T may now be obtained by first eliminating ϕ_T from Equations (E-38) and (E-39). This is accomplished with

$$\sin^2(\phi_T - \delta_G) + \cos^2(\phi_T - \delta_G) = 1 \quad (E-40)$$

Substitution into the above leads to the following expression in ψ_T :

$$A_T \sin \psi_T + B_T \cos \psi_T = C_T \quad (E-41)$$

where

$$A_T = \rho_G \cos \alpha_P + f_P \sin \alpha_P$$

$$B_T = \rho_G \sin \alpha_P - f_P \cos \alpha_P$$

$$C_T = \frac{a_G^2 - f_P^2 - b^2 - \rho_G^2}{2b}$$

Equation (E-41) is again solved in the manner of Equation (E-13)

$$\psi_T = 2 \tan^{-1} \frac{A_T \pm \sqrt{A_T^2 + B_T^2 - C_T^2}}{B_T + C_T} \quad (E-42)$$

The correct sign must again be determined from the geometric conditions.

The associated transition angle ϕ_T can now be obtained either with the help of Equation (E-38) or Equation (E-39):

$$\phi_T = \cos^{-1} \left[\frac{f_P \cos(\psi_T + \alpha_P) - r_G \sin(\psi_T + \alpha_P) - b}{a_G} \right] + \delta_G \quad (E-43)$$

or

$$\phi_T = \sin^{-1} \left[\frac{f_P \sin(\psi_T + \alpha_P) + r_G \cos(\psi_T + \alpha_P)}{a_G} \right] + \delta_G \quad (E-44)$$

VI. SENSING GEOMETRY FOR THE DETERMINATION OF CONTACT OF SUBSEQUENT TOOTH MESH

The following derives a computer sensing equation which indicates when contact is transferred from one tooth mesh to the succeeding one. Figure E-3 illustrates the case. The active mesh is in the round on flat mode and the subsequent mesh will make its initial contact in the round on round mode. This

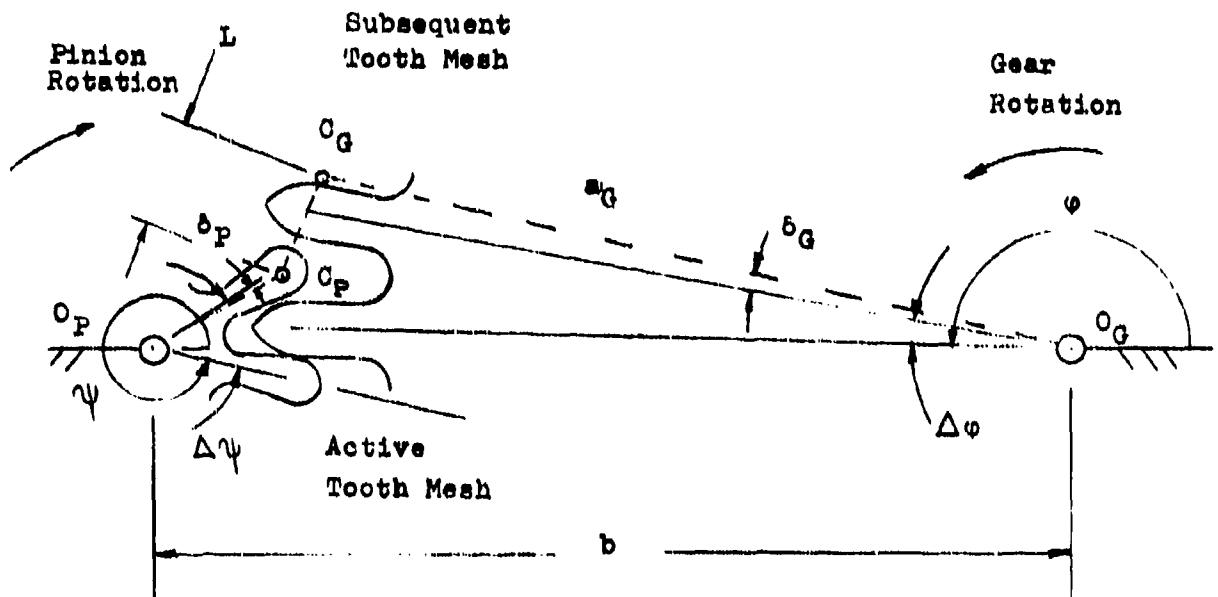


Figure E3
 Sensing Geometry for Contact of
 Subsequent Tooth Mesh

assertion is based on experience with the three gear and pinion combinations of the M125A1 booster. In each of these instances, the subsequent mesh makes contact before the round of the gear has left the flat of the pinion in the active mesh, i.e., $g < f_p$. (See work in section V.) It has also been found that initial contact of the subsequent mesh is always in the round on round mode. Generally, contact between the flat of the gear and the round of the pinion does not occur, and it has not been considered in this report. Section VII gives a criterion for the existence of this inverted round on flat mode of contact.

Once contact has been made by the subsequent mesh it becomes the new active mesh. This can be proven by the fact that, for a given angular velocity $\dot{\phi}$ of the gear, the angular velocity of the pinion is always larger in the initial stages of the round on round mode than in the final stages of the round on flat one. Thus, once the new mesh has made contact, the old one separates rapidly and the "contact ratio" is always unity.

The above may be shown theoretically by the position of the instant center of rotation between the gear and the pinion on line $O_G O_P$.

If $\Delta\phi$ and $\Delta\psi$ represent the angles between the individual tooth center lines of the gear and pinion, respectively, (see Figure E-3), the

closure equation for the subsequent mesh may be written in terms of the active mesh as follows:

$$\begin{aligned}
 a_p [\cos(\psi - \delta_p + \Delta\psi)\bar{I} + \sin(\psi - \delta_p + \Delta\psi)\bar{J}] + L_x\bar{I} + L_y\bar{J} \\
 = b\bar{I} + a_g [\cos(\phi - \delta_g - \Delta\phi)\bar{I} + \sin(\phi - \delta_g - \Delta\phi)\bar{J}]
 \end{aligned}
 \tag{E-45}$$

where L_x, L_y = components of the distance $L = C_p C_g$

ψ = pinion angle determined from round on flat
mode according to Equation (E-29)

The components L_x and L_y may be obtained from Equation (E-45):

$$L_x = b + a_g \cos(\phi - \delta_g - \Delta\phi) - a_p \cos(\psi - \delta_p + \Delta\psi)
 \tag{E-46}$$

and

$$L_y = a_g \sin(\phi - \delta_g - \Delta\phi) - a_p \sin(\psi - \delta_p + \Delta\psi)
 \tag{E-47}$$

Contact will have occurred when the distance L becomes equal to, or slightly smaller than, the sum of the two radii of curvature ρ_G and ρ_P . Thus, the criterion of contact becomes

$$\sqrt{L_x^2 + L_y^2} \leq \rho_G + \rho_P \quad (E-48)$$

VII. POSSIBILITY OF FLAT OF GEAR MAKING CONTACT WITH THE
ROUND PORTION OF THE PINION

Figure E-4 shows a transition configuration in which the flat part of the gear tooth makes contact with the circular arc of the pinion, i.e., $\overline{O_G S} = f_G$. The radius of curvature ρ_P of the pinion will only then be normal to the flat of the gear

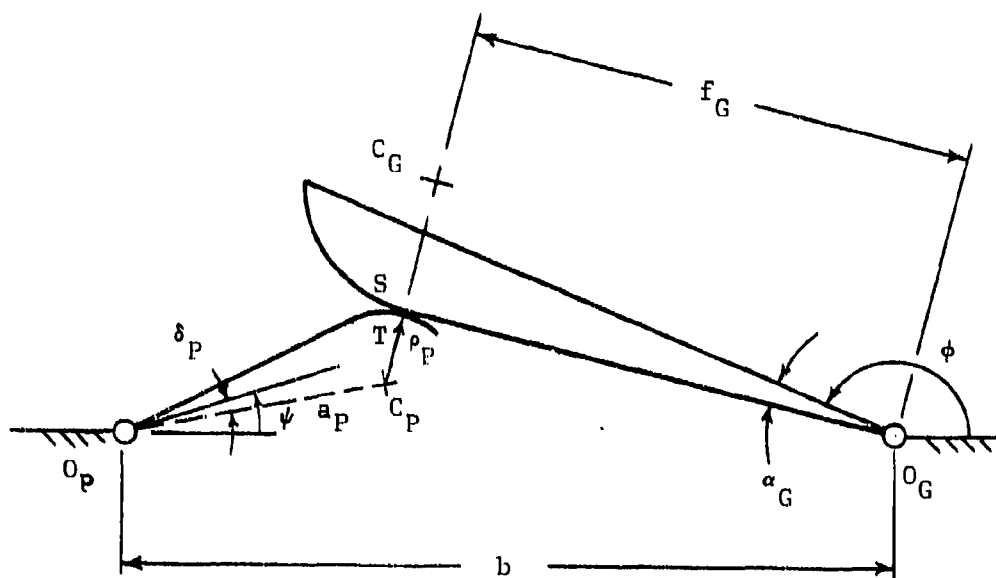


FIGURE E-4

FLAT OF GEAR CONTACTS ROUND OF PINION

when $\overline{O_G S} \leq f_G$. Accordingly, in order to avoid this type of contact, the following criterion must be met:

$$b > \left[a_P + \sqrt{f_G^2 + \rho_P^2} \right] \quad (E-49)$$

The three gear meshes of the M125A1 booster always satisfy equation (E-49), and therefore the initial contact is made in the round on round mode.

2. MOMENT INPUT-OUTPUT RELATIONSHIP FOR SINGLE STEP-UP GEAR MESH WITH OGIVAL TEETH

The present section concerns itself with the determination of the equilibrant moment M_o acting on the output pinion of a single ogival mesh, when the input moment M_{in} , which acts on the gear, is given. This relationship must be derived both for the round on round and for the round on flat phases of the motion. The directions of the pivot friction forces are again chosen such that the resulting moments oppose the motion of the respective component. (See Appendix A.) The magnitude of these friction moments is expressed in the manner of equation (A-2) of the aforementioned appendix. The direction of the friction force of the gear on the pinion is the same as the direction of the relative velocity $V_{S/T}$, of the gear contact point S with respect to the pinion contact point T. This will be expressed by the appropriate signum convention. It must also be remembered that the kinematic expressions must conform to the motion phase under consideration.

a. INPUT-OUTPUT RELATIONSHIP FOR THE ROUND ON ROUND PHASE OF MOTION

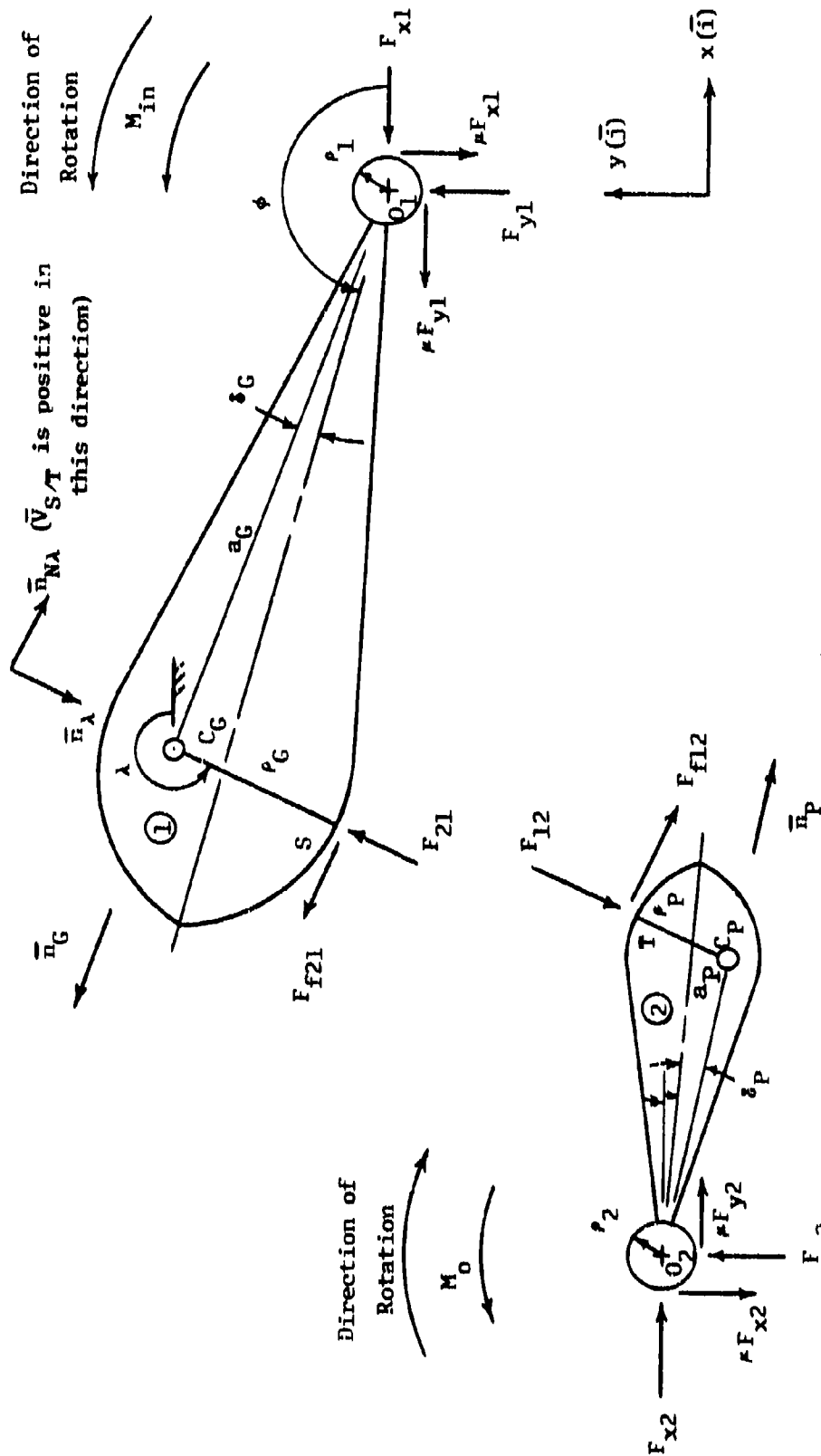
Figure E-5 shows the free body diagrams for the round on round phase of motion with the gear considered to be component no. 1 and the pinion defined as component no. 2. The contact forces F_{12} and F_{21} are expressed with the help of the unit vector \bar{n}_λ [see equation (E-2)]. This unit vector is always normal to both contacting surfaces at points S and T. The unit vector $\bar{n}_{N\lambda}$ is used to describe the direction of the friction forces at the contact point. The sense of these friction forces is determined with the help of

$$s = \frac{v_{S/T}}{|v_{S/T}|} \quad (E-50)$$

(See equation (E-20) for $\bar{v}_{S/T}$.) Since the friction force F_{f12} of the gear on the pinion has the same direction as the relative velocity $v_{S/T}$, one may write

$$\bar{F}_{f12} = \mu s F_{12} \bar{n}_{N\lambda} \quad (E-51)$$

where μ represents the coefficient of friction at the contact point.



Note: ϕ is positive in
ccw direction

FIGURE E-5

FREE BODY DIAGRAM FOR ROUND ON ROUND PHASE

Since

$$\bar{F}_{21} = -F_{12}\bar{n}_\lambda \quad (E-52)$$

the friction force of the pinion on the gear becomes

$$\bar{F}_{f21} = -\mu s F_{12}\bar{n}_{N\lambda} \quad (E-53)$$

I. FORCE AND MOMENT EQUILIBRIUM OF THE GEAR

The force equilibrium of the gear is assured when

$$-F_{12}\bar{n}_\lambda - \mu s F_{12}\bar{n}_{N\lambda} - F_{x1}\bar{i} + F_{y1}\bar{j} - \mu F_{y1}\bar{i} - \mu F_{x1}\bar{j} = 0 \quad (E-54)$$

In the above μ also stands for the pivot coefficient of friction.

Moment equilibrium is given by

$$M_{1n}\bar{k} - \mu p_1 \sqrt{F_{x1}^2 + F_{y1}^2} \bar{k} + [a_G\bar{n}_G + p_G\bar{n}_\lambda] \times [-F_{12}\bar{n}_\lambda - \mu s F_{12}\bar{n}_{N\lambda}] = 0 \quad (E-55)$$

The unit vector \bar{n}_G is defined by equation (E-1).

The following component equations may be obtained from equation (E-54):

$$-F_{12}\cos\lambda + \mu s F_{12}\sin\lambda - F_{x1} - \mu F_{y1} = 0 \quad (E-56)$$

and

$$-F_{12}\sin\lambda - \mu s F_{12}\cos\lambda + F_{y1} - \mu F_{x1} = 0 \quad (E-57)$$

After substitution and cross-multiplication, one obtains the moment expression, equation (E-55), in scalar form:

$$M_{1n} - \mu \rho_1 \sqrt{F_{x1}^2 + F_{y1}^2} + F_{12} \left[-\mu s \rho_G + a_G \sin(\phi - \delta_G - \lambda) - \mu s a_G \cos(\phi - \delta_G - \lambda) \right] = 0 \quad (E-58)$$

Simultaneous solution of equations (E-56) and (E-57) for F_{x1} and F_{y1} results in

$$F_{x1} = -F_{12} \left[\frac{(1 + \mu^2 s)\cos\lambda + \mu(1 - s)\sin\lambda}{1 + \mu^2} \right] \quad (E-59)$$

and

$$F_{y1} = F_{12} \left[\frac{(1 + \mu^2 s)\sin\lambda - \mu(1 - s)\cos\lambda}{1 + \mu^2} \right] \quad (E-60)$$

These results are now substituted in equation (E-58). Since s^2 is unity and always positive, the resulting expression for F_{12} has the following form:

$$F_{12} = \frac{M_{in}}{\mu(p_1 + s p_G) + s_G [\mu s \cos(\phi - \delta_G - \lambda) - \sin(\phi - \delta_G - \lambda)]}$$

(E-61)

II. FORCE AND MOMENT EQUILIBRIUM OF THE PINION

Force equilibrium of the pinion is assured by

$$F_{12} \bar{n}_\lambda + \mu s F_{12} \bar{n}_{N\lambda} + F_{x2} \bar{i} + F_{y2} \bar{j} + \mu F_{y2} \bar{i} - \mu F_{x2} \bar{j} = 0$$

(E-62)

Moment equilibrium must satisfy

$$M_O \bar{k} + \mu p_2 \sqrt{F_{x2}^2 + F_{y2}^2} \bar{k} + [a_P \bar{n}_P - r_P \bar{n}_\lambda] \times [F_{12} \bar{n}_\lambda + \mu s F_{12} \bar{n}_{N\lambda}] = 0$$

(E-63)

The unit vector \bar{n}_p is defined by equation (E-4).

Equation (E-62) gives rise to the following component equations:

$$F_{12}\cos\lambda - \mu s F_{12}\sin\lambda + F_{x2} + \mu F_{y2} = 0 \quad (E-64)$$

and

$$F_{12}\sin\lambda + \mu s F_{12}\cos\lambda + F_{y2} - \mu F_{x2} = 0 \quad (E-65)$$

The moment equation (E-63) becomes, in scalar form,

$$M_o + \mu p_2 \sqrt{F_{x2}^2 + F_{y2}^2} + F_{12} \left[-\mu s r_p - a_p \sin(\psi - \theta_p - \lambda) + \mu s a_p \cos(\psi - \theta_p - \lambda) \right] = 0 \quad (E-66)$$

Simultaneous solution of equations (E-64) and (E-65) for F_{x2} and F_{y2} results in

$$F_{x2} = F_{12} \left[\frac{\mu(1+s)\sin\lambda - (1-\mu^2 s)\cos\lambda}{1 + \mu^2} \right] \quad (E-67)$$

and

$$F_{y2} = -F_{12} \left[\frac{\mu(1+s)\cos\lambda + (1+\mu^2 s)\sin\lambda}{1 + \mu^2} \right] \quad (E-68)$$

The above expressions are now substituted into equation (E-66).

Again, s^2 is unity and always positive, and the following expression may be obtained for the contact force F_{12} in terms of the equilibrant moment M_0

$$F_{12} = \frac{M_0}{\mu(s_P r_P - r_2) - s_P [\mu s \cos(\psi - \delta_P - \lambda) - \sin(\psi - \delta_P - \lambda)]} \quad (\text{E-69})$$

III. MOMENT INPUT-OUTPUT RELATIONSHIP

When equations (E-61) and (E-69) are set equal to each other, one obtains the following input-output relationship:

$$M_0 = M_{in} \left[\frac{\mu(s_R r_P - r_2) - s_P [\mu s_R \cos(\psi - \delta_P - \lambda) - \sin(\psi - \delta_P - \lambda)]}{\mu(r_1 + s_R r_G) + s_G [\mu s_R \cos(\phi - \delta_G - \lambda) - \sin(\phi - \delta_G - \lambda)]} \right] \quad (\text{E-70})$$

To account for the fact that equ.(E-70) is only valid for the round on round phase of motion, the signum symbol has now been changed to s_R .

b. INPUT-OUTPUT RELATIONSHIP FOR ROUND ON FLAT PHASE OF MOTION

Figure E-6 gives the free body diagrams for the round on flat phase of the motion. Again, the gear is considered to be component no. 1, while the pinion is component no. 2. Using the unit vector \bar{n}_{NF} , of equation (E-22), which is normal to the flat side of the pinion to express the force \bar{F}_{12} of the gear on the pinion, one obtains

$$\bar{F}_{12} = -F_{12}\bar{n}_{NF} \quad (E-71)$$

The friction force of the gear on the pinion again has the same direction as the now applicable relative velocity $\bar{V}_{S/T}$ of equation (E-35). With

$$s = \frac{V_{S/T}}{|V_{S/T}|} \quad (E-72)$$

as the applicable signum convention, the friction force \bar{F}_{f12} becomes

$$\bar{F}_{f12} = \mu s F_{12} \bar{n}_F \quad (E-73)$$

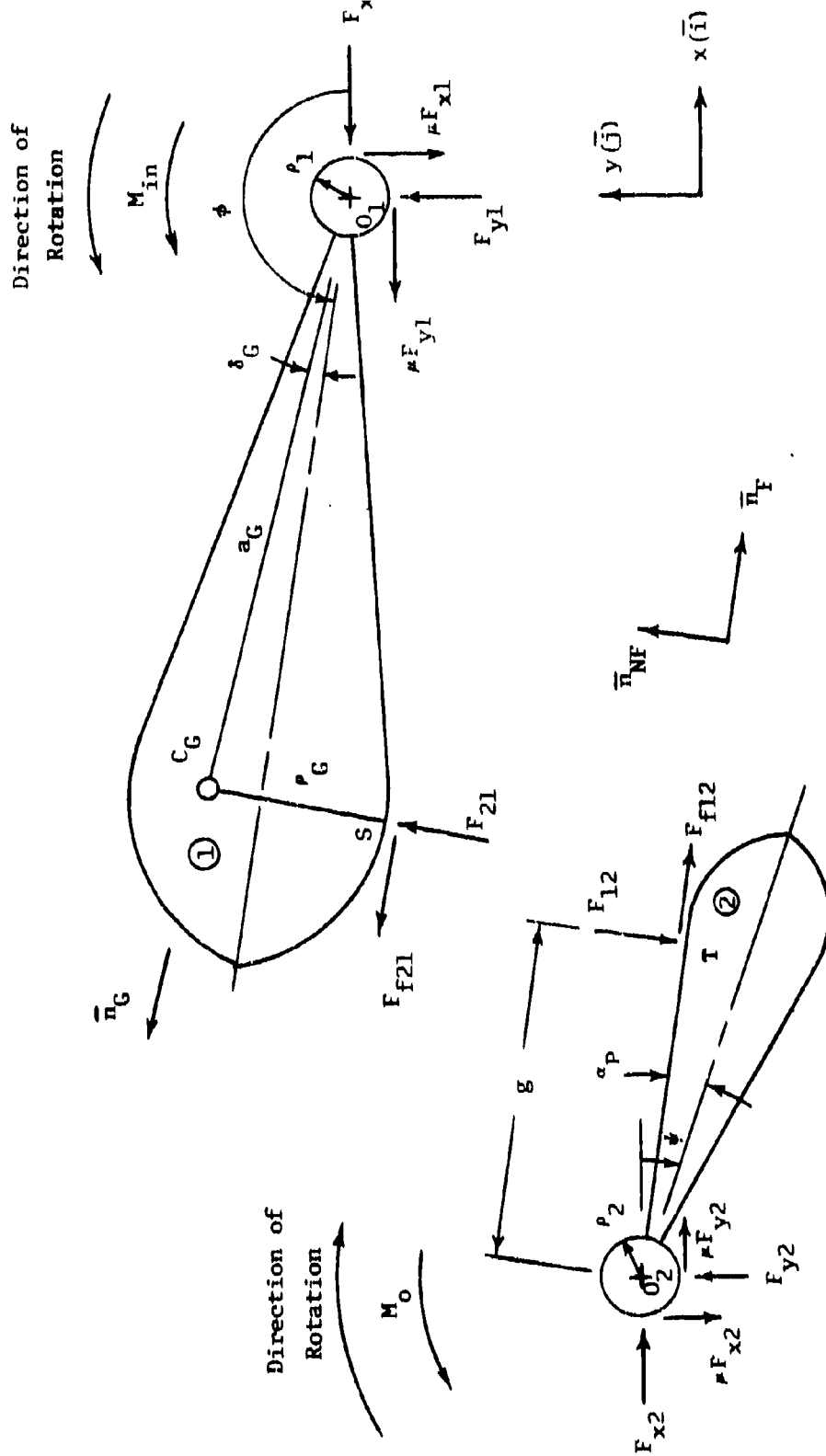


FIGURE E-6

FREE BODY DIAGRAM FOR ROUND ON FLAT PHASE

The contact force \bar{F}_{21} of the pinion on the gear and the associated friction force are equal and opposite to the forces given by equations (E-71) and (E-73) respectively. Thus,

$$\bar{F}_{21} = F_{12} \bar{n}_{NF} \quad (E-74)$$

and

$$\bar{F}_{f21} = -\mu s F_{12} \bar{n}_F \quad (E-75)$$

Note that the kinematics of the round on flat phase must now be used.

I. FORCE AND MOMENT EQUILIBRIUM OF THE GEAR

Force equilibrium of the gear is given by

$$F_{12} \bar{n}_{NF} - \mu s F_{12} \bar{n}_F - F_{x1} \bar{i} + F_{y1} \bar{j} - \mu F_{y1} \bar{i} - \mu F_{x1} \bar{j} = 0 \quad (E-76)$$

Moment equilibrium requires

$$M_{in} \bar{k} - \mu \rho_1 \sqrt{F_{x1}^2 + F_{y1}^2} \bar{k} + [s_G \bar{n}_G - \rho_G \bar{n}_{NF}] \times [F_{12} \bar{n}_{NF} - \mu s F_{12} \bar{n}_F] = 0 \quad (E-77)$$

Equation (E-76) furnishes the following component expressions

$$-F_{12}\sin(\psi + \alpha_P) - \mu s F_{12}\cos(\psi + \alpha_P) - F_{x1} - \mu F_{y1} = 0 \quad (E-78)$$

and

$$F_{12}\cos(\psi + \alpha_P) - \mu s F_{12}\sin(\psi + \alpha_P) + F_{y1} - \mu F_{x1} = 0 \quad (E-79)$$

The scalar form of equation (E-77) is given by

$$M_{in} - \mu p_1 \sqrt{F_{x1}^2 + F_{y1}^2} + F_{12}[-\mu s p_G + a_G \cos(\phi - \delta_G - \psi - \alpha_P) + \mu s a_G \sin(\phi - \delta_G - \psi - \alpha_P)] = 0 \quad (E-80)$$

Simultaneous solution of equations (E-78) and (E-79) for F_{x1} and F_{y1} furnishes

$$F_{x1} = F_{12} \left[\frac{\mu(1 - s)\cos(\psi + \alpha_P) - (1 + \mu^2 s)\sin(\psi + \alpha_P)}{1 + \mu^2} \right] \quad (E-81)$$

and

$$F_{y1} = -F_{12} \left[\frac{\mu(1 - s)\sin(\psi + \alpha_P) + (1 + \mu^2 s)\cos(\psi + \alpha_P)}{1 + \mu^2} \right] \quad (E-82)$$

The above results are now substituted into equation (E-80).

Since s^2 is again unity and positive at all times, the resulting expression for F_{12} becomes, in terms of M_{in} ,

$$F_{12} = \frac{M_{in}}{\mu(\rho_1 + s\rho_G) - a_G[\cos(\phi - \delta_G - \psi - \alpha_P) + \mu s \sin(\phi - \delta_G - \psi - \alpha_P)]}$$

(E-83)

II . FORCE AND MOMENT EQUILIBRIUM OF THE PINION

Force equilibrium of the pinion is expressed by

$$-F_{12}\bar{n}_{NF} + \mu s F_{12}\bar{n}_F + F_{x2}\bar{i} + F_{y2}\bar{j} + \mu F_{y2}\bar{i} - \mu F_{x2}\bar{j} = 0$$

(E-84)

Moment equilibrium requires that

$$M_o\bar{k} + \mu\rho_2\sqrt{F_{x2}^2 + F_{y2}^2}\bar{k} + g\bar{n}_F \times (-F_{12}\bar{n}_{NF}) = 0$$

(E-85)

Equation (E-84) furnishes the following component equations

$$F_{12}\sin(\psi + \alpha_P) + \mu s F_{12}\cos(\psi + \alpha_P) + F_{x2} + \mu F_{y2} = 0$$

(E-86)

and

$$-F_{12}\cos(\psi + \alpha_P) + \mu s F_{12}\sin(\psi + \alpha_P) + F_{y2} - \mu F_{x2} = 0$$

(E-87)

The scalar form of the moment equation (E-85) becomes

$$M_0 + \mu P_2 \sqrt{F_{x2}^2 + F_{y2}^2} - s F_{12} = 0$$

(E-88)

Simultaneous solution of equations (E-86) and (E-87) for F_{x2}

and F_{y2} leads to

$$F_{x2} = -F_{12} \left[\frac{(1 - \mu^2 s)\sin(\psi + \alpha_P) + \mu(1 + s)\cos(\psi + \alpha_P)}{1 + \mu^2} \right]$$

(E-89)

and

$$F_{y2} = F_{12} \left[\frac{(1 - \mu^2 s)\cos(\psi + \alpha_P) - \mu(1 + s)\sin(\psi + \alpha_P)}{1 + \mu^2} \right]$$

(E-90)

The above expressions are now substituted into equation (E-88).

Again, s^2 is unity and positive. The following expression for

F_{12} is now obtained

$$F_{12} = \frac{M_0}{\epsilon - \mu^2} \quad (E-91)$$

III. MOMENT INPUT-OUTPUT RELATIONSHIP

When equations (E-83) and (E-91) are set equal to each other, one obtains the following input-output relationship:

$$M_0 = M_{in} \left[\frac{\epsilon - \mu^2}{\mu(\rho_1 + s_F \rho_G) - s_G [\cos(\phi - \delta_G - \psi - \alpha_P) + \mu s_F \sin(\phi - \delta_G - \psi - \alpha_P)]} \right] \quad (E-92)$$

Note that the signum symbol has been changed to s_F in the above expression to account for the fact that the expression is only valid in the round on flat phase of motion.

APPENDIX F
COMPUTER MODELS FOR A SINGLE
STEP-UP GEAR MESH WITH CLOCK TEETH

The present appendix contains descriptions, listings and sample outputs of the following computer models relating to single step-up gear meshes containing clock (ogival) teeth

1. Program CLOCK 1: Kinematics of single pass step-up gear mesh with clock (ogival) teeth
2. Program CLOCK 2: Point and cycle efficiencies for single pass step-up gear mesh with clock (ogival) teeth

The relevant background, the input parameters, the manner of the computations, and the form of the output of each program are discussed in detail. The program proper forms the last part of each section.

1. Program CLOCK 1: Kinematics of Single Pass Step-Up Gear

Mesh With Clock (Ogival) Teeth

The program CLOCK 1 is based upon that portion of Appendix E which deals with the kinematics of single mesh step-up clock gearing. It may be used to check on the geometric performance of clock type meshes.

The nomenclature of the program is chosen to coincide as much as possible with that of Appendix D as well as that of Appendix E.

a. Input Parameters (see Program CLOCK 1, below)

The following parameters represent the input data for the program:

CAPRP = R_p , the pitch radius of the gear

RP = r_p , the pitch radius of the pinion

AG = a_G , the distance from the center of rotation of the gear to the center of curvature of the circular arc portion of the gear tooth

AP = a_p , the distance from the center of rotation of the pinion to the center of curvature of the circular arc portion of the pinion tooth

RHOG = ρ_G , the radius of curvature of the circular arc portion of the gear tooth

RHOP = ρ_p , the radius of curvature of the circular arc portion of the pinion tooth

TG = t_G , the maximum thickness of the gear tooth

TP = t_p , the maximum thickness of the pinion tooth

NG = n_G , the number of teeth of the gear

NP = n_p , the number of teeth of the pinion

K = range divisor

PHIDOT = $\dot{\phi} = 1$, all velocity computations are based on this value

b. Computations (see also COMMENT cards in program)

I. Computation of Gear Tooth Parameters

The following tooth parameters of the gear as well as of the pinion are first computed:

For the gear

CXG = c_{xG} (see eq. (D-1))

DELG = δ_G (see eq. (D-2))

CYG = c_{yG} (see eq. (D-3))

ROG = r_{oG} (see eq. (D-4))

GAMMG = γ_G (see eq. (D-5))

ETMING = v_{minG} (see eq. (D-8))

ETMAXG = v_{maxG} (see eq. (D-9))

For the pinion

CXP = c_{xP} (see eq. (D-1))

DELP = δ_P (see eq. (D-2))

CYP = c_{yP} (see eq. (D-3))

ROP = r_{oP} (see eq. (D-4))

GAMMP = γ_P (see eq. (D-5))

ALPHP = α_P (see eq. (D-6))

$ETMINP = r_{minp}$ (see eq. (D-8))

$ETMAXP = r_{maxp}$ (see eq. (D-9))

$FP = f_p$ (see eq. (D-7))

In general

$B = b$, the center distance between the gear and the pinion

$DPHI = \Delta\phi$, the angle between the center lines of adjacent gear teeth

$DPSI = \Delta\psi$, the angle between the center lines of adjacent pinion teeth

L (see eq. (E-10))

II. Determination of Transition Angle

In order to define the ranges for the round on round and the round on flat phases of motion, it is first necessary to locate the transition angles ϕ_T and ψ_T . This is accomplished with the help of the expression contained in section 1b-V, Appendix E. The transition angle ψ_T is first solved according to eq. (E-42). Since the solution furnishes two answers, i.e., the angles ψ_{T1} and ψ_{T2} , it is necessary to decide which of these is the desired one. The principal criterion for selecting the correct value of ψ_T is based on the motion of the contact point T with respect to the pinion. The first transition angles ψ_{T1} and ϕ_{T1} occur as the contact point moves from the round portion of the pinion to the flat one (for increasing values of ϕ). As this motion is continued, the distance g becomes smaller than the transition parameter f_p . Once g has reached its minimum, the contact point moves outward on the

pinion flat until g theoretically equals f_p once again. This part of the motion is never completed in actuality since the subsequent set of teeth takes over before g reaches this transition value. It is this second transition situation which corresponds to the transition angles ψ_{T2} and ϕ_{T2} . Since the round on flat equation does not recognize any limitation on the length of the pinion flat, an increase of ϕ over the value of ϕ_{T2} will have associated with it a theoretical value for g which is larger than f_p . Thus, one may identify the correct value of ϕ_T and ψ_T by noting that an increase in the angle ϕ must lead to an associated value of g which is smaller than f_p .

The program uses this criterion in the following manner after ψ_{T1} and ψ_{T2} are known:

A. Subroutine TRANS is called and the angle ϕ_{T1} , which is associated with ψ_{T1} , is computed with the help of eqs. (E-43) and (E-44).

B. The angle ϕ is made slightly larger than ϕ_{T1} to produce PHINEXT, and eq. (E-29) is used to find the associated angle PSINEX. Since there are two such angles, the subroutine selects the one which is closest to the value of transition angle ψ_{T1} . Subsequently, the associated value of g_1 is computed according to eq. (E-27).

C. Steps A and B are then repeated identically for the second transition angle ψ_{T2} . This results in the determination of g_2 .

D. Control remains with the main program, and that value of ψ_T is chosen for which the associated value of g is smaller

than f_p .

For checking purposes, a subsidiary test for the determination of the transition angle was added to the program. It is based on the idea that, for the correct transition angle ψ_T , the line representing the flat portion of the pinion will make a smaller angle with the center line $O_G O_P$ than will be the case for the incorrect one. To this end, TEST1 and TEST2 find both angles with the help of

$$\text{TEST} = 360^\circ - (\psi_T + \alpha_P) \quad (\text{F-1})$$

III. Determination of Correct Sign for Round on Flat Regime

The sign preceding the square root in eq. (E-29), for the round on flat regime, is determined with the help of the angle ψ_T . The condition which yields that angle ψ which is closest to ψ_T governs. The variable SIGNF is used for the sign under consideration.

IV. Computation of Final and Initial Values of φ and ψ

The final and initial values of the gear and pinion angles are found by continuously evaluating the round on flat equation (E-29), using the previously determined value of SIGNF, and simultaneously checking the contact condition for the subsequent set of teeth, as given by eq. (E-48). This loop is initiated at the transition angle and terminated once the condition of eq. (E-48) is met. This allows the simultaneous determination

of both the angles at which the first set of teeth loses contact and at which the second set of teeth comes into engagement. The latter is accomplished by subtracting $\Delta\varphi$ from the "loss of contact" angle φ_F and adding $\Delta\psi$ to the "loss of contact" angle ψ_F (see computations following statement label no. 70). PHIF and PSIFF represent the angles when contact is lost for a given mesh, while PHII and PSII stand for the angles when initial contact is made.

V. Determination of Correct Sign for Round on Round Regime

Eq. (E-13) is used to determine the angle ψ while the gear and pinion are in the round on round regime. The correct sign in eq. (E-13) is obtained by comparing the value of the angle ψ , as computed with PHII, with the value of PSII. SIGNR is the variable which furnishes this sign.

VI. Kinematics

Since the limits as well as the correct signs for both the round on round and the round on flat regimes are known, the various kinematic properties of interest may now be computed.

The angular increment DDPHI of the input angle is found by dividing the range from PHII to PHIF into K parts. (K is the range divisor.) The computational loop begins with statement label no. 110 and ends with the third card from the end of the main program. The computation is terminated when the angle φ exceeds PHIF.

A. Round on Round Regime

As long as PHI is smaller than the transition angle PHIT, the kinematics of the round on round phase of motion is computed. This results in the following:

$$\text{PSI} = \psi \text{ (see eq. (E-13))}$$

$$\text{LAMDA} = \lambda \text{ (see eqs. (E-14) and (E-15))}$$

$$\text{PSIDOT} = \dot{\psi} \text{ (see eq. (E-16))}$$

$$\text{VSTR} = \bar{V}_S/T \text{ for round on round (see eq. (E-20))}$$

$$\text{SR} = s \text{ (see eq. (E-50) for later use)}$$

$$\text{ETAPH} = \eta_P \text{ (see eqs. (E-6a) and (E-6b))}$$

$$\text{ETAGR} = \eta_G \text{ (see eq. (E-5)). For discussion of the usefulness of } \eta_P \text{ and } \eta_G, \text{ see output in section c below.)}$$

B. Round on Flat Regime

When PHI is larger than the transition angle PHIT, the kinematics of the round on flat phase is computed. This computation includes the following:

$$\text{PSI} = \psi \text{ (see eq. (E-29))}$$

$$G = g \text{ (see eq. (E-27))}$$

$$\text{PSIDOT} = \dot{\psi} \text{ (see eq. (E-30))}$$

$$\text{VSTF} = \bar{V}_S/T \text{ for round on flat (see eq. (E-35))}$$

$$\text{SF} = s \text{ (see eq. (E-72) for later use)}$$

$$\text{ETAGF} = \eta_{GF} \text{ (see eqs. (E-6c) and (E-6d))}$$

c. Output (see Program CLOCK 1, below)

As previously, the output of the program is best explained with the help of the sample problem at the end of the program. It contains the following:

I. Input Parameters

CAPRP = R_p = .47725 in. (1.212 cm)
RP = r_p = .09085 in. (0.231 cm)
AG = a_G = .47725 in. (1.212 cm)
AP = a_p = .09085 in. (0.231 cm)
RHOG = r_G = .03870 in. (0.098 cm)
RHOP = r_p = .01740 in. (0.044 cm)
TG = t_G = .03480 in. (0.088 cm)
TP = t_p = .02800 in. (0.071 cm)
NG = n_G = 42
NP = n_p = 8
K = 50

II. Computed Values

The following parameters are printed out:

DELGD = δ_G = 2.5880°
DELPD = δ_p = 2.1448°
GAMMPD = γ_p = 11.0418°
ALPHPD = α_p = 8.8970°
ETMINGD = $\gamma_{\min G}$ = 85.3488°
ETMAXGD = $\gamma_{\max G}$ = 144.0484°

$ETMINPD = \varphi_{minp} = 78.9582^\circ$
 $ETMAXPD = \varphi_{maxp} = 166.5870^\circ$
 $FP = f_p = .08917 \text{ in. } (0.226 \text{ cm})$

The printout concerning the transition angles consists of two lines. While the program automatically picks that transition configuration which leads to a decreasing value of g as φ is increased, both transition angles are printed out for checking purposes. Thus, one finds

$\varphi_{T1} = 186.36^\circ \quad \psi_{T1} = 308.63^\circ \quad g_1 = .0895 \text{ in. } (0.227 \text{ cm}) \quad TEST1 = 42.47^\circ$
 $\varphi_{T2} = 178.75^\circ \quad \psi_{T2} = 346.65^\circ \quad g_2 = .0888 \text{ in. } (0.226 \text{ cm}) \quad TEST2 = 4.45^\circ$

Clearly, the second line represents the solution since $g_2 = .0888$ for a slight increase in the angle φ over φ_T . This is less than the value of $f_p = .08917$. In addition, TEST2 furnishes the smaller number of degrees. Recall TEST represents the angle between the flat of the pinion the line connecting the pivots.

Furthermore, the program shows the initial and final angles of contact:

$PHIID =$ the angle φ at initial contact
 $PSIID =$ the angle ψ at initial contact
 $PHIFD =$ the angle φ at final contact
 $PSIFD =$ the angle ψ at final contact

Note that angle ϕ increases while the angle ψ decreases from the beginning to the end of the contact.

The computational loop begins with PHIID and ends with PHIFD. Further, when PHID reaches the approximate value of PHITD, the output shifts from round on round parameters to round on flat ones. The purpose of the multiple output throughout the motion of the mesh is to gain insight concerning the behavior of the mesh as well as to be able to check geometric values.

The following conclusions may be drawn for either of the phases as well as in general for the gears under consideration.

A. Round on Round Phase ($176.2623^\circ < \phi < 178.6623^\circ$)

PSIDOT, the angular velocity of the pinion, is negative, and at all times near the "gear ratio" of $42/8 = 5.25$.

SR is printed here only for checking purposes. It becomes important in the moment input-output analyses of program CLOCK 2.

The angles ETAGR and ETAPRD are of interest because one needs to make sure that the contact between gear and pinion does not occur too close to the respective tooth tips. This is necessary since the present mathematical model has a pointed tip while in a real situation the tips are rounded. Thus, if contact is sufficiently far from the tips of the teeth, the present model will give valid answers.

The range of ETAGR is approximately between 86° and 90° . This is considerably smaller than the ETMAXGD of approximately 144° and larger than the ETMINGD of approximately 85° . (The

latter shows that the round of the pinion tooth does not touch the flat of the gear tooth.)

The angle ETAPRD of the pinion tooth is always considerably smaller than ETMAXPD. Since contact is transferred to the flat portion of the pinion at the end of this phase of motion, ETAPRD almost equals ETMINPD at that point.

LAMDAD is given for general checking purposes only.

B. Round on Flat Phase ($178.6623^\circ < \phi < 184.834^\circ$)

The angular velocity $\dot{\psi}$ continues relatively smoothly after the transition. The distance g remains smaller than f_p , as expected, and it reaches a minimum of .0822 in. at $\phi \approx 182.5^\circ$. It is further to be noted that g never reaches the value of f_p again since the subsequent set of teeth takes over when $g = .08439$ in. (0.214 cm). For the present program to be valid, it is necessary that contact ends before the round on flat phase is completed.

As before, s_F is given for checking purposes only, and its value has been confirmed, just as was done for s_R , by graphical analysis (not shown).

The angle ETAGFD of the gear reaches a maximum of approximately 130° at the end of this phase. Since this is well below the maximum value ETMAXGD = 144° , there is enough margin for a tip radius on the gear tooth.

C. General Considerations

As expected for a direct contact mechanism of this type, the angular velocity ratio, as represented by PSIDOT, is not constant and has a greater absolute value at initial contact than at final contact. This indicates that the pinion will speed up somewhat as the subsequent set of teeth comes into contact, and that therefore, the original set of teeth loses contact at that instant. This means that the "effective contact ratio" is unity.

Program CLOCK 1

F-14

1 C PROGRAM CLOCK (INPUT-OUTPUT, TAPES=INPUT, TAP=0=OUTPUT)
C KINEMATICS OF SINGLE PASS STEP-UP GEAR MESH WITH CLOCK (OGIVAL) TEETH

5 REAL NP,AG,LX,LY,X,LAHQA,LANQAO
1 FORMAT(2F10.5)
READ(5,1)CAPRP,RP

READ(5,1)AG,AP

READ(5,1)RHOG,RHQP

READ(5,1)TG,TP

READ(5,2)NG,NP

2 FORMAT(2F10.8)

READ(5,3)K

3 FORMAT(F10.8)

PI = 3.14159

2 = PI/180.

PHIDOT = 1.

4 WRITE(6,*)CAPRP,RP,AG,AP

5 FORMAT(1E10.5,3E10.5) = F7.5,3X,MP = F7.5,3X,AP = F7.5,3X,

10P = F7.5,3X

6 FORMAT(1E10.5,3E10.5) = F7.5,3X,PHQP = F7.5,3X,

WRITE(6,*)TG,TP

7 FORMAT(1E10.5,3E10.5) = F7.5,3X,TP = F7.5,3X,

WRITE(6,*)NG,NP

8 FORMAT(1E10.5,3E10.5) = F7.5,3X,MP = F7.5,3X,

WRITE(6,*)K

9 FORMAT(1E10.5,3E10.5) = F7.5,3X,PHQP = F7.5,3X,

10 C COMPUTATION OF GEAR LOGIN PARAMETERS

C

C

C

C

C

C

C

C

C

C

C

C

C

C

C

C

C

C

C

C

C

C

C

C

C

C

C


```

1  SUMQU:LINE TRANS(RHOG*ALPAP*FP*AG*0,DEL6*0,PSIT,PHIT,6)
   WT = 2.24159
   ST = (FP*PSIT*ALPAP) + (RHOG*COS(PSIT*ALPAP))/AG
   CT = (FP*COS(PSIT*ALPAP) - (RHOG*SIN(PSIT*ALPAP)) - B)/AG
   PHIT = ATAN2(ST,CT) + DEL6
   IF (PHIT - LT - 0.1) PHIT = PHIT + 2.0*PI
   PHINEXT = PHIT + .102
   AF = B*CCOS(CT*PHIT) + B0*COS(PHINEXT - LEL6 - ALPAP)
   HF = B*SIN(ALPAP) - AG*SIN(PHINEXT - DEL6 - ALPAP)
   CF = RHOG
   MOOTF = AF*AF + HF*HF - CF*CF
   YF1 = AF + SQRT(MOOTF)
   YF2 = AF - SQRT(MOOTF)
   AF = YF1 + CF
   PSINEX1 = 2.0*ATAN2(YF1,YF2)
   PSINEX2 = 2.0*ATAN2(YF2,YF1)
   IF (PSINEX1 - LT - 0.1) PSINEX1 = PSINEX1 + 2.0*PI
   IF (PSINEX2 - LT - 0.1) PSINEX2 = PSINEX2 + 2.0*PI
   IF (ABS(PSINEX1 - PSIT) - LT - ABS(PSINEX2 - PSIT)) GO TO 1
   PSINEX1 = PSINEX2
   GO TO 2
2  PSINEX1 = PSINEX1
   CG = (AG*SIN(PHINEXT - DEL6) - RHOG*COS(PSINEX1*ALPAP))/SIN(PSINEX1
   L(ALPAP)
   DEL(UM)
   END

```

2510	359.8195	2510T	-5.2458	SF	-1.0	ETAGRD	64.7219	ETAGRD	91.6923	LAMOD	266.9022
2510	359.8204	2510T	-5.2461	SF	-1.0	ETAGRD	64.8959	ETAGRD	89.7758	LAMOD	267.0898
2510	359.8211	2510T	-5.2468	SF	-1.0	ETAGRD	64.9172	ETAGRD	86.7464	LAMOD	267.1389
2510	357.1314	2510T	-5.2581	SF	-1.0	ETAGRD	87.8587	ETAGRD	81.8137	LAMOD	267.1029
2510	356.2516	2510T	-5.2546	SF	-1.0	ETAGRD	87.2214	ETAGRD	86.9377	LAMOD	267.1066
2510	356.3136	2510T	-5.2493	SF	-1.0	ETAGRD	87.3145	ETAGRD	86.9291	LAMOD	267.1669
2510	354.4174	2510T	-5.2474	SF	-1.0	ETAGRD	87.3531	ETAGRD	85.1748	LAMOD	267.1978
2510	353.5138	2510T	-5.2752	SF	-1.0	ETAGRD	87.3503	ETAGRD	84.3476	LAMOD	267.8212
2510	352.6610	2510T	-5.2839	SF	-1.0	ETAGRD	86.1547	ETAGRD	83.5649	LAMOD	266.6178
2510	351.7621	2510T	-5.2933	SF	-1.0	ETAGRD	86.4628	ETAGRD	82.7722	LAMOD	266.7852
2510	354.7938	2510T	-5.3633	SF	-1.0	ETAGRD	86.7931	ETAGRD	82.6235	LAMOD	266.6255
2510	342.0438	2510T	-5.3137	SF	-1.0	ETAGRD	86.1521	ETAGRD	81.3811	LAMOD	266.4390
2510	349.9720	2510T	-5.3244	SF	-1.0	ETAGRD	85.3398	ETAGRD	80.6848	LAMOD	264.2224
2510	348.8693	2510T	-5.3353	SF	-1.0	ETAGRD	86.9541	ETAGRD	79.9347	LAMOD	265.9788
2510	347.1427	2510T	-5.3462	SF	-1.0	ETAGRD	86.3973	ETAGRD	79.2909	LAMOD	265.7878
2510	346.2252	2510T	-5.3468	SF	-1.0	ETAGRD		ETAGRD	91.1534		
2510	345.1421	2510T	-5.3892	SF	-1.0	ETAGRD	86.0031	ETAGRD	92.2409		
2510	344.3738	2510T	-5.4294	SF	-1.0	ETAGRD	86.8075	ETAGRD	93.3677		
2510	343.4494	2510T	-5.4554	SF	-1.0	ETAGRD	86.8722	ETAGRD	90.4522		
2510	342.5436	2510T	-5.4781	SF	-1.0	ETAGRD	86.0467	ETAGRD	95.5488		
2510	341.5629	2510T	-5.4974	SF	-1.0	ETAGRD	86.8623	ETAGRD	90.6731		
2510	340.6199	2510T	-5.5131	SF	-1.0	ETAGRD	86.2857	ETAGRD	97.7083		
2510	339.6779	2510T	-5.5252	SF	-1.0	ETAGRD	86.9534	ETAGRD	96.9054		
2510	338.7294	2510T	-5.5335	SF	-1.0	ETAGRD	86.2949	ETAGRD	100.9253		
2510	337.7754	2510T	-5.5306	SF	-1.0	ETAGRD	86.0455	ETAGRD	101.1458		
2510	336.8263	2510T	-5.5346	SF	-1.0	ETAGRD	86.8428	ETAGRD	102.2407		
2510	336.8771	2510T	-5.5353	SF	-1.0	ETAGRD	86.0868	ETAGRD	103.3874		
2510	334.9281	2510T	-5.5288	SF	-1.0	ETAGRD	86.9535	ETAGRD	104.5071		
2510	333.9629	2510T	-5.5168	SF	-1.0	ETAGRD	86.9431	ETAGRD	105.6293		
2510	331.8374	2510T	-5.5815	SF	-1.0	ETAGRD	86.0937	ETAGRD	106.7612		

PM10 = 181.4826	PM10 = 332.8664	PM100T = -5.4823	G = .08286	SF = 1.0	ETAGFD = 107.8542
PM10 = 181.5766	PM10 = 331.1581	PM100T = -5.4591	G = .08268	SF = 1.0	ETAGFD = 108.8635
PM10 = 181.7488	PM10 = 330.2245	PM100T = -5.4328	G = .08252	SF = 1.0	ETAGFD = 110.8695
PM10 = 181.9194	PM10 = 329.2959	PM100T = -5.4011	G = .08248	SF = 1.0	ETAGFD = 111.1496
PM10 = 182.0989	PM10 = 328.3729	PM100T = -5.3663	G = .08238	SF = 1.0	ETAGFD = 112.2629
PM10 = 182.2823	PM10 = 327.4562	PM100T = -5.3278	G = .08224	SF = 1.0	ETAGFD = 113.3511
PM10 = 182.4337	PM10 = 326.5464	PM100T = -5.2859	G = .08220	SF = 1.0	ETAGFD = 114.4323
PM10 = 182.6852	PM10 = 325.6441	PM100T = -5.2403	G = .08228	SF = 1.0	ETAGFD = 115.5068
PM10 = 182.7766	PM10 = 324.7499	PM100T = -5.1915	G = .08222	SF = 1.0	ETAGFD = 116.5717
PM10 = 182.9488	PM10 = 323.8644	PM100T = -5.1394	G = .08227	SF = 1.0	ETAGFD = 117.6284
PM10 = 183.1194	PM10 = 322.9886	PM100T = -5.0843	G = .08235	SF = 1.0	ETAGFD = 118.6794
PM10 = 183.2989	PM10 = 322.1213	PM100T = -5.0263	G = .08244	SF = 1.0	ETAGFD = 119.7195
PM10 = 183.4623	PM10 = 321.2648	PM100T = -4.9656	G = .08268	SF = 1.0	ETAGFD = 120.7425
PM10 = 183.5337	PM10 = 320.4198	PM100T = -4.9023	G = .08277	SF = 1.0	ETAGFD = 121.7597
PM10 = 183.8952	PM10 = 319.5842	PM100T = -4.8367	G = .08297	SF = 1.0	ETAGFD = 122.7668
PM10 = 183.9766	PM10 = 318.7688	PM100T = -4.7689	G = .08328	SF = 1.0	ETAGFD = 123.7698
PM10 = 184.1488	PM10 = 317.9492	PM100T = -4.6998	G = .08346	SF = 1.0	ETAGFD = 124.7438
PM10 = 184.3194	PM10 = 317.1484	PM100T = -4.6274	G = .08374	SF = 1.0	ETAGFD = 125.7166
PM10 = 184.4989	PM10 = 316.3628	PM100T = -4.5542	G = .08405	SF = 1.0	ETAGFD = 126.6731
PM10 = 184.6623	PM10 = 315.5885	PM100T = -4.4795	G = .08439	SF = 1.0	ETAGFD = 127.6188
PM10 = 184.8337	PM10 = 314.8270	PM100T = -4.4036	G = .08476	SF = 1.0	ETAGFD = 128.5517

2. Program Clock 2: Point and Cycle Efficiencies for Single
Pass Step-Up Gear Mesh With Clock
(Ogival) Teeth

The program CLOCK 2 furnishes the moment input-output relationship for a single step-up gear mesh with clock (ogival) teeth as derived in section 2 of Appendix E. This program uses the same kinematics as program CLOCK 1, and it differs from that program only in that it also determines both point and cycle efficiencies. Because of the above, sections a to c below will only contain discussions on those portions of the program which are different from CLOCK 1. The last section shows the complete program CLOCK 2.

a. Input Parameters (see Program CLOCK 2, below)

In addition to the input parameters of CLOCK 1, the following data must be supplied to the program:

MU = μ , the coefficient of friction at the gear and pinion pivots as well as at the contact point between the gear and the pinion

RHO1 = ρ_1 , the pivot radius of the gear

RHO2 = ρ_2 , the pivot radius of the pinion

b. Computations (See also COMMENT cards in program)

I. Computation of Gear Tooth Parameters

The computation of the gear tooth parameters is identical

with that given in program CLOCK 1.

II. Determination of Transition Angle

The transition angle is determined in the same manner as described in program CLOCK 1.

III. Determination of Correct Sign for Round on Flat Regime

This computation is also identical with that given in program CLOCK 1.

IV. Computation of Final and Initial Values of φ and ψ

This computation is also identical with that given in program CLOCK 1.

V. Determination of Correct Sign for Round on Round Regime

This computation is also identical with that given in program CLOCK 1.

VI. Kinematics, Point and Cycle Efficiencies

The angular increment DDPHI of the input angle is found in the same manner as shown in program CLOCK 1. While the initial, transition and final angles of the mesh are obtained in the same manner as shown in CLOCK 1, the computational loop of the program ranges from the initial angle PHII to one increment before the final angle PHIF. This is necessary in

order to accommodate the numerical integration for the cycle efficiency.

A. Round on Round Regime

As before for CLOCK 1, as long as PHI is smaller than the transition angle PHIT, the kinematics of the round on round phase of the motion is computed for each increment. These kinematic computations are identical with those given in CLOCK 1. The point efficiency in this phase of motion is obtained with the help of eq. (E-70) and takes the form of eq. (3), i.e.,

$$\epsilon_P = K_{ratio} \frac{M_o}{M_{in}} \quad (F-2)$$

Since the transmission ratio depends on the angular velocity ratio, and the input angular velocity is unity, eq. (F-2) becomes

$$\epsilon_P = \frac{M_o}{M_{in}} |\dot{\psi}| \quad (\text{POINTEF}) \quad (F-3)$$

B. Round on Flat Regime

When PHI is larger than the transition angle PHIT, the kinematics of the round on flat phase becomes applicable. While the computed kinematic quantities are identical with those of CLOCK 1, the present program contains an expression for the point efficiency for the round on flat phase of the motion. This expression is obtained with the help of eq. (E-92), and it

is computed in the manner of eq. (F-3) with the now current values of the output angular velocity PSIDOT.

C. Computation of Cycle Efficiency

Once the computational loop is terminated, the cycle efficiency is computed in the manner of eq. (C-10) of Appendix C, i.e.,

$$\epsilon_C = \frac{\Delta\phi \sum p}{(\phi_{FIN} - \phi_{IN})} \quad (\text{CYCLEFF}) \quad (\text{F-4})$$

The summation was accomplished inside the loop in terms of

$$MTOT = MTOT + POINTEF \quad (\text{F-5})$$

Further,

$\Delta\phi = DDPHI$ in the program, and similarly

$\phi_{FIN} = PHIF$ and

$\phi_{IN} = PHII$

c. Output (See sectiond below)

The output of CLOCK 2 is identical with that of CLOCK 1 with the exception that the point and cycle efficiencies are printed out. The identical geometric parameters are used, and therefore, the same kinematic output is obtained.

Program CLOCK 2

F-27

09/13/78 09:47.20

FTN 000420

70710 001=1

AF = B+COS(ALPHA) * AG+COS(PHI1-DELG-ALPHA)
 BF = B+SIN(ALPHA) * AG+SIN(PHI1-DELG-ALPHA)

CF = -PHOG
 MUOIF = AF*AF + BF*BF - CF*CF

YF1 = AF * SORT(MUOIF)
 YF2 = BF * SORT(MUOIF)

XF = BF * CF

PSIF1 = 2.0*ATAN2(YF1,XF)

PSIF2 = 2.0*ATAN2(YF2,XF)

IF(PSIF1 .LT. 0.0)PSIF1 = PSIF1 + 2.0*PI

IF(PSIF2 .LT. 0.0)PSIF2 = PSIF2 + 2.0*PI

IF(ABS(PSIF1-PSIF2) .LT. ABS(PSIF2-PSIF1))GO TO 10

SIGNF = -1.

GO TO 50

10 SIGNF = 1.

C COMPUTATION OF FINAL AND INITIAL VALUES OF PHI AND PSI

50 DO 60 I=1,1000

PHI0 = PHI0 + (1.0/77180.

PHI = PHI0 + Z

AF = B+COS(ALPHA) * AG+COS(PHI-DELG-ALPHA)

BF = B+SIN(ALPHA) * AG+SIN(PHI-DELG-ALPHA)

CF = -PHOG

MUOIF = AF*AF + BF*BF - CF*CF

IF(PSIF1-PSIF2 .GT. 0.0)PSIF1 = PSIF1 + 2.0*PI

IF(PSIF1 .LT. 0.0)PSIF1 = PSIF1 + 2.0*PI

LA = B * AG+COS(PHI-DELG-ALPHA) * AG+COS(PSIF-DELG-PSIF)

LY = AG+SIN(PHI-DELG-ALPHA) * AG+SIN(PSIF-DELG-PSIF)

IF(SORT(LA**2+LY**2) .GT. 0.0)GO TO 70

60 CONTINUE

70 PHIF = PHIF + PHI

PSIF = PSIF

PHI = PHIF + PHI

PSI = PSIF + PSI

IF(PSIF-DELG-PSIF .GT. 0.0)PSIF = PSIF + 2.0*PI

PHI0 = PHI0 + Z

PSI0 = PSI0 + Z

PHIF = PHIF + Z

PSIF = PSIF + Z

WRITE(6,8)PHI0,PSI0,PHIF,PSIF

80 FORMAT(10F10.4,10F10.4,10F10.4,10F10.4)

10PSIF = 0.0

C DETERMINATION OF CORRECT SIGN FOR WOUND ON WOUND REGIME

AF = SIGN(PHI-DELG, COS(PHI-DELG-ALPHA)) * B*AG + SIGN(PSIF-DELG, COS(PSIF-DELG-PSIF)) * B*AG

BF = COS(PHI-DELG) * B*AG - SIN(PHI-DELG-ALPHA) * B*AG

CF = LAPSE * B*AG - B*AG * LAPSE

10 AG+COS(PHI-DELG) * AG+COS(DELG)

MUOIF = AF*AF + BF*BF - CF*CF

YF1 = AF * SORT(MUOIF)

[illegible]

```

210 60 TO 150
120 AF = B0COS(ALPH) : A0COS(PHI-DELG-ALPH)
BF = B0SIN(ALPH) : A0SIN(PHI-DELG-ALPH)
CF = -B0D6
MOOF = AF*AF + BF*BF - CF*CF
VF = AF + BF + SIGN(SQRT(MOOF))
AF = BF + CF
PSI = 2.0ATAN2(VF,AF)
IF(PSI < 0) PSI = PSI + 2.0PI
PSI0 = PSI/2
G = IAGOSIN(PHI-DELG) - B0D6COS(PSI*ALPH)/SIN(PSI*ALPH)
AF0 = A0SIN(PHI-DELG-ALPH)
BF0 = A0COS(PHI-DELG-ALPH)
PSI00 = PRINT0(BF0SIN(PSI) + B0D6COS(PSI)/A0COS(PSI) - BF0
SIN(PSI))
VST = PHIDOT*(B0D6 + A0SIN(PSI*ALPH*ALPH*DELG))
BF = VST/ABS(VST)
IF(PSI0*ALPH0 < 0.99) IETAGD = (PHI-DELG-PSI-ALPH*PSI0*ALPH0)/2.1/7
IF(PSI0*ALPH0 < 0.99) IETAGD = (PHI-DELG-PSI-ALPH*PSI0*ALPH0)/2
EEN = 6 - INT(2000)
EFU = MO*(MO0 + SF*MO6) - A0*(COS(PHI-DELG-PSI-ALPH))
1. MUSEOSIN(PHI-DELG-PSI-ALPH)
POINTER = EFM/EFU*ABS(PSI00)
WRITE(6,136)PHI0,PSI0,PSI00,PSI,EF,ETAGD,POINTER
130 FORMAT(20.0PHI0,20.0PSI0,20.0PSI00,20.0F9.4,3X,PSI00,20.0F9.4,3X,
106 20.0F7.5,3X,0.5F,20.0F4.1,3X,ETAGD,20.0F9.4,3X,POINTER,20.0F9.3)
150 MTOF = MTOF + POINTER
60 TO 110
200 CYCLEFF = INT(0.0PHI/(PHI-PSI))
WRITE(6,210)CYCLEFF
210 FORMAT(20.0,5X,CYCLE EFFICIENCY,20.0F6.3)
STOP
END

```

1 SUBROUTINE TRANS(RHOG,ALPH,FP,SG,R,DELG,Z,PSIT,PHIT,G)

PI=3.14159

SI=(FP+SIN(PSIT*ALPH))/AG

CI=(FP+COS(PSIT*ALPH))/AG

PHIT=ATAN2(SI,CI)+SELE

IF(PHIT.LT.0.)PHIT=PHIT+2.*PI

PSINEA1=PHIT*.107

RF=8*COS(PSINEA1)-AG+COS(PHIT*PI-DELG-ALPH)

CF=8*SIN(PHIT*PI-DELG-ALPH)

ROOTF=AF*RF+BF*CF-CF*CF

YF1=AF+SQRT(ROOTF)

YF2=AF-SQRT(ROOTF)

XF=RF+CF

PSINEA1=2.*ATAN2(YF1,XF)

PSINEA2=2.*ATAN2(YF2,XF)

IF(PSINEA1.LT.0.)PSINEA1=PSINEA1+2.*PI

IF(PSINEA2.LT.0.)PSINEA2=PSINEA2+2.*PI

IF(ABS(PSINEA1-PSINEA2).LT.ABS(PSINEA2-PSINEA1))GO TO 1

PSINEA1=PSINEA2

GO TO 2

1 PSINEA1=PSINEA1

2 G=(AG+SIN(PHINEA1-DELG)-RHOG*COS(PSINEA1*ALPH))/SIN(PSINEA1

1*ALPH)

RETURN

END

$$50063^{\circ} = 49^{\circ} 52'16'' \pm 24 \quad 50116^{\circ} = 49^{\circ} 52'18'' = 49^{\circ} 52'19''$$

DATE = 11/28/80

Page 10 of 10

42-4261

$$E_{\text{eff}} = E_{\text{eff}} = 1, \dots$$

61. In the

25

5.
" 6

00017 2.1600 2.5500 2.7300

CA 3007 = 11-8019 61-2007 = 11-8070

SECRET

79-4587
 EIMLAPD = 149-5878

1685-1697

SMITHID = 104.3023 PSYID = 308.6744 G: = .9095 TEST1 = 42.07

$201:20 = 1/4, 7337$
 $251720 = 345, 064$
 $62 = 1438$
 $TEST2 = AAS$

PMIID = 176.2023 PMSID = 359.6276 PMIFO = 104.8137 PMSFO = 314.8276

951007	=	359.48195	951007	=	-5.24556	951007	=	94.7219	951007	=	93.6923	951007	=	.879
951008	=	358.9244	951008	=	-5.24531	951008	=	94.7219	951008	=	93.6923	951008	=	.879
951009	=	358.3689	951009	=	-5.24506	951009	=	94.7219	951009	=	93.6923	951009	=	.879
951010	=	357.8134	951010	=	-5.24481	951010	=	94.7219	951010	=	93.6923	951010	=	.879
951011	=	357.2579	951011	=	-5.24456	951011	=	94.7219	951011	=	93.6923	951011	=	.879
951012	=	356.7024	951012	=	-5.24431	951012	=	94.7219	951012	=	93.6923	951012	=	.879
951013	=	356.1469	951013	=	-5.24406	951013	=	94.7219	951013	=	93.6923	951013	=	.879
951014	=	355.5914	951014	=	-5.24381	951014	=	94.7219	951014	=	93.6923	951014	=	.879
951015	=	355.0359	951015	=	-5.24356	951015	=	94.7219	951015	=	93.6923	951015	=	.879
951016	=	354.4804	951016	=	-5.24331	951016	=	94.7219	951016	=	93.6923	951016	=	.879
951017	=	353.9249	951017	=	-5.24306	951017	=	94.7219	951017	=	93.6923	951017	=	.879
951018	=	353.3694	951018	=	-5.24281	951018	=	94.7219	951018	=	93.6923	951018	=	.879
951019	=	352.8139	951019	=	-5.24256	951019	=	94.7219	951019	=	93.6923	951019	=	.879
951020	=	352.2584	951020	=	-5.24231	951020	=	94.7219	951020	=	93.6923	951020	=	.879
951021	=	351.7029	951021	=	-5.24206	951021	=	94.7219	951021	=	93.6923	951021	=	.879
951022	=	351.1474	951022	=	-5.24181	951022	=	94.7219	951022	=	93.6923	951022	=	.879
951023	=	350.5919	951023	=	-5.24156	951023	=	94.7219	951023	=	93.6923	951023	=	.879
951024	=	350.0364	951024	=	-5.24131	951024	=	94.7219	951024	=	93.6923	951024	=	.879
951025	=	349.4809	951025	=	-5.24106	951025	=	94.7219	951025	=	93.6923	951025	=	.879
951026	=	348.9254	951026	=	-5.24081	951026	=	94.7219	951026	=	93.6923	951026	=	.879
951027	=	348.3699	951027	=	-5.24056	951027	=	94.7219	951027	=	93.6923	951027	=	.879
951028	=	347.8144	951028	=	-5.24031	951028	=	94.7219	951028	=	93.6923	951028	=	.879
951029	=	347.2589	951029	=	-5.24006	951029	=	94.7219	951029	=	93.6923	951029	=	.879
951030	=	346.7034	951030	=	-5.23981	951030	=	94.7219	951030	=	93.6923	951030	=	.879
951031	=	346.1479	951031	=	-5.23956	951031	=	94.7219	951031	=	93.6923	951031	=	.879
951032	=	345.5924	951032	=	-5.23931	951032	=	94.7219	951032	=	93.6923	951032	=	.879
951033	=	345.0369	951033	=	-5.23906	951033	=	94.7219	951033	=	93.6923	951033	=	.879
951034	=	344.4814	951034	=	-5.23881	951034	=	94.7219	951034	=	93.6923	951034	=	.879
951035	=	343.9259	951035	=	-5.23856	951035	=	94.7219						

PM10 = 187.5400	PS10 = 336.8703	PS100T = -5.5366	6 = .08420	SF = 1.0	ETAGFD = 192.2407	POINTEF = .055
PM10 = 187.7194	PS10 = 335.8771	PS100T = -5.5353	6 = .08388	SF = 1.0	ETAGFD = 193.3874	POINTEF = .052
PM10 = 187.8944	PS10 = 334.9207	PS100T = -5.5286	6 = .08358	SF = 1.0	ETAGFD = 194.5071	POINTEF = .048
PM10 = 187.6623	PS10 = 333.9426	PS100T = -5.5168	6 = .08331	SF = 1.0	ETAGFD = 195.6253	POINTEF = .044
PM10 = 187.2317	PS10 = 333.0375	PS100T = -5.5015	6 = .08307	SF = 1.0	ETAGFD = 196.7412	POINTEF = .041
PM10 = 187.4052	PS10 = 332.8905	PS100T = -5.4923	6 = .08286	SF = 1.0	ETAGFD = 197.8502	POINTEF = .037
PM10 = 187.5760	PS10 = 331.1501	PS100T = -5.4591	6 = .08268	SF = 1.0	ETAGFD = 198.9635	POINTEF = .034
PM10 = 187.7408	PS10 = 330.2245	PS100T = -5.4328	6 = .08252	SF = 1.0	ETAGFD = 199.0655	POINTEF = .030
PM10 = 187.9194	PS10 = 329.2959	PS100T = -5.4011	6 = .08248	SF = 1.0	ETAGFD = 199.1605	POINTEF = .027
PM10 = 187.9909	PS10 = 328.3729	PS100T = -5.3663	6 = .08238	SF = 1.0	ETAGFD = 199.2629	POINTEF = .023
PM10 = 187.2621	PS10 = 327.4552	PS100T = -5.3279	6 = .08224	SF = 1.0	ETAGFD = 199.3511	POINTEF = .019
PM10 = 187.4317	PS10 = 326.5464	PS100T = -5.2859	6 = .08220	SF = 1.0	ETAGFD = 199.4323	POINTEF = .016
PM10 = 187.6052	PS10 = 325.6441	PS100T = -5.2403	6 = .08220	SF = 1.0	ETAGFD = 199.5008	POINTEF = .012
PM10 = 187.7766	PS10 = 324.7496	PS100T = -5.1915	6 = .08222	SF = 1.0	ETAGFD = 199.5717	POINTEF = .009
PM10 = 187.9400	PS10 = 323.8644	PS100T = -5.1394	6 = .08227	SF = 1.0	ETAGFD = 199.6206	POINTEF = .005
PM10 = 187.1194	PS10 = 322.9886	PS100T = -5.0843	6 = .08235	SF = 1.0	ETAGFD = 199.6764	POINTEF = .002
PM10 = 187.2904	PS10 = 322.1213	PS100T = -5.0263	6 = .08246	SF = 1.0	ETAGFD = 199.7145	POINTEF = .000
PM10 = 187.4623	PS10 = 321.2448	PS100T = -4.9656	6 = .08260	SF = 1.0	ETAGFD = 199.7425	POINTEF = .000
PM10 = 187.6317	PS10 = 320.4196	PS100T = -4.9023	6 = .08277	SF = 1.0	ETAGFD = 199.7597	POINTEF = .000
PM10 = 187.8052	PS10 = 319.5862	PS100T = -4.8367	6 = .08297	SF = 1.0	ETAGFD = 199.7608	POINTEF = .000
PM10 = 187.9766	PS10 = 318.7600	PS100T = -4.7689	6 = .08320	SF = 1.0	ETAGFD = 199.7608	POINTEF = .000
PM10 = 187.1400	PS10 = 317.9432	PS100T = -4.6998	6 = .08346	SF = 1.0	ETAGFD = 199.7438	POINTEF = .000
PM10 = 187.3194	PS10 = 317.1498	PS100T = -4.6274	6 = .08374	SF = 1.0	ETAGFD = 199.7146	POINTEF = .000
PM10 = 187.4909	PS10 = 316.3628	PS100T = -4.5542	6 = .08405	SF = 1.0	ETAGFD = 199.6731	POINTEF = .000
PM10 = 187.6623	PS10 = 315.5805	PS100T = -4.4795	6 = .08439	SF = 1.0	ETAGFD = 199.6100	POINTEF = .000

CYCLE EFFICIENCY = .050

APPENDIX G
KINEMATICS OF TWO AND THREE STEP-UP GEAR TRAINS WITH CLOCK TEETH

Figure G-1 shows the basic configuration of a three step-up gear train used in certain fuze applications. The general layout is identical to that shown in Figure A-5 of Appendix A. Now, ogival type gear teeth are used instead of involute type ones. Again, it is required to find the equilibrant moment M_{o4} , acting on pinion no. 4 which holds the input moment, M_{in} , acting on gear no. 1, in equilibrium when both pivot and contact friction are taken into account, and when the fuze body spins. Appendix H gives the force and moment analyses for the determination of this moment input-output relationship. The same appendix also shows the derivation of such an input-output relationship for a two step-up gear train with ogival gear teeth which must operate in a spin environment. (Figure A-10 of Appendix A shows this type of configuration with involute teeth.) The present appendix lays the groundwork for the moment relationships of Appendix H by providing the kinematics of the three ogival gear meshes involved.

In each case both round on round and round on flat phases

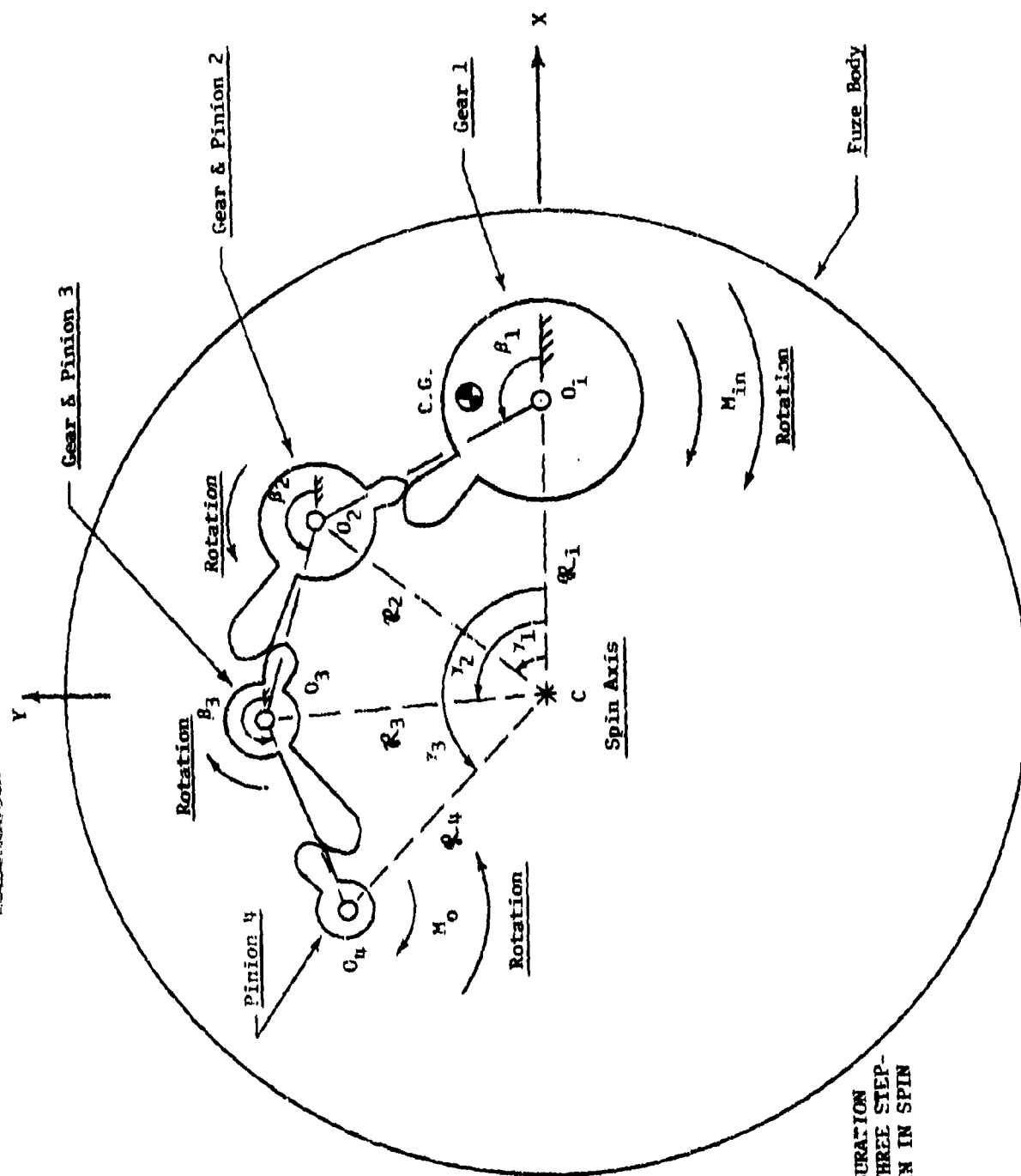


FIGURE G-1
BASIC CONFIGURATION
FOR OCIVAL THREE STEP-
UP GEAR TRAIN IN SPIN
ENVIRONMENT

of motion have to be considered. All derivations follow the pattern set in Section 1 of Appendix E. The derivations must take into account that the driving gears of meshes no. 1 and no. 3, i.e., between gear no. 1 and pinion no. 2 and between gear no. 3 and pinion no. 4, respectively, have clockwise rotations. The driving gear of mesh no. 2, i.e., between gear no. 2 and pinion no. 3, has counterclockwise rotation.

Finally, the inclinations of the various pivot to pivot centerlines with respect to the body-fixed X-axes, as represented by the angles β_1 , β_2 and β_3 , must be considered.

For the sake of simplicity, the notation will in most cases not differentiate between round on round and round on flat phases of motion. For example, the output angle, ψ_1 , and its derivatives will have the same symbol for both phases.

For definitions of angles β_1 and γ_1 as well as the distances Q_1 , see Appendix A-6.

1. KINEMATICS OF MESH NO. 1 (GEAR NO. 1 AND PINION NO. 2)

a. ROUND ON ROUND PHASE OF MOTION

Figure G-2 shows the round on round phase of the motion of mesh no. 1 in a schematic manner. Only the contacting faces of the gear and the pinion are indicated.

I. UNIT VECTORS

The unit vector in the direction O_1C_{G1} of the gear is given by

$$\bar{n}_{G1} = \cos(\phi_1 + \delta_{G1})\bar{i} + \sin(\phi_1 + \delta_{G1})\bar{j} \quad (G-1)$$

The unit vector in the direction $C_{G1}C_{P1}$ is given by

$$\bar{n}_{\lambda 1} = \cos\lambda_1\bar{i} + \sin\lambda_1\bar{j} \quad (G-2)$$

The unit vector normal to $\bar{n}_{\lambda 1}$ (in the right hand sense) becomes

$$\bar{n}_{N\lambda 1} = -\sin\lambda_1\bar{i} + \cos\lambda_1\bar{j} \quad (G-3)$$

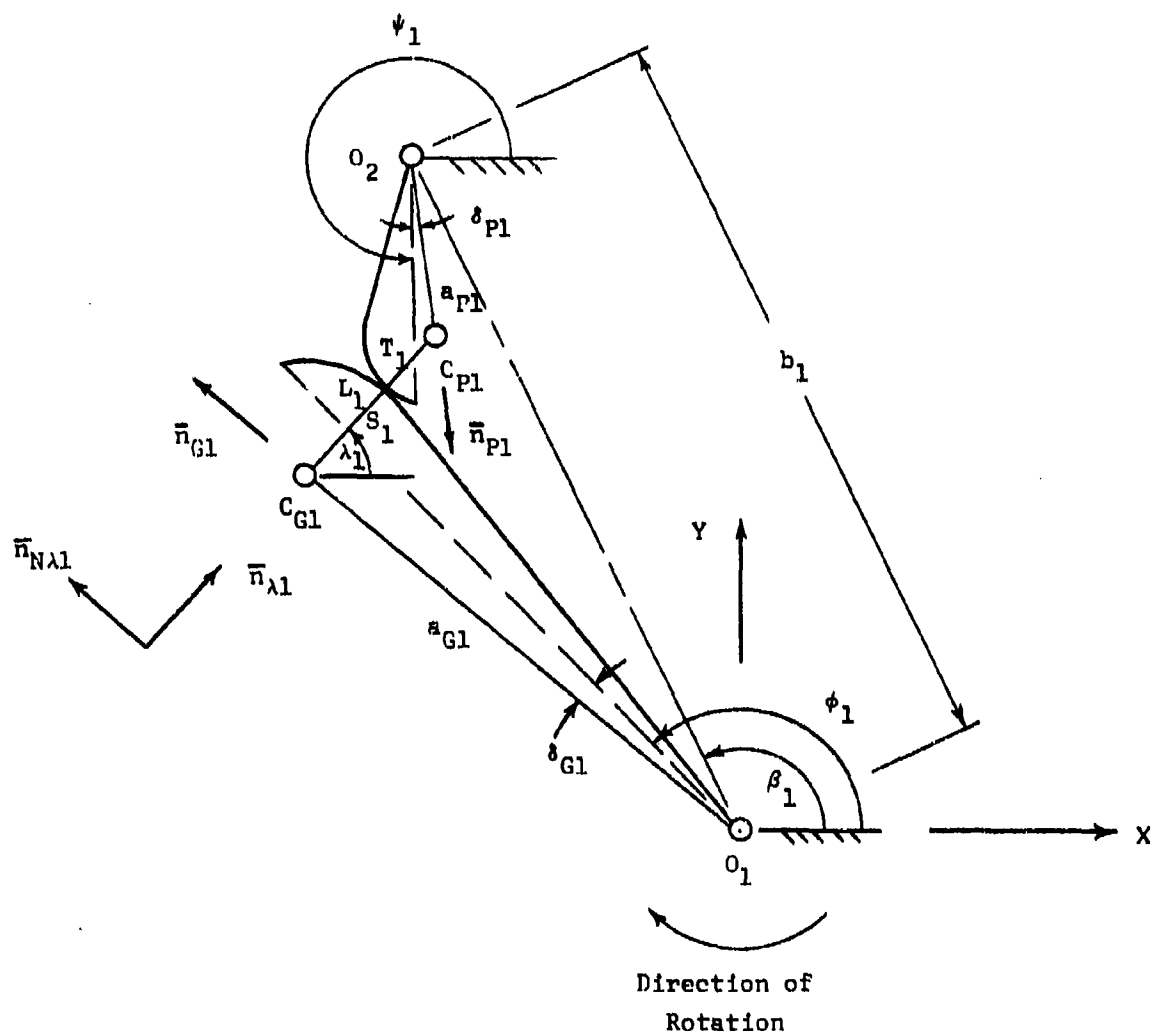


FIGURE G-2

ROUND ON ROUND PHASE FOR MESH NO. 1

The unit vector in the direction O_2C_{P1} is given by

$$\bar{n}_{P1} = \cos(\psi_1 + \delta_{P1})\bar{i} + \sin(\psi_1 + \delta_{P1})\bar{j} \quad (G-4)$$

Finally, the unit vector along the centerline, O_1O_2 , is given by

$$\bar{n}_{\beta 1} = \cos\beta_1\bar{i} + \sin\beta_1\bar{j} \quad (G-5)$$

II. DETERMINATION OF OUTPUT ANGLE ψ_1 AND "COUPLER" ANGLE λ_1

The loop equation of the equivalent four-bar linkage is given by

$$a_{G1}\bar{n}_{G1} + L_1\bar{n}_{\lambda 1} - a_{P1}\bar{n}_{P1} - b_1\bar{n}_{\beta 1} = 0 \quad (G-6)$$

$$\text{where } L_1 = \rho_{G1} + \rho_{P1} \quad (G-7)$$

With the appropriate substitution for the unit vectors, one obtains the following component equations:

$$a_{G1} \cos(\phi_1 + \delta_{G1}) + L_1 \cos \lambda_1 - b_1 \cos \beta_1 - a_{P1} \cos(\psi_1 + \delta_{P1}) = 0 \quad (G-8)$$

and

$$a_{G1} \sin(\phi_1 + \delta_{G1}) + L_1 \sin \lambda_1 - b_1 \sin \beta_1 - a_{P1} \sin(\psi_1 + \delta_{P1}) = 0 \quad (G-9)$$

To eliminate λ_1 , let

$$\sin^2 \lambda_1 + \cos^2 \lambda_1 = 1 \quad (G-10)$$

The above trigonometric functions are obtained from equations (G-8) and (G-9), respectively. Substitution into equation (G-10) furnishes

$$A_{1R} \sin \psi_1 + B_{1R} \cos \psi_1 = C_{1R} \quad (G-11)$$

where

$$A_{1R} = a_{G1} \sin(\phi_1 + \delta_{G1} - \delta_{P1}) - b_1 \sin(\beta_1 - \delta_{P1})$$

$$B_{1R} = a_{G1} \cos(\phi_1 + \delta_{G1} - \delta_{P1}) - b_1 \cos(\beta_1 - \delta_{P1})$$

$$C_{1R} = \frac{a_{P1}^2 + a_{G1}^2 + b_1^2 - L_1^2 - 2a_{G1}b_1 \cos(\phi_1 + \delta_{G1} - \beta_1)}{2a_{P1}}$$

Equation (G-11) is now solved for ψ_1 in the manner described in Appendix E in connection with equation (E-12), i.e.,

$$\psi_1 = 2 \tan^{-1} \frac{A_{1R} \pm \sqrt{A_{1R}^2 + B_{1R}^2 - C_{1R}^2}}{B_{1R} + C_{1R}} \quad (G-12)$$

The correct sign on equation (G-12) must be found from geometric considerations.

The coupler angle λ_1 may now be determined either from equation (G-8) or from equation (G-9). Thus,

$$\lambda_1 = \cos^{-1} \left[\frac{b_1 \cos \beta_1 + a_{p1} \cos(\psi_1 + \delta_{p1}) - a_{g1} \cos(\phi_1 + \delta_{g1})}{L_1} \right] \quad (G-13)$$

or

$$\lambda_1 = \sin^{-1} \left[\frac{b_1 \sin \beta_1 + a_{p1} \sin(\psi_1 + \delta_{p1}) - a_{g1} \sin(\phi_1 + \delta_{g1})}{L_1} \right] \quad (G-14)$$

III. DETERMINATION OF ANGULAR VELOCITY $\dot{\psi}_1$ OF PINION NO. 2

Differentiation of equation (G-11) with respect to time gives

$$\dot{\psi}_1 = \dot{\phi}_1 \left[\frac{B_{1RD} \cos \psi_1 - A_{1RD} \sin \psi_1 + C_{1RD}}{A_{1R} \cos \psi_1 - B_{1R} \sin \psi_1} \right] \quad (G-15)$$

where

$$A_{1RD} = a_{G1} \cos(\phi_1 + \delta_{G1} - \delta_{P1})$$

$$B_{1RD} = a_{G1} \sin(\phi_1 + \delta_{G1} - \delta_{P1})$$

$$C_{1RD} = \frac{a_{G1} b_1 \sin(\phi_1 + \delta_{G1} - \beta_1)}{a_{P1}}$$

IV. RELATIVE VELOCITY AT THE CONTACT POINT

The relative velocity $\bar{V}_{S1/T1_R}$ of the contact point S_1 on gear no. 1 with respect to point T_1 on pinion no. 2, represents the vectorial difference between the absolute velocities of these points. Thus,

$$\bar{V}_{S1/T1_R} = \bar{V}_{S1/C} - \bar{V}_{T1/C} \quad (G-16)$$

where C represents the spin center of the fuze body. If $\bar{\omega}$ stands for the angular velocity of the fuze body, then appropriate substitution into equation (G-16) gives (See also Figures G-1 and G-2)

$$\begin{aligned} \bar{V}_{S1/T1_R} = & \left[\bar{\omega} \times \bar{R}_1 + (\bar{\omega} + \bar{\phi}_1) \times (\bar{a}_{G1} + \bar{p}_{G1}) \right] \\ & - \left[\bar{\omega} \times \bar{R}_2 + (\bar{\omega} + \dot{\psi}_1) \times (\bar{a}_{P1} + \bar{p}_{P1}) \right] \end{aligned} \quad (G-17)$$

Since

$$\bar{\omega} \times [\bar{R}_1 + \bar{a}_{G1} + \bar{p}_{G1}] = \bar{\omega} \times [\bar{R}_2 + \bar{a}_{P1} + \bar{p}_{P1}] \quad (G-18)$$

because the position vectors in brackets are equal, equation (G-17) may be written

$$\begin{aligned}\bar{V}_{S1/T1_R} &= \bar{V}_{S1/O_1} - \bar{V}_{T1/O_2} \\ &= \dot{\bar{\phi}}_1 \times (\bar{a}_{G1} + \bar{r}_{G1}) - \dot{\bar{\psi}}_1 \times (\bar{a}_{P1} + \bar{r}_{P1})\end{aligned}\quad (G-19)$$

Note that $\bar{V}_{S1/T1_R}$ becomes the vectorial difference of the contact point velocities with respect to the fuze body.

Since this relative velocity is tangent to the contacting surfaces, it may be written as the vectorial difference of the velocity components along these surfaces. Accordingly, equation (G-19) becomes, with the help of the unit vector $\bar{n}_{N\lambda 1}$,

$$\begin{aligned}\bar{V}_{S1/T1_R} &= \left\{ \left[\dot{\bar{\phi}}_1 \bar{k} \times (\bar{a}_{G1} \bar{n}_{G1} + \bar{r}_{G1} \bar{n}_{\lambda 1}) \right] \cdot \bar{n}_{N\lambda 1} \right. \\ &\quad \left. - \left[\dot{\bar{\psi}}_1 \bar{k} \times (\bar{a}_{P1} \bar{n}_{P1} + \bar{r}_{P1} \bar{n}_{\lambda 1}) \right] \cdot \bar{n}_{N\lambda 1} \right\} \bar{n}_{N\lambda 1}\end{aligned}\quad (G-20)$$

Appropriate substitution of unit vectors given earlier in Section I and simplification results in

$$\begin{aligned} \nabla_{S1/T1R} = & \left\{ \dot{\psi}_1 [a_{G1} \cos(\psi_1 + \delta_{G1} - \lambda_1) + r_{G1}] \right. \\ & \left. - \dot{\psi}_1 [a_{P1} \cos(\psi_1 + \delta_{P1} - \lambda_1) - r_{P1}] \right\} \bar{E}_{N\lambda 1} \end{aligned} \quad (G-21)$$

b. ROUND ON FLAT PHASE OF MOTION

Figure G-3 shows a schematic view of mesh no. 1 in the round on flat phase of the motion.

I. UNIT VECTORS

The unit vector in the direction O_2T_1 is given by

$$\bar{n}_{F1} = \cos(\psi_1 - \alpha_{P1})\bar{i} + \sin(\psi_1 - \alpha_{P1})\bar{j} \quad (G-22)$$

The unit vector \bar{n}_{NF1} , in the direction $C_{G1}S_1$, is always normal to \bar{n}_{F1}

$$\bar{n}_{NF1} = -\sin(\psi_1 - \alpha_{P1})\bar{i} + \cos(\psi_1 - \alpha_{P1})\bar{j} \quad (G-23)$$

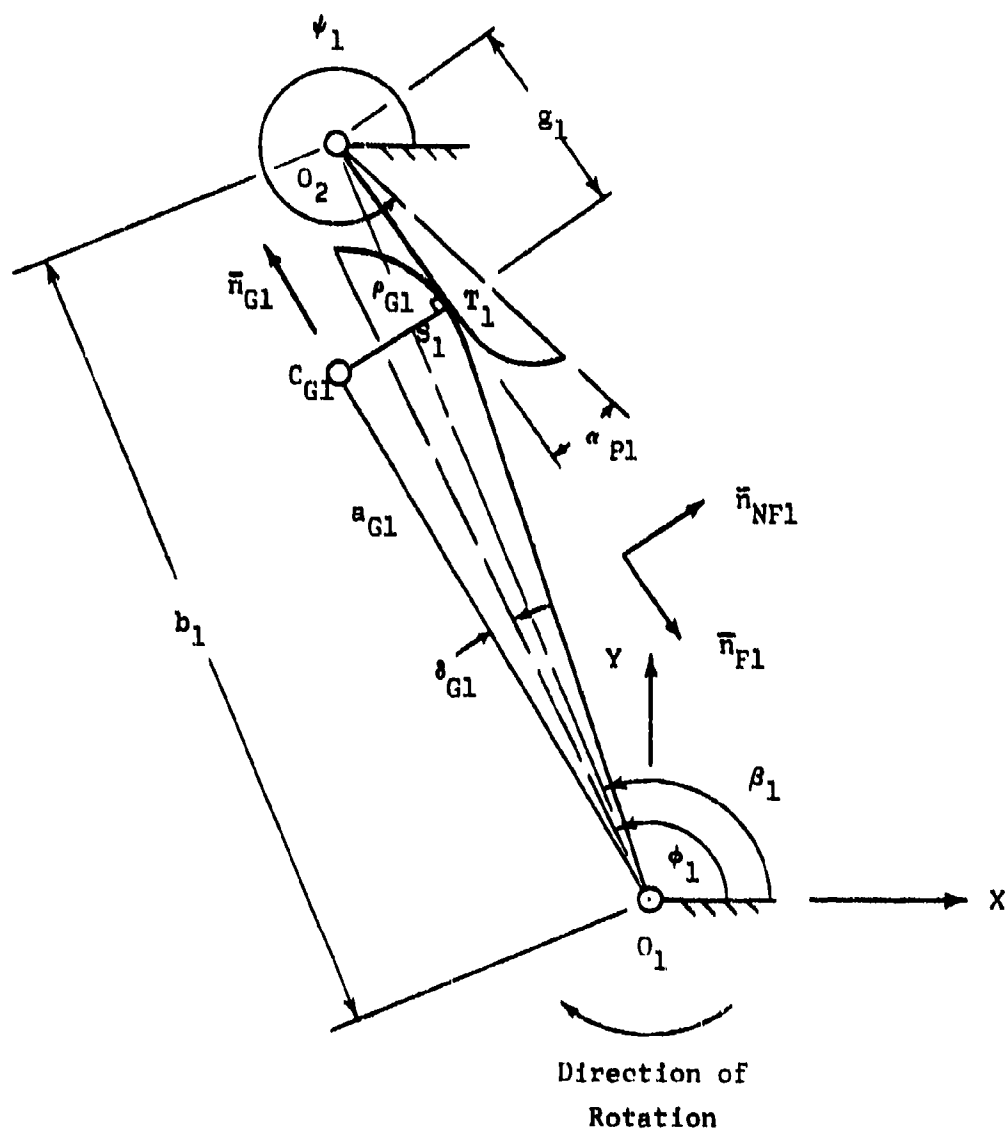


FIGURE G-3

ROUND ON FLAT PHASE FOR MESH NO. 1

II. DETERMINATION OF OUTPUT ANGLE ψ_1 AND DISTANCE g_1

The vector equation for the mechanism loop $O_1-C_{G1}-S_1-T_1-O_2$ has the form:

$$a_{G1}\bar{n}_{G1} + \rho_{G1}\bar{n}_{NF1} - g_1\bar{n}_{F1} - b_1\bar{n}_{\beta_1} = 0 \quad (G-24)$$

Substitution of equations (G-1), (G-5), (G-22) and (G-23) leads to the following component equations.

$$\begin{aligned} a_{G1}\cos(\phi_1 + \theta_{G1}) - \rho_{G1}\sin(\psi_1 - \alpha_{P1}) - b_1\cos\beta_1 - g_1\cos(\psi_1 - \alpha_{P1}) \\ = 0 \end{aligned} \quad (G-25)$$

and

$$\begin{aligned} a_{G1}\sin(\phi_1 + \theta_{G1}) + \rho_{G1}\cos(\psi_1 - \alpha_{P1}) - b_1\sin\beta_1 - g_1\sin(\psi_1 - \alpha_{P1}) \\ = 0 \end{aligned} \quad (G-26)$$

From equation (G-26) one obtains for the quantity g_1

$$g_1 = \frac{a_{G1}\sin(\phi_1 + \theta_{G1}) + \rho_{G1}\cos(\psi_1 - \alpha_{P1}) - b_1\sin\beta_1}{\sin(\psi_1 - \alpha_{P1})} \quad (G-27)$$

This expression is now substituted in equation (G-25). This leads to the following:

$$A_{1F} \sin \psi_1 + B_{1F} \cos \psi_1 = C_{1F} \quad (G-28)$$

where

$$A_{1F} = a_{G1} \cos(\phi_1 + \delta_{G1} + \alpha_{P1}) - b_1 \cos(\beta_1 + \alpha_{P1})$$

$$B_{1F} = -a_{G1} \sin(\phi_1 + \delta_{G1} + \alpha_{P1}) + b_1 \sin(\beta_1 + \alpha_{P1})$$

$$C_{1F} = \rho_{G1}$$

Equation (G-28) is solved for ψ_1 in the now customary manner:

$$\psi_1 = 2 \tan^{-1} \frac{A_{1F} \pm \sqrt{A_{1F}^2 + B_{1F}^2 - C_{1F}^2}}{B_{1F} + C_{1F}} \quad (G-29)$$

The appropriate sign is again found from geometric considerations.

III. DETERMINATION OF ANGULAR VELOCITY $\dot{\psi}_1$ DURING ROUND ON FLAT PHASE OF MOTION

Implicit differentiation of equation (G-28) with respect to time gives, for $\dot{\psi}_1$:

$$\dot{\psi}_1 = \dot{\phi}_1 \left[\frac{A_{1FD} \sin \psi_1 + B_{1FD} \cos \psi_1}{A_{1F} \cos \psi_1 - B_{1F} \sin \psi_1} \right] \quad (G-30)$$

where

$$A_{1FD} = a_{G1} \sin(\phi_1 + \delta_{G1} + \alpha_{P1})$$

$$B_{1FD} = a_{G1} \cos(\phi_1 + \delta_{G1} + \alpha_{P1})$$

IV. RELATIVE VELOCITY $\bar{V}_{S1/T1_F}$ AT CONTACT POINT DURING ROUND
ON FLAT PHASE OF MOTION

For the round on flat phase, the relative velocity $\bar{V}_{S1/T1_F}$ may be expressed by

$$\bar{V}_{S1/T1_F} = \bar{V}_{S1/O_1} - \bar{V}_{T1/O_2} \quad (G-31)$$

Now, this velocity has the direction of the unit vector $\pm \bar{n}_{F1}$. Since there is no velocity component along the pinion flank, equation (G-31) becomes

$$\begin{aligned} \bar{V}_{S1/T1_F} &= \bar{V}_{S1/O_1} \cdot \bar{n}_{F1} \\ &= \left\{ \left[\dot{\phi}_1 \times (a_{G1} \bar{n}_{G1} + r_{G1} \bar{n}_{NF1}) \right] \cdot \bar{n}_{F1} \right\} \bar{n}_{F1} \end{aligned} \quad (G-32)$$

Appropriate substitution of unit vectors furnishes

$$\bar{V}_{S1/T1_F} = \dot{\phi}_1 \left[a_{G1} \sin(\psi_1 - \alpha_{P1} - \phi_1 - \delta_{G1}) - r_{G1} \right] \bar{n}_{F1} \quad (G-33)$$

V. DETERMINATION OF TRANSITION ANGLES

The transition angle, ϕ_{1T} , and the corresponding angle, ψ_{1T} , are reached when the round or round phase is followed by the round on flat one. They are obtained by letting $g_1 = f_{p1}$ in the component equations (G-25) and (G-26). This gives

$$\begin{aligned} a_{G1} \cos(\phi_{1T} + \delta_{G1}) - p_{G1} \sin(\psi_{1T} - \alpha_{P1}) - b_1 \cos \beta_1 - f_{P1} \cos(\psi_{1T} - \alpha_{P1}) \\ = 0 \end{aligned} \quad (G-34)$$

and

$$\begin{aligned} a_{G1} \sin(\phi_{1T} + \delta_{G1}) + p_{G1} \cos(\psi_{1T} - \alpha_{P1}) - b_1 \sin \beta_1 - f_{P1} \sin(\psi_{1T} - \alpha_{P1}) \\ = 0 \end{aligned} \quad (G-35)$$

From the above, one obtains

$$\cos(\phi_{1T} + \delta_{G1}) = \frac{1}{a_{G1}} \left[p_{G1} \sin(\psi_{1T} - \alpha_{P1}) + b_1 \cos \beta_1 + f_{P1} \cos(\psi_{1T} - \alpha_{P1}) \right] \quad (G-36)$$

$$\sin(\phi_{1T} + \delta_{G1}) = \frac{1}{a_{G1}} \left[-p_{G1} \cos(\psi_{1T} - \alpha_{P1}) + b_1 \sin \beta_1 + f_{P1} \sin(\psi_{1T} - \alpha_{P1}) \right] \quad (G-37)$$

The angle ψ_{1T} is now obtained by letting

$$\sin^2(\phi_{1T} + \delta_{G1}) + \cos^2(\phi_{1T} + \delta_{G1}) = 1$$

This results in

$$A_{1T} \sin \psi_{1T} + B_{1T} \cos \psi_{1T} = C_{1T} \quad (G-38)$$

where

$$A_{1T} = \rho_{G1} \cos(\beta_1 + \alpha_{P1}) + f_{P1} \sin(\beta_1 + \alpha_{P1})$$

$$B_{1T} = -\rho_{G1} \sin(\beta_1 + \alpha_{P1}) + f_{P1} \cos(\beta_1 + \alpha_{P1})$$

$$C_{1T} = \frac{a_{G1}^2 - \rho_{G1}^2 - b_1^2 - f_{P1}^2}{2b_1}$$

Finally,

$$\psi_{1T} = 2 \tan^{-1} \frac{A_{1T} \pm \sqrt{A_{1T}^2 + B_{1T}^2 - C_{1T}^2}}{B_{1T} + C_{1T}} \quad (G-39)$$

The appropriate sign must be found from geometric considerations.

The associated angle ϕ_{1T} may be found with the help of either equation (G-36) or equation (G-37):

$$\phi_{1T} = \cos^{-1} \left[\frac{r_{G1} \sin(\psi_{1T} - \alpha_{P1}) + f_{P1} \cos(\psi_{1T} - \alpha_{P1}) + b_1 \cos \beta_1}{a_{G1}} \right] - \delta_{G1} \quad (G-40)$$

or

$$\phi_{1T} = \sin^{-1} \left[\frac{-r_{G1} \cos(\psi_{1T} - \alpha_{P1}) + f_{P1} \sin(\psi_{1T} - \alpha_{P1}) + b_1 \sin \beta_1}{a_{G1}} \right] - \delta_{G1} \quad (G-41)$$

VI. SENSING EQUATION FOR THE DETERMINATION OF CONTACT ON SUBSEQUENT TOOTH MESH

The following contact sensing equation is derived with the assumption that subsequent contact is made in the round on round phase of the motion, in the manner shown in Section VI of Appendix E. Now, the configuration is that of Figure G-2 where gear no. 1 rotates in a clockwise direction.

Before contact is made, the distance between the centers of curvature C_{G1} and C_{P1} is given by

$$\overline{C_{G1}C_{P1}} = L_{x1}\bar{i} + L_{y1}\bar{j} \quad (G-42)$$

If $\Delta\phi_1$ and $\Delta\psi_1$ represent the tooth spacing angles of gear no. 1 and pinion no. 2, respectively, the associated loop equation becomes (see Figures E-3 and G-2).

$$\begin{aligned} & a_{G1} [\cos(\phi_1 + \Delta\phi_1 + \delta_{G1})\bar{i} + \sin(\phi_1 + \Delta\phi_1 + \delta_{G1})\bar{j}] + L_{x1}\bar{i} + L_{y1}\bar{j} \\ & = b_1(\cos\beta_1\bar{i} + \sin\beta_1\bar{j}) + a_{P1} [\cos(\psi_1 - \Delta\psi_1 + \delta_{P1})\bar{i} + \sin(\psi_1 - \Delta\psi_1 + \delta_{P1})\bar{j}] \end{aligned} \quad (G-43)$$

where

ψ_1 = angle of pinion no. 2 as determined for the round on flat mode with equation (G-29)

The magnitudes of L_{x1} and L_{y1} are determined from the component form of equation (G-43), i.e.,

$$L_{x1} = b_1 \cos\beta_1 + a_{P1} \cos(\psi_1 - \Delta\psi_1 + \delta_{P1}) - a_{G1} \cos(\phi_1 + \Delta\phi_1 + \delta_{G1}) \quad (G-44)$$

and

$$L_{y1} = b_1 \sin\beta_1 + a_{P1} \sin(\psi_1 - \Delta\psi_1 + \delta_{P1}) - a_{G1} \sin(\phi_1 + \Delta\phi_1 + \delta_{G1}) \quad (G-45)$$

Contact will have occurred as soon as

$$\sqrt{L_{x1}^2 + L_{y1}^2} \leq p_{G1} + p_{P1}$$

(G-46)

2. KINEMATICS OF MESH NO. 2 (GEAR NO. 2 AND PINION NO. 3)

a. ROUND ON ROUND PHASE OF MOTION

Figure G-4 gives a schematic representation of the round on round phase of the motion. Only the contacting faces of the gear and the pinion are shown. It is to be noted that the input gear rotates in the counter-clockwise direction, and that the output angle ψ_1 of mesh no. 1 is identical to the input angle ϕ_2 of mesh no. 2.

I. UNIT VECTORS

The unit vector in the direction O_2C_{G2} of the gear is given by

$$\bar{n}_{G2} = \cos(\phi_2 - \delta_{G2})\bar{i} + \sin(\phi_2 - \delta_{G2})\bar{j} \quad (G-47)$$

The unit vector in the direction $C_{G2}C_{P2}$ is given by

$$\bar{n}_{\lambda 2} = \cos\lambda_2\bar{i} + \sin\lambda_2\bar{j} \quad (G-48)$$

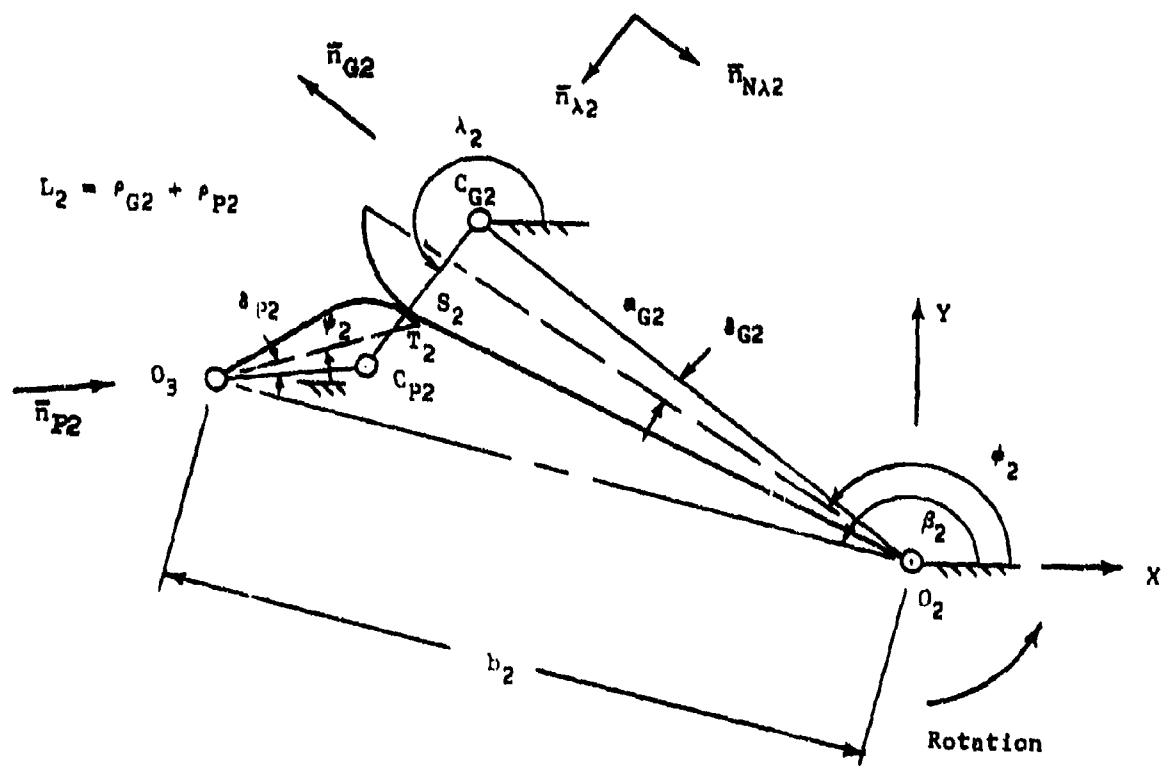


FIGURE G-4
ROUND ON ROUND PHASE FOR MESH NO. 2

The unit vector normal to $\bar{n}_{\lambda 2}$ in the right hand sense becomes

$$\bar{n}_{N\lambda 2} = -\sin\lambda_2 \bar{i} + \cos\lambda_2 \bar{j} \quad (G-49)$$

The pinion unit vector \bar{n}_{p2} , in the direction O_3C_{p2} , is represented by

$$\bar{n}_{p2} = \cos(\psi_2 - \delta_{p2}) \bar{i} + \sin(\psi_2 - \delta_{p2}) \bar{j} \quad (G-50)$$

Finally, the unit vector along the centerline O_2O_3 is given by

$$\bar{n}_{\beta 2} = \cos\beta_2 \bar{i} + \sin\beta_2 \bar{j} \quad (G-51)$$

II. DETERMINATION OF OUTPUT ANGLE ψ_2 AND "COUPLER" ANGLE λ_2

The loop equation of the equivalent four-bar linkage is given by

$$a_{G2} \bar{n}_{G2} + L_2 \bar{n}_{\lambda 2} - a_{p2} \bar{n}_{p2} - b_2 \bar{n}_{\beta 2} = 0 \quad (G-52)$$

where

$$L_2 = \rho_{G2} + \rho_{P2} \quad (G-53)$$

After substitution of the unit vector, as given earlier, one obtains the following component equations

$$a_{G2} \cos(\phi_2 - \delta_{G2}) + L_2 \cos \lambda_2 - a_{P2} \cos(\psi_2 - \delta_{P2}) - b_2 \cos \beta_2 = 0 \quad (G-54)$$

and

$$a_{G2} \sin(\phi_2 - \delta_{G2}) + L_2 \sin \lambda_2 - a_{P2} \sin(\psi_2 - \delta_{P2}) - b_2 \sin \beta_2 = 0 \quad (G-55)$$

To solve for the output angle ψ_2 in terms of the input angle ϕ_2 , substitute the expressions for $\sin \lambda_2$ and $\cos \lambda_2$, as obtained from the component equations (G-54) and (G-55), into

$$\sin^2 \lambda_2 + \cos^2 \lambda_2 = 1 \quad (G-56)$$

This leads to

$$A_{2R} \sin \psi_2 + B_{2R} \cos \psi_2 = C_{2R} \quad (G-57)$$

where

$$A_{2R} = b_2 \sin(\beta_2 + \delta_{P2}) - a_{G2} \sin(\phi_2 - \delta_{G2} + \delta_{P2})$$

$$B_{2R} = b_2 \cos(\beta_2 + \delta_{P2}) - a_{G2} \cos(\phi_2 - \delta_{G2} + \delta_{P2})$$

$$C_{2R} = \frac{L_2^2 - b_2^2 - a_{G2}^2 - a_{P2}^2 + 2a_{G2}b_2 \cos(\phi_2 - \delta_{G2} - \beta_2)}{2a_{P2}}$$

Equation (G-57) is then solved for ψ_2 in the manner discussed in Appendix E

$$\psi_2 = 2 \tan^{-1} \frac{A_{2R} \pm \sqrt{A_{2R}^2 + B_{2R}^2 - C_{2R}^2}}{B_{2R} + C_{2R}} \quad (G-58)$$

The correct sign must again be determined from geometric considerations

The angle λ_2 may now be determined either from equation (G-54) or equation (G-55)

$$\lambda_2 = \cos^{-1} \left[\frac{b_2 \cos \beta_2 + a_{P2} \cos(\psi_2 - \delta_{P2}) - a_{G2} \cos(\phi_2 - \delta_{G2})}{L_2} \right] \quad (G-59)$$

or

$$\lambda_2 = \sin^{-1} \left[\frac{b_2 \sin \beta_2 + a_{P2} \sin(\psi_2 - \delta_{P2}) - a_{G2} \sin(\phi_2 - \delta_{G2})}{L_2} \right] \quad (G-60)$$

III. DETERMINATION OF OUTPUT ANGULAR VELOCITY $\dot{\psi}_2$

Implicit differentiation of equation (G-57) with respect to time leads to

$$\dot{\psi}_2 = \dot{\phi}_2 \left[\frac{A_{2RD} \sin \psi_2 - B_{2RD} \cos \psi_2 - C_{2RD}}{A_{2R} \cos \psi_2 - B_{2R} \sin \psi_2} \right] \quad (G-61)$$

where

$$A_{2RD} = a_{G2} \cos(\phi_2 - \delta_{G2} + \delta_{p2})$$

$$B_{2RD} = a_{G2} \sin(\phi_2 - \delta_{G2} + \delta_{p2})$$

$$C_{2RD} = \frac{a_{G2} b_2 \sin(\phi_2 - \delta_{G2} - \beta_2)}{a_{p2}}$$

IV. RELATIVE VELOCITY AT THE CONTACT POINT

The relative velocity $\bar{V}_{S2/T2_R}$, of point S_2 on gear no. 2 with respect to point T_2 on pinion no. 3 has the direction of the unit vector $\bar{n}_{N\lambda 2}$. Thus, in the manner of equation (G-20).

$$\bar{V}_{S2/T2_R} = \left\{ \left[\dot{\phi}_2 \bar{k} \times (a_{G2} \bar{n}_{G2} + \rho_{G2} \bar{n}_{\lambda 2}) \right] \cdot \bar{n}_{N\lambda 2} - \left[\dot{\psi}_2 \bar{k} \times (a_{P2} \bar{n}_{P2} - \rho_{P2} \bar{n}_{\lambda 2}) \right] \cdot \bar{n}_{N\lambda 2} \right\} \bar{n}_{N\lambda 2} \quad (G-62)$$

Substitution of unit vectors yields

$$\bar{V}_{S2/T2_R} = \left\{ \dot{\phi}_2 [a_{G2} \cos(\phi_2 - \delta_{G2} - \lambda_2) + \rho_{G2}] - \dot{\psi}_2 [a_{P2} \cos(\psi_2 - \delta_{P2} - \lambda_2) - \rho_{P2}] \right\} \bar{n}_{N\lambda 2} \quad (G-63)$$

b. ROUND ON FLAT PHASE OF MOTION

Figure G-5 shows a schematic view of mesh no. 2 in the round on flat phase of the motion. Again, only the contacting sides of the gear teeth are indicated.

I. UNIT VECTORS

The unit vector in the direction O_3T_2 , along the flank of pinion no. 3, is given by

$$\bar{n}_{F2} = \cos(\psi_2 + \alpha_{p2})\bar{i} + \sin(\psi_2 + \alpha_{p2})\bar{j} \quad (G-64)$$

The unit vector \bar{n}_{NF2} , in the direction S_2C_{G2} , is normal to \bar{n}_{F2} in the right hand sense

$$\bar{n}_{NF2} = -\sin(\psi_2 + \alpha_{p2})\bar{i} + \cos(\psi_2 + \alpha_{p2})\bar{j} \quad (G-65)$$

II. DETERMINATION OF OUTPUT ANGLE ψ_2 AND DISTANCE g_2

The vector equation for the mechanism loop $O_2-C_{G2}-S_2-T_2-O_3$ has the form

$$a_{G2}\bar{n}_{G2} - p_{G2}\bar{n}_{NF2} - g_2\bar{n}_{F2} - b_2\bar{n}_{\beta 2} = 0 \quad (G-66)$$

Appropriate substitutions for the unit vectors furnish the following component equations.

$$\begin{aligned} a_{G2}\cos(\phi_2 - \delta_{G2}) + p_{G2}\sin(\psi_2 + \alpha_{P2}) - b_2\cos\beta_2 - g_2\cos(\psi_2 + \alpha_{P2}) \\ = 0 \end{aligned} \quad (G-67)$$

and

$$\begin{aligned} a_{G2}\sin(\phi_2 - \delta_{G2}) - p_{G2}\cos(\psi_2 + \alpha_{P2}) - b_2\sin\beta_2 - g_2\sin(\psi_2 + \alpha_{P2}) \\ = 0 \end{aligned} \quad (G-68)$$

From equation (G-68) one obtains the following expression for g_2

$$g_2 = \frac{a_{G2}\sin(\phi_2 - \delta_{G2}) - p_{G2}\cos(\psi_2 + \alpha_{P2}) - b_2\sin\beta_2}{\sin(\psi_2 + \alpha_{P2})} \quad (G-69)$$

This expression is now substituted into equation (G-67), and one obtains the following:

$$A_{2F} \sin \psi_2 + B_{2F} \cos \psi_2 = C_{2F} \quad (G-70)$$

where

$$A_{2F} = a_{G2} \cos(\phi_2 - \delta_{G2} - \alpha_{P2}) - b_2 \cos(\beta_2 - \alpha_{P2})$$

$$B_{2F} = -a_{G2} \sin(\phi_2 - \delta_{G2} - \alpha_{P2}) + b_2 \sin(\beta_2 - \alpha_{P2})$$

$$C_{2F} = -r_{G2}$$

Equation (G-70) is solved in the customary manner:

$$\psi_2 = 2 \tan^{-1} \frac{A_{2F} \pm \sqrt{A_{2F}^2 + B_{2F}^2 - C_{2F}^2}}{B_{2F} + C_{2F}} \quad (G-71)$$

The appropriate sign is again found from geometric considerations.

III. DETERMINATION OF ANGULAR VELOCITY $\dot{\psi}_2$ DURING ROUND ON FLAT PHASE OF MOTION

Implicit differentiation of equation (G-70) with respect to time gives the following expression for $\dot{\psi}_2$:

$$\dot{\psi}_2 = \dot{\phi}_2 \left[\frac{A_{2FD} \sin \psi_2 + B_{2FD} \cos \psi_2}{A_{2F} \cos \psi_2 - B_{2F} \sin \psi_2} \right] \quad (G-72)$$

where

$$A_{2FD} = a_{G2} \sin(\phi_2 - \delta_{G2} - \alpha_{P2})$$

$$B_{2FD} = a_{G2} \cos(\phi_2 - \delta_{G2} - \alpha_{P2})$$

IV. RELATIVE VELOCITY $\bar{V}_{S2/T2_F}$ AT CONTACT POINT DURING ROUND ON FLAT PHASE OF MOTION

Again, the relative velocity $\bar{V}_{S2/T2_F}$ consists only of that component of \bar{V}_{S2/O_2} which is directed along the pinion flank.

Thus,

$$\begin{aligned}
\bar{V}_{S2/T2_F} &= [\bar{V}_{S2/O_2} \cdot \bar{n}_{F2}] \bar{n}_{F2} \\
&= \left\{ [\dot{\phi}_2 \bar{k} \times (a_{G2} \bar{n}_{G2} - \rho_{G2} \bar{n}_{NF2})] \cdot \bar{n}_{F2} \right\} \bar{n}_{F2}
\end{aligned}
\tag{G-73}$$

Appropriate substitution of unit vectors gives

$$\bar{V}_{S2/T2_F} = \dot{\phi}_2 [a_{G2} \sin(\psi_2 + \alpha_{P2} - \phi_2 + \delta_{G2}) + \rho_{G2}] \bar{n}_{F2}
\tag{G-74}$$

V. DETERMINATION OF TRANSITION ANGLES

The transition angle ϕ_{2T} and the angle ψ_{2T} , which correspond to the transition from the round on round to the round on flat phase of motion, are obtained by letting $g_2 = f_{p2}$ in the component equations (G-67) and (G-68). From this one finds the following with $\phi_2 = \phi_{2T}$ and $\psi_2 = \psi_{2T}$:

$$\cos(\phi_{2T} - \delta_{G2}) = \frac{1}{a_{G2}} \left[-\rho_{G2} \sin(\psi_{2T} + \alpha_{P2}) + b_2 \cos \beta_2 + f_{p2} \cos(\psi_{2T} + \alpha_{P2}) \right]
\tag{G-75}$$

and

$$\sin(\phi_{2T} - \delta_{G2}) = \frac{1}{a_{G2}} \left[p_{G2} \cos(\psi_{2T} + \alpha_{P2}) + b_2 \sin \beta_2 + f_{P2} \sin(\psi_{2T} + \alpha_{P2}) \right] \quad (G-76)$$

The angle ψ_{2T} is now found by substituting the above expressions into

$$\sin^2(\phi_{2T} - \delta_{G2}) + \cos^2(\phi_{2T} - \delta_{G2}) = 1 \quad (G-77)$$

This results in

$$A_{2T} \sin \psi_{2T} + B_{2T} \cos \psi_{2T} = C_{2T} \quad (G-78)$$

where

$$A_{2T} = -p_{G2} \cos(\beta_2 - \alpha_{P2}) + f_{P2} \sin(\beta_2 - \alpha_{P2})$$

$$B_{2T} = p_{G2} \sin(\beta_2 - \alpha_{P2}) + f_{P2} \cos(\beta_2 - \alpha_{P2})$$

$$C_{2T} = \frac{a_{G2}^2 - p_{G2}^2 - b_2^2 - f_{P2}^2}{2 b_2}$$

Finally, in the usual way

$$\psi_{2T} = 2 \tan^{-1} \frac{A_{2T} \pm \sqrt{A_{2T}^2 + B_{2T}^2 - C_{2T}^2}}{B_{2T} + C_{2T}} \quad (G-79)$$

Again, the sign must be decided from geometric considerations.

The associated angle ϕ_{2T} may be found with the help of either equation (G-75) or equation (G-76), i.e.,

$$\phi_{2T} = \cos^{-1} \left[\frac{-p_{G2} \sin(\psi_{2T} + \alpha_{P2}) + b_2 \cos \beta_2 + f_{P2} \cos(\psi_{2T} + \alpha_{P2})}{a_{G2}} \right] + \delta_{G2} \quad (G-80)$$

or

$$\phi_{2T} = \sin^{-1} \left[\frac{p_{G2} \cos(\psi_{2T} + \alpha_{P2}) + b_2 \sin \beta_2 + f_{P2} \sin(\psi_{2T} + \alpha_{P2})}{a_{G2}} \right] + \delta_{G2} \quad (G-81)$$

VI. SENSING EQUATION FOR THE DETERMINATION OF CONTACT ON
SUBSEQUENT TOOTH MESH

The contact sensing equation for mesh no. 2 is derived similarly to that for mesh no. 1 before contact is made in the round on round mode. The distance between the centers of curvature C_{G2} and C_{P2} is given by

$$\overline{C_{G2}C_{P2}} = L_{x2}\bar{i} + L_{y2}\bar{j} \quad (G-82)$$

If $\Delta\phi_2$ and $\Delta\psi_2$ represent the tooth spacing angles of gear no. 2 and pinion no. 3 respectively, the associated loop equation becomes (see Figures E-3 and G-4)

$$\begin{aligned} & a_{G2} [\cos(\phi_2 - \Delta\phi_2 - \delta_{G2})\bar{i} + \sin(\phi_2 - \Delta\phi_2 - \delta_{G2})\bar{j}] + L_{x2}\bar{i} + L_{y2}\bar{j} \\ & - a_{P2} [\cos(\psi_2 + \Delta\psi_2 - \delta_{P2})\bar{i} + \sin(\psi_2 + \Delta\psi_2 - \delta_{P2})\bar{j}] \\ & - b_2 [\cos\beta_2\bar{i} + \sin\beta_2\bar{j}] = 0 \end{aligned} \quad (G-83)$$

Note that for mesh no. 2, the angular increment $\Delta\phi_2$ is negative while $\Delta\psi_2$ is positive. Further, as before, the angle ψ_2 must be

determined for the round on flat phase of the motion.

The magnitudes of L_{x2} and L_{y2} are determined from the components of equation (G-83), i.e.,

$$L_{x2} = b_2 \cos \beta_2 + a_{p2} \cos(\psi_2 + \Delta\psi_2 - \delta_{p2}) - a_{G2} \cos(\phi_2 - \Delta\phi_2 - \delta_{G2}) \quad (G-84)$$

while

$$L_{y2} = b_2 \sin \beta_2 + a_{p2} \sin(\psi_2 + \Delta\psi_2 - \delta_{p2}) - a_{G2} \sin(\phi_2 - \Delta\phi_2 - \delta_{G2}) \quad (G-85)$$

Contact will occur as soon as

$$\sqrt{L_{x2}^2 + L_{y2}^2} \leq r_{G2} + r_{P2} \quad (G-86)$$

3. KINEMATICS OF MESH NO. 3 (GEAR NO. 3 AND PINION NO. 4)

Since mesh no. 3 is kinematically equivalent to mesh no. 1, the kinematic equations for mesh no. 3 may be obtained from those for mesh no. 1. The angle β_3 must replace the angle β_1 and the center distance b_3 is used instead of b_1 . All parameters of gear no. 1 are replaced by those of gear no. 3 and the pinion parameters of pinion no. 4 are substituted for those of pinion no. 2.

It is to be noted that the input angle ϕ_3 of mesh no. 3 is identical to the output angle ψ_2 of mesh no. 2.

a. ROUND ON ROUND PHASE OF MOTION

The output angle ψ_3 is obtained with the help of equation (G-12)

$$\psi_3 = 2 \tan^{-1} \frac{A_{3R} \pm \sqrt{A_{3R}^2 + B_{3R}^2 - C_{3R}^2}}{B_{3R} + C_{3R}} \quad (G-87)$$

where

$$A_{3R} = a_{G3} \sin(\phi_3 + \delta_{G3} - \delta_{P3}) - b_3 \sin(\beta_3 - \delta_{P3})$$

$$B_{3R} = a_{G3} \cos(\phi_3 + \delta_{G3} - \delta_{P3}) - b_3 \cos(\beta_3 - \delta_{P3})$$

$$C_{3R} = \frac{a_{P3}^2 + a_{G3}^2 + b_3^2 - L_3^2 - 2a_{G3}b_3 \cos(\phi_3 + \delta_{G3} - \beta_3)}{2 a_{P3}}$$

and

$$L_3 = r_{G3} + r_{P3} \quad (G-88)$$

The angle λ_3 may be found with the help of equation (G-13) or equation (G-14)

$$\lambda_3 = \cos^{-1} \left[\frac{b_3 \cos \beta_3 + a_{P3} \cos(\psi_3 + \delta_{P3}) - a_{G3} \cos(\phi_3 + \delta_{G3})}{L_3} \right] \quad (G-89)$$

or

$$\lambda_3 = \sin^{-1} \left[\frac{b_3 \sin \beta_3 + a_{P3} \sin(\psi_3 + \delta_{P3}) - a_{G3} \sin(\phi_3 + \delta_{G3})}{L_3} \right] \quad (G-90)$$

The angular velocity $\dot{\psi}_3$ is obtained from equation (G-15)

$$\dot{\psi}_3 = \dot{\phi}_3 \left[\frac{B_{3RD} \cos \psi_3 - A_{3RD} \sin \psi_3 + C_{3RD}}{A_{3R} \cos \psi_3 - B_{3R} \sin \psi_3} \right] \quad (G-91)$$

where

$$A_{3RD} = a_{G3} \cos(\phi_3 + \delta_{G3} - \delta_{P3})$$

$$B_{3RD} = a_{G3} \sin(\phi_3 + \delta_{G3} - \delta_{P3})$$

$$C_{3RD} = \frac{a_{G3} b_3 \sin(\phi_3 + \delta_{G3} - \beta_3)}{a_{P3}}$$

The relative velocity $\bar{V}_{S3/T3R}$ becomes, according to Equation (G-21),

$$\bar{V}_{S3/T3R} = \left\{ \begin{aligned} &\dot{\phi}_3 [a_{G3} \cos(\phi_3 + \delta_{G3} - \lambda_3) + r_{G3}] \\ &- \dot{\psi}_3 [a_{P3} \cos(\psi_3 + \delta_{P3} - \lambda_3) - r_{P3}] \end{aligned} \right\} \bar{n}_{N\lambda 3} \quad (G-92)$$

where, according to equation (G-3),

$$\bar{n}_{N\lambda 3} = -\sin \lambda_3 \bar{i} + \cos \lambda_3 \bar{j} \quad (G-93)$$

b. ROUND ON FLAT PHASE OF MOTION

The output angle ψ_3 is obtained from equation (G-29)

$$\psi_3 = 2 \tan^{-1} \frac{A_{3F} \pm \sqrt{A_{3F}^2 + B_{3F}^2 - C_{3F}^2}}{B_{3F} + C_{3F}} \quad (G-94)$$

where

$$A_{3F} = a_{G3} \cos(\phi_3 + \delta_{G3} + \alpha_{P3}) - b_3 \cos(\beta_3 + \alpha_{P3})$$

$$B_{3F} = -a_{G3} \sin(\phi_3 + \delta_{G3} + \alpha_{P3}) + b_3 \sin(\beta_3 + \alpha_{P3})$$

$$C_{3F} = r_{G3}$$

The distance g_3 becomes, according to equation (G-27),

$$g_3 = \frac{a_{G3} \sin(\phi_3 + \delta_{G3}) + r_{G3} \cos(\psi_3 - \alpha_{P3}) - b_3 \sin \beta_3}{\sin(\psi_3 - \alpha_{P3})} \quad (G-95)$$

The angular velocity $\dot{\psi}_3$ for the round on flat phase of the motion is found from equation (G-30)

$$\dot{\psi}_3 = \dot{\phi}_3 \left[\frac{A_{3FD} \sin \psi_3 + B_{3FD} \cos \psi_3}{A_{3F} \cos \psi_3 - B_{3F} \sin \psi_3} \right] \quad (G-96)$$

where

$$A_{3FD} = a_{G3} \sin(\phi_3 + \delta_{G3} + \alpha_{P3})$$

$$B_{3FD} = a_{G3} \cos(\phi_3 + \delta_{G3} + \alpha_{P3})$$

The relative velocity $\bar{V}_{S3/T3_F}$ for the round on flat phase comes from equation (G-33)

$$\bar{V}_{S3/T3_F} = \dot{\phi}_3 \left[a_{G3} \sin(\psi_3 - \alpha_{P3} - \phi_3 - \delta_{G3}) - \rho_{G3} \right] \bar{n}_{F3} \quad (G-97)$$

where

$$\bar{n}_{F3} = \cos(\psi_3 - \alpha_{P3}) \bar{i} + \sin(\psi_3 - \alpha_{P3}) \bar{j} \quad (G-98)$$

according to equation (G-22).

The transition angle ψ_{3T} is obtained by way of equation (G-39)

$$\psi_{3T} = 2 \tan^{-1} \frac{A_{3T} \pm \sqrt{A_{3T}^2 + B_{3T}^2 - C_{3T}^2}}{B_{3T} + C_{3T}} \quad (G-99)$$

where

$$A_{3T} = \rho_{G3} \cos(\beta_3 + \alpha_{P3}) + f_{P3} \sin(\beta_3 + \alpha_{P3})$$

$$B_{3T} = -\rho_{G3} \sin(\beta_3 + \alpha_{P3}) + f_{P3} \cos(\beta_3 + \alpha_{P3})$$

$$C_{3T} = \frac{a_{G3}^2 - \rho_{G3}^2 - b_3^2 - f_{P3}^2}{2 b_3}$$

The associated angle ϕ_{3T} may be obtained from equation (G-40)
or from equation (G-41)

$$\phi_{3T} = \cos^{-1} \left[\frac{\rho_{G3} \sin(\psi_{3T} - \alpha_{P3}) + f_{P3} \cos(\psi_{3T} - \alpha_{P3}) + b_3 \cos \beta_3}{a_{G3}} \right] - \delta_{G3} \quad (G-100)$$

or

$$\phi_{3T} = \sin^{-1} \left[\frac{-\rho_{G3} \cos(\psi_{3T} - \alpha_{P3}) + f_{P3} \sin(\psi_{3T} - \alpha_{P3}) + b_3 \sin \beta_3}{a_{G3}} \right] - \delta_{G3} \quad (G-101)$$

Finally, the contact sensing equation is based on equations

(G-44) - (G-46). Contact will occur, when

$$\sqrt{L_{x3}^2 + L_{y3}^2} \leq \rho_{G3} + \rho_{P3} \quad (G-102)$$

where with the tooth spacing angles $\Delta\phi_3$ and $\Delta\psi_3$,

$$L_{x3} = b_3 \cos \beta_3 + a_{P3} \cos(\psi_3 - \Delta\psi_3 + \delta_{P3}) - a_{G3} \cos(\phi_3 + \Delta\phi_3 + \delta_{G3}) \quad (G-103)$$

and

$$L_{y3} = b_3 \sin \beta_3 + a_{P3} \sin(\psi_3 - \Delta\psi_3 + \delta_{P3}) - a_{G3} \sin(\phi_3 + \Delta\phi_3 + \delta_{G3}) \quad (G-104)$$

APPENDIX H
MOMENT INPUT-OUTPUT RELATIONSHIPS FOR TWO AND THREE STEP-UP
GEAR TRAINS WITH TEETH OPERATING IN A SPIN ENVIRONMENT

The following gives the derivations for the moment input-output relationships of two and three step-up gear trains which operate in a spin environment.

Figure G-1 of Appendix G shows the basic configuration of a three step-up gear train. The input moment, M_{1n} , which acts on gear no. 1, is held in equilibrium by the moment, M_{o4} , which acts on pinion no. 4.

Since in all three meshes there may either be round on round or round on flat type of contact, the force and moment analyses must account for various contact combinations. Table H-1 shows the eight different phase combinations which may occur in a three step-up gear train, and for which input-output relationships must be found. The two step-up gear train, which is shown in Figure A-10 of Appendix A for involute gearing, does not contain pinion 4 and gear no. 3. Here, the input moment M_{1n} , which acts on gear no. 1, is held in equilibrium by moment M_{o3} , which acts on pinion no. 3.

Case no.	Mesh No. 3 (Gear 3 & Pinion 4)	Mesh No. 2 (Gear 2 & Pinion 3)	Mesh No. 1 (Gear 1 & Pinion 2)
1	R	R	R
2	R	R	F
3	R	F	F
4	R	F	R
5	F	F	F
6	F	F	R
7	F	R	R
8	F	R	F

TABLE H-1

POSSIBLE COMBINATIONS OF PHASES FOR THREE STEP-UP GEAR TRAIN AS SHOWN IN FIGURE G-1

R = Round on Round

F = Round on Flat

When ogival teeth are involved, there are four possible phase combinations of the two remaining meshes. These are shown in Table H-2. Again input-output relationships must be obtained for each of them.

Case No.	Mesh No. 2 (Gear 2 & Pinion 3)	Mesh No. 1 (Gear 1 & Pinion 2)
1	R	R
2	R	F
3	F	F
4	F	R

TABLE H-2

POSSIBLE COMBINATIONS OF PHASES FOR TWO STEP-UP GEAR TRAIN AS SHOWN IN FIGURE A-10

R = Round on Round

F = Round on Flat

The unit vectors, mechanism angles and kinematic terms necessary for the following analyses were derived in Appendix G. (See also Appendix D for a description of the geometry of ogival teeth.) Certain terms used in connection with mesh no. 3 may be obtained from expressions derived for mesh no. 1 in Appendix G by the replacement of the appropriate subscript numbers, since the kinematics of these meshes are identical. The following additional nomenclature is used:

- R_1 = distance from spin axis C to pivot points O_1 of individual gears. ($i = 1, 2, 3, 4$ as applicable)
- γ_1 = angle of lines $R_1 = CO_1$ with respect to the body-fixed X-axis
- ω = spin velocity of fuze body
- m_1 = mass of various gears, pinions and gear-pinion combinations
- Q_1 = $m_1 R_1 \omega^2$, centrifugal force acting on individual gear components. (Now called Q_1 to differentiate it from the pinion contact point T_1 .)
- ρ_1 = pivot radius
- ρ_{p1} = radius of curvature of pinion tooth (ogival)
- ρ_{G1} = radius of curvature of gear tooth (ogival)
- μ = coefficient of friction at pivots as well as at contact point between gears and pinions

The pivot friction moments are obtained according to equation (A-3b) of Appendix A. They always oppose motion regardless of the assumption of direction of the pivot reactions F_{x1} and F_{y1} . To this end the pivot forces \tilde{F}_{x1} and \tilde{F}_{y1} , which represent the sums of the absolute values of their component parts, are added

algebraically. The algebraic addition of such modified reactions provides a conservative, i.e., a somewhat overstated friction moment.

The directions of the friction forces of the gears on the pinions are always those of the relative velocities \bar{V}_{S_1/T_1} , where points S_1 and T_1 are located at the contact points of the gears and pinions, respectively. This allows the introduction of a signum convention. For the round on round phases,

$$\mu_{1R} = \frac{V_{S_1/T_1R}}{|V_{S_1/T_1R}|} \quad (H-1)$$

For the round on flat phase, the convention becomes

$$\mu_{1F} = \frac{V_{S_1/T_1F}}{|V_{S_1/T_1F}|} \quad (H-2)$$

The expressions for the above relative velocities, which are different for round on round and for round on flat, are given in Appendix G.

1. INPUT-OUTPUT ANALYSIS OF THREE STEP-UP GEAR TRAIN

a. CASE NO. 1: RRR

1. FORCE AND MOMENT EQUILIBRIA OF PINION NO. 4

Figure H-1 shows a schematic free body diagram of pinion no. 4 in the round on round mode of contact. The equivalent four-bar linkage associated with mesh no. 3 is also indicated. The pinion is acted upon by the equilibrant moment M_{o4} in the direction opposite to its counterclockwise rotation. The contact force of gear no. 3 on the pinion is given by

$$\vec{F}_{34} = F_{34} \vec{E}_{\lambda 3} \quad (H-3)$$

The associated friction force exerted by the gear on the pinion has the direction of the relative velocity $\vec{V}_{s3/T3_R}$, as given by equation (G-92). With the use of the signum convention of equation (H-1) the friction force \vec{F}_{f34} becomes

$$\vec{F}_{f34} = \mu_{s3} F_{34} \vec{E}_{N\lambda 3} \quad (H-4)$$

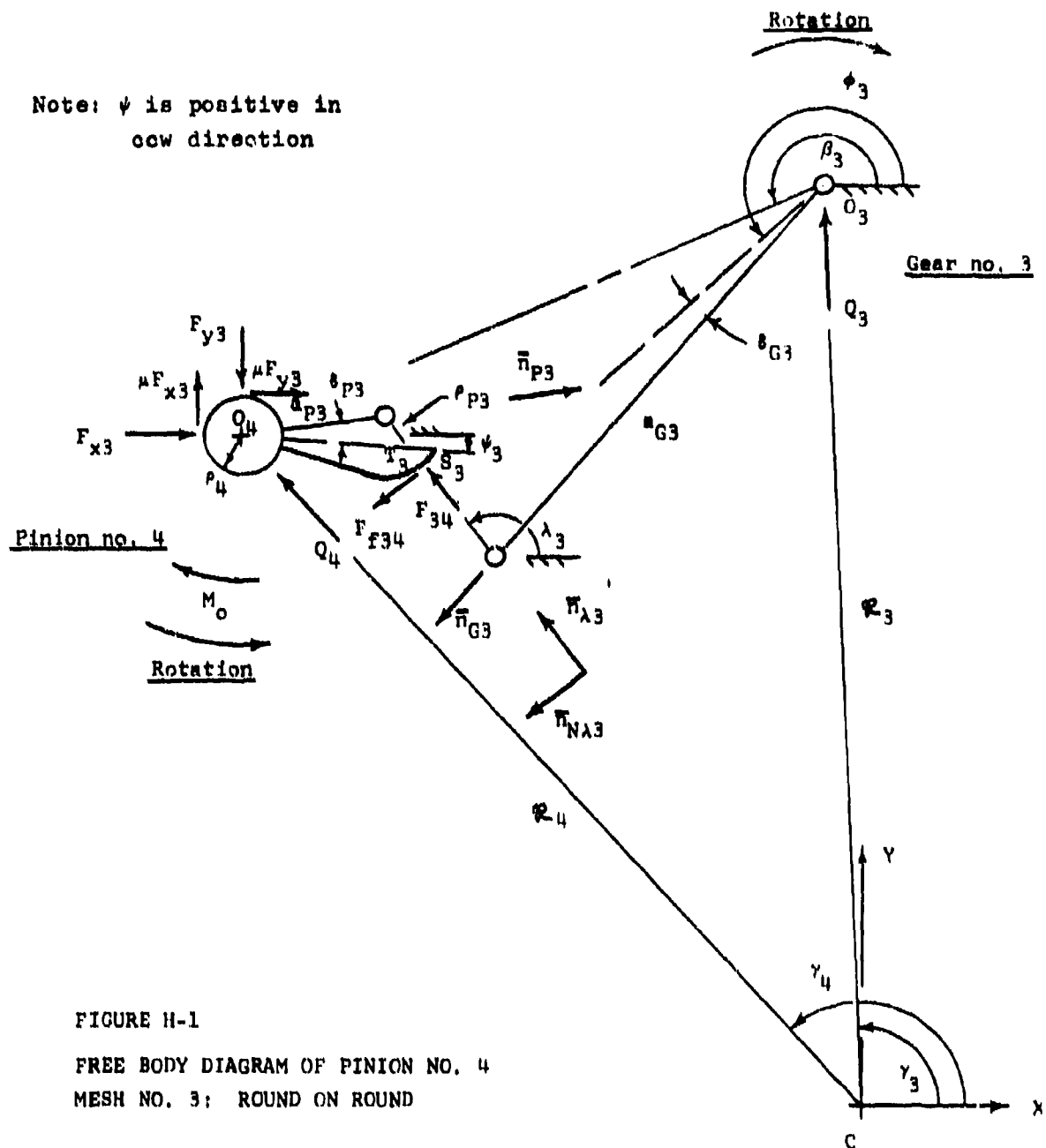
Rotation

FIGURE H-1

FREE BODY DIAGRAM OF PINION NO. 4
MESH NO. 3; ROUND ON ROUND

The centrifugal force, due to the pinion mass, is given by

$$\bar{Q}_4 = Q_4(\cos\gamma_4\bar{i} + \sin\gamma_4\bar{j}) \quad (H-5)$$

where

$$Q_4 = R_4 m_4 \omega^2 \quad (H-6)$$

Force equilibrium is given by

$$F_{34}\bar{n}_{\lambda 3} + \mu_{3R}F_{34}\bar{n}_{N\lambda 3} + F_{x4}\bar{i} + \mu F_{y4}\bar{i} - F_{y4}\bar{j} + \mu F_{x4}\bar{j} + \bar{Q}_4 = 0 \quad (H-7)$$

Moment equilibrium requires the following:

$$-M_{o4}\bar{k} - \mu\rho_4(\tilde{F}_{x4} + \tilde{F}_{y4})\bar{k} + (a_{p3}\bar{n}_{p3} - r_{p3}\bar{n}_{\lambda 3}) \times (F_{34}\bar{n}_{\lambda 3} + \mu_{3R}F_{34}\bar{n}_{N\lambda 3}) = 0 \quad (H-8)$$

Equation (H-7) furnishes the following component equations:

$$F_{34}\cos\lambda_3 - \mu_{3R}F_{34}\sin\lambda_3 + F_{x4} + \mu F_{y4} + Q_4\cos\gamma_4 = 0 \quad (H-9)$$

and

$$F_{34}\sin\lambda_3 + \mu_{3R}F_{34}\cos\lambda_3 - F_{y4} + \mu F_{x4} + Q_4\sin\gamma_4 = 0 \quad (H-10)$$

The scalar form of the moment equation becomes

$$-M_{o4} - \mu p_4(\tilde{F}_{x4} + \tilde{F}_{y4}) - F_{34} \left\{ a_{p3} [\sin(\psi_3 + \delta_{p3} - \lambda_3) - \mu s_{3R} \cos(\psi_3 + \delta_{p3} - \lambda_3)] + \mu s_{3R} p_3 \right\} = 0 \quad (H-11)$$

Simultaneous solution of equations (H-9) and (H-10) for F_{x4} and F_{y4} gives

$$F_{x4} = \frac{F_{34} [\mu(s_{3R} - 1) \sin \lambda_3 - (1 + \mu^2 s_{3R}) \cos \lambda_3] - Q_4 (\mu \sin \gamma_4 + \cos \gamma_4)}{1 + \mu^2} \quad (H-12)$$

and

$$F_{y4} = \frac{F_{34} [(1 + \mu^2 s_{3R}) \sin \lambda_3 + \mu(s_{3R} - 1) \cos \lambda_3] + Q_4 (\sin \gamma_4 - \mu \cos \gamma_4)}{1 + \mu^2} \quad (H-13)$$

The sum $\tilde{F}_{x4} + \tilde{F}_{y4}$ of equation (H-11) is now made up of equations (H-12) and (H-13) in the sense of equation (A-3b) of Appendix A

$$\tilde{F}_{x4} + \tilde{F}_{y4} = Q_4 A_1 + F_{34} A_2 + Q_4 A_3 + F_{34} A_4 \quad (H-14)$$

$$A_1 = \left| \frac{\mu \sin \gamma_4 + \cos \gamma_4}{1 + \mu^2} \right| \quad (H-15)$$

$$A_2 = \left| \frac{\mu(s_{3R} - 1)\sin \lambda_3 - (1 + \mu^2 s_{3R})\cos \lambda_3}{1 + \mu^2} \right| \quad (H-16)$$

$$A_3 = \left| \frac{\sin \gamma_4 - \mu \cos \gamma_4}{1 + \mu^2} \right| \quad (H-17)$$

$$A_4 = \left| \frac{(1 + \mu^2 s_{3R})\sin \lambda_3 + \mu(s_{3R} - 1)\cos \lambda_3}{1 + \mu^2} \right| \quad (H-18)$$

Equation (H-14) is now substituted into the moment equation (H-11) and the latter is solved for the contact force F_{34}

$$F_{34} = \frac{M_{o4}}{C_2} + \frac{Q_4 C_1}{C_2} \quad (H-19)$$

where

$$C_1 = \mu \rho_4 (A_1 + A_3)$$

$$C_2 = a_{P3} [\mu s_{3R} \cos(\psi_3 + \delta_{P3} - \lambda_3) - \sin(\psi_3 + \delta_{P3} - \lambda_3)] \\ - \mu [\rho_{P3} s_{3R} + \rho_4 (A_2 + A_4)]$$

II. FORCE AND MOMENT EQUILIBRIA OF GEAR AND PINION SET NO. 3

Figure H-2 gives a schematic free body diagram of the gear and pinion combination no. 3. Mesh no. 2 is also indicated to obtain the directions of the forces of gear no. 2 on pinion no. 3. The forces of pinion no. 4 on gear no. 3 are opposite to those given by equations (H-3) and (H-4) respectively. Thus, the contact force becomes

$$\bar{F}_{43} = -\bar{F}_{34} = -F_{34}\bar{n}_{\lambda 3} \quad (H-20)$$

The friction force of pinion no. 4 on gear no. 3 becomes:

$$\bar{F}_{f43} = -\bar{F}_{f34} = -\mu_{s3}F_{34}\bar{n}_{\lambda 3} \quad (H-21)$$

The contact force of gear no. 2 on pinion no. 3 is given by

$$\bar{F}_{23} = F_{23}\bar{n}_{\lambda 2} \quad (H-22)$$

while the associated friction force of gear no. 2 on pinion no. 3 becomes

$$\bar{F}_{f23} = \mu s_{2R} F_{23} \bar{n}_{N\lambda 2}$$

(H-23)

The pivot reactions F_{x3} and F_{y3} as well as the associated friction forces are drawn in a separate diagram in Figure H-2. As was the case earlier, the friction moment due to the friction forces again opposes rotation.

The centrifugal force, due to the mass of the combined gear and pinion no. 3, is given by

$$\bar{Q}_3 = Q_3(\cos \gamma_3 \bar{i} + \sin \gamma_3 \bar{j}) \quad (H-24)$$

where

$$Q_3 = m_3 \omega^2 \quad (H-25)$$

The force equilibrium of the combination is given by

$$\begin{aligned} -F_{34} \bar{n}_{\lambda 3} - \mu s_{3R} F_{34} \bar{n}_{N\lambda 3} + F_{23} \bar{n}_{\lambda 2} + \mu s_{2R} F_{23} \bar{n}_{N\lambda 2} + F_{x3} \bar{i} + \mu F_{y3} \bar{i} \\ + F_{y3} \bar{j} - \mu F_{x3} \bar{j} + \bar{Q}_3 = 0 \end{aligned} \quad (H-26)$$

The moment equation is given by

$$\begin{aligned} & \mu p_3 (\tilde{F}_{x3} + \tilde{F}_{y3}) \bar{k} + [a_{G3} \bar{n}_{G3} + p_{G3} \bar{n}_{\lambda 3}] \times [-F_{34} \bar{n}_{\lambda 3} - \mu s_{3R} F_{34} \bar{n}_{N\lambda 3}] \\ & + [a_{P2} \bar{n}_{P2} - p_{P2} \bar{n}_{\lambda 2}] \times [F_{23} \bar{n}_{\lambda 2} + \mu s_{2R} F_{23} \bar{n}_{N\lambda 2}] = 0 \end{aligned} \quad (H-27)$$

Equation (H-26) gives the following component expressions:

$$\begin{aligned} & -F_{34} \cos \lambda_3 + \mu s_{3R} F_{34} \sin \lambda_3 + Q_3 \cos \gamma_3 + F_{x3} + \mu F_{y3} + F_{23} \cos \lambda_2 \\ & - \mu s_{2R} F_{23} \sin \lambda_2 = 0 \end{aligned} \quad (H-28)$$

and

$$\begin{aligned} & -F_{34} \sin \lambda_3 - \mu s_{3R} F_{34} \cos \lambda_3 + Q_3 \sin \gamma_3 + F_{y3} - \mu F_{x3} + F_{23} \sin \lambda_2 \\ & + \mu s_{2R} F_{23} \cos \lambda_2 = 0 \end{aligned} \quad (H-29)$$

The scalar form of the moment equation (H-27) becomes

$$\begin{aligned} & \mu p_3 (\tilde{F}_{x3} + \tilde{F}_{y3}) - \mu s_{3R} p_{G3} F_{34} - \mu s_{2R} p_{P2} F_{23} + a_{G3} F_{34} [\sin(\phi_3 + \delta_{G3} - \lambda_3) \\ & - \mu s_{3R} \cos(\phi_3 + \delta_{G3} - \lambda_3)] + a_{P2} F_{23} [-\sin(\psi_2 - \delta_{P2} - \lambda_2) \\ & + \mu s_{2R} \cos(\psi_2 - \delta_{P2} - \lambda_2)] = 0 \end{aligned} \quad (H-30)$$

Simultaneous solution of equations (H-28) and (H-29) for the pivot reactions F_{x3} and F_{y3} gives

$$F_{x3} = \frac{1}{1 + \mu^2} \left\{ F_{34}[(1 - \mu^2 s_{3R})\cos\lambda_3 - \mu(1 + s_{3R})\sin\lambda_3] + \right. \\ F_{23}[\mu(1 + s_{2R})\sin\lambda_2 - (1 - \mu^2 s_{2R})\cos\lambda_2] + \\ \left. Q_3[\mu\sin\gamma_3 - \cos\gamma_3] \right\} \quad (H-31)$$

and

$$F_{y3} = \frac{1}{1 + \mu^2} \left\{ F_{34}[(1 - \mu^2 s_{3R})\sin\lambda_3 + \mu(1 + s_{3R})\cos\lambda_3] + \right. \\ F_{23}[(\mu^2 s_{2R} - 1)\sin\lambda_2 - \mu(1 + s_{2R})\cos\lambda_2] - \\ \left. Q_3[\sin\gamma_3 + \mu\cos\gamma_3] \right\} \quad (H-32)$$

The sum $\tilde{F}_{x3} + \tilde{F}_{y3}$ of equation (H-30) is now made up of equations (H-31) and (H-32) in the sense of equation (A-3b).

$$\tilde{F}_{x3} + \tilde{F}_{y3} = F_{34}A_5 + F_{23}A_6 + Q_3A_7 + F_{34}A_8 + F_{23}A_9 + Q_3A_{10} \quad (H-33)$$

where

$$A_5 = \left| \frac{(1 - \mu^2 s_{3R}) \cos \lambda_3 - \mu(1 + s_{3R}) \sin \lambda_3}{1 + \mu^2} \right| \quad (H-34)$$

$$A_6 = \left| \frac{\mu(1 + s_{2R}) \sin \lambda_2 - (1 - \mu^2 s_{2R}) \cos \lambda_2}{1 + \mu^2} \right| \quad (H-35)$$

$$A_7 = \left| \frac{\mu \sin \gamma_3 - \cos \gamma_3}{1 + \mu^2} \right| \quad (H-36)$$

$$A_8 = \left| \frac{(1 - \mu^2 s_{3R}) \sin \lambda_3 + \mu(1 + s_{3R}) \cos \lambda_3}{1 + \mu^2} \right| \quad (H-37)$$

$$A_9 = \left| \frac{(\mu^2 s_{2R} - 1) \sin \lambda_2 - \mu(1 + s_{2R}) \cos \lambda_2}{1 + \mu^2} \right| \quad (H-38)$$

$$A_{10} = \left| \frac{\sin \gamma_3 + \mu \cos \gamma_3}{1 + \mu^2} \right| \quad (H-39)$$

Equation (H-33) is now substituted into equation (H-30) and the resulting expression is solved for the contact force F_{23} . Thus,

$$F_{23} = \frac{-F_{34}C_3 - Q_3C_4}{C_5} \quad (H-40)$$

where

$$C_3 = \mu_P(A_5 + A_8) - \mu_{3R}P_{G3} + a_{G3}[\sin(\phi_3 + \delta_{G3} - \lambda_3) \\ - \mu_{3R}\cos(\phi_3 + \delta_{G3} - \lambda_3)]$$

$$C_4 = \mu_P(A_7 + A_{10})$$

$$C_5 = \mu_P(A_6 + A_9) - \mu_{2R}P_{P2} + a_{P2}[\mu_{2R}\cos(\psi_2 - \delta_{P2} - \lambda_2) \\ - \sin(\psi_2 - \delta_{P2} - \lambda_2)]$$

III. FORCE AND MOMENT EQUILIBRIA OF GEAR AND PINION SET NO. 2

Figure H-3 gives the free body diagram of the gear and pinion combination no. 2. In addition, mesh no. 1 is indicated to obtain the directions of the forces of gear no. 1 on pinion no. 2.

The forces of pinion no. 3 on gear no. 2 have directions opposite to those given by equation (H-22) and (H-23) respectively. Thus, the normal force is given by

$$\bar{F}_{32} = -F_{23}\bar{n}_{\lambda 2} \quad (H-41)$$

The friction force of pinion no. 3 on gear no. 2 becomes

$$\bar{F}_{f32} = -\mu_{s2}F_{23}\bar{n}_{\lambda 2} \quad (H-42)$$

The contact force of gear no. 1 on pinion no. 2 is given by

$$\bar{F}_{12} = F_{12}\bar{n}_{\lambda 1} \quad (H-43)$$

while the associated friction force of gear no. 1 on pinion no. 2 becomes

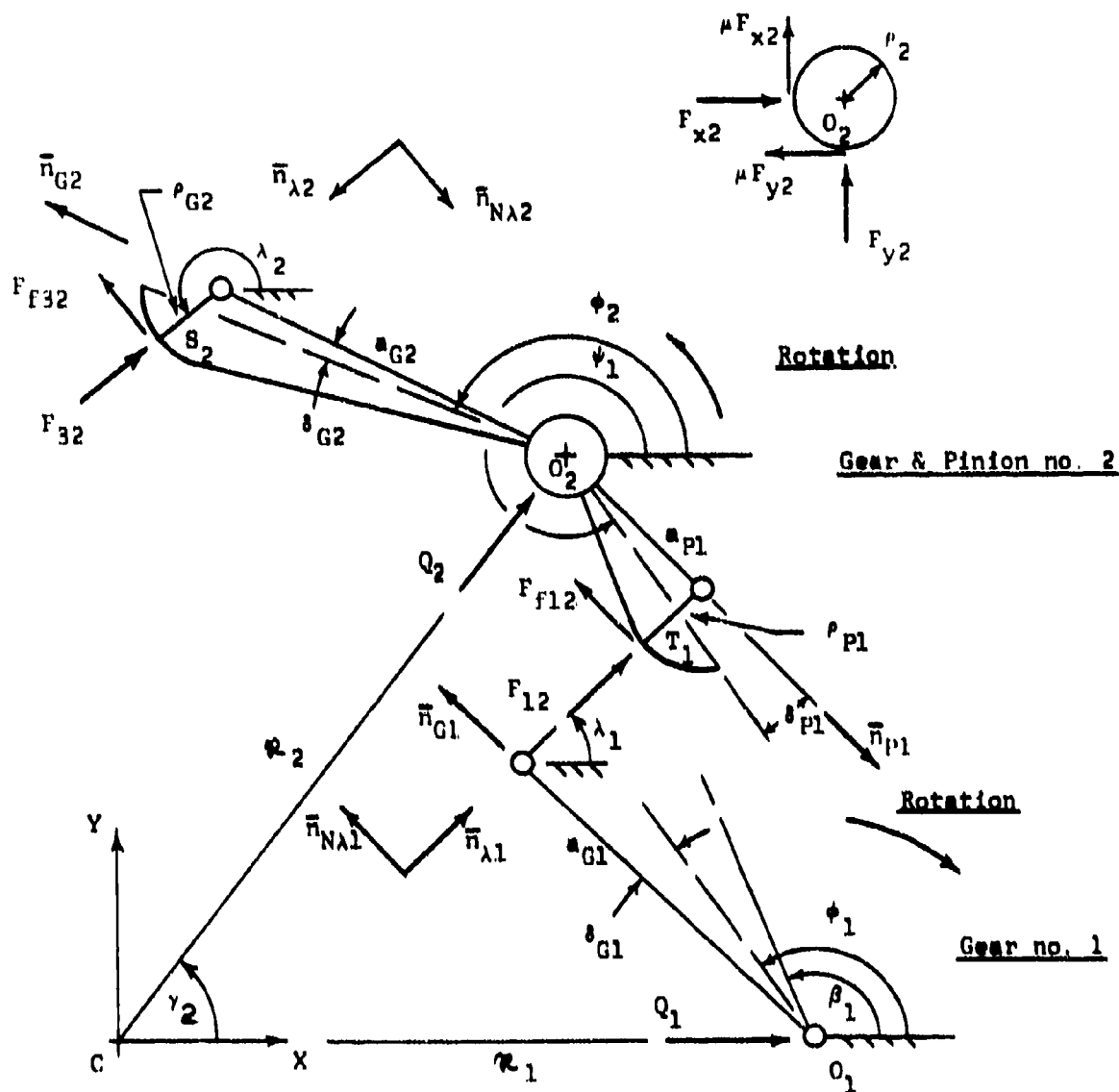


FIGURE H-3

FREE BODY DIAGRAM OF GEAR & PINION NO. 2

MESH NO. 2: ROUND ON ROUND

MESH NO. 1: ROUND ON ROUND

$$\bar{F}_{f12} = \mu_{21} R F_{12} \bar{n}_{N\lambda 1}$$

(H-44)

The pivot reactions, of the fuse body on the pivot shaft, together with the pivot friction forces, are shown in a separate diagram in Figure H-3. The centrifugal force, due to the mass of gear and pinion assembly no. 2, is given by

$$\bar{Q}_2 = Q_2 (\cos \gamma_2 \bar{i} + \sin \gamma_2 \bar{j}) \quad (H-45)$$

where

$$Q_2 = R_2 m_2 \omega^2 \quad (H-46)$$

Force equilibrium is assured by

$$\begin{aligned} -F_{23} \bar{n}_{\lambda 2} - \mu_{2R} F_{23} \bar{n}_{N\lambda 2} + F_{12} \bar{n}_{\lambda 1} + \mu_{21} R F_{12} \bar{n}_{N\lambda 1} + \bar{Q}_2 \\ + F_{x2} \bar{i} - \mu F_{y2} \bar{i} + F_{y2} \bar{j} + \mu F_{x2} \bar{j} = 0 \end{aligned} \quad (H-47)$$

Moment equilibrium must satisfy

$$\begin{aligned}
 & -\mu_2(\tilde{F}_{x2} + \tilde{F}_{y2})\bar{k} + [a_{G2}\bar{n}_{G2} + \rho_{G2}\bar{n}_{\lambda 2}] \times [-F_{23}\bar{n}_{\lambda 2} - \mu_{2R}F_{23}\bar{n}_{N\lambda 2}] \\
 & + [a_{P1}\bar{n}_{P1} - \rho_{P1}\bar{n}_{\lambda 1}] \times [F_{12}\bar{n}_{\lambda 1} + \mu_{1R}F_{12}\bar{n}_{N\lambda 1}] = 0 \quad (H-48)
 \end{aligned}$$

Equation (H-47) gives the following component expressions

$$\begin{aligned}
 & -F_{23}\cos\lambda_2 + \mu_{2R}F_{23}\sin\lambda_2 + F_{12}\cos\lambda_1 - \mu_{1R}F_{12}\sin\lambda_1 \\
 & + Q_2\cos\gamma_2 + F_{x2} - \mu F_{y2} = 0 \quad (H-49)
 \end{aligned}$$

and

$$\begin{aligned}
 & -F_{23}\sin\lambda_2 - \mu_{2R}F_{23}\cos\lambda_2 + F_{12}\sin\lambda_1 + \mu_{1R}F_{12}\cos\lambda_1 \\
 & + Q_2\sin\gamma_2 + F_{y2} + \mu F_{x2} = 0 \quad (H-50)
 \end{aligned}$$

The scalar form of the moment equation (H-48) becomes

$$\begin{aligned}
 & -\mu^2_2(\tilde{F}_{x2} + \tilde{F}_{y2}) + s_{G2}F_{23}[\sin(\phi_2 - \delta_{G2} - \lambda_2) - \mu s_{2R}\cos(\phi_2 - \delta_{G2} - \lambda_2)] \\
 & - \mu s_{2R}s_{G2}F_{23} + s_{P1}F_{12}[-\sin(\psi_1 + \delta_{P1} - \lambda_1) + \mu s_{1R}\cos(\psi_1 + \delta_{P1} - \lambda_1)] \\
 & - \mu s_{1R}s_{P1}F_{12} = 0
 \end{aligned} \tag{H-51}$$

Simultaneous solution of equations (H-49) and (H-50) for F_{x2} and F_{y2} leads to

$$\begin{aligned}
 F_{x2} = \frac{1}{1 + \mu^2} \bigg\{ & F_{23}[(1 + \mu^2 s_{2R})\cos\lambda_2 - \mu(s_{2R} - 1)\sin\lambda_2] \\
 & + F_{12}[\mu(s_{1R} - 1)\sin\lambda_1 - (1 + \mu^2 s_{1R})\cos\lambda_1] \\
 & + Q_2 [-\cos\gamma_2 - \mu\sin\gamma_2] \bigg\}
 \end{aligned} \tag{H-52}$$

and

$$\begin{aligned}
 F_{y2} = \frac{1}{1 + \mu^2} \bigg\{ & F_{23}[(1 + \mu^2 s_{2R})\sin\lambda_2 - \mu(1 - s_{2R})\cos\lambda_2] \\
 & + F_{12}[\mu(1 - s_{1R})\cos\lambda_1 - (1 + \mu^2 s_{1R})\sin\lambda_1] \\
 & + Q_2 [\mu\cos\gamma_2 - \sin\gamma_2] \bigg\}
 \end{aligned} \tag{H-53}$$

The sum of \tilde{F}_{x2} and \tilde{F}_{y2} of equation (H-51) is now made up of equations (H-52) and (H-53) in the sense of equation (A-3b) of Appendix A

$$\begin{aligned}\tilde{F}_{x2} + \tilde{F}_{y2} = & F_{23}A_{11} + F_{12}A_{12} + Q_2A_{13} + F_{23}A_{14} + F_{12}A_{15} \\ & + Q_2A_{16}\end{aligned}\quad (H-54)$$

where

$$A_{11} = \left| \frac{(1 + \mu^2 s_{2R}) \cos \lambda_2 - \mu(s_{2R} - 1) \sin \lambda_2}{1 + \mu^2} \right| \quad (H-55)$$

$$A_{12} = \left| \frac{\mu(s_{1R} - 1) \sin \lambda_1 - (1 + \mu^2 s_{1R}) \cos \lambda_1}{1 + \mu^2} \right| \quad (H-56)$$

$$A_{13} = \left| \frac{-\cos \gamma_2 - \mu \sin \gamma_2}{1 + \mu^2} \right| \quad (H-57)$$

$$A_{14} = \left| \frac{(1 + \mu^2 s_{2R}) \sin \lambda_2 - \mu(1 - s_{2R}) \cos \lambda_2}{1 + \mu^2} \right| \quad (H-58)$$

$$A_{15} = \left| \frac{\mu(1 - s_{1R}) \cos \lambda_1 - (1 + \mu^2 s_{1R}) \sin \lambda_1}{1 + \mu^2} \right| \quad (H-59)$$

$$A_{16} = \left| \frac{\mu \cos \gamma_2 - \sin \gamma_2}{1 + \mu^2} \right| \quad (H-60)$$

Equation (H-54) is now substituted into the moment equation (H-51).

The resulting expression is then solved for the contact force F_{12}

$$F_{12} = \frac{-F_{23}C_6 + Q_2C_7}{C_8} \quad (H-61)$$

where

$$C_6 = a_{g2} [\sin(\phi_2 - \delta_{g2} - \lambda_2) - \mu_{2R} \cos(\phi_2 - \delta_{g2} - \lambda_2)] \\ - \mu_{p2}(A_{11} + A_{14}) - \mu_{2R}^p Q_2$$

$$C_7 = \mu_{p2}(A_{13} + A_{16})$$

$$C_8 = - \left\{ a_{p1} [\sin(\psi_1 + \delta_{p1} - \lambda_1) - \mu_{1R} \cos(\psi_1 + \delta_{p1} - \lambda_1)] \right. \\ \left. + \mu_{p2}(A_{12} + A_{15}) + \mu_{1R}^p P_1 \right\}$$

IV. FORCE AND MOMENT EQUILIBRIA OF INPUT GEAR NO. 1

Figure H-4 represents the free body diagram of the input gear no. 1 which has the input moment M_{in} acting on it.

The forces of pinion no. 2 on gear no. 1 are given according to equations (H-43) and (H-44),

$$\bar{F}_{21} = -F_{12}\bar{n}_{\lambda 1} \quad (H-62)$$

and

$$\bar{F}_{f21} = -\mu s_1 R F_{12} \bar{n}_{N\lambda 1} \quad (H-63)$$

The moments due to the friction forces on the pivot oppose rotation as indicated.

The centrifugal force, due to the mass of gear no. 1, is given by

$$\bar{Q}_1 = Q_1 \bar{i} \quad (H-64)$$

where

$$Q_1 = \mathcal{R}_1 m_1 \omega^2 \quad (H-65)$$

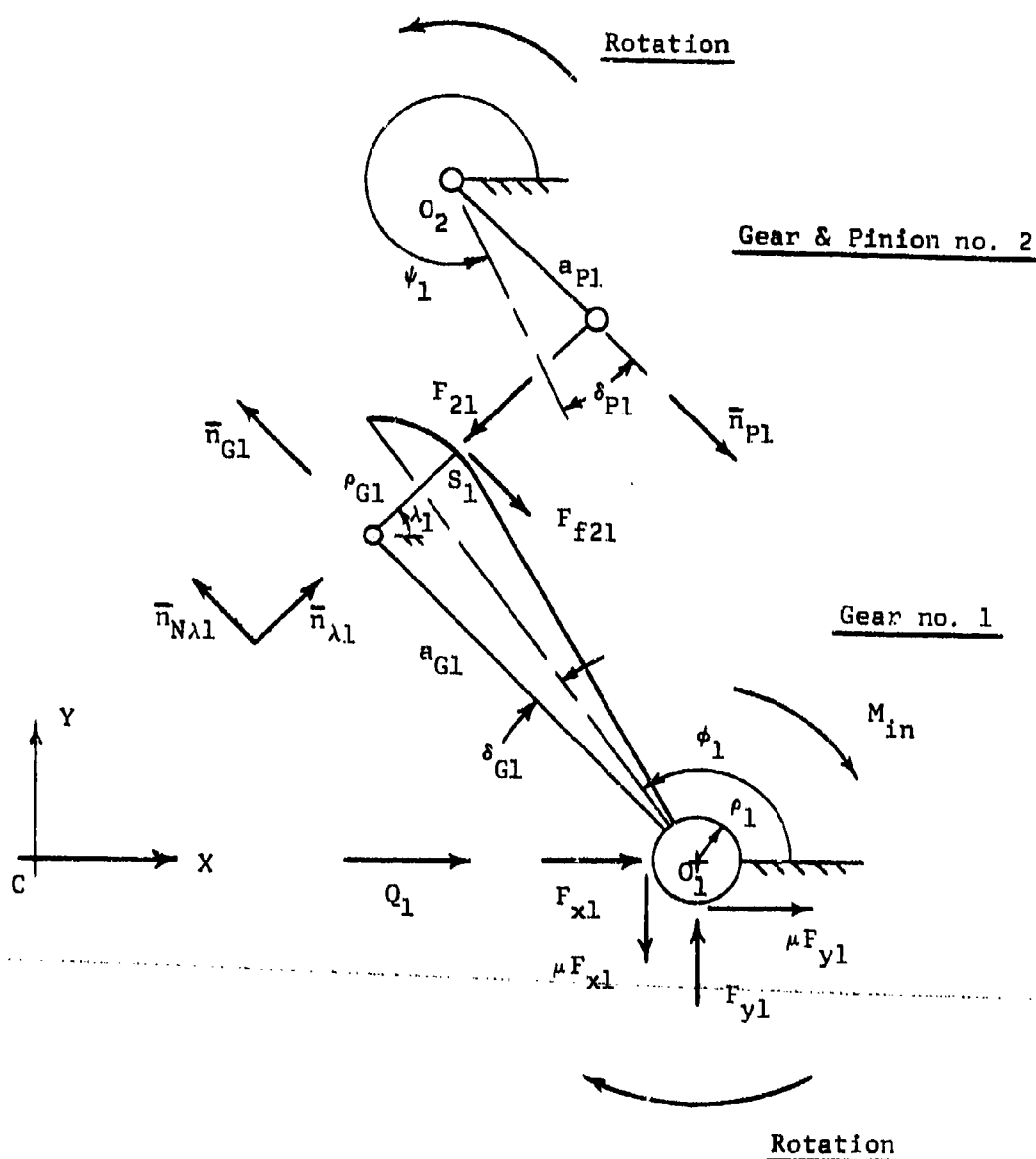


FIGURE H-4

FREE BODY DIAGRAM OF GEAR NO. 1

MESH NO. 1: ROUND ON ROUND

Force equilibrium requires, that

$$\begin{aligned}
 -F_{12}\bar{n}_{\lambda 1} - \mu s_{1R}F_{12}\bar{n}_{N\lambda 1} + \bar{Q}_1 + F_{x1}\bar{i} + \mu F_{y1}\bar{i} + F_{y1}\bar{j} \\
 - \mu F_{x1}\bar{j} = 0
 \end{aligned}
 \tag{H-66}$$

Moment equilibrium is given by.

$$\begin{aligned}
 \mu p_1(\tilde{F}_{x1} + \tilde{F}_{y1})\bar{k} - M_{1n}\bar{k} + [a_{G1}\bar{n}_{G1} + p_{G1}\bar{n}_{\lambda 1}] \times \\
 [-F_{12}\bar{n}_{\lambda 1} - \mu s_{1R}F_{12}\bar{n}_{N\lambda 1}] = 0
 \end{aligned}
 \tag{H-67}$$

Equation (H-66) furnishes the following component equations:

$$-F_{12}\cos\lambda_1 + \mu s_{1R}F_{12}\sin\lambda_1 + Q_1 + F_{x1} + \mu F_{y1} = 0 \tag{H-68}$$

and

$$-F_{12}\sin\lambda_1 - \mu s_{1R}F_{12}\cos\lambda_1 + F_{y1} - \mu F_{x1} = 0 \tag{H-69}$$

The scalar form of equation (H-67) becomes

$$\begin{aligned}
 \mu p_1(\tilde{F}_{x1} + \tilde{F}_{y1}) - M_{1n} + a_{G1}F_{12}[\sin(\phi_1 + \delta_{G1} - \lambda_1) \\
 - \mu s_{1R}\cos(\phi_1 + \delta_{G1} - \lambda_1)] - \mu s_{1R}p_{G1}F_{12} = 0
 \end{aligned}
 \tag{H-70}$$

The simultaneous solution of equations (H-68) and (H-69) furnishes

$$F_{x1} = \frac{1}{1 + \mu^2} \left\{ F_{12} [(1 - \mu^2 s_{1R}) \cos \lambda_1 - \mu(1 + s_{1R}) \sin \lambda_1] - Q_1 \right\} \quad (H-71)$$

and

$$F_{y1} = \frac{1}{1 + \mu^2} \left\{ F_{12} [(1 - \mu^2 s_{1R}) \sin \lambda_1 + \mu(1 + s_{1R}) \cos \lambda_1] - \mu Q_1 \right\} \quad (H-72)$$

Then, with the same reasoning as before,

$$\tilde{F}_{x1} + \tilde{F}_{y1} = F_{12} A_{17} + Q_1 A_{18} + F_{12} A_{19} + Q_1 A_{20} \quad (H-73)$$

where

$$A_{17} = \left| \frac{(1 - \mu^2 s_{1R}) \cos \lambda_1 - \mu(1 + s_{1R}) \sin \lambda_1}{1 + \mu^2} \right| \quad (H-74)$$

$$A_{18} = \left| \frac{1}{1 + \mu^2} \right| \quad (H-75)$$

$$A_{19} = \left| \frac{(1 - \mu^2 s_{1R}) \sin \lambda_1 + \mu(1 + s_{1R}) \cos \lambda_1}{1 + \mu^2} \right| \quad (H-76)$$

$$A_{20} = \left| \frac{\mu}{1 + \mu^2} \right| \quad (H-77)$$

Equation (H-73) is now substituted into equation (H-70) and the result is solved for the contact force F_{12}

$$F_{12} = \frac{M_{1n} - Q_1 C_9}{C_{10}} \quad (H-78)$$

where

$$C_9 = \mu p_1 (A_{18} + A_{20})$$

$$C_{10} = \mu p_1 (A_{17} + A_{19}) + a_{G1} [\sin(\phi_1 + \delta_{G1} - \lambda_1) - \mu s_{1R} \cos(\phi_1 + \delta_{G1} - \lambda_1)] - \mu s_{1R} p_{G1}$$

V. MOMENT INPUT-OUTPUT RELATIONSHIP

Equations (H-61) and (H-78), which are both expressions in F_{12} , are now set equal to each other and the result is solved for F_{23}

$$F_{23} = \frac{-c_8}{c_6 c_{10}} (M_{1n} - Q_1 c_9) + \frac{c_7}{c_6} Q_2 \quad (\text{H-79})$$

The above is now equated to equation (H-40) and the result is solved for F_{34}

$$F_{34} = \frac{c_5 c_8 (M_{1n} - Q_1 c_9) - c_5 c_{10} c_7 Q_2 - c_4 c_6 c_{10} Q_3}{c_3 c_6 c_{10}} \quad (\text{H-80})$$

Finally equation (H-80) is equated to equation (H-19). This permits the determination of the equilibrant moment M_{o41} (for case no. 1: RRR)

$$M_{o41} = M_{1n} \frac{c_2 c_5 c_8}{c_3 c_6 c_{10}} - Q_1 \frac{c_2 c_5 c_8 c_9}{c_3 c_6 c_{10}} - Q_2 \frac{c_2 c_5 c_7}{c_3 c_6} - Q_3 \frac{c_2 c_4}{c_3} - Q_4 c_1 \quad (\text{H-81})$$

b. CASE NO. 2: RRF

Since only mesh 1 is now assumed to be in the round on flat phase of motion, the forces F_{34} and F_{23} remain as given by equations (H-19) and (H-40), respectively.

I. FORCE AND MOMENT EQUILIBRIA OF GEAR AND PINION SET NO. 2

Figure H-5 shows the free body diagram of the gear and pinion set with the necessary portions of mesh no. 1.

The forces of pinion no. 3 on gear no. 2 are given by equations (H-41) and (H-42), i.e.,

$$\bar{F}_{32} = -F_{23}\bar{N}_{\lambda 2} \quad (H-82)$$

and

$$\bar{F}_{f32} = -\mu_s 2R F_{23} \bar{N}_{\lambda 2} \quad (H-83)$$

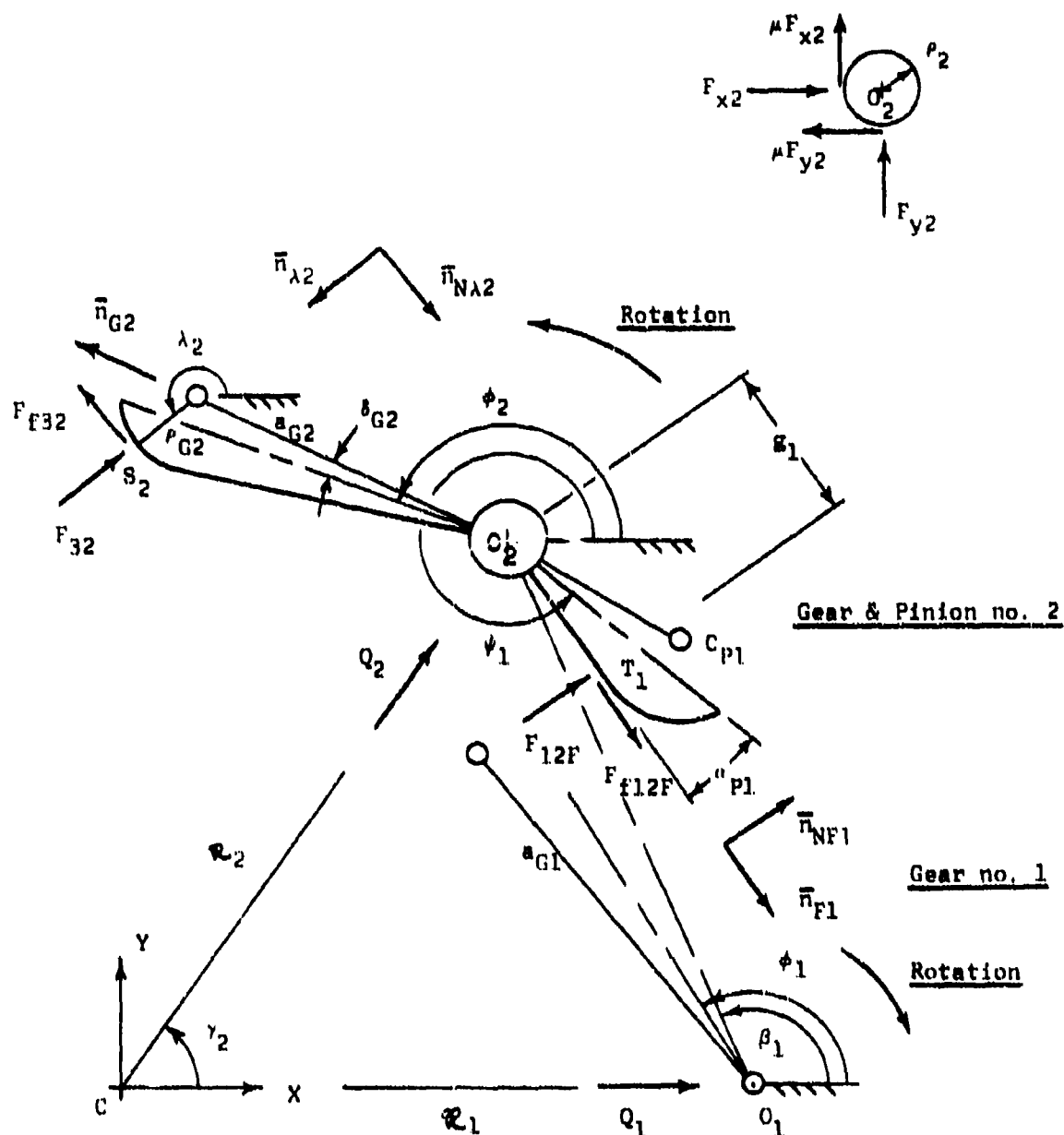


FIGURE H-5

FREE BODY DIAGRAM OF GEAR & PINION NO. 2

MESH NO. 2: ROUND ON ROUND

MESH NO. 1: ROUND ON FLAT

The contact force of gear no. 1 on pinion no. 2 is now given by

$$\bar{F}_{12F} = F_{12F} \bar{n}_{NF1} \quad (H-84)$$

(Note that the additional subscript F is introduced to distinguish round on flat from round on round contact.)

The associated friction force is given by

$$\bar{F}_{f12F} = \mu s_{1F} F_{12F} \bar{n}_{F1} \quad (H-85)$$

(See equation (H-2) for s_{1F} .)

The pivot reactions, together with the pivot friction forces, are shown in a separate diagram in Figure H-5. As before, the pivot friction moments oppose rotation.

The centrifugal force \bar{Q}_2 is again given by equations (H-45) and (H-46).

Force equilibrium is given by

$$\begin{aligned} -F_{23} \bar{n}_{\lambda 2} - \mu s_{2R} F_{23} \bar{n}_{N\lambda 2} + F_{12F} \bar{n}_{NF1} + \mu s_{1F} F_{12F} \bar{n}_{F1} + \bar{Q}_2 \\ + F_{x2} \bar{i} - \mu F_{y2} \bar{i} + F_{y2} \bar{j} + \mu F_{x2} \bar{j} = 0 \end{aligned} \quad (H-86)$$

Moment equilibrium about point O_2 requires

$$\begin{aligned}
 -\mu_2(\bar{F}_{x2} + \bar{F}_{y2})\bar{k} + [\bar{a}_{G2}\bar{H}_{G2} + \bar{r}_{G2}\bar{H}_{\lambda 2}] \times [-F_{23}\bar{H}_{\lambda 2} - \mu_{2R}F_{23}\bar{H}_{N\lambda 2}] \\
 + \bar{s}_1\bar{H}_{F1} \times F_{12}\bar{H}_{NF1} = 0
 \end{aligned}
 \tag{H-87}$$

Note that since the line of action of the friction force F_{f12} passes through point O_2 , this friction force exerts no moment about point O_2 .

Equation (H-86) furnishes the following component equations:

$$\begin{aligned}
 -F_{23}\cos\lambda_2 + \mu_{2R}F_{23}\sin\lambda_2 - F_{12}\sin(\psi_1 - \alpha_{P1}) + \mu_{1F}F_{12}\cos(\psi_1 - \alpha_{P1}) \\
 + F_{x2} - \mu F_{y2} + Q_2\cos\gamma_2 = 0
 \end{aligned}
 \tag{H-88}$$

and

$$\begin{aligned}
 -F_{23}\sin\lambda_2 - \mu_{2R}F_{23}\cos\lambda_2 + F_{12}\cos(\psi_1 - \alpha_{P1}) + \mu_{1F}F_{12}\sin(\psi_1 - \alpha_{P1}) \\
 + F_{y2} + \mu F_{x2} + Q_2\sin\gamma_2 = 0
 \end{aligned}
 \tag{H-89}$$

The scalar form of the moment equation (H-87) becomes

$$-\mu p_2(\tilde{F}_{x2} + \tilde{F}_{y2}) + a_{Q2}F_{23}[\sin(\phi_2 - \phi_{Q2} - \lambda_2) - \mu a_{2R}\cos(\phi_2 - \phi_{Q2} - \lambda_2)] \\ - \mu a_{2R}\phi_{Q2}F_{23} + F_{12}\phi_1 = 0 \quad (H-90)$$

Simultaneous solution of these component equations for F_{x2} and F_{y2} leads to

$$F_{x2} = \frac{1}{1 + \mu^2} \left\{ F_{23}[\mu(1 - a_{2R})\sin\lambda_2 + (1 + \mu^2 a_{2R})\cos\lambda_2] \right. \\ \left. + F_{12}[(1 - \mu^2 a_{1R})\sin(\psi_1 - \alpha_{p1}) - \mu(1 + a_{1R})\cos(\psi_1 - \alpha_{p1})] \right. \\ \left. - Q_2[\mu\sin\gamma_2 + \cos\gamma_2] \right\} \quad (H-91)$$

and

$$F_{y2} = \frac{1}{1 + \mu^2} \left\{ F_{23}[(1 + \mu^2 a_{2R})\sin\lambda_2 - \mu(1 - a_{2R})\cos\lambda_2] \right. \\ \left. + F_{12}[-\mu(1 + a_{1R})\sin(\psi_1 - \alpha_{p1}) + (\mu^2 a_{1R} - 1)\cos(\psi_1 - \alpha_{p1})] \right. \\ \left. + Q_2[-\sin\gamma_2 + \mu\cos\gamma_2] \right\} \quad (H-92)$$

The sum ($\tilde{F}_{x2} + \tilde{F}_{y2}$) of equation (H-90) is now made up of equations (H-91) and (H-92) in the sense of equation (A-3b) of Appendix A

$$\tilde{F}_{x2} + \tilde{F}_{y2} = F_{23}A_{21} + F_{12}A_{22} + Q_2A_{23} + F_{23}A_{24} + F_{12}A_{25} + Q_2A_{26} \quad (H-93)$$

where

$$A_{21} = \left| \frac{\mu(1 - s_{2R})\sin\lambda_2 + (1 + \mu^2 s_{2R})\cos\lambda_2}{1 + \mu^2} \right| \quad (H-94)$$

$$A_{22} = \left| \frac{(1 - \mu^2 s_{1R})\sin(\psi_1 - \alpha_{P1}) - \mu(1 + s_{1R})\cos(\psi_1 - \alpha_{P1})}{1 + \mu^2} \right| \quad (H-95)$$

$$A_{23} = \left| \frac{\mu\sin\gamma_2 + \cos\gamma_2}{1 + \mu^2} \right| \quad (H-96)$$

$$A_{24} = \left| \frac{(1 + \mu^2 s_{2R})\sin\lambda_2 - \mu(1 - s_{2R})\cos\lambda_2}{1 + \mu^2} \right| \quad (H-97)$$

$$A_{25} = \left| \frac{-\mu(1 + s_{1R})\sin(\psi_1 - \alpha_{P1}) + (\mu^2 s_{1R} - 1)\cos(\psi_1 - \alpha_{P1})}{1 + \mu^2} \right| \quad (H-98)$$

$$A_{26} = \left| \frac{-\sin \gamma_2 + \mu \cos \gamma_2}{1 + \mu^2} \right| \quad (H-99)$$

Equation (H-93) is now substituted into equation (H-90), and the resulting expression is solved for the contact force F_{12F}

$$F_{12F} = \frac{-F_{23}C_{11} + Q_2C_{12}}{C_{13}} \quad (H-100)$$

where

$$C_{11} = A_{Q2} [\sin(\phi_2 - \delta_{Q2} - \lambda_2) - \mu_{2R} \cos(\phi_2 - \delta_{Q2} - \lambda_2)] \\ - \mu P_2 (A_{21} + A_{24}) - \mu_{2R} P_{Q2}$$

$$C_{12} = \mu P_2 (A_{23} + A_{26})$$

$$C_{13} = \delta_1 - \mu P_2 (A_{22} + A_{25})$$

II. FORCE AND MOMENT EQUILIBRIA OF INPUT GEAR NO. 1

Figure H-6 represents the free body diagram of input gear no. 1.

The forces of pinion no. 2 on this gear are given, according to equations (H-84) (H-85) ,

$$\bar{F}_{21F} = -F_{12F}\bar{n}_{NF1} \quad (H-101)$$

and

$$\bar{F}_{f21F} = -\mu s_{1F}F_{12F}\bar{n}_{F1} \quad (H-102)$$

The moments due to the pivot friction forces oppose the indicated rotation due to the moment M_{1n} .

The centrifugal force \bar{Q}_1 has been defined by equations (H-64) and (H-65).

The force equilibrium equation is given by

$$\begin{aligned} -F_{12F}\bar{n}_{NF1} - \mu s_{1F}F_{12F}\bar{n}_{F1} + Q_1\bar{i} + F_{x1}\bar{i} + \mu F_{y1}\bar{i} + F_{y1}\bar{j} - \mu F_{x1}\bar{j} \\ = 0 \end{aligned} \quad (H-103)$$

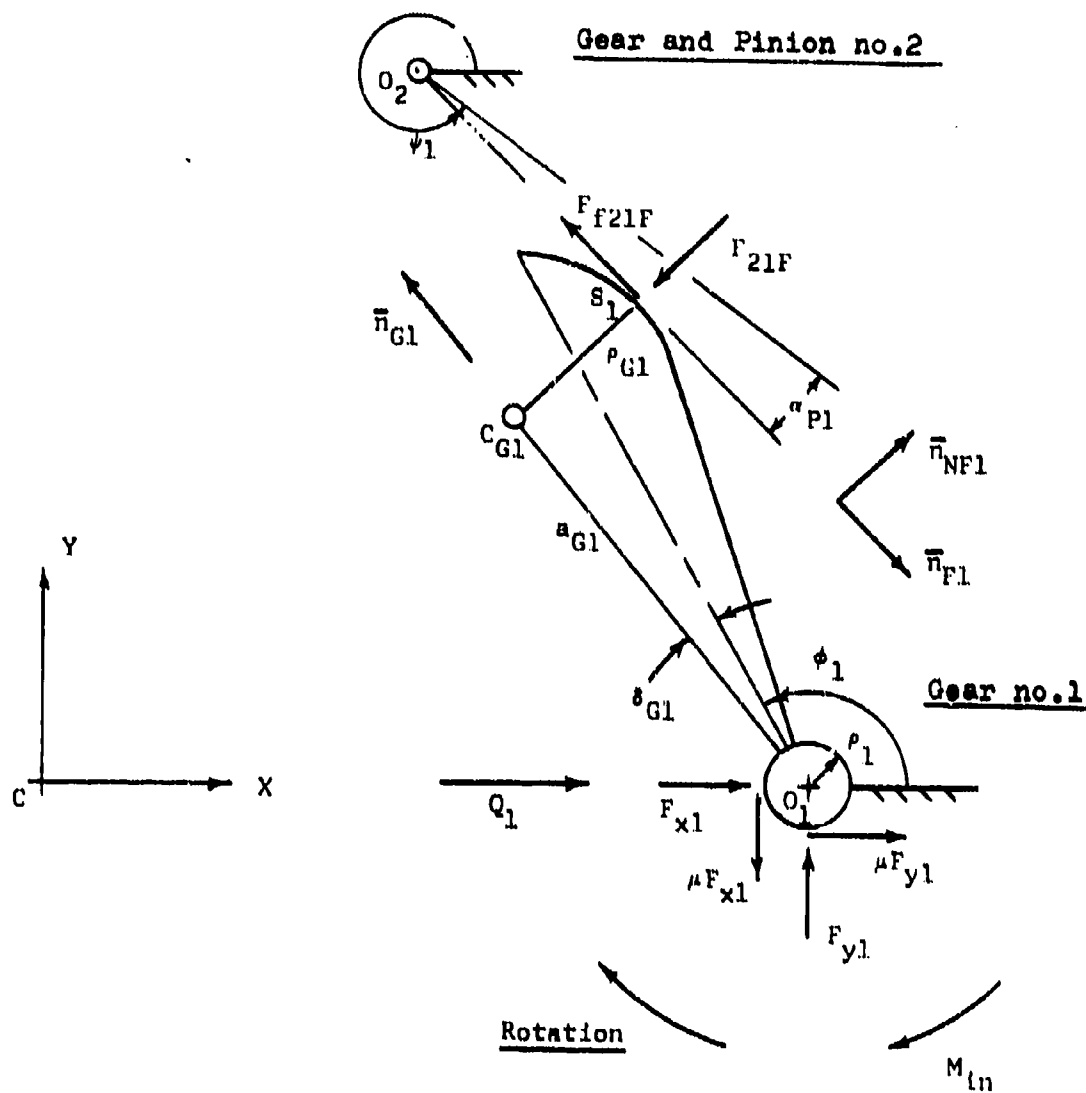


FIGURE H-6
FREE BODY DIAGRAM OF GEAR NO. 1
MECH NO. 1: ROUND ON FLAT

The moment equilibrium equation becomes

$$-M_{1n} \bar{k} + \mu \rho_1 (\tilde{F}_{x1} + \tilde{F}_{y1}) \bar{k} + [a_{G1} \bar{n}_{G1} + \rho_{G1} \bar{n}_{NF1}] \times [-F_{12F} \bar{n}_{NF1} - \mu s_{1F} F_{12F} \bar{n}_{F1}] = 0 \quad (H-104)$$

Equation (H-103) furnishes the following component expressions

$$F_{12F} \sin(\psi_1 - \alpha_{P1}) - \mu s_{1F} F_{12F} \cos(\psi_1 - \alpha_{P1}) + Q_1 + F_{x1} + \mu F_{y1} = 0 \quad (H-105)$$

and

$$-F_{12F} \cos(\psi_1 - \alpha_{P1}) - \mu s_{1F} F_{12F} \sin(\psi_1 - \alpha_{P1}) + F_{y1} - \mu F_{x1} = 0 \quad (H-106)$$

The scalar form of the moment equation (H-104) becomes

$$-M_{1n} + \mu \rho_1 (\tilde{F}_{x1} + \tilde{F}_{y1}) + \mu s_{1F} \rho_{G1} F_{12F} + a_{G1} F_{12F} [-\cos(\phi_1 + \delta_{G1} - \psi_1 + \alpha_{P1}) + \mu s_{1F} \sin(\phi_1 + \delta_{G1} - \psi_1 + \alpha_{P1})] = 0 \quad (H-107)$$

Simultaneous solution of equations (H-105) and (H-106) for F_{x1} and F_{y1} furnishes

$$F_{x1} = \frac{F_{12F} [-(1 + \mu^2 s_{1F}) \sin(\psi_1 - \alpha_{P1}) + \mu (s_{1F} - 1) \cos(\psi_1 - \alpha_{P1})] - Q_1}{1 + \mu^2} \quad (H-108)$$

and

$$F_{y1} = \frac{F_{12F}[(1 + \mu^2 s_{1F})\cos(\psi_1 - \alpha_{P1}) + \mu(s_{1F} - 1)\sin(\psi_1 - \alpha_{P1})] - \mu Q_1}{1 + \mu^2} \quad (H-109)$$

Now let

$$\tilde{F}_{x1} + \tilde{F}_{y1} = F_{12F}A_{27} + Q_1A_{28} + F_{12F}A_{29} + Q_1A_{30} \quad (H-110)$$

where

$$A_{27} = \left| \frac{-(1 + \mu^2 s_{1F})\sin(\psi_1 - \alpha_{P1}) + \mu(s_{1F} - 1)\cos(\psi_1 - \alpha_{P1})}{1 + \mu^2} \right| \quad (H-111)$$

$$A_{28} = \left| \frac{1}{1 + \mu^2} \right| \quad (H-112)$$

$$A_{29} = \left| \frac{\mu(s_{1F} - 1)\sin(\psi_1 - \alpha_{P1}) + (1 + \mu^2 s_{1F})\cos(\psi_1 - \alpha_{P1})}{1 + \mu^2} \right| \quad (H-113)$$

$$A_{30} = \left| \frac{\mu}{1 + \mu^2} \right| \quad (H-114)$$

Equation (H-110) is now substituted into the moment equation (H-107).

This furnishes

$$F_{12F} = \frac{M_{1n} - Q_1 C_{14}}{C_{15}} \quad (H-115)$$

where

$$C_{14} = \mu P_1 (A_{28} + A_{30})$$

$$C_{15} = \mu P_1 (A_{27} + A_{29}) + \mu S_1 F^P G_1$$

$$+ a_{G1} [\mu S_1 F^P \sin(\phi_1 + \delta_{G1} - \psi_1 + \alpha_{P1}) - \cos(\phi_1 + \delta_{G1} - \psi_1 + \alpha_{P1})]$$

III. MOMENT INPUT-OUTPUT RELATIONSHIP

Equations (H-100) and (H-115), which are both expressions in F_{12} , are now set equal to each other and the result is solved for F_{23}

$$F_{23} = \frac{-c_{13}}{c_{11}c_{15}} (M_{1n} - q_1 c_{14}) + q_2 \frac{c_{12}}{c_{11}} \quad (H-116)$$

The above expression is now equated to equation (H-40) and solved for F_{34}

$$F_{34} = \frac{c_5 c_{13}}{c_3 c_{11} c_{15}} (M_{1n} - q_1 c_{14}) - q_2 \frac{c_5 c_{12}}{c_3 c_{11}} - q_3 \frac{c_4}{c_3} \quad (H-117)$$

Finally, this expression is set equal to equation (H-19) and the result is solved for the equilibrant moment M_{o42} (for case 2: RRF)

$$M_{o42} = M_{1n} \frac{c_2 c_5 c_{13}}{c_3 c_{11} c_{15}} - q_1 \frac{c_2 c_5 c_{13} c_{14}}{c_3 c_{11} c_{15}} - q_2 \frac{c_2 c_5 c_{12}}{c_3 c_{11}} - q_3 \frac{c_2 c_4}{c_3} - q_4 c_1 \quad (H-118)$$

c. CASE NO. 3: RFF

With both meshes no. 1 and no. 2 in the round on flat phase of motion, only force F_{34} of the round on round phase can be incorporated for the present case. The equilibrium equations for gear and pinion set no. 3, gear and pinion set no. 2 and the input gear no. 1 must be newly derived.

I. FORCE AND MOMENT EQUILIBRIA OF GEAR AND PINION SET NO. 3

Figure H-7 shows the free body diagram of gear and pinion set no. 3, together with the necessary outline of mesh no. 2.

The forces of pinion no. 4 on gear no. 3 are given by equations (H-20) and (H-21)

$$\bar{F}_{43} = -F_{34}\bar{n}_{\lambda 3} \quad (H-119)$$

and

$$\bar{F}_{f43} = -\mu_{3R}F_{34}\bar{n}_{N\lambda 3} \quad (H-120)$$

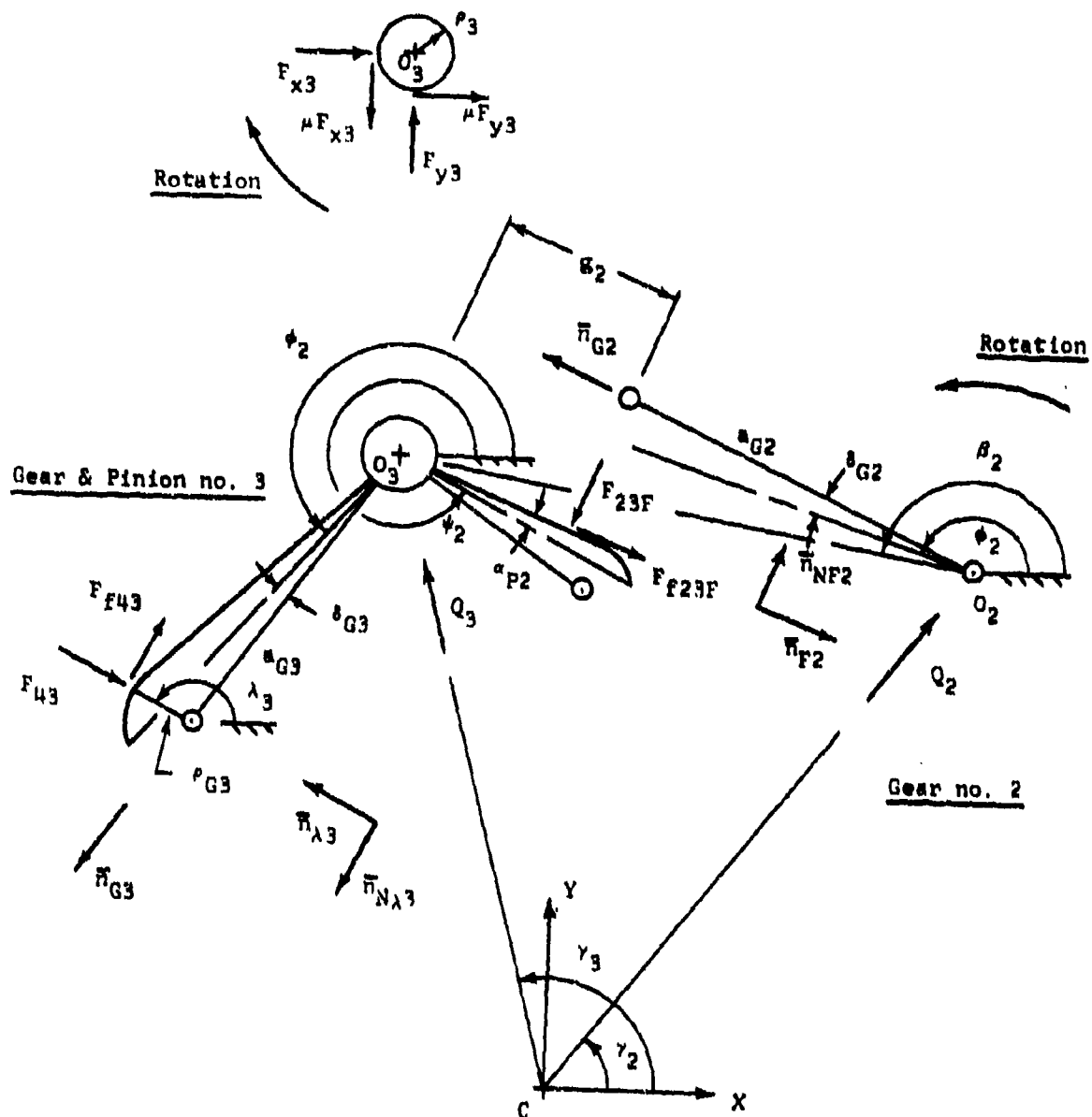


FIGURE H-7

FREE BODY DIAGRAM OF GEAR & PINION NO. 3

MESH NO. 3: ROUND ON ROUND

MESH NO. 2: ROUND ON FLAT

The normal contact force of gear no. 2 on pinion no. 3 is given by

$$\bar{F}_{23F} = -F_{23F}\bar{n}_{F2} \quad (H-121)$$

The associated friction force is given by

$$\bar{F}_{f23F} = \mu_{s2F}F_{23F}\bar{n}_{F2} \quad (H-122)$$

The pivot friction forces are chosen so that the resulting friction moments oppose the indicated rotation. The centrifugal force \bar{Q}_3 is that of equations (H-24) and (H-25).

Force equilibrium is given by

$$\begin{aligned} -F_{34}\bar{n}_{\lambda 3} - \mu_{s3R}F_{34}\bar{n}_{N\lambda 3} - F_{23F}\bar{n}_{F2} + \mu_{s2F}F_{23F}\bar{n}_{F2} + \bar{Q}_3 \\ + F_{x3}\bar{i} + \mu_{Fy3}\bar{i} + F_{y3}\bar{j} - \mu_{Fx3}\bar{j} = 0 \end{aligned} \quad (H-123)$$

Moment equilibrium about point O_3 is given by

$$\begin{aligned} \mu_{F3}(\bar{F}_{x3} + \bar{F}_{y3})\bar{k} + [\bar{a}_{O3}\bar{n}_{O3} + \bar{r}_{O3}\bar{n}_{\lambda 3}] \times [-F_{34}\bar{n}_{\lambda 3} - \mu_{s3R}F_{34}\bar{n}_{N\lambda 3}] \\ + \bar{e}_2\bar{n}_{F2} \times \bar{F}_{23F} = 0 \end{aligned} \quad (H-124)$$

Note that the friction force F_{f23} exerts no moment about point O_3 .

Equation (H-123) furnishes the following component equations:

$$\begin{aligned} -F_{34}\cos\lambda_3 + \mu_{3R}F_{34}\sin\lambda_3 + Q_3\cos\gamma_3 + F_{x3} + \mu F_{y3} + F_{23}\sin(\psi_2 + \alpha_{p2}) \\ + \mu_{2R}F_{23}\cos(\psi_2 + \alpha_{p2}) = 0 \end{aligned} \quad (H-125)$$

and

$$\begin{aligned} -F_{34}\sin\lambda_3 - \mu_{3R}F_{34}\cos\lambda_3 + Q_3\sin\gamma_3 + F_{y3} - \mu F_{x3} - F_{23}\cos(\psi_2 + \alpha_{p2}) \\ + \mu_{2R}F_{23}\sin(\psi_2 + \alpha_{p2}) = 0 \end{aligned} \quad (H-126)$$

The scalar form of the moment equation (H-124) becomes

$$\begin{aligned} \mu_{p3}(\tilde{F}_{x3} + \tilde{F}_{y3}) + a_{03}F_{34}[\sin(\phi_3 + \delta_{03} - \lambda_3) - \mu_{3R}\cos(\phi_3 + \delta_{03} - \lambda_3)] \\ - \mu_{3R}a_{03}F_{34} - \delta_2 F_{23} = 0 \end{aligned} \quad (H-127)$$

Simultaneous solution of equations (H-125) and (H-126) for F_{x3} and F_{y3} leads to

$$F_{x3} = \frac{1}{1 + \mu^2} \left\{ F_{34} [(1 - \mu^2 a_{3R}) \cos \lambda_3 - \mu(1 + a_{3R}) \sin \lambda_3] \right. \\ \left. + F_{23} [-\mu(1 + a_{2F}) \cos(\psi_2 + \alpha_{P2}) - (1 - \mu^2 a_{2F}) \sin(\psi_2 + \alpha_{P2})] \right. \\ \left. + Q_3 [\mu \sin \gamma_3 - \cos \gamma_3] \right\} \quad (H-128)$$

and

$$F_{y3} = \frac{1}{1 + \mu^2} \left\{ F_{34} [(1 - \mu^2 a_{3R}) \sin \lambda_3 + \mu(1 + a_{3R}) \cos \lambda_3] \right. \\ \left. + F_{23} [(1 - \mu^2 a_{2F}) \cos(\psi_2 + \alpha_{P2}) - \mu(1 + a_{2F}) \sin(\psi_2 + \alpha_{P2})] \right. \\ \left. - Q_3 [\sin \gamma_3 + \mu \cos \gamma_3] \right\} \quad (H-129)$$

The sum $\tilde{F}_{x3} + \tilde{F}_{y3}$ of equation (H-127) is now made up of equations (H-128) and (H-129) in the sense of equation (A-5b)

$$\tilde{F}_{x3} + \tilde{F}_{y3} = F_{34} A_{31} + F_{23} A_{32} + Q_3 A_{33} + F_{34} A_{34} + F_{23} A_{35} + Q_3 A_{36} \quad (H-130)$$

where

$$A_{31} = \left| \frac{(1 - \mu^2 s_{3R}) \cos \lambda_3 - \mu(1 + s_{3R}) \sin \lambda_3}{1 + \mu^2} \right| \quad (H-131)$$

$$A_{32} = \left| \frac{-\mu(1 + s_{2F}) \cos(\psi_2 + \alpha_{P2}) - (1 - \mu^2 s_{2F}) \sin(\psi_2 + \alpha_{P2})}{1 + \mu^2} \right| \quad (H-132)$$

$$A_{33} = \left| \frac{\mu \sin \gamma_3 - \cos \gamma_3}{1 + \mu^2} \right| \quad (H-133)$$

$$A_{34} = \left| \frac{(1 - \mu^2 s_{3R}) \sin \lambda_3 + \mu(1 + s_{3R}) \cos \lambda_3}{1 + \mu^2} \right| \quad (H-134)$$

$$A_{35} = \left| \frac{(1 - \mu^2 s_{2F}) \cos(\psi_2 + \alpha_{P2}) - \mu(1 + s_{2F}) \sin(\psi_2 + \alpha_{P2})}{1 + \mu^2} \right| \quad (H-135)$$

$$A_{36} = \left| \frac{\sin \gamma_3 + \mu \cos \gamma_3}{1 + \mu^2} \right| \quad (H-136)$$

Equation (H-130) is now substituted into equation (H-127) and the result is solved for F_{23F}

$$F_{23R} = \frac{-F_{34}C_{16} - Q_3C_{17}}{C_{18}}$$

(H-137)

where

$$C_{16} = \mu P_3(A_{31} + A_{34}) + a_{Q3}[\sin(\phi_3 + \delta_{Q3} - \lambda_3) \\ - \mu_{3R} \cos(\phi_3 + \delta_{Q3} - \lambda_3)] - \mu_{3R} P_{Q3}$$

$$C_{17} = \mu P_3(A_{33} + A_{36})$$

$$C_{18} = \mu P_3(A_{32} + A_{35}) - \delta_2$$

II. FORCE AND MOMENT EQUILIBRIA OF GEAR AND PINION SET NO. 2

Figure H-8 shows the free body diagram of the gear and pinion set no. 2.

The forces of pinion no. 3 on gear no. 2 are equal and opposite to those given by equations (H-121) and (H-122), i.e.,

$$\bar{F}_{32F} = F_{23F} \bar{n}_{NF2} \quad (H-138)$$

and

$$\bar{F}_{f32F} = -\mu_{2F} F_{23F} \bar{n}_{NF2} \quad (H-139)$$

The forces of gear no. 1 on pinion no. 2 are those of equations (H-84) and (H-85).

The pivot friction is accounted for in the usual manner and the centrifugal force \bar{Q}_2 is given by equation (H-45).

Force equilibrium is given by

$$\begin{aligned} F_{23F} \bar{n}_{NF2} - \mu_{2F} F_{23F} \bar{n}_{NF2} + F_{12F} \bar{n}_{NF1} + \mu_{1F} F_{12F} \bar{n}_{NF1} + \bar{Q}_2 + F_{x2} \bar{i} - \mu F_{y2} \bar{i} \\ + F_{y2} \bar{j} + \mu F_{x2} \bar{j} = 0 \end{aligned} \quad (H-140)$$

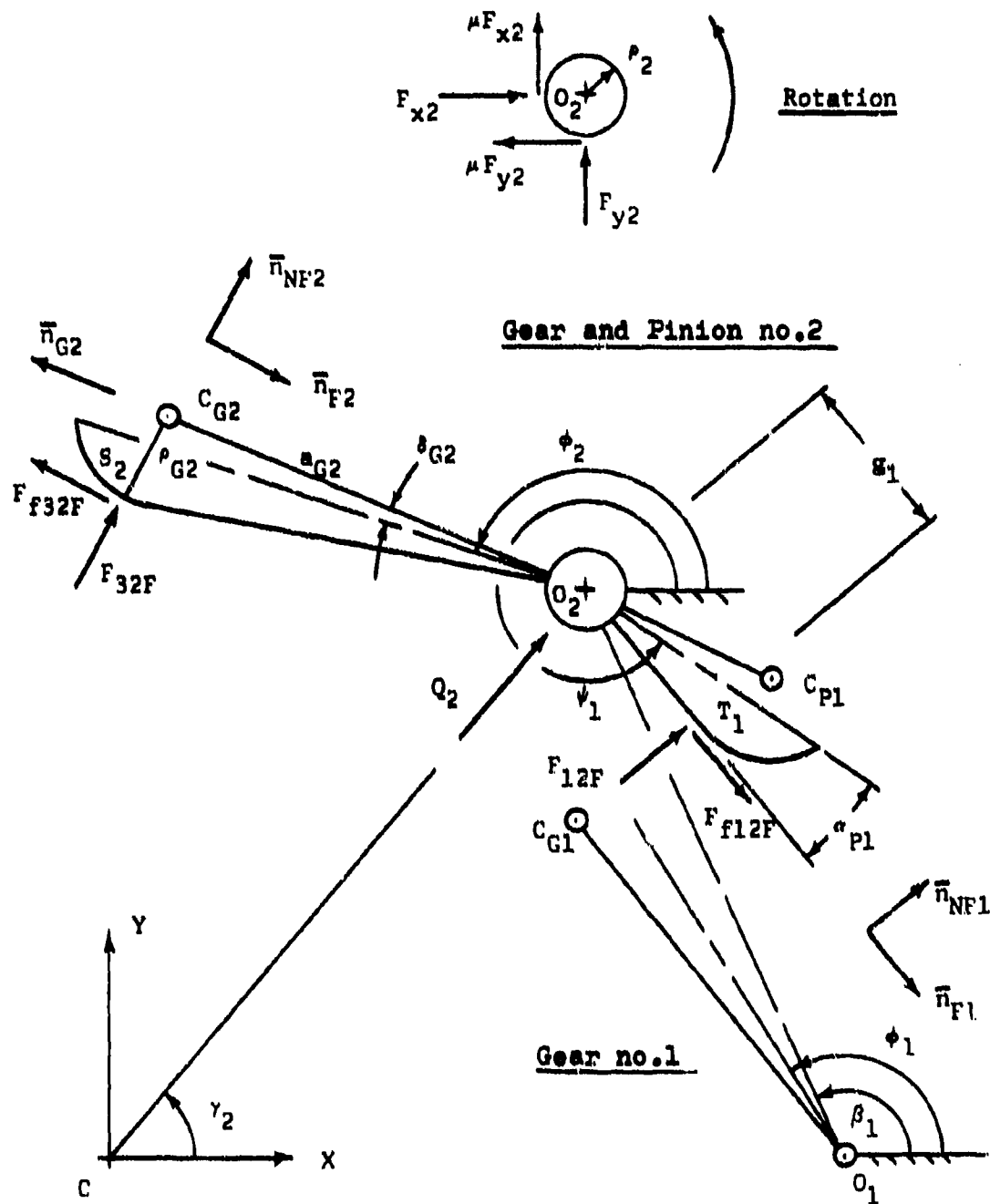


FIGURE H-8

FREE BODY DIAGRAM OF GEAR & PINION NO. 2

MESH NO. 2: ROUND ON FLAT

MESH NO. 1: ROUND ON FLAT

Moment equilibrium about point O_2 requires

$$\begin{aligned}
 -\mu_2(\tilde{F}_{x2} + \tilde{F}_{y2})\bar{k} + [a_{G2}\bar{n}_{G2} - r_{G2}\bar{n}_{NF2}] \times [F_{23}\bar{n}_{NF2} - \mu_2 F_{23}\bar{n}_{F2}] \\
 + s_1\bar{n}_{F1} \times F_{12}\bar{n}_{NF1} = 0
 \end{aligned}
 \tag{H-141}$$

Equation (H-140) gives the component equations

$$\begin{aligned}
 -F_{23}\sin(\psi_2 + \alpha_{P2}) - \mu_2 F_{23}\cos(\psi_2 + \alpha_{P2}) + Q_2\cos\gamma_2 + F_{x2} - \mu F_{y2} \\
 - F_{12}\sin(\psi_1 - \alpha_{P1}) + \mu_1 F_{12}\cos(\psi_1 - \alpha_{P1}) = 0
 \end{aligned}
 \tag{H-142}$$

and

$$\begin{aligned}
 F_{23}\cos(\psi_2 + \alpha_{P2}) - \mu_2 F_{23}\sin(\psi_2 + \alpha_{P2}) + Q_2\sin\gamma_2 + F_{y2} + \mu F_{x2} \\
 + F_{12}\cos(\psi_1 - \alpha_{P1}) + \mu_1 F_{12}\sin(\psi_1 - \alpha_{P1}) = 0
 \end{aligned}
 \tag{H-143}$$

The scalar form of the moment equation (H-141) becomes

$$\begin{aligned}
 & -\mu p_2(\tilde{F}_{x2} + \tilde{F}_{y2}) + a_{G2} F_{23F} [\cos(\phi_2 - \delta_{G2} - \psi_2 - \alpha_{P2}) \\
 & + \mu s_{2F} \sin(\phi_2 - \delta_{G2} - \psi_2 - \alpha_{P2})] - \mu s_{2F} p_{G2} F_{23F} + \xi_1 F_{12F} = 0
 \end{aligned}
 \tag{H-144}$$

Simultaneous solution of the component equations (H-142) and (H-143) for F_{x2} and F_{y2} leads to

$$\begin{aligned}
 F_{x2} = \frac{1}{1 + \mu^2} \bigg\{ & F_{23F} [(1 + \mu^2 s_{2F}) \sin(\psi_2 + \alpha_{P2}) + \mu(s_{2F} - 1) \cos(\psi_2 + \alpha_{P2})] \\
 & + F_{12F} [(1 - \mu^2 s_{1F}) \sin(\psi_1 - \alpha_{P1}) - \mu(1 + s_{1F}) \cos(\psi_1 - \alpha_{P1})] \\
 & - Q_2 [\mu \sin \gamma_2 + \cos \gamma_2] \bigg\}
 \end{aligned}
 \tag{H-145}$$

and

$$\begin{aligned}
 F_{y2} = \frac{1}{1 + \mu^2} \bigg\{ & F_{23F} [\mu(s_{2F} - 1) \sin(\psi_2 + \alpha_{P2}) - (1 + \mu^2 s_{2F}) \cos(\psi_2 + \alpha_{P2})] \\
 & - F_{12F} [\mu(1 + s_{1F}) \sin(\psi_1 - \alpha_{P1}) + (1 - \mu^2 s_{1F}) \cos(\psi_1 - \alpha_{P1})] \\
 & + Q_2 [\mu \cos \gamma_2 - \sin \gamma_2] \bigg\}
 \end{aligned}
 \tag{H-146}$$

The sum $\tilde{F}_{x2} + \tilde{F}_{y2}$ of equation (H-144) is now made up of equations (H-145) and (H-146) in the sense of equation (A-3b)

$$\tilde{F}_{x2} + \tilde{F}_{y2} = F_{23F}A_{37} + F_{12F}A_{38} + Q_2A_{39} + F_{23F}A_{40} + F_{12F}A_{41} + Q_2A_{42} \quad (H-147)$$

where

$$A_{37} = \left| \frac{(1 + \mu^2 s_{2F})\sin(\psi_2 + \alpha_{P2}) + \mu(s_{2F} - 1)\cos(\psi_2 + \alpha_{P2})}{1 + \mu^2} \right| \quad (H-148)$$

$$A_{38} = \left| \frac{(1 - \mu^2 s_{1F})\sin(\psi_1 - \alpha_{P1}) - \mu(1 + s_{1F})\cos(\psi_1 - \alpha_{P1})}{1 + \mu^2} \right| \quad (H-149)$$

$$A_{39} = \left| \frac{\mu \sin \gamma_2 + \cos \gamma_2}{1 + \mu^2} \right| \quad (H-150)$$

$$A_{40} = \left| \frac{\mu(s_{2F} - 1)\sin(\psi_2 + \alpha_{P2}) - (1 + \mu^2 s_{2F})\cos(\psi_2 + \alpha_{P2})}{1 + \mu^2} \right| \quad (H-151)$$

$$A_{41} = \left| \frac{\mu(1 + s_{1F})\sin(\psi_1 - \alpha_{P1}) + (1 - \mu^2 s_{1F})\cos(\psi_1 - \alpha_{P1})}{1 + \mu^2} \right| \quad (H-152)$$

$$A_{42} = \left| \frac{\mu \cos \gamma_2 - \sin \gamma_2}{1 + \mu^2} \right| \quad (H-153)$$

Equation (H-147) is now substituted into equation (H-144) and the result is solved for F_{12F}

$$F_{12F} = \frac{-F_{23F}C_{19} + Q_2C_{20}}{C_{21}} \quad (H-154)$$

where

$$C_{19} = -\mu P_2(A_{37} + A_{40}) + s_{G2}[\cos(\phi_2 - \delta_{G2} - \psi_2 - \alpha_{P2}) + \mu s_{2F}\sin(\phi_2 - \delta_{G2} - \psi_2 - \alpha_{P2})] - \mu s_{2F}P_{G2}$$

$$C_{20} = \mu P_2(A_{39} + A_{42})$$

$$C_{21} = -\mu P_2(A_{38} + A_{41}) + S_1$$

III. FORCE AND MOMENT EQUILIBRIA OF INPUT GEAR NO. 1

While the numerical values of the force F_{21F} and its associated friction force F_{12F} , both acting on gear no. 1, are peculiar to the present combination of contact phases, its functional relationship to the input moment M_{1n} and the centrifugal force Q_1 is identical to that derived in section 1b-II of this appendix. (See also Figure H-6.)

According to equation (H-115), one obtains for F_{12F}

$$F_{12F} = \frac{M_{1n} - Q_1 C_{14}}{C_{15}} \quad (H-155)$$

IV. MOMENT INPUT-OUTPUT RELATIONSHIP

Equations (H-154) and (H-155), both in F_{12F} , are set equal to each other and the result is solved for F_{23F}

$$F_{23F} = \frac{-C_{21}}{C_{15}C_{19}} (M_{1n} - Q_1 C_{14}) + Q_2 \frac{C_{20}}{C_{19}} \quad (H-156)$$

The above is now equated to equation (H-137) and the result is solved for F_{34}

$$F_{34} = \frac{C_{18}C_{21}}{C_{15}C_{16}C_{19}} (M_{1n} - Q_1 C_{14}) - Q_2 \frac{C_{18}C_{20}}{C_{16}C_{19}} - Q_3 \frac{C_{17}}{C_{16}} \quad (H-157)$$

Finally, equation (H-157) is equated to equation (H-19), which corresponds to the round on round phase of mesh no. 3. The result is solved for the equilibrant moment M_{043} (for case 3: RFF)

$$M_{043} = M_{1n} \frac{C_2 C_{18} C_{21}}{C_{15} C_{16} C_{19}} - Q_1 \frac{C_2 C_{14} C_{18} C_{21}}{C_{15} C_{16} C_{19}} - Q_2 \frac{C_2 C_{18} C_{20}}{C_{16} C_{19}} - Q_3 \frac{C_2 C_{17}}{C_{16}} - Q_4 C_1 \quad (H-158)$$

d. CASE NO. 4: RFR

For this contact combination force F_{34} may be taken from the results of case no. 1 [see equation (H-19)], since mesh no. 3 is in the round on round phase of motion. The force F_{23F} of case no. 3, i.e., equation (H-137), also is incorporated.

The input-output relationship of the gear and pinion combination no. 2 must be newly derived, i.e., the force F_{12} must be expressed in terms of the contact force F_{32F} and the centrifugal force Q_2 . Finally, the results of the equilibrium equations for the input gear no. 1 of case no. 1 are used. For this case of contact, the force F_{12} is given by equation (H-78).

I. FORCE AND MOMENT EQUILIBRIA OF GEAR AND PINION SET NO. 2

Figure H-9 shows the free body diagram of gear and pinion set no. 2 with the necessary portions of mesh no. 1.

The forces of pinion no. 3 on gear no. 2 were given by equations (H-138) and (H-139)

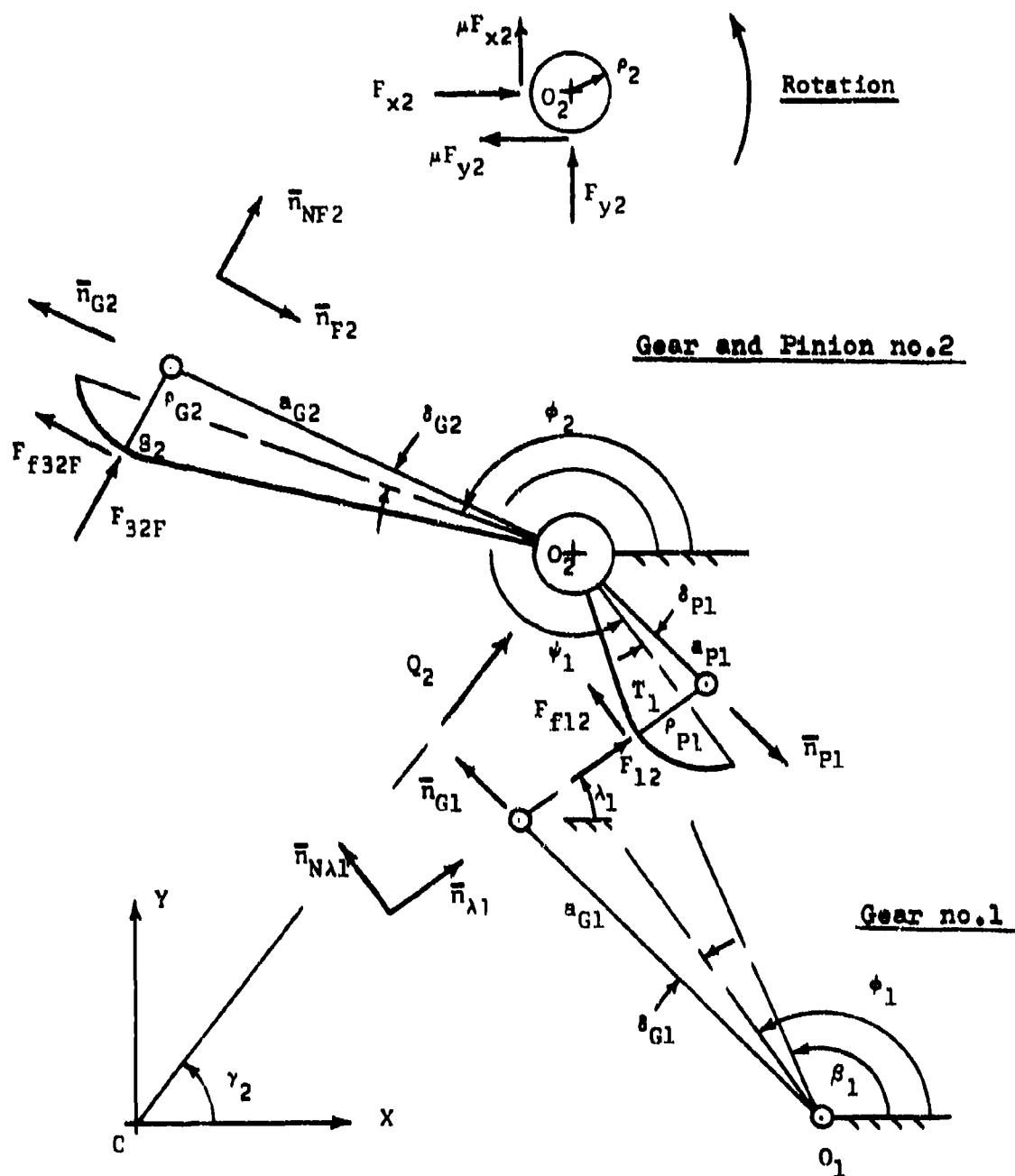


FIGURE H-9

FREE BODY DIAGRAM OF GEAR & PINION NO. 2

MESH NO. 2: ROUND ON FLAT

MESH NO. 1: ROUND ON ROUND

$$\bar{F}_{32F} = F_{23F} \bar{n}_{NF2} \quad (H-159)$$

and

$$\bar{F}_{f32F} = -\mu s_{2F} F_{23F} \bar{n}_{F2} \quad (H-160)$$

The forces of gear no. 1 on pinion no. 2 are given by equations (H-43) and (H-44)

$$\bar{F}_{12} = F_{12} \bar{n}_{\lambda 1} \quad (H-161)$$

and

$$\bar{F}_{f12} = \mu s_{1R} F_{12} \bar{n}_{N\lambda 1} \quad (H-162)$$

The centrifugal force \bar{Q}_2 is given by equation (H-45). The pivot reactions and friction forces are handled as before.

Force equilibrium is given by

$$\begin{aligned} F_{23F} \bar{n}_{NF2} - \mu s_{2F} F_{23F} \bar{n}_{F2} + F_{12} \bar{n}_{\lambda 1} + \mu s_{1R} F_{12} \bar{n}_{N\lambda 1} + \bar{Q}_2 + F_{x2} \bar{i} - \mu F_{y2} \bar{i} \\ + F_{y2} \bar{j} + \mu F_{x2} \bar{j} = 0 \end{aligned} \quad (H-163)$$

Moment equilibrium about point O_2 is given by

$$\begin{aligned}
 & -\mu P_2(\tilde{F}_{x2} + \tilde{F}_{y2}) + [a_{G2}\bar{E}_{G2} - \rho_{G2}\bar{E}_{NF2}] \times [F_{23}F_{NF2} - \mu s_2 F_{23}F_{NF2}] \\
 & + [a_{P1}\bar{n}_{P1} - \rho_{P1}\bar{n}_{\lambda 1}] \times [F_{12}\bar{n}_{\lambda 1} + \mu s_1 R F_{12}\bar{n}_{N\lambda 1}] = 0 \quad (H-164)
 \end{aligned}$$

Equation (H-163) gives the following component equations

$$\begin{aligned}
 & -F_{23}F_{NF2} \sin(\psi_2 + \alpha_{P2}) - \mu s_2 F_{23}F_{NF2} \cos(\psi_2 + \alpha_{P2}) + F_{x2} - \mu F_{y2} + F_{12} \cos \lambda_1 \\
 & - \mu s_1 R F_{12} \sin \lambda_1 + Q_2 \cos \gamma_2 = 0 \quad (H-165)
 \end{aligned}$$

and

$$\begin{aligned}
 & F_{23}F_{NF2} \cos(\psi_2 + \alpha_{P2}) - \mu s_2 F_{23}F_{NF2} \sin(\psi_2 + \alpha_{P2}) + F_{y2} + \mu F_{x2} + F_{12} \sin \lambda_1 \\
 & + \mu s_1 R F_{12} \cos \lambda_1 + Q_2 \sin \gamma_2 = 0 \quad (H-166)
 \end{aligned}$$

The scalar form of the moment equation (H-164) becomes

$$\begin{aligned}
 & - p_2(\tilde{F}_{x2} + \tilde{F}_{y2}) + a_{G2}F_{23F}[\cos(\phi_2 - \delta_{G2} - \psi_2 - \alpha_{P2}) \\
 & + \mu s_{2F}\sin(\phi_2 - \delta_{G2} - \psi_2 - \alpha_{P2})] - \mu s_{2F}^p G_2 F_{23F} - \mu s_{1R}^p P_1 F_{12} \\
 & + a_{P1}F_{12}[\mu s_{1R}\cos(\psi_1 + \delta_{P1} - \lambda_1) - \sin(\psi_1 + \delta_{P1} - \lambda_1)] = 0
 \end{aligned}
 \tag{H-167}$$

Simultaneous solution of the force component equations (H-165)

and (H-166) for F_{x2} and F_{y2} results in

$$\begin{aligned}
 F_{x2} = \frac{1}{1 + \mu^2} \bigg\{ & F_{23F}[(1 + \mu^2 s_{2F})\sin(\psi_2 + \alpha_{P2}) - \mu(1 - s_{2F})\cos(\psi_2 + \alpha_{P2})] \\
 & + F_{12}[\mu(s_{1R} - 1)\sin\lambda_1 - (1 + \mu^2 s_{1R})\cos\lambda_1] \\
 & - Q_2[\mu\sin\gamma_2 + \cos\gamma_2] \bigg\}
 \end{aligned}
 \tag{H-168}$$

and

$$\begin{aligned}
 F_{y2} = \frac{1}{1 + \mu^2} \bigg\{ & F_{23F}[\mu(s_{2F} - 1)\sin(\psi_2 + \alpha_{P2}) - (1 + \mu^2 s_{2F})\cos(\psi_2 + \alpha_{P2})] \\
 & + F_{12}[-(1 + \mu^2 s_{1R})\sin\lambda_1 + \mu(1 - s_{1R})\cos\lambda_1] \\
 & + Q_2[-\sin\gamma_2 + \mu\cos\gamma_2] \bigg\}
 \end{aligned}
 \tag{H-169}$$

The sum $\tilde{F}_{x2} + \tilde{F}_{y2}$ of equation(H-167) is now made up of equations (H-168) and (H-169) in the usual manner

$$\tilde{F}_{x2} + \tilde{F}_{y2} = F_{23}A_{43} + F_{12}A_{44} + Q_2A_{45} + F_{23}A_{46} + F_{12}A_{47} + Q_2A_{48} \quad (H-170)$$

where

$$A_{43} = \left| \frac{(1 + \mu^2 s_{2F}) \sin(\psi_2 + \alpha_{P2}) - \mu(1 - s_{2F}) \cos(\psi_2 + \alpha_{P2})}{1 + \mu^2} \right| \quad (H-171)$$

$$A_{44} = \left| \frac{\mu(s_{1R} - 1) \sin \lambda_1 - (1 + \mu^2 s_{1R}) \cos \lambda_1}{1 + \mu^2} \right| \quad (H-172)$$

$$A_{45} = \left| \frac{\mu \sin \gamma_2 + \cos \gamma_2}{1 + \mu^2} \right| \quad (H-173)$$

$$A_{46} = \left| \frac{\mu(s_{2F} - 1) \sin(\psi_2 + \alpha_{P2}) - (1 + \mu^2 s_{2F}) \cos(\psi_2 + \alpha_{P2})}{1 + \mu^2} \right| \quad (H-174)$$

$$A_{47} = \left| \frac{-(1 + \mu^2 s_{1R}) \sin \lambda_1 + \mu(1 - s_{1R}) \cos \lambda_1}{1 + \mu^2} \right| \quad (H-175)$$

$$A_{48} = \left| \frac{-\sin \gamma_2 + \mu \cos \gamma_2}{1 + \mu^2} \right| \quad (H-176)$$

Equation (H-170) is now substituted into the moment equation (H-167) and the result is solved for F_{12}

$$F_{12} = \frac{-F_{23}C_{22} + Q_2C_{23}}{C_{24}} \quad (H-177)$$

where

$$C_{22} = -\mu p_2(A_{43} + A_{46}) + a_{g2}[\cos(\phi_2 - \delta_{g2} - \psi_2 - \alpha_{p2}) + \mu a_{2f}\sin(\phi_2 - \delta_{g2} - \psi_2 - \alpha_{p2})] - \mu a_{2f}p_{g2}$$

$$C_{23} = \mu p_2(A_{45} + A_{48})$$

$$C_{24} = -\mu p_2(A_{44} + A_{47}) + a_{p1}[\mu a_{1R}\cos(\psi_1 + \delta_{p1} - \lambda_1) - \sin(\psi_1 + \delta_{p1} - \lambda_1)] - \mu a_{1R}p_{p1}$$

II. MOMENT INPUT-OUTPUT RELATIONSHIP

Equations (H-177) and (H-78) are now set equal to each other and the result is solved for F_{23F}

$$F_{23F} = \frac{-C_{24}}{C_{10}C_{22}} (M_{1n} - Q_1 C_9) + Q_2 \frac{C_{23}}{C_{22}} \quad (H-178)$$

The above is now equated to equation (H-137) to obtain F_{34}

$$F_{34} = \frac{C_{18}C_{24}}{C_{10}C_{16}C_{22}} (M_{1n} - Q_1 C_9) - Q_2 \frac{C_{18}C_{23}}{C_{16}C_{22}} - Q_3 \frac{C_{17}}{C_{16}} \quad (H-179)$$

Finally equations (H-179) and (H-19) are set equal to each other and the equilibrant moment M_{o44} (For case 4: RFR) is determined

$$\begin{aligned} M_{o44} = M_{1n} \frac{C_2 C_{18} C_{24}}{C_{10} C_{16} C_{22}} - Q_1 \frac{C_2 C_9 C_{18} C_{24}}{C_{10} C_{16} C_{22}} - Q_2 \frac{C_2 C_{18} C_{23}}{C_{16} C_{22}} - Q_3 \frac{C_2 C_{17}}{C_{16}} \\ - Q_4 C_1 \end{aligned} \quad (H-180)$$

e. CASE NO. 5: FFF

For this contact combination it is necessary to determine new expressions for the force F_{34F} of gear no. 3 on pinion no. 4, and for force F_{23F} of gear no. 2 on pinion no. 3.

Equation (H-156), derived for case 3, and which relates force F_{23F} to the input moment M_{in} , may be used for the determination of the final input-output relationship.

I. FORCE AND MOMENT EQUILIBRIA OF PINION NO. 4

Figure H-10 gives the free body diagram of pinion no. 4 in the round on flat phase of motion with gear no. 3.

The equilibrant moment M_{o4} acts in a clockwise direction and opposes the counter-clockwise rotation of the pinion.

The normal contact force \bar{F}_{34F} is given by

$$\bar{F}_{34F} = F_{34F} \bar{H}_{NF3} \quad (H-181)$$

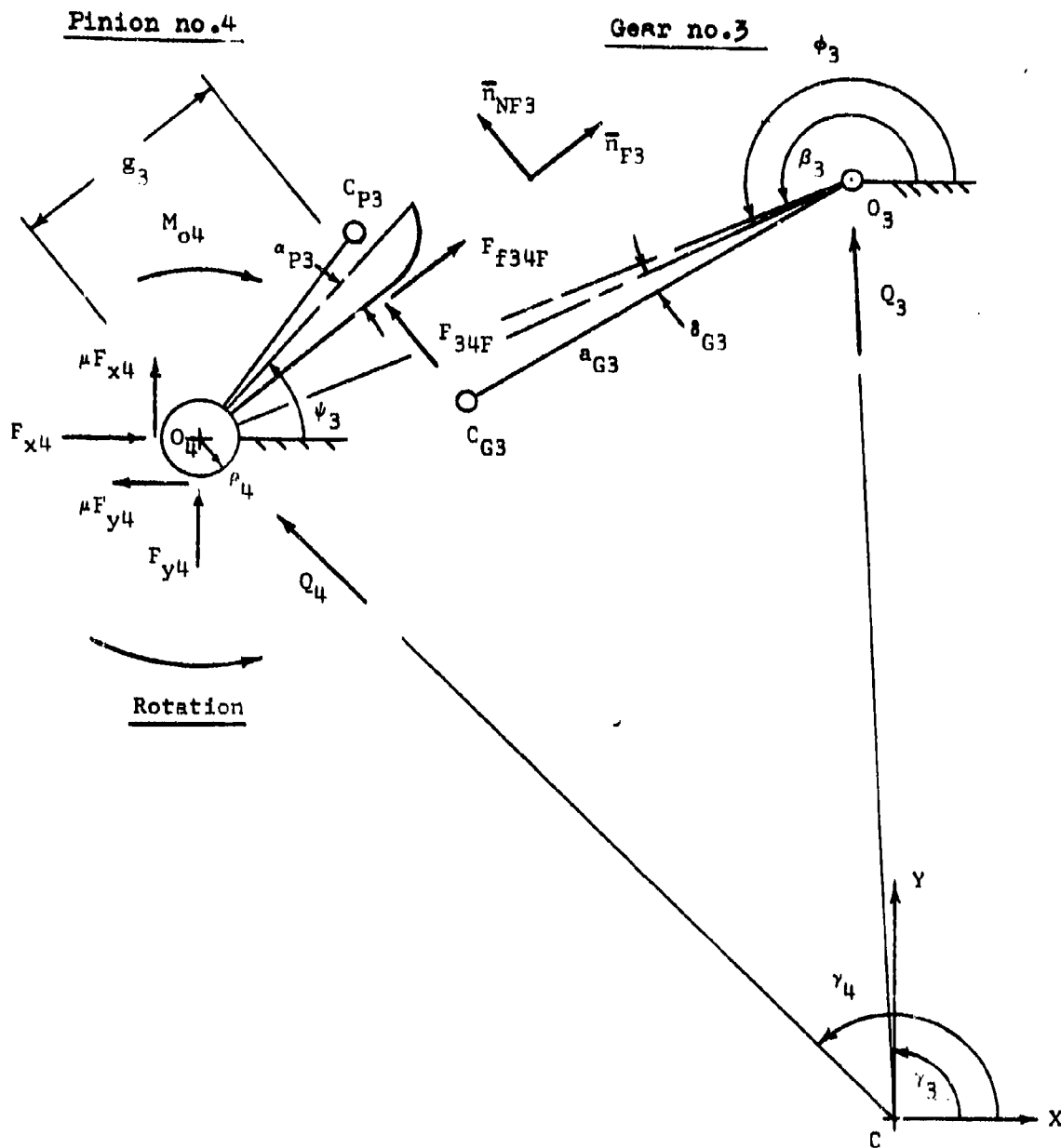


FIGURE H-10
FREE BODY DIAGRAM OF PINION NO. 4
MESH NO. 3: ROUND ON FLAT

The associated friction force becomes

$$\bar{F}_{f34F} = \mu s_3 F_{34F} \bar{n}_{F3} \quad (H-182)$$

The centrifugal force \bar{Q}_4 is given by equation (H-5) and the pivot friction forces are chosen such that they oppose rotation.

Force equilibrium is given by

$$\begin{aligned} F_{34F} \bar{n}_{NF3} + \mu s_3 F_{34F} \bar{n}_{F3} + F_{x4} \bar{i} - \mu F_{y4} \bar{i} + F_{y4} \bar{j} + \mu F_{x4} \bar{j} \\ + Q_4 (\cos \gamma_4 \bar{i} + \sin \gamma_4 \bar{j}) = 0 \end{aligned} \quad (H-183)$$

Moment equilibrium about point O_4 requires that

$$-M_{O4} \bar{k} - \mu \rho_4 (\tilde{F}_{x4} + \tilde{F}_{y4}) \bar{k} + s_3 \bar{n}_{F3} \times F_{34F} \bar{n}_{NF3} = 0 \quad (H-184)$$

Note that the friction force F_{f34F} does not exert a moment about point O_4 , since its line of action passes through it.

Equation (H-183) furnishes the following component equations

$$\begin{aligned} -F_{34F} \sin(\psi_3 - \alpha_{P3}) + \mu s_3 F_{34F} \cos(\psi_3 - \alpha_{P3}) + F_{x4} - \mu F_{y4} \\ + Q_4 \cos \gamma_4 = 0 \end{aligned} \quad (H-185)$$

and

$$F_{34F} \cos(\psi_3 - \alpha_{p3}) + \mu s_{3F} F_{34F} \sin(\psi_3 - \alpha_{p3}) + F_{y4} + \mu F_{x4} + Q_4 \sin \gamma_4 = 0 \quad (H-186)$$

The scalar form of the moment equation (H-184) becomes

$$-M_{o4} - \mu \rho_4 (\tilde{F}_{x4} + \tilde{F}_{y4}) + \epsilon_3 F_{34F} = 0 \quad (H-187)$$

Simultaneous solution of equations (H-185) and (H-186) for F_{x4} and F_{y4} results in

$$F_{x4} = \frac{1}{1 + \mu^2} \left\{ F_{34F} [(1 - \mu^2 s_{3F}) \sin(\psi_3 - \alpha_{p3}) - \mu(1 + s_{3F}) \cos(\psi_3 - \alpha_{p3})] + Q_4 [-\mu \sin \gamma_4 - \cos \gamma_4] \right\} \quad (H-188)$$

and

$$F_{y4} = \frac{1}{1 + \mu^2} \left\{ F_{34F} [-\mu(1 + s_{3F}) \sin(\psi_3 - \alpha_{p3}) - (1 - \mu^2 s_{3F}) \cos(\psi_3 - \alpha_{p3})] + Q_4 [-\sin \gamma_4 + \mu \cos \gamma_4] \right\} \quad (H-189)$$

The sum $\tilde{F}_{x4} + \tilde{F}_{y4}$ of equation (H-187) is now made up of equations (H-188) and (H-189) in the sense of equation (A-3b)

$$\tilde{F}_{x4} + \tilde{F}_{y4} = F_{34F}A_{49} + Q_4A_{50} + F_{34F}A_{51} + Q_4A_{52} \quad (H-190)$$

where

$$A_{49} = \left| \frac{(1 - \mu^2 s_{3F}) \sin(\psi_3 - \alpha_{P3}) - \mu(1 + s_{3F}) \cos(\psi_3 - \alpha_{P3})}{1 + \mu^2} \right| \quad (H-191)$$

$$A_{50} = \left| \frac{-\mu \sin \gamma_4 - \cos \gamma_4}{1 + \mu^2} \right| \quad (H-192)$$

$$A_{51} = \left| \frac{-\mu(1 + s_{3F}) \sin(\psi_3 - \alpha_{P3}) - (1 - \mu^2 s_{3F}) \cos(\psi_3 - \alpha_{P3})}{1 + \mu^2} \right| \quad (H-193)$$

$$A_{52} = \left| \frac{-\sin \gamma_4 + \mu \cos \gamma_4}{1 + \mu^2} \right| \quad (H-194)$$

Equation (H-190) is now substituted into equation (H-187) and the result is solved for F_{34F}

$$F_{34F} = \frac{M_{04} + Q_4 C_{25}}{C_{26}} \quad (H-195)$$

where

$$C_{25} = \mu p_4 (A_{50} + A_{52})$$

$$C_{26} = \delta_3 - \mu p_4 (A_{49} + A_{51})$$

II. FORCE AND MOMENT EQUILIBRIA OF GEAR AND PINION SET NO. 3

Figure H-11 gives the free body diagram of gear and pinion combination no. 3. Both mesh 3 and mesh 2 are in their round on flat phase of contact.

The forces of pinion 4 on gear 3 are equal to, but opposite in direction to, those given by equations (H-181) and (H-182)

$$\bar{F}_{43F} = -F_{34F}\bar{n}_{NF3} \quad (H-196)$$

and

$$\bar{F}_{f43F} = -\mu_{s3F}F_{34F}\bar{n}_{F3} \quad (H-197)$$

The forces of gear 2 on pinion 3 are given by

$$\bar{F}_{23F} = -F_{23F}\bar{n}_{NF2} \quad (H-198)$$

and

$$\bar{F}_{f23F} = -\mu_{s2F}F_{23F}\bar{n}_{F2} \quad (H-199)$$

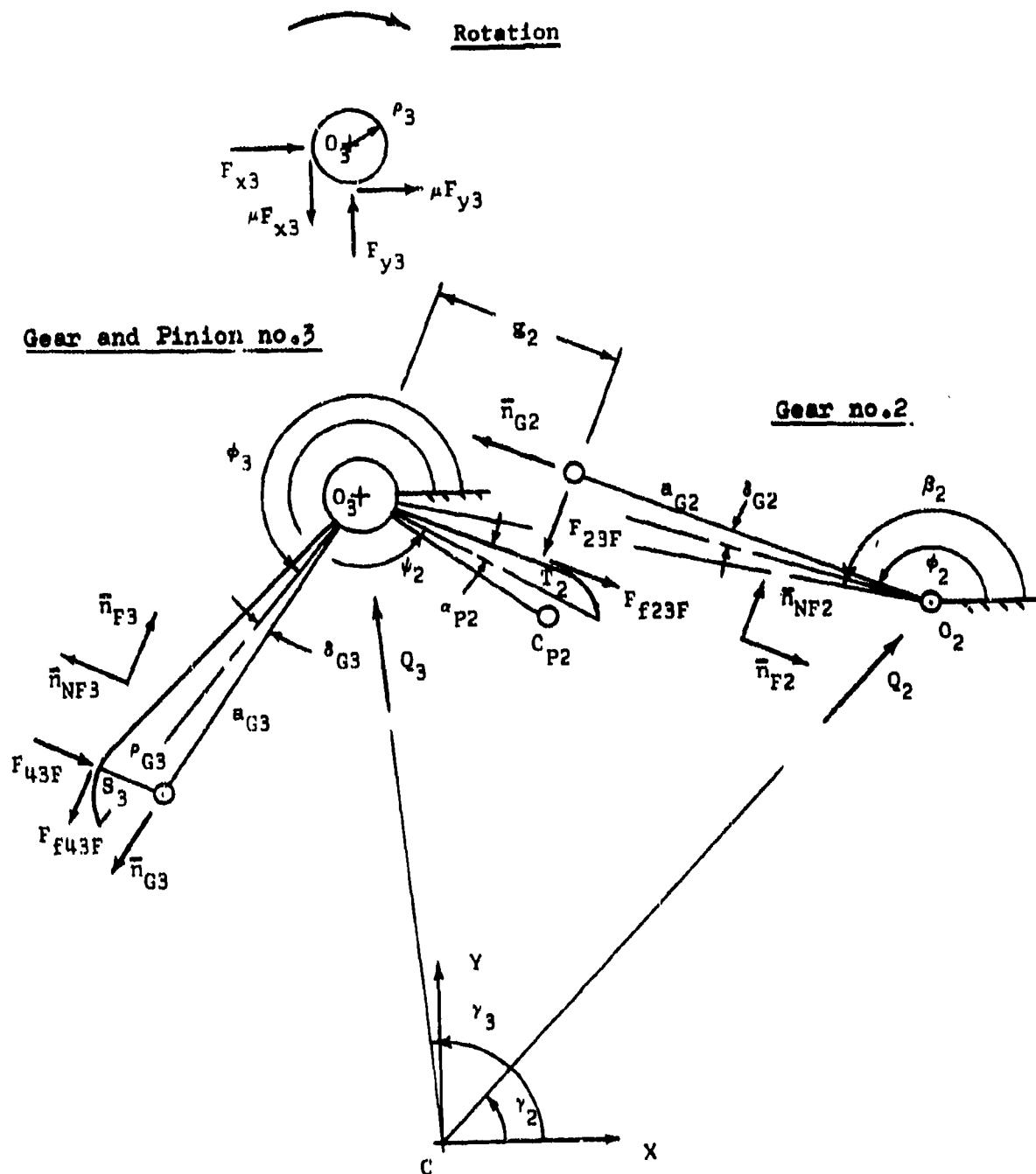


FIGURE H-11

FREE BODY DIAGRAM OF GEAR & PINION NO. 3

MESH NO. 3: ROUND ON FLAT

MESH NO. 2: ROUND ON FLAT

The pivot forces and moments are chosen in the usual manner and the centrifugal force \bar{Q}_3 is defined by equation (H-24).

Force equilibrium is given by

$$\begin{aligned} -F_{34}\bar{n}_{NF3} - \mu_{s3}F_{34}\bar{n}_{F3} - F_{23}\bar{n}_{NF2} + \mu_{s2}F_{23}\bar{n}_{F2} + \bar{Q}_3 + F_{x3}\bar{i} \\ + \mu_{Fy3}\bar{i} + F_{y3}\bar{j} - \mu_{Fx3}\bar{j} = 0 \end{aligned} \quad (H-200)$$

Moment equilibrium about point O_3 requires that

$$\begin{aligned} \mu_{F3}(\bar{F}_{x3} + \bar{F}_{y3})\bar{k} + [a_{G3}\bar{n}_{G3} + r_{G3}\bar{n}_{NF3}] \times [-F_{34}\bar{n}_{NF3} - \mu_{s3}F_{34}\bar{n}_{F3}] \\ + b_{2}\bar{n}_{F2} \times (-)F_{23}\bar{n}_{NF2} = 0 \end{aligned} \quad (H-201)$$

Note that the friction force F_{f23F} does not exert a moment about point O_3 .

Equation (H-200) furnishes, after all necessary substitutions, the following component equations:

$$\begin{aligned} F_{34}\sin(\psi_3 - \alpha_{P3}) - \mu_{s3}F_{34}\cos(\psi_3 - \alpha_{P3}) + Q_3\cos\gamma_3 + F_{x3} + \mu_{Fy3} \\ + F_{23}\sin(\psi_2 + \alpha_{P2}) + \mu_{s2}F_{23}\cos(\psi_2 + \alpha_{P2}) = 0 \end{aligned} \quad (H-202)$$

and

$$\begin{aligned}
 & -F_{34} \cos(\psi_3 - \alpha_{p3}) - \mu s_{3F} F_{34} \sin(\psi_3 - \alpha_{p3}) + Q_3 \sin \gamma_3 + F_{y3} - \mu F_{x3} \\
 & - F_{23} \cos(\psi_2 + \alpha_{p2}) + \mu s_{2F} F_{23} \sin(\psi_2 + \alpha_{p2}) = 0 \quad (H-203)
 \end{aligned}$$

The scalar form of the moment equation (H-201) becomes

$$\begin{aligned}
 & \mu p_3 (\tilde{F}_{x3} + \tilde{F}_{y3}) + s_{G3} F_{34} [-\cos(\phi_3 + \delta_{G3} - \psi_3 + \alpha_{p3}) \\
 & + \mu s_{3F} \sin(\phi_3 + \delta_{G3} - \psi_3 + \alpha_{p3})] + \mu s_{3F} p_{G3} F_{34} - s_{2F} F_{23} = 0 \\
 & \quad (H-204)
 \end{aligned}$$

Simultaneous solution of the component equations (H-202) and (H-203) for F_{x3} and F_{y3} gives

$$\begin{aligned}
 F_{x3} = \frac{1}{1 + \mu^2} \bigg\{ & F_{34} \left[-(1 + \mu^2 s_{3F}) \sin(\psi_3 - \alpha_{p3}) + \mu (s_{3F} - 1) \cos(\psi_3 - \alpha_{p3}) \right] \\
 & + F_{23} \left[(\mu^2 s_{2F} - 1) \sin(\psi_2 + \alpha_{p2}) - \mu (1 + s_{2F}) \cos(\psi_2 + \alpha_{p2}) \right] \\
 & + Q_3 [\mu \sin \gamma_3 - \cos \gamma_3] \bigg\} \quad (H-205)
 \end{aligned}$$

and

$$F_{y3} = \frac{1}{1 + \mu^2} \left\{ F_{34F} [\mu(s_{3F} - 1)\sin(\psi_3 - \alpha_{P3}) + (1 + \mu^2 s_{3F})\cos(\psi_3 - \alpha_{P3})] \right. \\ \left. + F_{23F} [-\mu(1 + s_{2F})\sin(\psi_2 + \alpha_{P2}) + (1 - \mu^2 s_{2F})\cos(\psi_2 + \alpha_{P2})] \right. \\ \left. + Q_3 [-\sin\gamma_3 - \mu\cos\gamma_3] \right\} \quad (H-206)$$

The sum $\tilde{F}_{x3} + \tilde{F}_{y3}$ is now made up from equations (H-205) and (H-206)

$$\tilde{F}_{x3} + \tilde{F}_{y3} = F_{34F}A_{53} + F_{23F}A_{54} + Q_3A_{55} + F_{34F}A_{56} + F_{23F}A_{57} + Q_3A_{58} \quad (H-207)$$

where

$$A_{53} = \left| \frac{-(1 + \mu^2 s_{3F})\sin(\psi_3 - \alpha_{P3}) + \mu(s_{3F} - 1)\cos(\psi_3 - \alpha_{P3})}{1 + \mu^2} \right| \quad (H-208)$$

$$A_{54} = \left| \frac{(\mu^2 s_{2F} - 1)\sin(\psi_2 + \alpha_{P2}) - \mu(1 + s_{2F})\cos(\psi_2 + \alpha_{P2})}{1 + \mu^2} \right| \quad (H-209)$$

$$A_{55} = \left| \frac{\mu\sin\gamma_3 - \cos\gamma_3}{1 + \mu^2} \right| \quad (H-210)$$

$$A_{56} = \left| \frac{\mu(a_{3F} - 1)\sin(\psi_3 - \alpha_{P3}) + (1 + \mu^2 a_{3F})\cos(\psi_3 - \alpha_{P3})}{1 + \mu^2} \right| \quad (H-211)$$

$$A_{57} = \left| \frac{-\mu(1 + a_{2F})\sin(\psi_2 + \alpha_{P2}) + (1 - \mu^2 a_{2F})\cos(\psi_2 + \alpha_{P2})}{1 + \mu^2} \right| \quad (H-212)$$

$$A_{58} = \left| \frac{\sin\gamma_3 + \mu\cos\gamma_3}{1 + \mu^2} \right| \quad (H-213)$$

Equation (H-207) is now substituted into equation (H-204).

The result is solved for F_{23F}

$$F_{23F} = \frac{-F_{34F}C_{27} - Q_3C_{28}}{C_{29}} \quad (H-214)$$

where

$$C_{27} = \mu^2 P_3 (A_{53} + A_{56}) + a_{G3} [-\cos(\phi_3 + \delta_{G3} - \psi_3 + \alpha_{P3}) + \mu a_{3F} \sin(\phi_3 + \delta_{G3} - \psi_3 + \alpha_{P3})] + \mu a_{3F} P_{G3}$$

$$C_{28} = \mu^2 P_3 (A_{55} + A_{58})$$

$$C_{29} = \mu^2 P_3 (A_{54} + A_{57}) - G_2$$

III. MOMENT INPUT-OUTPUT RELATIONSHIP

Equation (H-156) is an expression for F_{23F} as a function of the moment M_{1n} and the centrifugal forces Q_1 and Q_2 , when both meshes no. 1 and no. 2 are in the round on flat phase of motion. This expression for F_{23F} is now equated to equation (H-214). The result is solved for F_{34F}

$$F_{34F} = \frac{C_{21}C_{29}}{C_{15}C_{19}C_{27}} (M_{1n} - Q_1C_{14}) - Q_2 \frac{C_{20}C_{29}}{C_{19}C_{27}} - Q_3 \frac{C_{28}}{C_{27}} \quad (H-215)$$

The above is now equated to equation (H-195) and the resulting expression is used to determine the equilibrant moment M_{o45} (for Case 5: FFF)

$$M_{o45} = M_{1n} \frac{C_{21}C_{26}C_{29}}{C_{15}C_{19}C_{27}} - Q_1 \frac{C_{14}C_{21}C_{26}C_{29}}{C_{15}C_{19}C_{27}} - Q_2 \frac{C_{20}C_{26}C_{29}}{C_{19}C_{27}} - Q_3 \frac{C_{26}C_{28}}{C_{27}} - Q_4C_{25} \quad (H-216)$$

f. CASE NO. 6: FFR

MOMENT INPUT-OUTPUT RELATIONSHIP

The moment input-output relationship for this contact combination can be assembled entirely from previously derived component relationships. As for case no. 4, mesh no. 1 is in the round on round phase while mesh no. 2 is in the round on flat phase. Therefore, equation (H-178), which relates the force F_{23F} to the input moment M_{in} , may be used. The input-output relationship of the gear and pinion set no. 3, i.e. the relationship between the forces F_{34F} and F_{23F} , is given by equation (H-214) of case no. 5. The force F_{34F} may be obtained from equation (H-195). This expression was also derived for a round on flat contact in case no. 5.

Thus, equation (H-178) is first set equal to equation (H-214) and the result is solved for the force F_{34F}

$$F_{34F} = \frac{c_{24}c_{29}}{c_{10}c_{22}c_{27}} (M_{in} - Q_1c_9) - Q_2 \frac{c_{23}c_{29}}{c_{22}c_{27}} - Q_3 \frac{c_{28}}{c_{27}} \quad (H-217)$$

The above expression is now set equal to equation (H-195).

This then allows the determination of the equilibrant moment

M_{046} for the present contact combination.

$$\begin{aligned}
 M_{046} = M_{1n} \frac{C_{24}C_{26}C_{29}}{C_{10}C_{22}C_{27}} &- Q_1 \frac{C_9C_{24}C_{26}C_{29}}{C_{10}C_{22}C_{27}} - Q_2 \frac{C_{23}C_{26}C_{29}}{C_{22}C_{27}} \\
 &- Q_3 \frac{C_{26}C_{28}}{C_{27}} - Q_4 C_{25}
 \end{aligned}
 \tag{H-218}$$

A. CASE NO. 7: FRR

For the present contact combination the expression for force F_{34F} may be taken over from equation (H-195) of case no. 5. The input-output relationship of gear and pinion set no. 3, which relates the forces F_{34F} and F_{23} , must be newly derived. The relationship between force F_{23} and the input moment M_{1n} is taken from case no. 1 in the form of equation (H-79).

I. FORCE AND MOMENT EQUILIBRIA OF GEAR AND PINION SET NO. 3

Figure H-12 gives the free body diagram of gear and pinion set no. 3. Mesh no. 3 is in the round on flat phase of contact, while mesh no. 2 is in the round on round one.

The forces of pinion no. 4 on gear no. 3 are equal to, but opposite in direction to those given by equations (H-181) and (H-182)

$$\bar{F}_{43F} = - F_{34F} \bar{n}_{NF3} \quad (H-219)$$

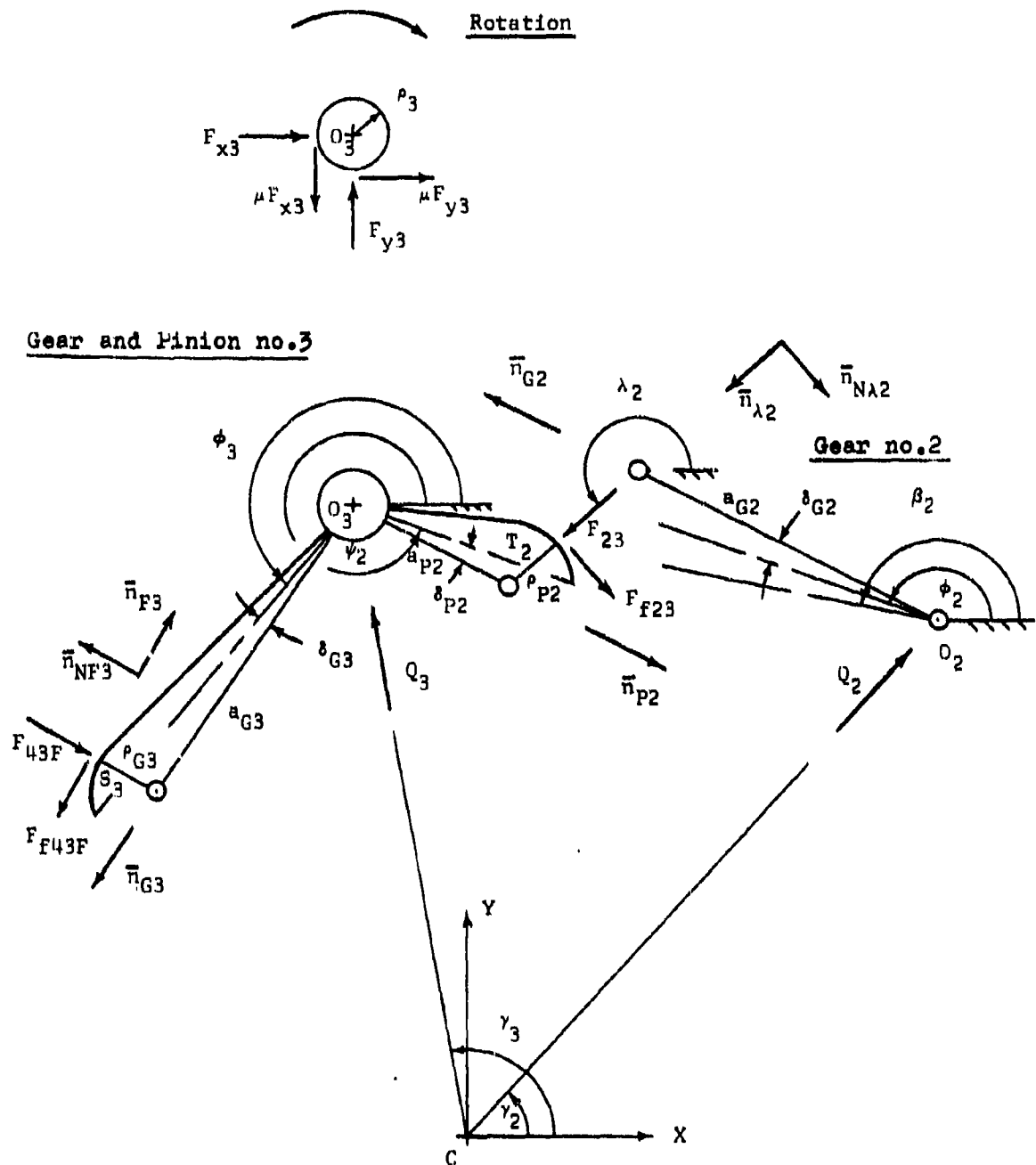


FIGURE H-12

FREE BODY DIAGRAM OF GEAR & PINION NO. 3

MESH NO. 3: ROUND ON FLAT

MESH NO. 2: ROUND ON ROUND

and

$$\bar{F}_{f43F} = -\mu_{s3F} F_{34F} \bar{n}_{F3} \quad (H-220)$$

The forces of gear no. 2 on pinion no. 3 are given by

$$\bar{F}_{23} = F_{23} \bar{n}_{\lambda 2} \quad (H-221)$$

and

$$\bar{F}_{f23} = \mu_{s2R} F_{23} \bar{n}_{N\lambda 2} \quad (H-222)$$

The pivot reactions are chosen in the same manner as before.

The centrifugal force \bar{Q}_3 was defined by equation (H-24).

Force equilibrium of the gear set requires

$$\begin{aligned} -F_{34F} \bar{n}_{NF3} - \mu_{s3F} F_{34F} \bar{n}_{F3} + F_{23} \bar{n}_{\lambda 2} + \mu_{s2R} F_{23} \bar{n}_{N\lambda 2} + \bar{Q}_3 + F_{x3} \bar{i} \\ + \mu_{Fy3} \bar{i} + F_{y3} \bar{j} - \mu_{Fx3} \bar{j} = 0 \end{aligned} \quad (H-223)$$

Moment equilibrium about point O_3 is given by

$$\begin{aligned} & \mu_{P3}(\tilde{F}_{x3} + \tilde{F}_{y3})\bar{k} + [a_{G3}\bar{n}_{G3} + \rho_{G3}\bar{n}_{NF3}] \times [-F_{34}\bar{n}_{NF3} - \mu_{S3}F_{34}\bar{n}_{F3}] \\ & + [a_{P2}\bar{n}_{P2} - \rho_{P2}\bar{n}_{\lambda 2}] \times [F_{23}\bar{n}_{\lambda 2} + \mu_{S2}F_{23}\bar{n}_{N\lambda 2}] = 0 \end{aligned} \quad (H-224)$$

Equation (H-223) gives the following component expressions

$$\begin{aligned} & F_{34}\sin(\psi_3 - \alpha_{P3}) - \mu_{S3}F_{34}\cos(\psi_3 - \alpha_{P3}) + Q_3\cos\gamma_3 + F_{x3} + \mu F_{y3} \\ & + F_{23}\cos\lambda_2 - \mu_{S2}F_{23}\sin\lambda_2 = 0 \end{aligned} \quad (H-225)$$

and

$$\begin{aligned} & -F_{34}\cos(\psi_3 - \alpha_{P3}) - \mu_{S3}F_{34}\sin(\psi_3 - \alpha_{P3}) + Q_3\sin\gamma_3 + F_{y3} - \mu F_{x3} \\ & + F_{23}\sin\lambda_2 + \mu_{S2}F_{23}\cos\lambda_2 = 0 \end{aligned} \quad (H-226)$$

The scalar form of the moment equation (H-224) becomes

$$\begin{aligned}
 & \mu P_3(\tilde{F}_{x3} + \tilde{F}_{y3}) + a_{G3}F_{34}[-\cos(\psi_3 + \delta_{G3} - \psi_3 + \alpha_{P3}) \\
 & + \mu s_{3F}\sin(\psi_3 + \delta_{G3} - \psi_3 + \alpha_{P3})] + \mu s_{3F}P_{G3}F_{34} \\
 & + a_{P2}F_{23}[-\sin(\psi_2 - \delta_{P2} - \lambda_2) + \mu s_{2R}\cos(\psi_2 - \delta_{P2} - \lambda_2)] \\
 & - \mu s_{2R}P_{P2}F_{23} = 0
 \end{aligned} \tag{H-227}$$

Simultaneous solution of the component equations (H-225) and (H-226) for F_{x3} and F_{y3} results in:

$$\begin{aligned}
 F_{x3} = \frac{1}{1 + \mu^2} \bigg\{ & F_{34}[-(1 + \mu^2 s_{3F})\sin(\psi_3 - \alpha_{P3}) + \mu(s_{3F} - 1)\cos(\psi_3 - \alpha_{P3})] \\
 & + F_{23} [\mu(1 + s_{2R})\sin\lambda_2 + (\mu^2 s_{2R} - 1)\cos\lambda_2] \\
 & + Q_3 [\mu\sin\gamma_3 - \cos\gamma_3] \bigg\}
 \end{aligned} \tag{H-228}$$

and

$$F_{y3} = \frac{1}{1 + \mu^2} \left\{ F_{34F} [\mu(s_{3F} - 1)\sin(\psi_3 - \alpha_{P3}) + (1 + \mu^2 s_{3F})\cos(\psi_3 - \alpha_{P3})] \right. \\ \left. + F_{23} [(\mu^2 s_{2R} - 1)\sin\lambda_2 - \mu(1 + s_{2R})\cos\lambda_2] \right. \\ \left. + Q_3 [-s\sin\gamma_3 - \mu\cos\gamma_3] \right\} \quad (H-229)$$

The sum $\tilde{F}_{x3} + \tilde{F}_{y3}$ in equation (H-227) is now made up from equations (H-228) and (H-229) in the sense of equation (A-3b)

$$\tilde{F}_{x3} + \tilde{F}_{y3} = F_{34F}A_{59} + F_{23}A_{60} + Q_3A_{61} + F_{34F}A_{62} + F_{23}A_{63} + Q_3A_{64} \quad (H-230)$$

where

$$A_{59} = \left| \frac{-(1 + \mu^2 s_{3F})\sin(\psi_3 - \alpha_{P3}) + \mu(s_{3F} - 1)\cos(\psi_3 - \alpha_{P3})}{1 + \mu^2} \right| \quad (H-231)$$

$$A_{60} = \left| \frac{\mu(1 + s_{2R})\sin\lambda_2 + (\mu^2 s_{2R} - 1)\cos\lambda_2}{1 + \mu^2} \right| \quad (H-232)$$

$$A_{61} = \left| \frac{\mu s\sin\gamma_3 - \cos\gamma_3}{1 + \mu^2} \right| \quad (H-233)$$

$$A_{62} = \left| \frac{\mu(a_{3F} - 1)\sin(\psi_3 - \alpha_{P3}) + (1 + \mu^2 a_{3F})\cos(\psi_3 - \alpha_{P3})}{1 + \mu^2} \right| \quad (H-234)$$

$$A_{63} = \left| \frac{(\mu^2 a_{2R} - 1)\sin\lambda_2 - \mu(1 + a_{2R})\cos\lambda_2}{1 + \mu^2} \right| \quad (H-235)$$

$$A_{64} = \left| \frac{-\sin\gamma_3 - \mu\cos\gamma_3}{1 + \mu^2} \right| \quad (H-236)$$

Equation (H-230) is now substituted into the moment equation (H-227)

and the resulting expression is solved for F_{23}

$$F_{23} = \frac{-F_{34}C_{30} - Q_3C_{31}}{C_{32}} \quad (H-237)$$

where

$$C_{30} = \mu P_3(A_{59} + A_{62}) - a_{Q3}[\cos(\psi_3 + \delta_{Q3} - \psi_3 + \alpha_{P3}) \\ - \mu a_{3F}\sin(\psi_3 + \delta_{Q3} - \psi_3 + \alpha_{P3})] + \mu a_{3F}P_{Q3}$$

$$C_{31} = \mu P_3(A_{61} + A_{64})$$

$$C_{32} = \mu^p_3(A_{60} + A_{63}) - a_{P2}[\sin(\psi_2 - \delta_{P2} - \lambda_2) - \mu^s_{2R}\cos(\psi_2 - \delta_{P2} - \lambda_2)]$$

$$- \mu^s_{2R}P_2$$

II. MOMENT INPUT-OUTPUT RELATIONSHIP

Equation (H-79), which gives the force F_{23} in terms of M_{1n} , Q_1 and Q_2 for the appropriate contact combinations, is now set equal to equation (H-237). Subsequently, one finds the following formulation for F_{34F} :

$$F_{34F} = \frac{C_{8C32}}{C_{6C10C30}} (M_{1n} - Q_1 C_9) - Q_2 \frac{C_{7C32}}{C_{6C30}} - Q_3 \frac{C_{31}}{C_{30}} \quad (H-238)$$

The above expression is now set equal to equation (H-195) which gives F_{34F} in terms of M_{04} and Q_4 . The determination of the equilibrant moment M_{047} (for case 7: FRR) is now possible. Thus,

$$M_{047} = M_{1n} \frac{c_8^c c_{26}^c c_{32}^c}{c_6^c c_{10}^c c_{30}^c} - q_1 \frac{c_8^c c_9^c c_{26}^c c_{32}^c}{c_6^c c_{10}^c c_{30}^c} - q_2 \frac{c_7^c c_{26}^c c_{32}^c}{c_6^c c_{30}^c}$$

$$- q_3 \frac{c_{26}^c c_{31}^c}{c_{30}^c} - q_4 c_{25}^c$$

(H-239)

h. CASE NO. 8: FRF

MOMENT INPUT-OUTPUT RELATIONSHIP

The input-output relationship for this contact combination can also be assembled entirely from existing expressions. With mesh no. 2 in the round on round phase of contact and mesh no. 1 in the round on flat one, the relationship between force F_{23} and the moment M_{1n} is that of case no. 2. Equation (H-116) is applicable. The input-output relationship of gear and pinion set no. 3, which relates F_{34F} to F_{23} , was derived for case no. 7 and is given by equation (H-237). Finally, with mesh no. 3 in the round on flat phase, one uses equation (H-195) for the relationship between force F_{34F} and moment M_{o4} . Thus, equation (H-116) is first set equal to equation (H-237) to obtain an expression for force F_{34F}

$$F_{34F} = \frac{c_{13}c_{32}}{c_{11}c_{15}c_{30}} (M_{1n} - q_1 c_{14}) - q_2 \frac{c_{12}c_{32}}{c_{11}c_{30}} - q_3 \frac{c_{31}}{c_{30}} \quad (H-240)$$

The above expression is now set equal to equation (H-195). This allows the determination of M_{048} (for case 8: FRF)

$$\begin{aligned}
 M_{048} = & M_{1n} \frac{C_{13}C_{26}C_{32}}{C_{11}C_{15}C_{30}} - Q_1 \frac{C_{13}C_{14}C_{26}C_{32}}{C_{11}C_{15}C_{30}} - Q_2 \frac{C_{12}C_{26}C_{32}}{C_{11}C_{30}} \\
 & - Q_3 \frac{C_{26}C_{31}}{C_{30}} - Q_4 C_{25} \quad (H-241)
 \end{aligned}$$

2. INPUT-OUTPUT ANALYSIS OF TWO STEP-UP GEAR TRAIN

The following gives derivations for the moment input-output relationships associated with the four possible contact combinations of a two step-up gear train. (See Table H-2).

a. CASE NO. 1: RR

For this contact combination, the relationship between the equilibrant moment M_{o3} and force F_{23} , both acting on pinion no. 3, must first be newly obtained. The relationships between forces F_{23} and F_{12} of gear and pinion set no. 2, as well as between force F_{12} and input moment M_{1n} of gear no. 1, may be taken from case no. 1 of the three step-up gear train analysis. Equations (H-61) and (H-78), respectively, are applicable.

I. FORCE AND MOMENT EQUILIBRIA OF PINION NO. 3

Figure H-13 shows a schematic free body diagram of pinion no. 3 in the round on round phase of contact. The equilibrant

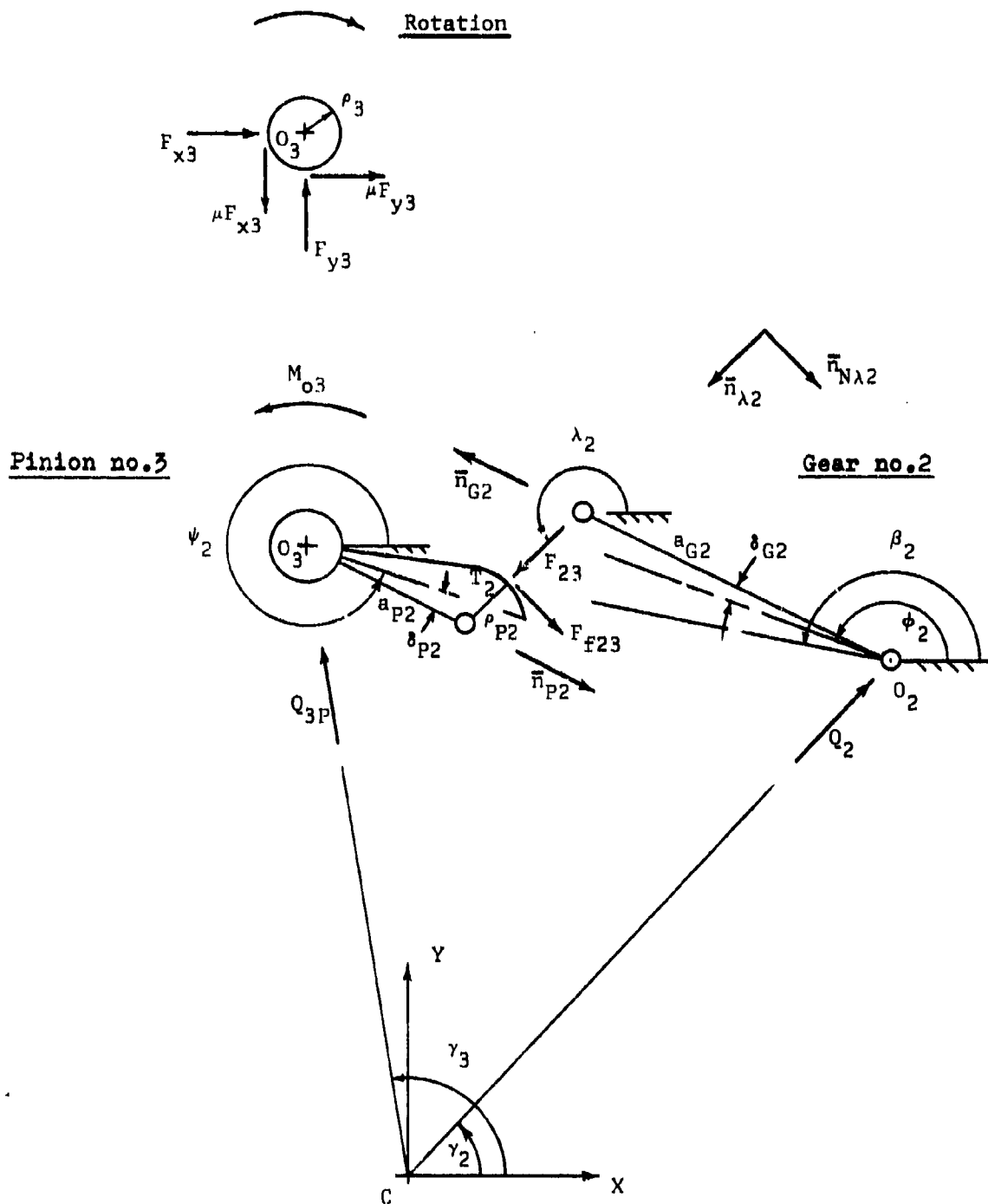


FIGURE H-13

FREE BODY DIAGRAM OF PINION NO. 3
MESH NO. 2: ROUND ON ROUND

moment M_{o3} acts in the direction opposite to the clockwise rotation of the pinion. The normal contact force of gear no. 2 on pinion no. 3 is given by

$$\bar{F}_{23} = F_{23} \bar{n}_{\lambda 2} \quad (H-242)$$

The associated friction force becomes

$$\bar{F}_{f23} = \mu_{s2R} F_{23} \bar{n}_{\lambda 2} \quad (H-243)$$

The pivot reactions are chosen in the usual manner.

The centrifugal force \bar{Q}_{3p} is now due to the mass m_{3p} of the pinion alone, i.e.,

$$\bar{Q}_{3p} = Q_{3p} (\cos \gamma_3 \bar{i} + \sin \gamma_3 \bar{j}) \quad (H-244)$$

where

$$Q_{3p} = m_{3p} r_3 \omega^2 \quad (H-245)$$

Force equilibrium of the pinion is assured by

$$F_{23}\bar{n}_{\lambda 2} + \mu s_{2R}F_{23}\bar{n}_{N\lambda 2} + F_{x3}\bar{i} + \mu F_{y3}\bar{i} + F_{y3}\bar{j} - \mu F_{x3}\bar{j} + \bar{Q}_{3P} = 0$$

(H-246)

Moment equilibrium about point O_3 is given by

$$\mu \rho_3(\tilde{F}_{x3} + \tilde{F}_{y3})\bar{k} + M_{O3}\bar{k} + [a_{P2}\bar{n}_{P2} - \rho_{P2}\bar{n}_{\lambda 2}] \times [F_{23}\bar{n}_{\lambda 2} + \mu s_{2R}F_{23}\bar{n}_{N\lambda 2}]$$

$$= 0$$

(H-247)

Equation (H-246) gives the following component expressions

$$F_{23}\cos\lambda_2 - \mu s_{2R}F_{23}\sin\lambda_2 + F_{x3} + \mu F_{y3} + Q_{3P}\cos\gamma_3 = 0 \quad (H-248)$$

and

$$F_{23}\sin\lambda_2 + \mu s_{2R}F_{23}\cos\lambda_2 + F_{y3} - \mu F_{x3} + Q_{3P}\sin\gamma_3 = 0 \quad (H-249)$$

The scalar form of the moment equation (H-247) becomes

$$\begin{aligned} \mu^2(\tilde{F}_{x3} + \tilde{F}_{y3}) + M_{03} - \mu s_{2R} p_{2R} F_{23} + s_{2R} F_{23} [-\sin(\psi_2 - \delta_{p2} - \lambda_2) \\ + \mu s_{2R} \cos(\psi_2 - \delta_{p2} - \lambda_2)] = 0 \end{aligned} \quad (H-250)$$

Simultaneous solution of equations (H-248) and (H-249) for the forces F_{x3} and F_{y3} gives

$$\begin{aligned} F_{x3} = \frac{1}{1 + \mu^2} \left\{ F_{23} [\mu(1 + s_{2R}) \sin \lambda_2 + (\mu^2 s_{2R} - 1) \cos \lambda_2] \right. \\ \left. + Q_{3P} [\mu \sin \gamma_3 - \cos \gamma_3] \right\} \end{aligned} \quad (H-251)$$

and

$$\begin{aligned} F_{y3} = \frac{1}{1 + \mu^2} \left\{ F_{23} [(\mu^2 s_{2R} - 1) \sin \lambda_2 - \mu(1 + s_{2R}) \cos \lambda_2] \right. \\ \left. + Q_{3P} [-\sin \gamma_3 - \mu \cos \gamma_3] \right\} \end{aligned} \quad (H-252)$$

The sum $\tilde{F}_{x3} + \tilde{F}_{y3}$ of equation (H-250) is now made up from equations (H-251) and (H-252) in the sense of equation (A-3b)

$$\tilde{F}_{x3} + \tilde{F}_{y3} = F_{23}A_{65} + Q_{3P}A_{66} + F_{23}A_{67} + Q_{3P}A_{68} \quad (H-253)$$

where

$$A_{65} = \left| \frac{\mu(1 + s_{2R})\sin\lambda_2 + (\mu^2 s_{2R} - 1)\cos\lambda_2}{1 + \mu^2} \right| \quad (H-254)$$

$$A_{66} = \left| \frac{\mu\sin\gamma_3 - \cos\gamma_3}{1 + \mu^2} \right| \quad (H-255)$$

$$A_{67} = \left| \frac{(\mu^2 s_{2R} - 1)\sin\lambda_2 - \mu(1 + s_{2R})\cos\lambda_2}{1 + \mu^2} \right| \quad (H-256)$$

$$A_{68} = \left| \frac{-\sin\gamma_3 - \mu\cos\gamma_3}{1 + \mu^2} \right| \quad (H-257)$$

Equation (H-253) is now substituted into the moment equation (H-250) and the result is solved for F_{23}

$$F_{23} = \frac{-M_{03} - Q_{3P}C_{33}}{C_{34}} \quad (H-258)$$

where

$$C_{33} = \mu p_3 (A_{66} + A_{68})$$

$$C_{34} = \mu p_3 (A_{65} + A_{67}) - \mu s_{2R} p_2$$

$$+ s_{P2} [\mu s_{2R} \cos(\psi_2 - \delta_{P2} - \lambda_2) - \sin(\psi_2 - \delta_{P2} - \lambda_2)]$$

II. MOMENT INPUT-OUTPUT RELATIONSHIP

In the derivation for case 1 of the three step-up gear train it was shown that if one sets equations (H-61) and (H-78) equal to each other, one obtains the following relationship [i.e., equation (H-79)] between force F_{23} and the input moment M_{1n} :

$$F_{23} = \frac{-c_8}{c_6 c_{10}} (M_{1n} - Q_1 c_9) + Q_2 \frac{c_7}{c_6} \quad (\text{H-259})$$

The above expression is now set equal to equation (H-258), and the result is solved for the equilibrant moment M_{o31} (for case 1: RR)

$$M_{o31} = M_{1n} \frac{c_8 c_{34}}{c_6 c_{10}} - Q_1 \frac{c_8 c_9 c_{34}}{c_6 c_{10}} - Q_2 \frac{c_7 c_{34}}{c_6} - Q_3 P c_{33} \quad (\text{H-260})$$

b. CASE NO. 2: RF

MOMENT INPUT-OUTPUT RELATIONSHIP

The moment equation for the present case, in which mesh no. 1 is in the round on flat phase and mesh no. 2 in the round on round one, may be derived entirely from existing relationships. Equation (H-116) gives an expression for the force F_{23} in terms of the input moment M_{1n} and the centrifugal forces Q_1 and Q_2 for the present combination of contacts in both meshes. When this expression, from case no. 2 of the three step-up gear train, is set equal to equation (H-259) of case no. 1 of the two step-up gear train, one obtains for M_{032} (case no. 2: RF)

$$M_{032} = M_{1n} \frac{C_{13}C_{34}}{C_{11}C_{15}} - Q_1 \frac{C_{13}C_{14}C_{34}}{C_{11}C_{15}} - Q_2 \frac{C_{12}C_{34}}{C_{11}} - Q_3P_{33}$$

(H-261)

c. CASE NO. 3: FF

For this contact combination, where both meshes no. 1 and no.2 are in the round on flat phase, the relationship between the equilibrant moment M_{03} and the normal contact force F_{23F} , both acting on pinion no. 3, must first be determined. The resulting expression in F_{23F} can then be set equal to the relationship between F_{23F} and the input moment M_{1n} , which is given by equation (H-156), and which was derived in conjunction with case no. 3 of the three step-up gear train.

I. FORCE AND MOMENT EQUILIBRIA OF PINION NO. 3

Figure H-14 shows the free body diagram of pinion no. 3 in the round on flat phase of contact. Again, the equilibrant moment M_{03} acts in a counter-clockwise direction. The normal force F_{23F} of gear no. 2 on pinion no. 3 is given by

$$\bar{F}_{23F} = - F_{23F} \bar{n}_{NF2} \quad (H-262)$$

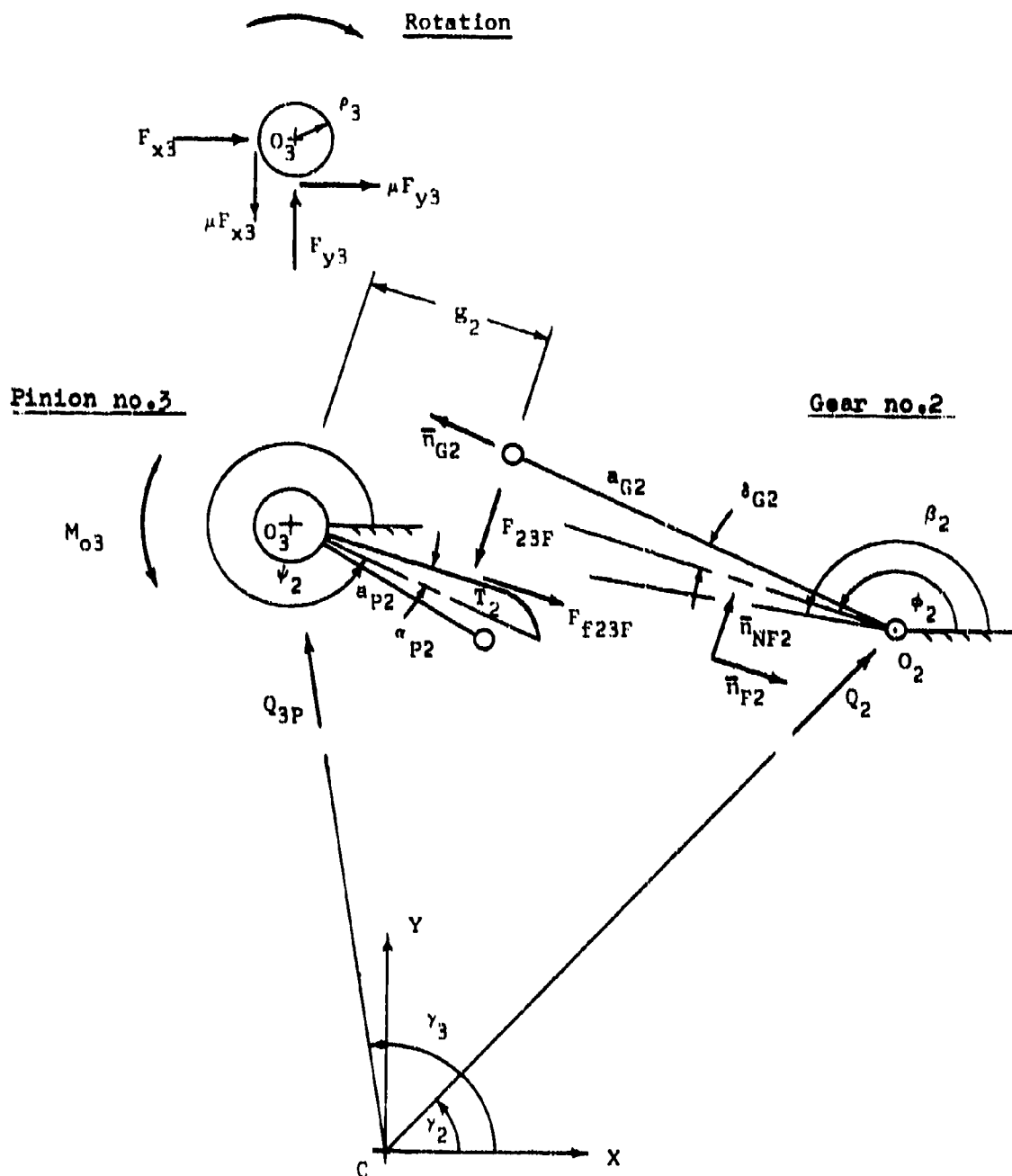


FIGURE H-14

FREE BODY DIAGRAM OF PINION NO. 3
MESH NO. 2: ROUND ON FLAT

The associated friction force of gear no. 2 on pinion no. 3 becomes

$$\bar{F}_{f23F} = \mu_{s2F} F_{23F} \bar{n}_{F2} \quad (H-263)$$

The pivot reactions and pivot friction forces are chosen in the usual manner. The centrifugal force \bar{Q}_{3P} was given previously by equation (H-244).

The force equilibrium expression becomes

$$-F_{23F} \bar{n}_{NF2} + \mu_{s2F} F_{23F} \bar{n}_{F2} + F_{x3} \bar{i} + \mu_{Fy3} \bar{i} + F_{y3} \bar{j} - \mu_{Fx3} \bar{j} + \bar{Q}_{3P} = 0 \quad (H-264)$$

Moment equilibrium about point O_3 is assured by

$$\mu_{P3} (\bar{F}_{x3} + \bar{F}_{y3}) \bar{k} + M_{O3} \bar{k} + s_2 \bar{n}_{F2} \times (-) F_{23F} \bar{n}_{NF2} = 0 \quad (H-265)$$

As always before, the friction force F_{f23F} exerts no moment about point O_3 .

Equation (H-264) gives the following component expressions

$$F_{23}\sin(\psi_2 + \alpha_{p2}) + \mu s_{2F}F_{23}\cos(\psi_2 + \alpha_{p2}) + F_{x3} + \mu F_{y3} + Q_{3p}\cos\gamma_3 = 0 \quad (H-266)$$

and

$$-F_{23}\cos(\psi_2 + \alpha_{p2}) + \mu s_{2F}F_{23}\sin(\psi_2 + \alpha_{p2}) + F_{y3} - \mu F_{x3} + Q_{3p}\sin\gamma_3 = 0 \quad (H-267)$$

The scalar form of the moment equation (H-265) is given by

$$\mu p_3(\tilde{F}_{x3} + \tilde{F}_{y3}) + M_{o3} - s_{2F}F_{23}r = 0 \quad (H-268)$$

Simultaneous solution of equations (H-266) and (H-267) for F_{x3} and F_{y3} leads to

$$F_{x3} = \frac{1}{1 + \mu^2} \left\{ F_{23}r [(\mu^2 s_{2F} - 1)\sin(\psi_2 + \alpha_{p2}) - \mu(1 + s_{2F})\cos(\psi_2 + \alpha_{p2})] + Q_{3p}[\mu\sin\gamma_3 - \cos\gamma_3] \right\} \quad (H-269)$$

$$F_{y3} = \frac{1}{1 + \mu^2} \left\{ F_{23F} [-\mu(1 + s_{2F})\sin(\psi_2 + \alpha_{P2}) + (1 - \mu^2 s_{2F})\cos(\psi_2 + \alpha_{P2})] \right. \\ \left. + Q_{3P} [-\sin\gamma_3 - \mu\cos\gamma_3] \right\} \quad (H-270)$$

The sum $\tilde{F}_{x3} + \tilde{F}_{y3}$ of equation (H-268) is now made up of equations (H-269) and (H-270) in the sense of equation (A-3b)

$$\tilde{F}_{x3} + \tilde{F}_{y3} = F_{23F}A_{69} + Q_{3P}A_{70} + F_{23F}A_{71} + Q_{3P}A_{72} \quad (H-271)$$

where

$$A_{69} = \left| \frac{(\mu^2 s_{2F} - 1)\sin(\psi_2 + \alpha_{P2}) - \mu(1 + s_{2F})\cos(\psi_2 + \alpha_{P2})}{1 + \mu^2} \right| \quad (H-272)$$

$$A_{70} = \left| \frac{\mu\sin\gamma_3 - \cos\gamma_3}{1 + \mu^2} \right| \quad (H-273)$$

$$A_{71} = \left| \frac{-\mu(1 + s_{2F})\sin(\psi_2 + \alpha_{P2}) + (1 - \mu^2 s_{2F})\cos(\psi_2 + \alpha_{P2})}{1 + \mu^2} \right| \quad (H-274)$$

$$A_{72} = \left| \frac{-\sin\gamma_3 - \mu\cos\gamma_3}{1 + \mu^2} \right| \quad (H-275)$$

Equation (H-271) is now substituted into the moment equation (H-268), and the result is solved for F_{23F}

$$F_{23F} = \frac{-M_{03} - Q_{3P}C_{35}}{C_{36}} \quad (H-276)$$

where

$$C_{35} = \mu P_3(A_{70} + A_{72})$$

$$C_{36} = \mu P_3(A_{69} + A_{71}) - S_2$$

II. MOMENT INPUT-OUTPUT RELATIONSHIP

The moment input-output relationship for the present case is obtained, as stated earlier, by setting equation (H-276) equal to equation (H-156) and solving the resulting expression for the equilibrant moment M_{033} (case no. 3: FF)

$$M_{033} = M_{1n} \frac{C_{21}C_{36}}{C_{15}C_{19}} - Q_1 \frac{C_{14}C_{21}C_{36}}{C_{15}C_{19}} - Q_2 \frac{C_{20}C_{36}}{C_{19}} - Q_{3P}C_{35} \quad (H-277)$$

d. CASE NO. 4: FR

MOMENT INPUT-OUTPUT RELATIONSHIP

The moment input-output relationship for this case, where mesh no. 1 is in round on round contact while mesh no. 2 is in the round on flat phase, may also be derived entirely by assembling existing relationships.

Equation (H-276), of the previous section, gives force F_{23F} in terms of the equilibrant moment M_{o3} when mesh no. 2 is in the round on flat phase. Equation (H-178), derived for case no. 4 (RFR) of the three step-up gear train, relates this force F_{23F} to the input moment M_{in} .

Thus, one first sets equations (H-178) and (H-276) equal to each other and then solves the result for M_{o34} (case 4: FR)

$$M_{o34} = M_{in} \frac{C_{24}C_{36}}{C_{10}C_{22}} - Q_1 \frac{C_9C_{24}C_{36}}{C_{10}C_{22}} - Q_2 \frac{C_{23}C_{36}}{C_{22}} - Q_{3P}C_{35}$$

(H-278)

APPENDIX I
COMPUTER MODELS FOR THREE AND TWO STEP-UP GEAR TRAINS
WITH CLOCK TEETH OPERATING IN A SPIN ENVIRONMENT

The following appendix contains descriptions, listings and sample outputs of the computer models relating to step-up gear trains containing clock (ogival) gear teeth:

1. Program CLOCK 3: Point and cycle efficiencies for three pass clock (ogival) step-up gear train in spin environment.
2. Program CLOCK 4: Point and cycle efficiencies for two pass clock (ogival) step-up gear train in spin environment.

The relevant background, the input parameters, the manner of the computations and the form of the output of each program are discussed in detail. The program proper forms the last part of each section.

1. Program CLOCK 3: Point and Cycle Efficiencies for Three
Pass Clock (Ogival) Step-Up Gear Train
in Spin Environment

The kinematics of program CLOCK 3 is based on the work in Appendix G, while the moment input-output relationships are derived in section 1 of Appendix H. The nomenclature of the program is chosen to coincide as much as possible with the above appendices. It is to be noted that, even though the fuze related geometry produces different expressions for the various meshes, the kinematic computations of the individual meshes are very similar to those shown in CLOCK 1 in Appendix F for the single mesh in the standard position. It is also assumed that all three meshes will have been tested by program CLOCK 1 for their geometric suitability, i.e. whether there is enough room for tip radii.

a. Input Parameters (see Program CLOCK 3, below)

The following parameters represent the input data for the program (for explanations and nomenclature, see sections 1 and 2 of Appendix F, as well as section 3 of Appendix C):

MU, coefficient of friction, as before

RPM, spin velocity

CAPRP1, CAPRP2, CAPRP3, RP2, RP3, RP4, pitch radii of gears and
pinions with nomenclature
of Fig. G-1

RHOG1, RHOG2, RHOG3, RHOP1, RHOP2, RHOP3, radii of curvature of circular arc portion of gear and pinion teeth

$ACG1, ACG2, ACG3^* = a_{CG1}$, distance from the center of rotation of the gear of the 1th mesh to the center of curvature of the circular arc portion of the gear tooth. (Unless otherwise noted, this and all following numbering schemes refer to those associated with the mesh mechanics as given in the text of Appendices G and H.)

$ACP1, ACP2, ACP3 = a_{CP1}$, distance from the center of rotation of the pinion of the 1th mesh to the center of curvature of the circular arc portion of the pinion tooth

$R1, R2, R3, R4 = R_1$ (nomenclature of Fig. G-1)

$TG1, TG2, TG3, TP1, TP2, TP3$, maximum thickness of gear and pinion teeth (mesh nomenclature)

$NG1, NG2, NG3, NP2, NP3, NP4$, numbers of teeth in various gears and pinions (nomenclature of Fig. G-1)

$RHO1, RHO2, RHO3, RHO4$, gear and/or pinion pivot radii (nomenclature of Fig. G-1)

$M1, M2, M3, M4$, masses of gear and/or pinion combinations

MD, see program INVOL 3

*Since many parts of the computer program were written before the nomenclature for these distances was changed in the report from a_{CG1} and a_{CP1} to a_{G1} and a_{P1} , there is a certain discrepancy between the program and the report.

K, range divisor

PHDOT1 = -1, all velocity computations are based on this value.

The input motion in the fuze gearing model is negative (see Fig. (G-1)).

b. Computations (see also COMMENT cards in program)

I. Computation of Gear Tooth Parameters

The tooth parameters of the gears and pinions of all three meshes are first computed. These computations are essentially the same as those shown in program CLOCK 1 for a single mesh. Certain parameters are omitted because they have been checked separately by using CLOCK 1 and are not required for the kinematics of CLOCK 3.

In addition, the pivot to pivot distances B1, B2 and B3 are obtained.

II. Computation of MIN, GAMMAS and BETAS

To begin with, the program computes the input moment

$$MIN = M_{in} = md\omega^2 \quad (I-1)$$

Subsequently, the angles $\gamma_2, \gamma_3, \gamma_4$ and $\beta_1, \beta_2, \beta_3$ are established according to the expressions of section 6b of Appendix A.

III. Computation of Other Parameters

The angles $\Delta\phi_1$ and $\Delta\psi_1$ between the centerlines of adjacent gear and pinion teeth, respectively, are determined in this

section of the computations. In addition, the lengths L_1 are found (see eqs. (G-7), (G-53) and (G-88)). Finally, the centrifugal forces Q_1 , Q_2 , Q_3 and Q_4 are computed according to eqs. (H-65), (H-46), (H-25) and (H-6), respectively.

IV. Preliminary Computations for Mesh 1

A. Determination of Transition Angle

The primary consideration for determining the transition angles in the fuze related clock gear meshes is identical with that used in Appendix F. The transition angle ψ_T is established as that angle for which, depending upon whether the input angle φ has counterclockwise or clockwise motion, a small increase or decrease in φ , respectively, will cause the associated value of g to become smaller than its transition value f_p . Since the gear of mesh 1 turns in a clockwise direction, the above increment of φ will be negative.

The program uses this criterion in the following manner:

(a) Transition angles ψ_{1T1} and ψ_{1T2} are computed according to eq. (G-39).

(b) The subroutine TRANS1 (which is valid for meshes in which the input gear has clockwise rotation, as is the case also for mesh 3) is called, and the angle φ_{1T1} (PHIT), which is associated with ψ_{1T1} , is computed with the help of eqs. (G-40) and (G-41).

(c) The angle φ is made slightly smaller than φ_{1T1} to produce the angle PHINEXT, and eq. (G-29) is used to find the associated angle PSINEX. Since there are two such angles, the

subroutine selects the one which is closest in value to the transition angle ψ_{1T1} . Subsequently, the associated value of g_{11} is computed according to eq. (G-27).

(d) Steps (b) and (c) are then repeated identically for the second transition angle ψ_{1T2} . This results in the determination of g_{12} .

(e) Control returns to the main program, and that value of ψ_{1T} is chosen for which the associated value of g_1 is smaller than f_{p1} .

For checking, a subsidiary test, which is similar to the one shown in Appendix F, is added to the program. It is based on the idea that, for the correct transition angle ψ_{1T} , the line representing the flat portion of the pinion will make a smaller angle with the centerline O_1O_2 than will be the case for the incorrect one. TEST11 and TEST12 find these angles with the help of the expressions shown below. These expressions hold for all values of β_1 and make use of a new variable ψ_{test} , which had to be introduced since the tests require that the transition angles be expressed in a range between -180° and $+180^\circ$. Thus,

For $0^\circ < \psi_{test} < 180^\circ$

$$TEST11 = |\pi - \beta_1 + \psi_{test} - \alpha_{p1}| \quad (I-2)$$

For $-180^\circ < \psi_{test} < 0^\circ$

$$TEST12 = |\pi + \beta_1 - (\psi_{test} + 2\pi - \alpha_{p1})| \quad (I-3)$$

To determine the angle ψ_{test} , let

$$\psi_{\text{test}} = \psi_{1T} \text{ if } -180^\circ < \psi_{1T} < 180^\circ \quad (\text{I-4})$$

$$\psi_{\text{test}} = \psi_{1T} + 2\pi \text{ if } \psi_{1T} < -180^\circ \quad (\text{I-5})$$

$$\psi_{\text{test}} = \psi_{1T} - 2\pi \text{ if } \psi_{1T} > 180^\circ \quad (\text{I-6})$$

B. Determination of Correct Sign for Round on Flat Regime

The sign preceding the square root in eq. (G-29), for the round on flat regime, is determined with the help of φ_{1T} . The condition yielding that angle ψ_{1F} which is closest to the angle ψ_{1T} governs. The variable SIGNIF is used for the sign in question.

C. Computation of Final and Initial Values of φ_1 and ψ_1

The final and initial values of the gear and pinion angles φ_1 and ψ_1 , respectively, are found by continuously evaluating the round on flat regime eq. (G-29), using the previously determined value of SIGNIF, and simultaneously checking the contact condition for the subsequent set of teeth as given by eq. (G-46). This loop is initiated at the transition angle φ_{1T} , and it is terminated when the condition of eq. (G-46) is met. This allows the determination of the angles PHILF and PSILFF, at which the first set of teeth loses contact, as well as of the angles PHILI and PSILI at which the second set of teeth simultaneously comes into engagement. The initial engagement angles PHILI and PSILI are obtained by adding φ_1 to the "loss of contact" angle PHILF

and by subtracting $\Delta\psi_1$ from the "loss of contact" angle PSI1FF .

D. Determination of Correct Sign for Round on Round Regime

Eq. (G-12) is used to determine the angle ψ_1 , while the gear and pinion are in the round on round regime. The correct sign for this expression is obtained by comparing the value ψ_1 , as computed with PHI1I , with the value for PSI1I . SIGN1R is the variable used for the desired sign.

V. Preliminary Computations for Mesh 2

A. Determination of Transition Angle

The primary criterion for determining the transition angle is again similar to that used in Appendix F and described earlier for mesh 1.

(a) Transition angles ψ_{2T1} and ψ_{2T2} are computed according to eq. (G-79).

(b) The subroutine TRANS2 , which is valid for meshes in which the input gear has counterclockwise rotation, is called, and the angle φ_{2T1} , which is associated with ψ_{2T1} is computed, with the help of eqs. (G-80) and (G-81).

(c) The angle φ_2 is made slightly larger than φ_{2T1} to produce the angle PHINEXT , and eq. (G-71) is used to find the associated output angle PSINEX . Since there are two such angles, the subroutine selects the one which is closest to the transition value ψ_{2T1} . Subsequently, the associated value of S_{21} is computed according to eq. (G-69).

(d) Steps (b) and (c) are then repeated identically for the second transition angle ψ_{2T2} . This results in the determination of g_{22} .

(e) Control returns to the main program, and that value of ψ_{2T} is chosen for which the associated value of g_2 is smaller than f_{p2} .

The procedure for the associated subsidiary test for the transition angle is similar to that for mesh 1 and is given by

For $0^\circ < \psi_{\text{test}} < 180^\circ$

$$\text{TEST21} = |\pi - \beta_2 + \psi_{\text{test}} + \alpha_{p2}| \quad (\text{I-7})$$

For $-180^\circ < \psi_{\text{test}} < 0^\circ$

$$\text{TEST22} = |\beta_2 + \pi - (\psi_{\text{test}} + 2\pi + \alpha_{p2})| \quad (\text{I-8})$$

To determine the angle ψ_{test} , let

$$\psi_{\text{test}} = \psi_{2T} \quad \text{if} \quad -180^\circ < \psi_{2T} < 180^\circ \quad (\text{I-9})$$

$$\psi_{\text{test}} = \psi_{2T} + 2\pi \quad \text{if} \quad \psi_{2T} < -180^\circ \quad (\text{I-10})$$

$$\psi_{\text{test}} = \psi_{2T} - 2\pi \quad \text{if} \quad \psi_{2T} > 180^\circ \quad (\text{I-11})$$

B. Determination of Correct Sign for Round on Flat Regime

The sign preceding the square root in eq. (G-71), for the round on flat regime, is determined with the help of ψ_{2T} . The condition yielding that angle ψ_{2F} which is closest to the angle ψ_{2T} governs. The variable SIGN2F is used for the sign in question.

C. Computation of Final and Initial Values of φ_2 and ψ_2

The final and initial values of the gear and pinion angles φ_2 and ψ_2 , respectively, are found by continuously evaluating the round on flat eq. (G-71), using the previously determined value of SIGN2F, and simultaneously checking the contact condition for the subsequent set of teeth, as given by eq. (G-86). This loop is initiated at the transition angle φ_{2T} and is terminated when the condition of eq. (G-86) is met. (Recall that in meshes 1 and 3 the driving gear turns clockwise, while in mesh 2 it turns in a counterclockwise direction.) This allows the determination of the two angles PHI2F and PSI2FF at which the first set of teeth loses contact as well as of the angles PHI2I and PSI2I at which the second set of teeth simultaneously comes into contact. The initial engagement angles PHI2I and PSI2I are obtained by subtracting $\Delta\varphi_2$ from the "loss of contact" angle PHI2F and by adding $\Delta\psi_2$ to the "loss of contact" angle PSI2FF.

D. Determination of Correct Sign for Round on Round Regime

Eq. (G-58) is used to determine the angle ψ_2 while the gear and pinion are in the round on round phase of motion. The correct sign for this expression is obtained by comparing the value of ψ_2 , as computed with PHI2I, with the previously obtained value for PSI2I. SIGN2R is the variable used for the desired sign.

VI. Preliminary Computations for Mesh 3

A. Determination of Transition Angle

The determination of the transition angles for mesh 3 runs along parallel lines to the one shown for mesh 1 since the driving gear also rotates in a clockwise direction. In all cases, the parameters of section 3 of Appendix G are used.

(a) Transition angles ψ_{3T1} and ψ_{3T2} are computed with the help of eq. (G-99).

(b) The subroutine TRANS1 determines the angle ψ_{3T1} , associated with ψ_{3T1} , according to eqs. (G-100) and (G-101).

(c) PHINEXT, which is now obtained by a decrease of the angle ψ_3 from ψ_{3T1} , serves as the input variable of eq. (G-94), and is used to determine PSINEX. Appropriate controls, as described before, determine the angle ψ_{3T1} . In addition, the associated value of g_{31} is computed with the help of eq. (G-95).

(d) Steps (b) and (c) are again repeated for the second transition angle ψ_{3T2} and g_{22} is determined.

(e) After control is returned to the main program, that value of ψ_{3T} is chosen for which the associated value of g_3 is smaller than f_{p3} .

The subsidiary test for the transition angles runs parallel to that described for mesh 1, i.e.,

For $0^\circ < \psi_{\text{test}} < 180^\circ$

$$\text{TEST31} = |\pi - \beta_3 + \psi_{\text{test}} - \alpha_{p3}| \quad (\text{I-12})$$

For $-180^\circ < \psi_{\text{test}} < 0^\circ$

$$\text{TEST32} = |\pi + \beta_3 - (\psi_{\text{test}} + 2\pi - \alpha_{p3})| \quad (\text{I-13})$$

To determine the angle ψ_{test} , let

$$\psi_{\text{test}} = \psi_{3T} \text{ if } -180^\circ < \psi_{3T} < 180^\circ \quad (\text{I-14})$$

$$\psi_{\text{test}} = \psi_{3T} + 2\pi \text{ if } \psi_{3T} < -180^\circ \quad (\text{I-15})$$

$$\psi_{\text{test}} = \psi_{3T} - 2\pi \text{ if } \psi_{3T} > 180^\circ \quad (\text{I-16})$$

B. Determination of Correct Sign for Round on Flat Regime

The sign preceding the square root in eq. (G-94), for the round on flat regime, is determined with the help of the angle φ_{3T} . The condition yielding that angle ψ_{3F} which is closest to the angle ψ_{3T} will govern. The variable SIGN3F is used for the sign in question.

C. Computation of Final and Initial Values of φ_3 and ψ_3

The final and initial values of the gear and pinion angles φ_3 and ψ_3 , respectively, are found by continuously evaluating the round on flat regime eq. (G-94), using the previously determined value of SIGN3F, and simultaneously checking the contact condition for the subsequent set of teeth, as given by eq. (G-102). This loop is initiated at the transition angle φ_{3T} , and it is terminated when the condition of eq. (G-102) is met. This allows the determination of the two angles PHI3F and PSI3FF at which the first set of teeth loses contact as well

as the angles PHI3I and PSI3I at which the second set of teeth simultaneously comes into contact. The initial engagement angles PHI3I and PSI3I are obtained by adding $\Delta\phi_3$ to the "loss of contact" angle PHI3F and by subtracting $\Delta\phi_3$ from the "loss of contact" angle PSI3F .

D. Determination of Correct Sign for Round on Round Regime

Eq. (G-87) is used to determine the angle ϕ_3 while the gear and pinion are in the round on round phase of motion. The correct sign for this expression is obtained by comparing the value of ϕ_3 , as computed with PHI3I , with the previously obtained value for PSI3I . SIGN3R is the variable used for the desired sign.

VII. Gear Train Motion Model: Kinematics, Point and Cycle Efficiency

The simulation of the gear train model, which is necessary for the computation of both POINTEF and CYCLEFF , is found in a loop, starting with statement label no. 29 (card no. 458) and ending with card no. 812. The motions of the individual driving gears are initialized at their respective angles PHI1I , PHI2I and PHI3I . (This again is arbitrary.) The meshes will be in round on round contact until they reach their respective transition angles PHI1T , PHI2T and PHI3T . Once the transition angles are passed, the meshes will be in round on flat contact. These regimes continue until the final angles PHI1F , PHI2F and PHI3F are reached.

The increment DDPHI1 of the angle PHI1 of the input gear 1

is obtained from an adaptation of eqs. (A-211) and (A-213), in which tooth numbers, rather than base circle radii, are used. The increment $DDPHI2$ of gear 2 is related to the increment of the pinion angle $PSI1$. Similarly, the increment $DDPHI3$ is obtained with the help of the pinion angle $PSI2$.

While the motion of gear 1 is terminated when the angle $PHI1$ reaches the angle $PHI1F$ (or rather $PHI1F + DDPHI1$ for moment summation purposes), both gears 2 and 3 must be reset to their respective starting angles whenever their final angles $PHI2F$ and $PHI3F$ are reached.

The appropriate choice of moment equation depends upon which of the eight possible combinations of contact conditions, as indicated by Table H-1, is applicable.

The following discusses the kinematics of the individual meshes as well as the determination of the point and cycle efficiencies in greater detail.

A. Kinematics

(1) Mesh 1

Depending on whether $PHI1$ is larger or smaller than $PHI1T$, the parameters of the round on round or the round on flat regime are computed. (Recall that gear 1 turns in a clockwise direction.)

For the round on round phase, the following calculations are made:

ψ_1 , according to eq. (G-11), and with the help of the previously
 determined SIGN1R
 λ_1 , according to eqs. (G-13) and (G-14)
 $\dot{\psi}_1$, according to eq. (G-15)
 $V_{S1}/T1R$, according to eq. (G-20)
 $s1R$, according to eq. (H-1) as adapted to mesh 1

For the round on flat phase, the following calculations
 are made:

ψ_1 , according to eq. (G-29), and with the help of the previously
 determined SIGN1F
 $s1$, according to eq. (G-27)
 $\dot{\psi}_1$, according to eq. (G-30)
 $V_{S1}/T1F$, according to eq. (G-33)
 $s1F$, according to eq. (H-2) as adapted to mesh 1

(2) Mesh 2

The increment DDPHI2 for each round of computation is
 obtained with the help of the change in the angle ψ_1 between
 the present and the previous computation, i.e., as shown at
 statement label no. 31

$$DDPHI2 = PSI1 - PSI1P \quad (I-17)$$

For the first round of computations, the "previous" ψ_1 , i.e.,
 $PSI1P$, is equal to $PSI1I$.

It must be recalled that gear 2 rotates in a positive
 direction, and therefore, the angle ϕ_2 increases with continued

motion. The angle PHI2 is re-indexed to PHI2I once it becomes larger than PHI2F.

As for mesh 1, comparison with the transition angle decides whether the mesh is in the round on round or in the round on flat regime.

The following round on round parameters are calculated:

- ψ_2 , according to eq. (G-58), and with the help of the previously determined SIGN2R
- λ_2 , according to eqs. (G-59) and (G-60)

Note that the "input angular velocity" for mesh 2, i.e., $\dot{\psi}_2$, equals the momentary value of $\dot{\psi}_1$.

- $\dot{\psi}_2$, according to eq. (G-61)
- V_{S2}/T_{2R} , according to eq. (G-63)
- s_{2R} , according to eq. (H-1) as adapted to mesh 2

For the round on flat phase, the following calculations are made:

- ψ_2 , according to eq. (G-71), and with the help of the previously determined SIGN2F
- g_2 , according to eq. (G-69)

Again, $\dot{\psi}_2$ equals the momentary value of $\dot{\psi}_1$

- $\dot{\psi}_2$, according to eq. (G-72)
- V_{S2}/T_{2F} , according to eq. (G-74)
- s_{2F} , according to eq. (H-2) as adapted to mesh 2

(3) Mesh 3

The increment DDPHI3, for each round of computation, is obtained with the help of the change in the angle ψ_2 between the present and the previous computation, i.e., as shown at statement label no. 33:

$$\text{DDPHI3} = \text{PSI2} - \text{PSI2P} \quad (\text{I-18})$$

For the first round of computations, the "previous" ψ_2 , i.e., PSI2P, is equal to PSI2I.

Gear 3 rotates in a negative (clockwise) direction, and therefore, the angle φ_3 decreases with continued rotation. The angle PHI3, which represents this angle, is re-indexed to PHI3I once it becomes smaller than PHI3F.

As for meshes 1 and 2, comparison with the applicable transition angle decides whether the mesh is in the round on round or in the round on flat regime.

The following round on round parameters are calculated:

- ψ_3 , according to eq. (G-87), and with the help of the previously determined SIGN3R
- λ_3 , according to eqs. (G-89) and (G-90)

Note that the "input angular velocity" for mesh 3, i.e., $\dot{\psi}_3$, equals the momentary value of $\dot{\psi}_2$.

- $\dot{\psi}_3$, according to eq. (G-91)
- $V_{S3/T3R}$, according to eq. (G-92)
- s_{3R} , according to eq. (H-1) as adapted to mesh 3

For the round on flat phase, the following calculations are made:

ψ_3 , according to eq. (G-94), and with the help of the previously determined SIGN3F

s_3 , according to eq. (G-95)

Again, $\dot{\phi}_3$ is equal to the momentary value of $\dot{\psi}_2$.

$\dot{\psi}_3$, according to eq. (G-96)

V_{S3}/T_{3F} , according to eq. (G-97)

s_{3F} , according to eq. (H-2) as adapted to mesh 3

B. Moment Computations, Point and Cycle Efficiencies

Regardless of the combination of contact conditions, the point efficiency is computed according to eq. (3), i.e.,

$$\epsilon_p = \text{POINTEF} = K_{\text{ratio}} \frac{M_{o41}}{M_{1n}} \quad (\text{I-19})$$

where, with $\dot{\phi}_1 = -1$,

$$K_{\text{ratio}} = |\dot{\psi}_3| \quad (\text{I-20})$$

The cycle efficiency determination is based on eq. (C-10) in Appendix C, which represents an adaptation of eq. (4):

$$\epsilon_c = \frac{\Delta\phi_1 \Sigma \epsilon_p}{\phi_{1FIN} - \phi_{1IN}} \quad (\text{I-21})$$

(See page C-18.) The associated expression in the program, at statement label no. 45 becomes

$$\text{CYCLEFF} = -\text{MTOT} * \text{DDPHI1} / (\text{PHI1F} - \text{PHI1I})$$

(I-22)

where

$$\text{MTOT} = \text{MTOT} + \text{POINTEF}$$

(I-23)

The moment computations begin with the statement label no. 35 ,and initially consist of the determination of the variables A1 to A64 and C1 to C32 of section 1 of Appendix H. The governing contact combination (see also Table H-1) is determined with the help of the 8 moment control statements, which start with card no.737 . Once the appropriate combination is established, the program is directed to one of the 8 associated moment expressions. These expressions for M_{041} coincide in nomenclature with those given by eqs. (H-81), (H-118), (H-158), (H-180), (H-216), (H-218), (H-239) and (H-241). They are listed in the above order, beginning with statement label no. 36 and ending with statement label no. 43 .

In devising the control statements, the manner of rotation of the individual mesh input gears had to be taken into account. Thus:

For mesh 3:

Round on round (R) corresponds to

$$\text{PHI3I} > \text{PHI3} > \text{PHI3T}$$

Round on flat (F) corresponds to

$$\text{PHI3T} > \text{PHI3} > \text{PHI3F}$$

For mesh 2:

Round on round (R) corresponds to

$$\text{PHI2I} < \text{PHI2} < \text{PHI2T}$$

Round on flat (F) corresponds to

$$\text{PHI2T} < \text{PHI2} < \text{PHI2F}$$

For mesh 1:

Round on round (R) corresponds to

$$\text{PHI1I} > \text{PHI1} > \text{PHI1T}$$

Round on flat (F) corresponds to

$$\text{PHI1T} > \text{PHI1} > \text{PHI1F}$$

c. Output (see Program CLOCK 3, below)

The output of the program is best explained with the help of the sample problem at the end of the program.

I. Input Parameters

Mesh 1

$$\text{CAPRP1} = \text{Rp1} = .47725 \text{ in. (1.212 cm)}$$

$$\text{RP2} = \text{rp2} = .09085 \text{ in. (0.231 cm)}$$

$$\text{ACG1} = \text{aG1} = .47725 \text{ in. (1.212 cm)}$$

$$\text{ACP1} = \text{ap1} = .09085 \text{ in. (0.231 cm)}$$

$$\text{RHOG1} = \text{pG1} = .03870 \text{ in. (0.098 cm)}$$

$$\text{RHOP1} = \text{pP1} = .01740 \text{ in. (0.044 cm)}$$

$$\text{TG1} = \text{tG1} = .03480 \text{ in. (0.088 cm)}$$

$$\text{TP1} = \text{tP1} = .02800 \text{ in. (0.071 cm)}$$

$$\text{NG1} = \text{nG1} = 42$$

$$\text{NP2} = \text{nP2} = 8$$

Mesh 2

CAPRP2 = R_{P2} = .20670 in. (0.525 cm)
RP3 = r_{P3} = .06890 in. (0.175 cm)
ACG2 = a_{G2} = .20670 in. (0.525 cm)
ACP2 = a_{P2} = .06890 in. (0.175 cm)
RHOG2 = r_{G2} = .02070 in. (0.053 cm)
RHOP2 = r_{P2} = .01040 in. (0.026 cm)
TG2 = t_{G2} = .02520 in. (0.064 cm)
TP2 = t_{P2} = .02080 in. (0.053 cm)
NG2 = n_{G2} = 27
NP3 = n_{P3} = 9

Mesh 3

CAPRP3 = R_{P3} = .17560 in. (0.446 cm)
RP4 = r_{P4} = .05905 in. (0.150 cm)
ACG3 = a_{G3} = .17560 in. (0.446 cm)
ACP3 = a_{P3} = .05905 in. (0.150 cm)
RHOG3 = r_{G3} = .01910 in. (0.049 cm)
RHOP3 = r_{P3} = .00875 in. (0.022 cm)
TG3 = t_{G3} = .02170 in. (0.055 cm)
TP3 = t_{P3} = .01750 in. (0.044 cm)
NG3 = n_{G3} = 27
NP4 = n_{P4} = 9

In addition

MU = μ = .2
RPM = 1000
M1 = m_1 = $.69515 \times 10^{-4}$ lb-sec²/in. (12.171 g)

$M2 = m_2 = .97028 \times 10^{-5} \text{ lb-sec}^2/\text{in.} (1.699 \text{ g})$
 $M3 = m_3 = .70027 \times 10^{-5} \text{ lb-sec}^2/\text{in.} (1.226 \text{ g})$
 $M4 = m_4 = .79188 \times 10^{-6} \text{ lb-sec}^2/\text{in.} (0.139 \text{ g})$
 $R1 = R_1 = .750 \text{ in.} (1.905 \text{ cm})$
 $R2 = R_2 = .750 \text{ in.} (1.905 \text{ cm})$
 $R3 = R_3 = .750 \text{ in.} (1.905 \text{ cm})$
 $R4 = R_4 = .750 \text{ in.} (1.905 \text{ cm})$
 $RHO1 = \rho_1 = .060 \text{ in.} (0.152 \text{ cm})$
 $RHO2 = \rho_2 = .030 \text{ in.} (0.076 \text{ cm})$
 $RHO3 = \rho_3 = .025 \text{ in.} (0.064 \text{ cm})$
 $RHO4 = \rho_4 = .020 \text{ in.} (0.051 \text{ cm})$
 $MD = md^2 = .15 \times 10^{-4} \text{ lb-sec}^2 \text{ in.} (16.944 \text{ g} \cdot \text{cm}^2)$
 $K = 25$

II. Computed Values

At the beginning of the output, one finds $MIN = M_{1n}$.

Subsequently, the following are listed for each mesh:

f_{p1} , the length of the pinion flats

β_1 , the fuse body pivot to pivot line angles

ψ_{T1} and ϕ_{T1} , the transition angles as well as the associated subsidiary tests

ϕ_{IN1} and ψ_{IN1} , the initial angles

ϕ_{FIN1} and ψ_{FIN1} , the final angles

Finally, for the full range of the input angle ϕ_1 , the point efficiency $POINTEF$ is listed, in addition to other parameters which are useful for checking purposes. Note that $DPSI1$, $DPSI2$

and DPSI3 represent $\dot{\psi}_1$, $\dot{\psi}_2$ and $\dot{\psi}_3$, respectively. The cycle efficiency CYCLEFF is found at the end of the output.

Program CLOCK 3

```

1      PROGRAM CLOCKS(INPUT,OUTPUT,TAPES=INPUT,TAPE6=OUTPUT)
      C
      C POINT AND CYCLE EFFICIENCIES FOR THREE PASS CLOCK (OGIVAL) STEP UP
      C GEAR TRAIN IN SPIN ENVIRONMENT
      C
5      REAL MU,LAEDA1,LAEDA2,LAEDA3,MO4,MO41,MO42,MO43,MO44,MO45,MO46,MO4
17,MO48,LX1,LV1,L1,LX2,LV2,L2,LX3,LV3,L3,NP2,NP3,NP4,MG1,MG2,MG3,M1
24,M1,M2,M3,M4,MTOT,MO,LL1,LL2,LL3,K
1      READ (5,61) MU,RPM,CAPRP1,CAPRP2,CAPRP3,RP2,RP3,RP4,ACG1,ACG2,ACG3
      C
10     1,ACP1,ACP2,ACP3,ISTOP
      READ (5,62) R1,R2,R3,R4
      READ (5,63) RHOG1,RHOG2,RHOG3,RHOP1,RHOP2,RHOP3
      READ (5,64) TG1,TG2,TG3,TP1,TP2,TP3
      READ (5,65) MG1,MG2,MG3,NP2,NP3,NP4
      READ (5,66) M1,M2,M3,M4
      READ (5,67) RH01,RH02,RH03,RH04,MO,K
      PI=3.14159
      Z=PI/180.
      OMEGA=RPM*2.*PI/60.
      OM2=OMEGA*OMEGA
      PHOIT=-1.

      C
      C COMPUTATION OF GEAR TOOTH PARAMETERS
      C
      C
25     CXG1=RHOG1-TG1/2.
      DELG1=ASIN(CXG1/CAPRP1)
      CXP1=RHOP1-TP1/2.
      DELP1=ASIN(CXP1/RP2)
      GAMMP1=ASIN(RHOP1/RP2)
      ALPH1=GAMMP1-DELP1
      FP1=ACP1-COS(GAMMP1)
      B1=LAPRP1-RP2
      CXG2=RHOG2-TG2/2.
      DELG2=ASIN(CXG2/CAPRP2)
      CXP2=RHOP2-TP2/2.
      DELP2=ASIN(CXP2/RP3)
      GAMMP2=ASIN(RHOP2/RP3)
      ALPH2=GAMMP2-DELP2
      FP2=ACP2-COS(GAMMP2)
      B2=LAPRP2-RP3
      CXG3=RHOG3-TG3/2.
      DELG3=ASIN(CXG3/CAPRP3)
      CXP3=RHOP3-TP3/2.
      DELP3=ASIN(CXP3/RP4)
      GAMMP3=ASIN(RHOP3/RP4)
      ALPH3=GAMMP3-DELP3
      FP3=ACP3-COS(GAMMP3)
      B3=LAPRP3-RP4

      C
      C COMPUTATION OF MIN, GAMMAS AND BETAS
      C
50     MIN=MO-OM2
      DELTA2=ACOS(((CAPRP1+RP2)*(CAPRP1+RP2)+R1-R1-R2-R2)/(2.*R1*(CAPRP1

```


I-27

```

160      GO TO 6
165      5 SIGNIF=1.
      C
      C      COMPUTATION OF FINAL AND INITIAL VALUES OF PHI AND PSI FOR MESH 1
      C
      8 DO 7 I=1,2000
        PHID1=PHI1TD-(I-1-)/100.
        PHI1=PHID1+Z
        A1F=ACG1+COS(PHI1+DELGI+ALPHP1)-B1+COS(BETA1+ALPHP1)
        B1F=-ACG1+SIN(PHI1+DELGI+ALPHP1)+B1+SIN(BETA1+ALPHP1)
        C1F=RHOG1
        ROOT1F=A1F+A1F+B1F-B1F-C1F+C1F
        Y1F=A1F+SIGN1F+SQRT(ROOT1F)
        X1F=B1F+C1F
        PSI1F=2.*ATAN2(Y1F,X1F)
        IF (PSI1F.LT.0.) PSI1F=PSI1F+2.*PI
        LX1=B1+COS(BETA1)+ACG1+COS(PSI1F-DPSI1+DELPI)-ACG1+COS(PHI1+DPHI1+
        1DELGI)
        LY1=B1+SIN(BETA1)+ACG1+SIN(PSI1F-DPSI1+DELPI)-ACG1+SIN(PHI1+DPHI1+
        1DELGI)
        LL1=SQRT(LX1*LX1+LY1*LY1)
        DELE1=LL1-1
        IF (DELE1.LE.0.) GO TO 8
      7 CONTINUE
      8 PHI1F=PHI1
        PSI1FF=PSI1F
        PHI1I=PHI1F+DPHI1
        PSI1I=PSI1FF-DPSI1
        IF (PSI1I.LT.0.) PSI1I=PSI1I+2.*PI
        PHI1ID=PHI1I/Z
        PSI1ID=PSI1I/Z
        PHI1FD=PHI1F/Z
        PSI1FD=PSI1FF/Z
        WRITE (6,74) PHI1ID,PSI1ID,PHI1FD,PSI1FD
      C
      C      DETERMINATION OF CORRECT SIGN FOR ROUND ON ROUND REGIME OF MESH 1
      C
        A1R=ACG1+SIN(PHI1I+DELGI-DELPI)-B1+SIN(BETA1-DELP1)
        B1R=ACG1+COS(PHI1I+DELGI-DELPI)-B1+COS(BETA1-DELP1)
        C1R=(ACG1-ACG1+ACG1+ACG1+B1-B1-L1+L1-2.*ACG1+B1+COS(PHI1I+DELGI-BE
        1TA1))/(2.*ACPT)
        ROOT1R=A1R+A1R+B1R-B1R-C1R+C1R
        Y1R1=A1R+SQRT(ROOT1R)
        X1R2=A1R-SQRT(ROOT1R)
        X1R=B1R+C1R
        PSI1R1=2.*ATAN2(Y1R1,X1R)
        PSI1R2=2.*ATAN2(Y1R2,X1R)
        IF (PSI1R1.LT.0.) PSI1R1=PSI1R1+2.*PI
        IF (PSI1R2.LT.0.) PSI1R2=PSI1R2+2.*PI
        IF (ABS(PSI1I-PSI1R1).LT.ABS(PSI1I-PSI1R2)) GO TO 9
        SIGN1R=-1.
        GO TO 10
      9 SIGN1R=1.

```

A 160
 A 161
 A 162
 A 163
 A 164
 A 165
 A 166
 A 167
 A 168
 A 169
 A 170
 A 171
 A 172
 A 173
 A 174
 A 175
 A 176
 A 177
 A 178
 A 179
 A 180
 A 181
 A 182
 A 183
 A 184
 A 185
 A 186
 A 187
 A 188
 A 189
 A 190
 A 191
 A 192
 A 193
 A 194
 A 195
 A 196
 A 197
 A 198
 A 199
 A 200
 A 201
 A 202
 A 203
 A 204
 A 205
 A 206
 A 207
 A 208
 A 209
 A 210
 A 211
 A 212

```

C
C      PRELIMINARY COMPUTATIONS FOR MESH 2
C
C      DETERMINATION OF TRANSITION ANGLE OF MESH 2
C
10  A21=-RHOG2*COS(BETA2-ALPHP2)+FP2*SIN(BETA2-ALPHP2)
    B21=RHOG2*SIN(BETA2-ALPHP2)+FP2*COS(BETA2-ALPHP2)
    C21=(ACG2*ACG2-RHOG2-RHOG2-B2-B2-FP2*FP2)/(2.*B2)
    ROOT21=A21+A21*B21-B21-C21*C21
    Y211=A21+SQRT(ROOT21)
    Y212=A21-SQRT(ROOT21)
    X21=B21+C21
    PSI211=2.*ATAN2(Y211,X21)
    PSI212=2.*ATAN2(Y212,X21)
    PSITE21=PSI211
    PSITE22=PSI212
    IF (PSI211.GT.PI) PSITE21=PSI211-2.*PI
    IF (PSI211.LT.PI) PSITE21=PSITE21+2.*PI
    IF (PSI212.GT.PI) PSITE22=PSITE22-2.*PI
    IF (PSI212.LT.PI) PSITE22=PSITE22+2.*PI
    IF (PSITE21-GE.0.) TEST21=ABS(PI-BETA2+PSITE21+ALPHP2)/Z
    IF (PSITE21-LT.0.) TEST21=ABS(BETA2+PI-(PSITE21+2.*PI+ALPHP2))/Z
    IF (PSITE22-GE.0.) TEST22=ABS(PI-BETA2+PSITE22+ALPHP2)/Z
    IF (PSITE22-LT.0.) TEST22=ABS(BETA2+PI-(PSITE22+2.*PI+ALPHP2))/Z
    IF (PSITE21.LT.0.) PSITE21=PSITE21+2.*PI
    IF (PSITE22.LT.0.) PSITE22=PSITE22+2.*PI
    PSITE21=PSITE21/Z
    PSITE22=PSITE22/Z
    WRITE (6,48) PSITE21,TEST21
    WRITE (6,49) PSITE22,TEST22
    CALL TRANS2 (RHOG2,ALPHP2,BETA2,FP2,ACG2,B2,DELG2,Z,PSITE21,PHI2T1,
1G21)
    IF (G21-GT.FP2) GO TO 11
    PHI2T=PHI2T1
    PSITE2=PSITE21
    GO TO 13
11  CALL TRANS2 (RHOG2,ALPHP2,BETA2,FP2,ACG2,B2,DELG2,Z,PSITE22,PHI2T2,
1G22)
    IF (G22-LT.FP2) GO TO 12
    WRITE (6,75)
    STOP
12  PHI2T=PHI2T2
    PSITE2=PSITE22
13  IF (PHI2T-LT.0.) PHI2T=PHI2T+2.*PI
    IF (PSITE2-LT.0.) PSITE2=PSITE2+2.*PI
    PHI2TD=PHI2T/Z
    PSITE2D=PSITE2/Z
    WRITE (6,76) PHI2TD,PSITE2D
C
C      DETERMINATION OF CORRECT SIGN FOR ROUND ON FLAT REGIME OF MESH 2
C
A2F=ACG2*COS(PHI2T-DELG2-ALPHP2)-B2*COS(BETA2-ALPHP2)
B2F=-ACG2*SIN(PHI2T-DELG2-ALPHP2)+B2*SIN(BETA2-ALPHP2)

```

```

270 C2F=-RHOG2
    ROOT2F=A2F+A2F+B2F-B2F-C2F-C2F
    Y2F1=A2F+SQRT(ROOT2F)
    Y2F2=A2F-SQRT(ROOT2F)
    X2F=B2F+C2F
    PSI2F1=2.*ATAN2(Y2F1,X2F)
    PSI2F2=2.*ATAN2(Y2F2,X2F)
    IF (PSI2F1.LT.0.) PSI2F1=PSI2F1+2.*PI
    IF (PSI2F2.LT.0.) PSI2F2=PSI2F2+2.*PI
    IF (ABS(PSI2F1-PSI2T)-LT.ABS(PSI2F2-PSI2T)) GO TO 14
    PSI2F10=PSI2F1/Z
    PSI2F20=PSI2F2/Z
    SIGN2F=-1.
    GO TO 15
    14 SIGN2F=1.
    C
    C
    C
    280 COMPUTATION OF FINAL AND INITIAL VALUES OF PHI AND PSI FOR MESH 2
    C
    C
    C
    15 DO 16 I=1,1000
        PHID2=PHI2TD+(1-1)/100.
        PHI2=PHID2+Z
        A2F=ACG2+COS(PHI2-DELG2-ALPHP2)-B2+COS(BETA2-ALPHP2)
        B2F=-ACG2+SIN(PHI2-DELG2-ALPHP2)+B2+SIN(BETA2-ALPHP2)
        C2F=-RHOG2
        ROOT2F=A2F+A2F+B2F-B2F-C2F-C2F
        Y2F=A2F+SIGN2F*SQRT(ROOT2F)
        X2F=B2F+C2F
        PSI2F=2.*ATAN2(Y2F,X2F)
        IF (PSI2F.LT.0.) PSI2F=PSI2F+2.*PI
        LX2=B2+COS(BETA2)+ACP2+COS(PSI2F+DPSI2-DELG2)-ACG2+COS(PHI2-DPHI2-DELG2)
        LY2=B2+SIN(BETA2)+ACP2+SIN(PSI2F+DPSI2-DELG2)-ACG2+SIN(PHI2-DPHI2-DELG2)
        LL2=SQRT(LX2*LX2+LY2*LY2)
        DELEL2=LL2-L2
        IF (DELEL2.LE.0.) GO TO 17
    16 CONTINUE
    17 PHI2F=PHI2
        PSI2FF=PSI2F
        PHI2I=PHI2F-DPHI2
        PSI2I=PSI2FF-DPSI2
        IF (PSI2I.GT.2.*PI) PSI2I=PSI2I-2.*PI
        PHI2ID=PHI2I/Z
        PSI2ID=PSI2I/Z
        PHI2FD=PHI2F/Z
        PSI2FD=PSI2FF/Z
        WRITE (6,77) PHI2ID,PSI2ID,PHI2FD,PSI2FD
    C
    C
    C
    310 DETERMINATION OF CORRECT SIGN FOR ROUND ON ROUND REGIME OF MESH 2
    C
    C
    315 A2R=B2+SIN(BETA2+DELG2)-ACG2+SIN(PHI2I-DELG2+DELG2)
        B2P=B2+COS(BETA2+DELG2)-ACG2+COS(PHI2I-DELG2+DELG2)
        C2R=(L2-L2-B2-ACG2+ACG2-ACP2+2.*ACG2+B2+COS(PHI2I-DELG2-BE

```

```

320      1TA21)/(2.*ACP2)
      ROOT2R=A2R+A2R*B2R-B2R-C2R-C2R
      Y2R1=A2R+SORT(ROOT2R)
      X2R=B2R+C2R
      PSI2R1=2.*ATAN2(Y2R1,X2R)
      PSI2R2=2.*ATAN2(Y2R2,X2R)
      IF (PSI2R1.LT.0.) PSI2R1=PSI2R1+2.*PI
      IF (PSI2R2.LT.0.) PSI2R2=PSI2R2+2.*PI
      IF (ABS(PSI21-PSI2R1).LT.ABS(PSI21-PSI2R2)) GO TO 18
      SIGN2R=-1.
      GO TO 19
330      18 SIGN2R=1.
      C
      C
      C
      C
335      PRELIMINARY COMPUTATIONS FOR MESH 3
      DETERMINATION OF TRANSITION ANGLE OF MESH 3
19      A3T=RHO*G3-COS(BETA3+ALPHAP3)+FP3-SIN(BETA3+ALPHAP3)
      B3T=-RHO*G3-SIN(BETA3+ALPHAP3)+FP3-COS(BETA3+ALPHAP3)
      C3T=(ACG3+ACG3-RHO*G3-B3T-B3T-C3T-C3T)/(2.*B3)
      ROOT3T=A3T+A3T+B3T+B3T-C3T-C3T
      Y3T1=A3T+SORT(ROOT3T)
      X3T2=A3T-SORT(ROOT3T)
      X3T=B3T+C3T
      PSI3T1=2.*ATAN2(Y3T1,X3T)
      PSI3T2=2.*ATAN2(Y3T2,X3T)
      PSI3T3=PSI3T1
      PSI3T32=PSI3T2
      IF (PSI3T1.GT.PI) PSI3T31=PSI3T1-2.*PI
      IF (PSI3T1.LT.-PI) PSI3T31=PSI3T1+2.*PI
      IF (PSI3T2.GT.PI) PSI3T32=PSI3T2-2.*PI
      IF (PSI3T2.LT.-PI) PSI3T32=PSI3T2+2.*PI
      IF (PSI3T31-GE.0.) TEST31=ABS(PI-BETA3+PSITE31-ALPHAP3)/Z
      IF (PSI3T31.LT.0.) TEST31=ABS(PI-BETA3-(PSITE31+2.*PI-ALPHAP3))/Z
      IF (PSITE32-GE.0.) TEST32=ABS(PI-BETA3+PSITE32-ALPHAP3)/Z
      IF (PSITE32.LT.0.) TEST32=ABS(PI-BETA3-(PSITE32+2.*PI-ALPHAP3))/Z
      IF (PSI3T1.LT.0.) PSI3T1=PSI3T1+2.*PI
      IF (PSI3T2.LT.0.) PSI3T2=PSI3T2+2.*PI
      PSI3T1D=PSI3T1/Z
      PSI3T2D=PSI3T2/Z
      WRITE (6,50) PSI3T1D,TEST31
      WRITE (6,51) PSI3T2D,TEST32
      CALL TRANS1 (RHO*G3,ALPHAP3,BETA3,FP3,ACG3,B3,DEL*G3,Z,PSI3T1,PHI3T1,
1G31)
      IF (G31.GT.FP3) GO TO 20
      PHI3T=PHI3T1
      PSI3T=PSI3T1
      GO TO 22
20      CALL TRANS1 (RHO*G3,ALPHAP3,BETA3,FP3,ACG3,B3,DEL*G3,Z,PSI3T2,PHI3T2,
1G32)
      IF (G32.LT.FP3) GO TO 21
      WRITE (5,78)
370

```

PROGRAM CLOCK3 74/74 OPT=1

```

375      STOP
      21 PHI3T=PHI3T2
      PSI3T=PSI3T2
      22 IF (PHI3T.LT.0.) PHI3T=PHI3T+2.*PI
      IF (PSI3T.LT.0.) PSI3T=PSI3T+2.*PI
      PHI3TD=PHI3T/Z
      PSI3TD=PSI3T/Z
      WRITE (6,79) PHI3TD,PSI3TD
      380      DETERMINATION OF CORRECT SIGN FOR ROUND ON FLAT REGIME OF MESH 3
      C
      C
      A3F=ACG3*COS(PHI3T+DELG3+ALPH3)-B3*COS(BETA3+ALPH3)
      B3F=-ACG3*SIN(PHI3T+DELG3+ALPH3)+B3*SIN(BETA3+ALPH3)
      C3F=RHOG3
      ROOT3F=A3F+B3F+C3F
      Y3F1=A3F+SQRT(ROOT3F)
      Y3F2=A3F-SQRT(ROOT3F)
      X3F=B3F+C3F
      390      PSI3F1=2.*ATAN2(Y3F1,X3F)
      PSI3F2=2.*ATAN2(Y3F2,X3F)
      IF (PSI3F1.LT.0.) PSI3F1=PSI3F1+2.*PI
      IF (PSI3F2.LT.0.) PSI3F2=PSI3F2+2.*PI
      IF (ABS(PSI3F1-PSI3T).LT.ABS(PSI3F2-PSI3T)) GO TO 23
      SIGN3F=-1.
      GO TO 24
      395      23 SIGN3F=1.
      C
      C
      400      COMPUTATION OF FINAL AND INITIAL VALUES OF PHI AND PSI FOR MESH 3
      C
      24 DO 25 I=1,2000
      PHID3=PHI3TD-(I-1.)/100.
      PHI3=PHID3+Z
      A3F=ACG3*COS(PHI3+DELG3+ALPH3)-B3*COS(BETA3+ALPH3)
      B3F=-ACG3*SIN(PHI3+DELG3+ALPH3)+B3*SIN(BETA3+ALPH3)
      C3F=RHOG3
      ROOT3F=A3F+B3F+C3F
      Y3F1=A3F+SQRT(ROOT3F)
      Y3F2=A3F-SQRT(ROOT3F)
      X3F=B3F+C3F
      410      PSI3F=2.*ATAN2(Y3F1,X3F)
      IF (PSI3F.LT.0.) PSI3F=PSI3F+2.*PI
      LX3=B3*COS(BETA3)+ACP3*COS(PSI3F-DPSI3+DELP3)-ACG3*COS(PHI3+DPHI3+
      1DELG3)
      LY3=B3*SIN(BETA3)+ACP3*SIN(PSI3F-DPSI3+DELP3)-ACG3*SIN(PHI3+DPHI3+
      1DELG3)
      415      LL3=SQRT(LX3*LY3+LY3*LY3)
      DELEL3=LL3-L3
      IF (DELEL3.LE.0.) GO TO 26
      25 CONTINUE
      26 PHI3F=PHI3
      PSI3F=PSI3F
      PHI3I=PHI3F+DPHI3
      PSI3I=PSI3F+DPSI3
      IF (PSI3I.LT.0.) PSI3I=PSI3I+2.*PI

```

```

425 IF (PSI3I.LT.0.) PSI3I=PSI3I+2.*PI A 425
    PHI3ID=PHI3I/Z A 426
    PSI3ID=PSI3I/Z A 427
    PHI3FD=PHI3F/Z A 428
    PSI3FD=PSI3FF/Z A 429
    WRITE (6,80) PHI3ID,PSI3ID,PHI3FD,PSI3FD A 430
C
C DETERMINATION OF CORRECT SIGN OF ROUND ON ROUND REGIME FOR MESH 3 A 431
C A 432
A 433
A 434
A 435
A 436
A 437
A 438
A 439
A 440
A 441
A 442
A 443
A 444
A 445
A 446
A 447
A 448
A 449
A 450
A 451
A 452
A 453
A 454
A 455
A 456
A 457
A 458
A 459
A 460
A 461
A 462
A 463
A 464
A 465
A 466
A 467
A 468
A 469
A 470
A 471
A 472
A 473
A 474
A 475
A 476
A 477

    A3R=ACG3*SIN(PHI3I+DELG3-DELP3)-B3*SIN(BETA3-DELP3)
    B3R=ACG3*COS(PHI3I+DELG3-DELP3)-B3*COS(BETA3-DELP3)
    C3R=(ACP3*ACP3+ACG3*ACG3+B3-L3-L3-2.*ACG3*B3*COS(PHI3I+DELG3-BE
    ITA3))/ (2.*ACP3)
    ROOT3R=A3R*A3R+B3R*B3R-C3R*C3R
    Y3R1=A3R+SQRT(ROOT3R)
    Y3R2=A3R-SQRT(ROOT3R)
    X3R=B3R+C3R
    PSI3R1=2.*ATAN2(Y3R1,X3R)
    PSI3R2=2.*ATAN2(Y3R2,X3R)
    IF (PSI3R1.LT.0.) PSI3R1=PSI3R1+2.*PI
    IF (PSI3R2.LT.0.) PSI3R2=PSI3R2+2.*PI
    IF (ABS(PHI3I-PSI3R1).LT.ABS(PHI3I-PSI3R2)) GO TO 27
    SIGN3R=-1.
    GO TO 28
27 SIGN3R=1.
C
C GEAR TRAIN MOTION MODEL, KINEMATICS C
C
28 DOPHI1=NP2*NP3*(PHI3I-PHI3F)/(K*NG1*NG2)
    PHI1=PHI1+DOPHI1
    WRITE (6,52)
29 PHI1=PHI1-DOPHI1
    PHI1D=PHI1/Z
    IF (PHI1.LE.PHI1F+DOPHI1) GO TO 45
C
C MESH 1 C
C
    IF (PHI1.LE.PHI1T) GO TO 30
    A1R=ACG1*SIN(PHI1+DELG1-DELP1)-B1*SIN(BETA1-DELP1)
    B1R=ACG1*COS(PHI1+DELG1-DELP1)-B1*COS(BETA1-DELP1)
    C1R=(ACPI*ACPI+ACG1*ACG1+B1-L1-L1-2.*ACG1*B1*COS(PHI1+DELG1-BE
    ITA1))/ (2.*ACPI)
    ROOT1R=A1R*A1R+B1R*B1R-C1R*C1R
    Y1R=A1R+SIGN1R*SQRT(ROOT1R)
    X1R=B1R+C1R
    PSI1=2.*ATAN2(Y1R,X1R)
    IF (PSI1.LT.0.) PSI1=PSI1+2.*PI
    PSI1D=PSI1/Z
    IF (ABS(PHI1-PHI1T).LT.0.0001) PSI1I=PSI1
    IF (ABS(PHI1-PHI1T).LT..0001) PSI1T=PSI1T
    SLAM1=(B1*COS(BETA1)+ACP1*SIN(PHI1+DELP1)-ACG1*SIN(PHI1+DELG1))/L1
    CLAM1=(B1*COS(BETA1)+ACP1*COS(PHI1+DELG1)-ACG1*COS(PHI1+DELG1))/L1
    LAMDA1=ATAN2(SLAM1,CLAM1)

```

```

480      IF (LAMBDA1.LT.0.) LAMBDA1=LAMBDA1+2.*PI
      PSDOIT1=PHOG1*ACG1*(B1/ACP1*SIN(PHI1+DELG1-BETA1))+SIN(PHI1-PSI11+DE
      1LG1-DELP1))/(A1R+COS(PSI11)-B1R*SIN(PSI11))
      VST1R=PHOOT1*(ACG1+COS(PHI1+DELG1-LAMBDA1)+RHOG1)-PSOOT1*(ACP1+COS(
      1PSI1+DELP1-LAMBDA1))-RHOP1)
      SIR=VST1R/ABS(VST1R)
      GO TO 31
485      30 A1F=ACG1+COS(PHI1+DELG1+ALPH1)-B1+COS(BETA1+ALPH1)
      B1F=-ACG1+SIN(PHI1+DELG1+ALPH1)+B1+SIN(BETA1+ALPH1)
      C1F=RHOG1
      ROOT1F=A1F+A1F+B1F+B1F-C1F+C1F
      Y1F=A1F+SIGN1F*SQRT(ROOT1F)
      X1F=B1F+C1F
      PSI11=2.*ATAN2(Y1F,X1F)
      IF (PSI11.LT.0.) PSI11=PSI11+2.*PI
      PS11D=PSI11/Z
      G1=(ACG1+SIN(PHI1+DELG1)+RHOG1+COS(PSI11-ALPH1)-B1+SIN(BETA1))/SIN
      1(PSI1-ALPH1)
      PSDOIT1=PHOOT1*(ACG1+COS(PHI1-PSI11+DELG1+ALPH1))/(A1F+COS(PSI11)-B1
      1F+SIN(PSI11))
      VST1F=PHOOT1*(ACG1+SIN(PSI1-ALPH1)-PHI1-DELG1)-RHOG1)
      S1F=VST1F/ABS(VST1F)
      MESH 2
      C
      C
      C
500      31 DOPHI2=PSI1-PSI1P
      IF (ABS(PHI1-PHI11).LT.0.0001) PHI2=PHI21
      PHI2=PHI2+DOPHI2
      PSI1P=PSI1
      IF (PHI2.GT.PHI2F) PHI2=PHI21
      PHI2D=PHI2/Z
      IF (PHI2-GE-PHI21) CD TO 32
      A2R=B2*SIN(BETA2+DELP2)-ACG2*SIN(PHI2-DELG2+DELP2)
      B2R=B2*COS(BETA2+DELP2)-ACG2+COS(PHI2-DELG2+DELP2)
      C2R=(L2-B2-B2-ACG2+ACG2-ACP2+ACP2+2.*ACG2-B2+COS(PHI2-DELG2-BET
      1A2))/2.*ACP2)
      ROOT2R=A2R+A2R+B2R+B2R-C2R+C2R
      Y2R=A2R+SIGN2R*SQRT(ROOT2R)
      X2R=B2R+C2R
      PSI2=2.*ATAN2(Y2R,X2R)
      IF (PSI2.LT.0.) PSI2=PSI2+2.*PI
      PS12D=PSI2/Z
      IF (ABS(PHI2-PHI21).LT.0.0001) PSI21=PSI2
      IF (ABS(PHI2-PHI21).LT.0.0001) PSI2P=PSI21
      SLAW2=(B2+SIN(BETA2)+ACP2+SIN(PSI2-DELP2)-ACG2+SIN(PHI2-DELG2))/L2
      CLAW2=(B2+COS(BETA2)+ACP2+COS(PSI2-DELP2)-ACG2+COS(PHI2-DELG2))/L2
      LAMDA2=ATAN2(SLAW2,CLAW2)
      IF (LAMDA2.LT.0.) LAMDA2=LAMDA2+2.*PI
      PHOOT2=PSOOT1
      PSOOT2=PHOOT2*ACG2*(-SIN(PHI2-PSI2-DELG2+DELP2)-B2/ACP2+SIN(PHI2-B
      1ELG2-BETA2))/(A2R+COS(PSI2)-B2R*SIN(PSI2))
      VST2R=PHOOT2*(ACG2+COS(PHI2-DELG2-LAMBDA2)+RHOG2)-PSOOT2*(ACP2+COS(
      1PSI2-DELP2-LAMBDA2)-RHOP2)

```



```

585      ROOT3F=A3F+A3F*B3F+B3F*B3F-C3F-C3F
      Y3F=A3F+SIGK3F*SQRT(ROOT3F)
      X3F=B3F+C3F
      PS13=2.*ATAN2(Y3F,X3F)
      IF (PS13.LT.0.) PS13=PS13+2.*PI
      PS130=PS13/2
      G3=(ACG3+SIN(PHI13+DELG3)+BHG3-COS(PS13-ALPHP3)-B3-SIN(DELTA3))/SIN
      1(PS13-ALPHP3)
      PHOOT3=PSOOT2
      PSOOT3=PHOOT3+ACG3-COS(PHI13-PS13+DELG3+ALPHP3)/(A3F+COS(PS13)-B3F+
      1SIN(PS13))
      VST3F=PHOOT3*(ACG3+SIN(PS13-ALPHP3-PHI13-DELG3)-BHG3)
      S3F=VST3F/ABS(VST3F)

C
C      MOMENT COMPUTATIONS
C
600      DM=1.-MU+MU
      A1=ABS((MU+SIN(GAMMA4)+COS(GAMMA4))/DM)
      A2=ABS((MU*(S3R-1.)*SIN(LAMDA3)-(1.-MU+MU*S3R)*COS(LAMDA3))/DM)
      A3=ABS((SIN(GAMMA4)-MU+COS(GAMMA4))/DM)
      A4=ABS(((1.-MU+MU*S3R)*SIN(LAMDA3)+MU*(S3R-1.)*COS(LAMDA3))/DM)
      A5=ABS(((1.-MU+MU*S3R)*COS(LAMDA3)-MU*(1.+S3R)*SIN(LAMDA3))/DM)
      A6=ABS((MU*(1.+S3R)*SIN(LAMDA2)-(1.-MU+MU*S3R)*COS(LAMDA2))/DM)
      A7=ABS((MU+SIN(GAMMA3)-COS(GAMMA3))/DM)
      A8=ABS(((1.-MU+MU*S3R)*SIN(LAMDA3)+MU*(1.+S3R)*COS(LAMDA3))/DM)
      A9=ABS(((MU+MU*S3R-1.)*SIN(LAMDA2)-MU*(1.+S3R)*COS(LAMDA2))/DM)
      A10=ABS((SIN(GAMMA3)+MU+COS(GAMMA3))/DM)
      A11=ABS(((1.-MU+MU*S3R)*COS(LAMDA2)-MU*(S3R-1.)*SIN(LAMDA2))/DM)
      A12=ABS((MU*(S3R-1.)*SIN(LAMDA1)-(1.-MU+MU*S3R)*COS(LAMDA1))/DM)
      A13=ABS((-COS(GAMMA2)-MU*SIN(GAMMA2))/DM)
      A14=ABS(((1.-MU+MU*S3R)*SIN(LAMDA2)-MU*(1.-S3R)*COS(LAMDA2))/DM)
      A15=ABS((MU*(1.-S3R)*COS(LAMDA1)-(1.-MU+MU*S3R)*SIN(LAMDA1))/DM)
      A16=ABS((MU+COS(GAMMA2)-SIN(GAMMA2))/DM)
      A17=ABS(((1.-MU+MU*S3R)*COS(LAMDA1)-MU*(1.+S3R)*SIN(LAMDA1))/DM)
      A18=ABS(1./DM)
      A19=ABS(((1.-MU+MU*S3R)*SIN(LAMDA1)+MU*(1.+S3R)*COS(LAMDA1))/DM)
      A20=ABS(MU/DM)
      A21=ABS((MU*(1.-S3R)*SIN(LAMDA2)+(1.-MU+MU*S3R)*COS(LAMDA2))/DM)
      A22=ABS(((1.-MU+MU*S3F)*SIN(PS11-ALPHP1)-MU*(1.+S3F)*COS(PS11-ALPH
      1P1))/DM)
      A23=ABS((MU+SIN(GAMMA2)+COS(GAMMA2))/DM)
      A24=ABS(((1.-MU+MU*S3R)*SIN(LAMDA2)-MU*(1.-S3R)*COS(LAMDA2))/DM)
      A25=ABS((1.-MU*(1.+S3F)*SIN(PS11-ALPHP1)+(MU+MU*S3F-1.)*COS(PS11-ALP
      1HP1))/DM)
      A26=ABS((-SIN(GAMMA2)+MU+COS(GAMMA2))/DM)
      A27=ABS((-1.-MU+MU*S3F)*SIN(PS11-ALPHP1)+MU*(S3F-1.)*COS(PS11-ALP
      1HP1))/DM)
      A28=ABS(1./DM)
      A29=ABS((MU*(S3F-1.)*SIN(PS11-ALPHP1)+(1.-MU+MU*S3F)*COS(PS11-ALPH
      1P1))/DM)
      A30=ABS(MU/DM)
      A31=ABS(((1.-MU+MU*S3R)*COS(LAMDA3)-MU*(1.+S3R)*SIN(LAMDA3))/DM)
      A32=ABS((-MU*(1.+S3F)*COS(PS12+ALPHP2)-(1.-MU+MU*S3F)*SIN(PS12+ALP

```

```

1HP2))/DM)
A33=ABS((MU+SIN(GAMMA3)-COS(GAMMA3))/DM)
A34=ABS((MU*(1.+S3F)+COS(LAMDA3)+(1.-MU+MU*S3F)*SIN(LAMDA3))/DM)
A35=ABS((1.-MU+MU*S2F)*COS(PSI2+ALPH2)-MU*(1.+S2F)*SIN(PSI2+ALPH
1P2))/DM)
A36=ABS((SIN(GAMMA3)+MU)*COS(GAMMA3))/DM)
A37=ABS((1.-MU+MU*S2F)*SIN(PSI2+ALPH2)+MU*(S2F-1.)*COS(PSI2+ALPH
1P2))/DM)
A38=ABS((1.-MU+MU*S1F)*SIN(PSI1-ALPH1)-MU*(1.+S1F)*COS(PSI1-ALPH
1P1))/DM)
A39=ABS((MU+SIN(GAMMA2)+COS(GAMMA2))/DM)
A40=ABS((MU*(S2F-1.)*SIN(PSI2+ALPH2)-(1.-MU+MU*S2F)*COS(PSI2+ALPH
1P2))/DM)
A41=ABS((1.-MU*(1.+S1F)*SIN(PSI1-ALPH1)+(MU+MU*S1F-1.)*COS(PSI1-ALPH
1HP1))/DM)
A42=ABS((MU+COS(GAMMA2)-SIN(GAMMA2))/DM)
A43=ABS((1.-MU+MU*S2F)*SIN(PSI2+ALPH2)-MU*(1.-S2F)*COS(PSI2+ALPH
1P2))/DM)
A44=ABS((MU*(S1F-1.)*SIN(LAMDA1)-(1.-MU+MU*S1F)*COS(LAMDA1))/DM)
A45=ABS((MU+SIN(GAMMA2)+COS(GAMMA2))/DM)
A46=ABS((MU*(S2F-1.)*SIN(PSI2+ALPH2)-(1.-MU+MU*S2F)*COS(PSI2+ALPH
1P2))/DM)
A47=ABS((1.-MU+MU*S1F)*SIN(LAMDA1)+MU*(1.-S1F)*COS(LAMDA1))/DM)
A48=ABS((1.-SIN(GAMMA2)+MU+COS(GAMMA2))/DM)
A49=ABS((1.-MU+MU*S3F)*SIN(PSI3-ALPH3)-MU*(1.+S3F)*COS(PSI3-ALPH
1P3))/DM)
A50=ABS((1.-MU+SIN(GAMMA4)-COS(GAMMA4))/DM)
A51=ABS((1.-MU*(1.+S3F)*SIN(PSI3-ALPH3)-(1.-MU+MU*S3F)*COS(PSI3-ALPH
1HP3))/DM)
A52=ABS((1.-SIN(GAMMA4)+MU+COS(GAMMA4))/DM)
A53=ABS((1.-MU+MU*S3F)*SIN(PSI3-ALPH3)+MU*(S3F-1.)*COS(PSI3-ALPH
1HP3))/DM)
A54=ABS((1.-MU+MU*S2F-1.)*SIN(PSI2+ALPH2)-MU*(1.+S2F)*COS(PSI2+ALPH
1P2))/DM)
A55=ABS((MU+SIN(GAMMA3)-COS(GAMMA3))/DM)
A56=ABS((MU*(S3F-1.)*SIN(PSI3-ALPH3)+(1.-MU+MU*S3F)*COS(PSI3-ALPH
1P3))/DM)
A57=ABS((1.-MU*(1.+S2F)*SIN(PSI2+ALPH2)+(1.-MU+MU*S2F)*COS(PSI2+ALPH
1HP2))/DM)
A58=ABS((1.-SIN(GAMMA3)-MU+COS(GAMMA3))/DM)
A59=ABS((1.-MU+MU*S3F)*SIN(PSI3-ALPH3)+MU*(S3F-1.)*COS(PSI3-ALPH
1HP3))/DM)
A60=ABS((MU*(1.+S2F)*SIN(LAMDA2)+(MU+MU*S2F-1.)*COS(LAMDA2))/DM)
A61=ABS((MU+SIN(GAMMA3)-COS(GAMMA3))/DM)
A62=ABS((MU*(S3F-1.)*SIN(PSI3-ALPH3)+(1.-MU+MU*S3F)*COS(PSI3-ALPH
1P3))/DM)
A63=ABS((1.-MU+MU*S2F-1.)*SIN(LAMDA2)-MU*(1.+S2F)*COS(LAMDA2))/DM)
A64=ABS((1.-SIN(GAMMA3)-MU+COS(GAMMA3))/DM)
C1=MU+RH04*(A1+A3)
C2=ACP3*(MU+S3F+COS(PSI3+DELPH3-LAMDA3)-SIN(PSI3+DELPH3-LAMDA3))-MU*
1(RHOP3+S3F+RH04*(A2+A4))
C3=MU+RH03*(A5+A8)-MU*S3F+RH03+ACG3*(SIN(PSI3+DELPH3-LAMDA3)-MU*S3
1R=COS(PSI3+DELPH3-LAMDA3))

```

```

690 C4=RU+RHO3*(A7+A10)
691 C5=RU+RHO3*(A6+A9)-RU+S2R+RHOP2+ACP2*(RU+S2R+COS(PSI2-DELP2-LAMDA2
692 1)-SIN(PSI2-DELP2-LAMDA2))
693 C6=ACG2*(SIN(PHI2-DELG2-LAMDA2)-RU+S2R+COS(PHI2-DELG2-LAMDA2))-RU+
694 RHOP2*(A11+A14)-RU+RHOG2+S2R
695 C7=RU+RHO2*(A13+A16)
696 C8=-ACP1*(SIN(PSI1+DELP1-LAMDA1)-RU+S1R+COS(PSI1+DELP1-LAMDA1))+RU
697 1U+RHO2*(A12+A15)+RU+S1R+RHOP1)
698 C9=RU+RHO1*(A18+A20)
699 C10=RU+RHO1*(A17+A19)+ACG1*(SIN(PHI1+DELG1-LAMDA1)-RU+S1R+COS(PHI1
700 1+DELG1-LAMDA1))-RU+S1R+RHOP1)
701 C11=ACG2*(SIN(PHI2-DELG2-LAMDA2)-RU+S2R+COS(PHI2-DELG2-LAMDA2))-RU
702 1+RHO2*(A21+A24)-RU+RHOG2+S2R
703 C12=RU+RHO2*(A23+A26)
704 C13=GI-RU+RHO2*(A27+A25)
705 C14=RU+RHO1*(A28+A30)
706 C15=RU+RHO1*(A27+A29)+RU+S1F+RHOG1+ACG1*(RU+S1F+SIN(PHI1+DELG1-PSI
707 1+ALPH1))-COS(PHI1+DELG1-PSI1+ALPH1))
708 C16=RU+RHO3*(A31+A34)+ACG3*(SIN(PHI3+DELG3-LAMDA3)-RU+S3R+COS(PHI3
709 1+DELG3-LAMDA3))-RU+RHOG3+RU+S3R
710 C17=RU+RHO3*(A33+A36)
711 C18=RU+RHO3*(A32+A35)-G2
712 C19=-RU+RHO2*(A37+A40)+ACG2*(COS(PHI2-DELG2-PSI2-ALPH2)+RU+S2F+SI
713 1M(PHI2-DELG2-PSI2-ALPH2))-RU+S2F+RHOG2
714 C20=RU+RHO2*(A39+A42)
715 C21=-RU+RHO2*(A38+A41)+G1
716 C22=-RU+RHO2*(A43+A46)+ACG2*(COS(PHI2-DELG2-PSI2-ALPH2)+RU+S2F+SI
717 1M(PHI2-DELG2-PSI2-ALPH2))-RU+S2F+RHOG2
718 C23=RU+RHO3*(A45+A48)
719 C24=-RU+RHO2*(A44+A47)+ACP1*(RU+S1R+COS(PSI1+DELP1-LAMDA1))-SIN(PSI
720 1+DELP1-LAMDA1))-RU+S1R+RHOP1
721 C25=RU+RHO4*(A50+A52)
722 C26=GI-RU+RHO4*(A49+A51)
723 C27=RU+RHO3*(A53+A56)+ACG3*(-COS(PHI3+DELG3-PSI3+ALPH3)+RU+S3F+SI
724 1M(PHI3+DELG3-PSI3+ALPH3))+RU+S3F+RHOG3
725 C28=RU+RHO3*(A55+A58)
726 C29=RU+RHO3*(A54+A57)-G2
727 C30=RU+RHO3*(A59+A62)-ACG3*(COS(PHI3+DELG3-PSI3+ALPH3)-RU+S3F+SIN
728 1(PHI3+DELG3-PSI3+ALPH3))+RU+S3F+RHOG3
729 C31=RU+RHO3*(A61+A64)
730 C32=RU+RHO3*(A60+A63)-ACP2*(SIN(PSI2-DELP2-LAMDA2)-RU+S2R+COS(PSI2
731 1-DELP2-LAMDA2))-RU+S2R+RHOP2
732 C
733 C
734 C
735 IF ((PHI1-GE.PHI1T).AND.(PHI2-LE.PHI2T).AND.(PHI3-GE.PHI3T)) GO TO
736 1 36
737 IF ((PHI1-LE.PHI1T).AND.(PHI2-LE.PHI2T).AND.(PHI3-GE.PHI3T)) GO TO
738 1 37
739 IF ((PHI1-LE.PHI1T).AND.(PHI2-GE.PHI2T).AND.(PHI3-GE.PHI3T)) GO TO
740 1 38
741 IF ((PHI1-GE.PHI1T).AND.(PHI2-GE.PHI2T).AND.(PHI3-GE.PHI3T)) GO TO
742 1 39

```

```

745      IF ((PHI11.LE.PHI11).AND.(PHI12.GE.PHI12).AND.(PHI13.LE.PHI13)) GO TO 743
1 40      IF ((PHI11.GE.PHI11).AND.(PHI12.GE.PHI12).AND.(PHI13.LE.PHI13)) GO TO 745
1 41      IF ((PHI11.GE.PHI11).AND.(PHI12.LE.PHI12).AND.(PHI13.LE.PHI13)) GO TO 746
1 42      IF ((PHI11.LE.PHI11).AND.(PHI12.LE.PHI12).AND.(PHI13.LE.PHI13)) GO TO 748
1 43      IF ((PHI11.LE.PHI11).AND.(PHI12.LE.PHI12).AND.(PHI13.LE.PHI13)) GO TO 749
      A 750
      A 751
      A 752
      A 753
      A 754
      A 755
      A 756
      A 757
      A 758
      A 759
      A 760
      A 761
      A 762
      A 763
      A 764
      A 765
      A 766
      A 767
      A 768
      A 769
      A 770
      A 771
      A 772
      A 773
      A 774
      A 775
      A 776
      A 777
      A 778
      A 779
      A 780
      A 781
      A 782
      A 783
      A 784
      A 785
      A 786
      A 787
      A 788
      A 789
      A 790
      A 791
      A 792
      A 793
      A 794
      A 795

C      MOMENT EXPRESSIONS
C
36      MD41=MIN=C2+C5+C8/(C3+C6+C10)-Q4+C1-Q2+C3+C5+C7/(C3+C6)-Q3+C2+C4/C
      MD4-MD41
      POINTEF=ABS(PSOOT3)*MD4/MIN
      WRITE (6,53) PHI10,PHI20,PHI30,PSI10,PSI20,PSI30,PSOOT1,PSOOT2,PSO
      10T3,S1R,S2R,S3R,POINTEF
      GO TO 44
37      MD42=MIN=C2+C5+C13/(C3+C11+C15)-Q1+C2+C5+C13+C14/(C3+C11+C15)-Q2+C
      12+C5+C12/(C3+C11)-Q3+C2+C4/C3-Q4+C1
      MD4=MD42
      POINTEF=ABS(PSOOT3)*MD4/MIN
      WRITE (6,54) PHI10,PHI20,PHI30,PSI10,PSI20,PSI30,PSOOT1,PSOOT2,PSO
      10T3,S2R,S3R,S1F,G1,POINTEF
      GO TO 44
38      MD43=MIN=C2+C18+C21/(C15+C16+C19)-Q1+C2+C14+C18+C21/(C15+C16+C19)-
      102+C2+C18+C20/(C16+C19)-Q3+C2+C17/C16-Q4+C1
      MD4=MD43
      POINTEF=ABS(PSOOT3)*MD4/MIN
      WRITE (6,55) PHI10,PHI20,PHI30,PSI10,PSI20,PSI30,PSOOT1,PSOOT2,PSO
      10T3,S3R,S1F,G1,S2F,G2,POINTEF
      GO TO 44
39      MD44=MIN=C2+C18+C24/(C16+C16+C22)-Q1+C2+C9+C18+C24/(C16+C16+C22)-Q
      12+C2+C18+C23/(C16+C22)-Q3+C2+C17/C16-Q4+C1
      MD4=MD44
      POINTEF=ABS(PSOOT3)*MD4/MIN
      WRITE (6,56) PHI10,PHI20,PHI30,PSI10,PSI20,PSI30,PSOOT1,PSOOT2,PSO
      10T3,S1R,S3R,S2F,G2,POINTEF
      GO TO 44
40      MD45=MIN=C2+C26+C29/(C15+C19+C27)-Q1+C14+C21+C26+C29/(C15+C19+C27)
      1)-Q2+C20+C26+C29/(C19+C27)-Q3+C26+C28/C27-Q4+C25
      MD4=MD45
      POINTEF=ABS(PSOOT3)*MD4/MIN
      WRITE (6,57) PHI10,PHI20,PHI30,PSI10,PSI20,PSI30,PSOOT1,PSOOT2,PSO
      10T3,S1F,G1,S2F,G2,S3F,G3,POINTEF
      GO TO 44
41      MD46=MIN=C24+C26+C29/(C10+C22+C27)-Q1+C9+C24+C26+C29/(C10+C22+C27)
      1-Q2+C23+C26+C29/(C22+C27)-Q3+C26+C28/C27-Q4+C25
      MD4=MD46
      POINTEF=ABS(PSOOT3)*MD4/MIN
      WRITE (6,58) PHI10,PHI20,PHI30,PSI10,PSI20,PSI30,PSOOT1,PSOOT2,PSO
      10T3,S1R,S2F,G2,S3F,G3,POINTEF
      GO TO 44

```

```

42 MD47=MIN=C8-C26-C32/(C6-C19-C30)-01-C8-C9-C26-C32/(C6-C19-C30)-02-
1C7-C26-C32/(C6-C30)-03-C26-C31/C30-Q4-C25
MD4=MD47
POINTEF=ABS(PSOOT3)*MD4/MIN
WRITE (6.59) PHI10,PHI20,PHI30,PSI10,PSI20,PSI30,PSOOT1,PSOOT2,PSO
1073,51R,52R,53F,G3,POINTEF
GO TO 44
43 MD48=MIN=C13-C26-C32/(C11-C15-C30)-01-C13-C14-C26-C32/(C11-C15-C30
1)-02-C12-C26-C32/(C11-C30)-03-C26-C31/C30-Q4-C25
MD4=MD48
POINTEF=ABS(PSOOT3)*MD4/MIN
WRITE (6.60) PHI10,PHI20,PHI30,PSI10,PSI20,PSI30,PSOOT1,PSOOT2,PSO
1073,52R,51F,G1,53F,G3,POINTEF
44 NTOT=NTOT+POINTEF
GO TO 29
45 CYCLEFF=NTOT*DDPHI1/(PHI1F-PHI11)
WRITE (6.61) CYCLEFF
NTOT=0.
IF (ISTOP.NE.0) GO TO 1
STOP
C
46 FORMAT (6X,9APSI111D =,F9.4,3X,8NTEST11 =,F9.4)
47 FORMAT (6X,9APSI112D =,F9.4,3X,8NTEST12 =,F9.4//)
48 FORMAT (6X,9APSI121D =,F9.4,3X,8NTEST21 =,F9.4)
49 FORMAT (6X,9APSI122D =,F9.4,3X,8NTEST22 =,F9.4//)
50 FORMAT (6X,9APSI131D =,F9.4,3X,8NTEST31 =,F9.4)
51 FORMAT (6X,9APSI132D =,F9.4,3X,8NTEST32 =,F9.4//)
52 FORMAT (120H0 PHI1 PHI2 PHI3 PSI1 PSI2 PSI3 DPSI1 DPSI2
1 DPSI3 51R 52R 53R 51F G1 52F G2 53F G3 POINTEF
2/)
53 FORMAT (6X,6(F4.0,2X),3(F5.0,2X),3(F3.0,2X),36X,F5.3)
54 FORMAT (6X,6(F4.0,2X),3(F5.0,2X),5X,3(F3.0,2X),F5.3,26X,F5.3)
55 FORMAT (6X,6(F4.0,2X),3(F5.0,2X),10X,F3.0,2X,F3.0,2X,F5.3,2X,F3.0,
12X,F5.3,14X,F5.3)
56 FORMAT (6X,6(F4.0,2X),3(F5.0,2X),F3.0,7X,F3.0,14X,F3.0,2X,F5.3,14X
1,F5.3)
57 FORMAT (6X,6(F4.0,2X),3(F5.0,2X),15X,3(F3.0,2X,F5.3,2X),F5.3)
58 FORMAT (6X,6(F4.0,2X),3(F5.0,2X),F3.0,24X,F3.0,2X,F5.3,2X,F3.0,2X,
1F5.3,2X,F5.3)
59 FORMAT (6X,6(F4.0,2X),3(F5.0,2X),2(F3.0,2X),24X,F3.0,2X,F5.3,2X,F5
1,3)
60 FORMAT (6X,6(F4.0,2X),3(F5.0,2X),5X,F3.0,7X,F3.0,2X,F5.3,14X,F3.0,
12X,F5.3,2X,F5.3)
61 FORMAT (F10.3,F10.0/6F10.5/6F10.5/11)
62 FORMAT (6F10.4)
63 FORMAT (6F10.4)
64 FORMAT (6F10.0)
65 FORMAT (4F10.4/F10.4/F10.6)
66 FORMAT (1H1,5X,5MIN =,F8.4,3X,4MMU =,F6.3,3X,5MRPM =,F6.0//6X,8MC
1APR21 =,F8.5,3X,8MCAPR2 =,F8.5,3X,8MCAPR3 =,F8.5//6X,5MRP2 =,F8.
25,3X,5MRP3 =,F8.5,3X,5MRP4 =,F8.5//6X,8HACG1 =,F8.5,3X,8HACG2 =,F8
35,3X,8HACG3 =,F8.5//6X,8HACP1 =,F8.5,3X,8HACP2 =,F8.5,3X,8HACP3 =
A 796
A 797
A 798
A 799
A 800
A 801
A 802
A 803
A 804
A 805
A 806
A 807
A 808
A 809
A 810
A 811
A 812
A 813
A 814
A 815
A 816
A 817
A 818
A 819
A 820
A 821
A 822
A 823
A 824
A 825
A 826
A 827
A 828
A 829
A 830
A 831
A 832
A 833
A 834
A 835
A 836
A 837
A 838
A 839
A 840
A 841
A 842
A 843
A 844
A 845
A 846
A 847
A 848

```

I-41

```

1  SUBROUTINE TRANS1 (RHOG,ALPHP,BETA,FP,ACG,B,DELG,Z,PSIT,PHIT,G)
    PI=3.14159
    SI=(-RHOG*COS(PSIT-ALPHP)+B*SIN(BETA)+FP*SIN(PSIT-ALPHP))/ACG
    CT=(RHOG*SIN(PSIT-ALPHP)+B*COS(BETA)+FP*COS(PSIT-ALPHP))/ACG
    PHIT=ATAN2(ST,CT)-DELG
    PHINEXT=PHIT-.1*Z
    AF=ACG*COS(PHINEXT+DELG+ALPHP)-B*COS(BETA+ALPHP)
    BF=-ACG*SIN(PHINEXT+DELG+ALPHP)+B*SIN(BETA+ALPHP)
    CF=RHOG
    ROOTF=AF*AF+BF*BF+CF*CF
    YF1=AF+SQRT(ROOTF)
    YF2=AF-SQRT(ROOTF)
    XF=BF+CF
    PSINEX1=2.*ATAN2(YF1,XF)
    PSINEX2=2.*ATAN2(YF2,XF)
    IF (PSINEX1.LT.0.) PSINEX1=PSINEX1+2.*PI
    IF (PSINEX2.LT.0.) PSINEX2=PSINEX2+2.*PI
    IF (ABS(PSINEX1-PSIT).LT.ABS(PSINEX2-PSIT)) GO TO 1
    PSINEX1=PSINEX2
    GO TO 2
2  PSINEX1=PSINEX1
    G=(ACG*SIN(PHINEXT+DELG)+RHOG*COS(PSINEX1-ALPHP)-B*SIN(BETA))/SIN(
    1 PSINEX1-ALPHP)
    RETURN
    END
25

```

14.52.13

08/01/79

FTN 4.6+420

74/74 OPT=1

SUBROUTINE TRANS2

```

1  SUBROUTINE TRANS2 (RHOG,ALPHP,BETA,FP,ACG,B,DELG,Z,PSIT,PHIT,G)
   PI=3.14159
   ST=(RHOG*COS(PSIT+ALPHP)+B*SIN(BETA)+FP*SIN(PSIT+ALPHP))/ACG
   CT=(-RHOG*SIN(PSIT+ALPHP)+B*COS(BETA)+FP*COS(PSIT+ALPHP))/ACG
   PHIT=ATAN2(ST,CT)+DELG
   PHINEXT=PHIT+.1*Z
   AF=ACG*COS(PHINEXT-DELG-ALPHP)-B*COS(BETA-ALPHP)
   BF=-ACG*SIN(PHINEXT-DELG-ALPHP)+B*SIN(BETA-ALPHP)
   CF=-RHOG
   ROOTF=AF+BF+CF*CF
   YF1=AF+SQRT(ROOTF)
   YF2=AF-SQRT(ROOTF)
   XF=BF+CF
   PSINEX1=2.*ATAN2(YF1,XF)
   PSINEX2=2.*ATAN2(YF2,XF)
   IF (PSINEX1.LT.0.) PSINEX1=PSINEX1+2.*PI
   IF (PSINEX2.LT.0.) PSINEX2=PSINEX2+2.*PI
   IF (ABS(PSINEX1-PSIT).LT.ABS(PSINEX2-PSIT)) GO TO 1
   PSINEX1=PSINEX2
   GO TO 2
1  PSINEX1=PSINEX1
2  G=(ACG*SIN(PHINEXT-DELG)-RHOG*COS(PSINEX1+ALPHP)-B*SIN(BETA))/SIN(
   PSINEX1+ALPHP)
   RETURN
   END

```

MIN = .1645 BU = .200 RPM = 1000.
 CAPRP1 = .47725 CAPRP2 = .20670 CAPRP3 = .17560
 RP2 = .09085 RP3 = .06890 RP4 = .05905
 ACG1 = .47725 ACG2 = .20670 ACG3 = .17560
 ACP1 = .09085 ACP2 = .06890 ACP3 = .05905
 R1 = .75000 R2 = .75000 R3 = .75000 R4 = .75000
 RHOG1 = .03870 RHOG2 = .02670 RHOG3 = .01910 RHOP1 = .01740 RHOP2 = .01040 RHOP3 = .00875
 TGI = .33480 TGI2 = .02520 TGI3 = .02170 TP1 = .02800 TP2 = .02080 TP3 = .01750
 MGI = 42. MG2 = 27. MG3 = 27. MP2 = 8. MP3 = 9. MP4 = 9.
 M1 = .69515E-04 M2 = .97028E-05 M3 = .70027E-05 M4 = .79188E-06
 RH01 = .060 RH02 = .030 RH03 = .025 RH04 = .020
 WD = .1500E-04
 K = 25.0
 PHOOT1 = -1.0
 FPI = .08917 FP2 = .06811 FP3 = .05840
 BETA10 = 112.2552 BETA20 = 145.0978 BETA30 = 164.6850
 PSI1T10 = 305.6017 TEST11 = 4.4495
 PSI1T20 = 343.6259 TEST12 = 42.4736
 PHI1T10 = 113.5016 PSI1T10 = 305.6017
 PHI1T20 = 115.9930 PSI1T20 = 292.4283 PHI1T10 = 107.4216 PSI1T20 = 337.4283
 PSI2T10 = 286.9442 TEST21 = 29.4719
 PSI2T20 = 312.0785 TEST22 = 4.3377
 PHI2T10 = 142.0461 PSI2T10 = 312.0785
 PHI2T20 = 136.7828 PSI2T20 = 330.9531 PHI2T10 = 150.1161 PSI2T20 = 290.9531
 PSI3T10 = 357.5003 TEST31 = 4.2938
 PSI3T20 = 25.1346 TEST32 = 31.9282
 PHI3T10 = 166.7857 PSI3T10 = 357.5003
 PHI3T20 = 173.6791 PSI3T20 = 336.8610 PHI3T10 = 160.3457 PSI3T20 = 15.8610
 PHI1 PHI2 PHI3 PSI1 PSI2 PSI3 DPS11 DPS12 DPS13 S1R S2R S3R S1F G1 S2F G2 S3F G3
 116. 137. 174. 292. 331. 337. 5. -16. 59. 1. -1. 1.

.468

114.	148.	167.	304.	297.	356.	5.	-16.	47.	-1.	-1.	1.	.066	1.	.058	.526
114.	148.	167.	304.	297.	356.	5.	-16.	47.	-1.	-1.	1.	.066	1.	.058	.520
114.	148.	166.	304.	296.	360.	5.	-16.	48.	-1.	-1.	1.	.066	1.	.058	.515
114.	148.	166.	304.	296.	1.	5.	-16.	48.	-1.	-1.	1.	.066	1.	.057	.509
114.	149.	165.	304.	295.	3.	5.	-15.	47.	-1.	-1.	1.	.066	1.	.057	.504
114.	149.	164.	304.	295.	4.	5.	-15.	47.	-1.	-1.	1.	.066	1.	.057	.499
114.	149.	164.	305.	294.	6.	5.	-15.	47.	-1.	-1.	1.	.066	1.	.056	.494
114.	149.	163.	305.	294.	8.	5.	-15.	46.	-1.	-1.	1.	.066	1.	.056	.490
114.	149.	163.	305.	293.	9.	5.	-15.	46.	-1.	-1.	1.	.066	1.	.056	.485
114.	149.	162.	305.	293.	11.	5.	-15.	45.	-1.	-1.	1.	.066	1.	.056	.480
114.	150.	162.	305.	292.	12.	5.	-15.	45.	-1.	-1.	1.	.066	1.	.056	.475
114.	150.	161.	305.	292.	14.	5.	-15.	43.	-1.	-1.	1.	.066	1.	.056	.470
113.	137.	161.	306.	331.	15.	5.	-15.	42.	-1.	-1.	1.	.067	1.	.056	.465
113.	137.	161.	306.	331.	15.	5.	-15.	42.	-1.	-1.	1.	.067	1.	.056	.465
113.	137.	160.	306.	330.	17.	5.	-16.	47.	-1.	-1.	1.	.067	1.	.056	.481
113.	137.	174.	306.	330.	337.	5.	-16.	47.	-1.	-1.	1.	.067	1.	.056	.479
113.	137.	173.	306.	329.	339.	5.	-16.	51.	-1.	-1.	1.	.089	1.	.056	.492
113.	138.	173.	307.	329.	340.	5.	-16.	50.	-1.	-1.	1.	.089	1.	.056	.499
113.	138.	173.	307.	329.	340.	5.	-16.	49.	-1.	-1.	1.	.089	1.	.056	.506
113.	138.	172.	307.	328.	342.	5.	-16.	49.	-1.	-1.	1.	.088	1.	.056	.513
113.	138.	171.	307.	328.	344.	5.	-16.	48.	-1.	-1.	1.	.088	1.	.056	.519
113.	138.	171.	307.	327.	345.	5.	-16.	48.	-1.	-1.	1.	.088	1.	.056	.525
113.	138.	170.	307.	327.	347.	5.	-16.	48.	-1.	-1.	1.	.088	1.	.056	.531
113.	138.	170.	308.	326.	348.	5.	-16.	48.	-1.	-1.	1.	.088	1.	.056	.537
113.	139.	169.	308.	325.	350.	5.	-16.	48.	-1.	-1.	1.	.088	1.	.056	.543
113.	139.	168.	308.	325.	352.	5.	-16.	48.	-1.	-1.	1.	.088	1.	.056	.548
113.	139.	168.	308.	324.	353.	5.	-16.	49.	-1.	-1.	1.	.088	1.	.056	.546
113.	139.	168.	308.	324.	355.	5.	-16.	49.	-1.	-1.	1.	.088	1.	.056	.542
113.	140.	166.	309.	323.	357.	5.	-16.	49.	-1.	-1.	1.	.087	1.	.058	.539
113.	140.	166.	309.	322.	358.	5.	-16.	49.	-1.	-1.	1.	.087	1.	.058	.536
113.	140.	165.	309.	322.	2.	5.	-16.	50.	-1.	-1.	1.	.087	1.	.058	.533
113.	140.	165.	309.	321.	3.	5.	-16.	50.	-1.	-1.	1.	.087	1.	.057	.530
113.	140.	164.	309.	320.	5.	5.	-16.	50.	-1.	-1.	1.	.087	1.	.057	.528
113.	140.	164.	310.	320.	7.	5.	-16.	50.	-1.	-1.	1.	.087	1.	.056	.525
113.	141.	163.	310.	319.	9.	5.	-16.	50.	-1.	-1.	1.	.087	1.	.056	.523
113.	141.	163.	310.	319.	10.	5.	-16.	50.	-1.	-1.	1.	.087	1.	.056	.520
113.	141.	162.	310.	318.	12.	5.	-16.	50.	-1.	-1.	1.	.087	1.	.056	.517
113.	141.	162.	310.	318.	14.	5.	-16.	49.	-1.	-1.	1.	.087	1.	.056	.514
113.	141.	161.	310.	317.	15.	5.	-16.	48.	-1.	-1.	1.	.086	1.	.056	.511
113.	142.	160.	311.	317.	17.	5.	-17.	47.	-1.	-1.	1.	.086	1.	.056	.508
113.	142.	174.	311.	316.	337.	5.	-17.	51.	-1.	-1.	1.	.086	1.	.056	.505
113.	142.	173.	311.	315.	339.	5.	-17.	51.	-1.	-1.	1.	.086	1.	.056	.525
112.	142.	173.	311.	315.	340.	6.	-17.	51.	-1.	-1.	1.	.086	1.	.056	.529
112.	142.	172.	311.	314.	342.	6.	-17.	50.	-1.	-1.	1.	.086	1.	.056	.532
112.	143.	171.	312.	314.	344.	6.	-17.	50.	-1.	-1.	1.	.086	1.	.056	.536
112.	143.	171.	312.	313.	345.	6.	-17.	50.	-1.	-1.	1.	.086	1.	.056	.538
112.	143.	170.	312.	313.	347.	6.	-17.	50.	-1.	-1.	1.	.086	1.	.056	.541
112.	143.	170.	312.	312.	349.	6.	-17.	50.	-1.	-1.	1.	.086	1.	.056	.543
112.	143.	169.	312.	311.	350.	6.	-17.	50.	-1.	-1.	1.	.085	1.	.056	.546
112.	143.	169.	313.	311.	352.	6.	-17.	50.	-1.	-1.	1.	.085	1.	.056	.548
112.	144.	168.	313.	310.	354.	6.	-17.	50.	-1.	-1.	1.	.085	1.	.056	.549
112.	144.	167.	313.	310.	356.	6.	-17.	51.	-1.	-1.	1.	.085	1.	.056	.541
112.	144.	166.	313.	309.	357.	6.	-17.	51.	-1.	-1.	1.	.085	1.	.056	.534
112.	144.	166.	313.	309.	359.	6.	-17.	52.	-1.	-1.	1.	.085	1.	.056	.527
112.	144.	166.	313.	308.	1.	6.	-17.	52.	-1.	-1.	1.	.085	1.	.058	.520
112.	145.	165.	314.	307.	2.	6.	-17.	52.	-1.	-1.	1.	.085	1.	.057	.514
112.	145.	165.	314.	307.	4.	6.	-17.	52.	-1.	-1.	1.	.085	1.	.057	.507
112.	145.	164.	314.	306.	6.	6.	-17.	52.	-1.	-1.	1.	.085	1.	.056	.501
112.	145.	163.	314.	306.	8.	6.	-17.	52.	-1.	-1.	1.	.085	1.	.056	.496
112.	145.	163.	314.	305.	10.	6.	-17.	52.	-1.	-1.	1.	.085	1.	.056	.490
112.	145.	162.	315.	305.	11.	6.	-17.	51.	-1.	-1.	1.	.085	1.	.056	.484
112.	145.	162.	315.	305.	11.	6.	-17.	51.	-1.	-1.	1.	.085	1.	.056	.478

108.	140.	167.	336.	320.	357.	5.	-14.	41.	-1.	-1.	1.	.084	1.	.058	.470
108.	140.	167.	336.	320.	358.	5.	-14.	41.	-1.	-1.	1.	.084	1.	.058	.467
108.	141.	166.	337.	320.	359.	4.	-13.	41.	-1.	-1.	1.	.084	1.	.058	.465
108.	141.	166.	337.	319.	1.	4.	-13.	41.	-1.	-1.	1.	.084	1.	.057	.464
108.	141.	165.	337.	319.	2.	4.	-13.	41.	-1.	-1.	1.	.084	1.	.057	.462
108.	141.	165.	337.	318.	3.	4.	-13.	41.	-1.	-1.	1.	.085	1.	.057	.460
107.	141.	164.	337.	318.	5.	4.	-13.	41.	-1.	-1.	1.	.085	1.	.057	.458
107.	141.	164.	337.	317.	6.	4.	-13.	41.	-1.	-1.	1.	.085	1.	.056	.456

CYCLE EFFICIENCY = .491

2. Program CLOCK 4: Point and Cycle Efficiencies for Two Pass
Clock (Oxival) Step-Up Gear Train in
Spin Environment

The kinematics of program CLOCK 4 is again based on the work in Appendix G. The moment input-output relationships are derived in section 2 of Appendix H. This program is in many ways very similar to CLOCK 3 with the exception that only two meshes are involved, and therefore, wherever possible, reference will be made to CLOCK 3. Again, it is assumed that the two meshes will have been tested by program CLOCK 1 for their geometric suitability. The format of the following is identical to that used in section 1 of this appendix. For the sake of clarity, it will be helpful to refer to these parallel descriptions.

a. Input Parameters (see Program CLOCK 4, below)

The following parameters represent the input data for the program (for explanation, refer to section 1a of this appendix):

MU

RPM

CAPRP1, CAPRP2, RP2, RP3

RHOG1, RHOG2, RHOP1, RHOP2

ACG1, ACG2, ACP1, ACP2

R1, R2, R3

TG1, TG2, TP1, TP2

NG1, NG2, NP2, NP3

RHO1, RHO2, RHO3

M1, M2, M3

MD

K

PHDOT1 = -1

b. Computations (see also COMMENT cards in program)

I. Computation of Gear Tooth Parameters

The required computations are identical to those in CLOCK 3.

II. Computation of MIN, GAMMAS and BETAS

The input moment is computed in the manner of eq. (I-1).

In addition, the angles γ_2 , γ_3 , β_1 and β_2 are found according to the expressions given in section 6b of Appendix A.

III. Computation of Other Parameters

The computation of the angles $\Delta\varphi_1$ and $\Delta\psi_1$, the length L_1 as well as the centrifugal forces Q_1 , Q_2 and Q_3 (called Q_{3p} by eq. (H-245)) are identical to those described in the parallel section dealing with CLOCK 3.

IV. Preliminary Computations for Mesh 1

The preliminary computations for mesh 1 are identical to those given in section 1-IV of this appendix.

V. Preliminary Computations for Mesh 2

The preliminary computations for mesh 2 are identical to those given in section 1-V of this appendix.

VI. Gear Train Motion Model: Kinematics, Point and Cycle Efficiencies

The simulation of the gear train model, which is necessary for the determination of both `POINTEF` and `CYCLEFF`, is found in a loop starting with statement label no.20 and ending with card no.531. The motions of the individual driving gears are initialized at their respective angles PHI1I and PHI2I . The meshes will be in round on round contact until they reach their respective transition angles PHI1T and PHI2T . After the transition angles are passed, the meshes will be in round on flat contact. These regimes continue until the final angles PHI1F and PHI2F are reached.

The increment DDPHI1 of the input gear 1 is obtained from an adaptation of eqs. (A-207) and (A-208), in which tooth numbers, rather than base circle radii are used. The increment DDPHI2 of gear 2 is related to the increment of the pinion angle PSI1 .

While the motion of gear 1 is terminated when the angle PHI1 reaches the magnitude PHI1F (or rather $\text{PHI1F} + \text{DDPHI1}$ for moment summation purposes), gear 2 must be reset to its starting angle PHI2I whenever its final angle PHI2F has been reached.

The appropriate choice of moment equation depends upon which of the four possible combinations of contact conditions, as indicated by Table H-2, is applicable.

The following discusses the kinematics of the individual meshes as well as the determination of the point and cycle efficiencies where they differ from the description in section 1 of this appendix.

A. Kinematics

The program only utilizes the kinematics of meshes 1 and 2. These are identical with those for program CLOCK 3, as given in section 1.

B. Moment Computations, Point and Cycle Efficiencies

Regardless of the combination of contact conditions, the point efficiency is computed according to eq. (3), i.e.,

$$\eta_p = \text{POINTER} = K_{\text{ratio}} \frac{M_{031}}{M_{1n}} \quad (\text{I-24})$$

where, with $\dot{\phi}_1 = -1$

$$K_{\text{ratio}} = |\dot{\psi}_2| \quad (\text{I-25})$$

The cycle efficiency determination is based on eqs. (I-21) to (I-23).

The moment computations begin with the statement label no.24, and initially consist of the determination of selected variables between A11 and A72 and selected variables between C6 and C36, as applicable to the analyses of section 2 of Appendix H. The governing contact combination (see also Table H-2) is determined with the help of the four moment control statements, which start with card no.498. Once the appropriate combination is established, the program is directed to one of the four associated moment expressions. These expressions for M_{031} coincide with those given by eqs. (H-260), (H-261), (H-277) and (H-278). They are listed in the above

order beginning with statement label no.25 and ending with statement label no.28 .

The rationale of the control statements for meshes 1 and 2 is identical to that given for program CLOCK 3 (see section 1-VIIB of this appendix).

c. Output (see Program CLOCK 4, below)

The output of the program is best explained with the help of the sample problem at the end of the program.

I. Input Parameters

Mesh 1

CAPRP1 = R_{P1} = .47725 in. (1.212 cm)
RP2 = r_{P2} = .09085 in. (0.231 cm)
ACG1 = a_{G1} = .47725 in. (1.212 cm)
ACP1 = a_{P1} = .09085 in. (0.231 cm)
RHOG1 = ρ_{G1} = .03870 in. (0.098 cm)
RHOP1 = ρ_{P1} = .01740 in. (0.044 cm)
TG1 = t_{G1} = .03480 in. (0.088 cm)
TP1 = t_{P1} = .02800 in. (0.71 cm)
NG1 = n_{G1} = 42
NP2 = n_{P2} = 8

Mesh 2

CAPRP2 = R_{P2} = .20670 in. (0.525 cm)
RP3 = r_{P3} = .06890 in. (0.175 cm)
ACG2 = a_{G2} = .20670 in. (0.525 cm)
ACP2 = a_{P2} = .06890 in. (0.175 cm)

RHOG2 = ρ_{G2} = .02070 in. (0.053 cm)
 RHOP2 = ρ_{P2} = .01040 in. (0.026 cm)
 TG2 = t_{G2} = .02520 in. (0.064 cm)
 TP2 = t_{P2} = .02080 in. (0.053 cm)
 NG2 = n_{G2} = 27
 NP3 = n_{P3} = 9

In addition

MU = .2
 RPM = 1000
 M1 = m_1 = $.69515 \times 10^{-4}$ lb-sec²/in. (12.171 g)
 M2 = m_2 = $.97028 \times 10^{-5}$ lb-sec²/in. (1.699 g)
 M3 = m_3 = $.10780 \times 10^{-5}$ lb-sec²/in. (0.189 g)
 R1 = R_1 = .750 in. (1.905 cm)
 R2 = R_2 = .750 in. (1.905 cm)
 R3 = R_3 = .750 in. (1.905 cm)
 RHO1 = ρ_1 = .060 in. (0.152 cm)
 RHO2 = ρ_2 = .030 in. (0.076 cm)
 RHO3 = ρ_3 = .025 in. (0.051 cm)
 MD = md^2 = $.15 \times 10^{-4}$ lb-sec² in. (16.944 g - cm²)
 K = 25

II. Computed Values

At the beginning of the output, one finds MIN = M_{in} .
 Subsequently, the following are listed for each mesh:

f_{P1} , the length of the pinion flats
 β_1 , the fuze body pivot to pivot line angles

ψ_{T1} and φ_{T1} , the transition angles as well as the associated subsidiary tests

φ_{IN1} and ψ_{IN1} , the initial angles

φ_{FIN1} and ψ_{FIN1} , the final angles

Finally, for the full range of the input angle φ_1 , the point efficiency POINTEF is listed, in addition to other parameters which are useful for checking purposes. Note that DPSI1 and DPSI2 represent $\dot{\psi}_1$ and $\dot{\psi}_2$, respectively. The cycle efficiency CYCLEFF is found at the end of the output.

Program CLOCK 4

I-57

07/31/79 11.35.22

FTN 4.6+420

74/74 OPT=1

PROGRAM CLOCK4

1		PROGRAM CLOCK4(INPUT,OUTPUT,TAPE5=INPUT,TAPE6=OUTPUT)	A 1
	C		A 2
	C	POINT AND CYCLE EFFICIENCIES FOR TWO PASS CLOCK (OGIVAL) STEP-UP	A 3
	C	GEAR TRAIN IN SPIN ENVIRONMENT	A 4
5	C		A 5
		REAL MU, LAMDA1, LAMDA2, LX1, LY1, L1, LX2, LY2, L2, NP2, NP3, NG1, NG2, MIN, M1	A 6
		1.32, M3, M03, M031, M032, M033, M034, MTOT, MD, LL1, LL2, K	A 7
		1 READ (5.40) MU, RPM, CAPRP1, CAPRP2, RP2, RP3, ACG1, ACG2, ACP1, ACP2, ISTOP	A 8
		READ (5.58) R1, R2, R3	A 9
		READ (5.41) RHOG1, RHOG2, RHOP1, RHOP2	A 10
10		READ (5.42) TGT, TG2, TPT, TP2	A 11
		READ (5.43) NG1, NG2, NP2, NP3	A 12
		READ (5.61) M1, M2, M3	A 13
		READ (5.44) RHOT, RHOD2, RHOD3, MD, K, J1, J2	A 14
15		P1=3.14159	A 15
		Z=PI/180.	A 16
		OMEGA=KPM*2.*PI/60.	A 17
		OM2=OMEGA*OMEGA	A 18
		PHOO11=-1.	A 19
20	C	COMPUTATION OF GEAR TOOTH PARAMETERS FOR BOTH MESHES	A 20
	C		A 21
	C		A 22
		CXG1=RHOG1-TG1/2.	A 23
		DELGI=ASIN(CXG1/CAPRP1)	A 24
		CXP1=RHOP1-TP1/2.	A 25
25		DELP1=ASIN(CXP1/RP2)	A 26
		GAMMP1=ASIN(RHOP1/RP2)	A 27
		ALPHP1=GAMMP1-DELP1	A 28
		FPI=ACP1-COS(GAMMP1)	A 29
		B1=CAPRP1+RP2	A 30
30		CXG2=RHOG2-TG2/2.	A 31
		DELG2=ASIN(CXG2/CAPRP2)	A 32
		CXP2=RHOP2-TP2/2.	A 33
		DELP2=ASIN(CXP2/RP3)	A 34
35		GAMMP2=ASIN(RHOP2/RP3)	A 35
		ALPHP2=GAMMP2-DELP2	A 36
		FP2=ACP2-COS(GAMMP2)	A 37
		B2=CAPRP2+RP3	A 38
40	C	COMPUTATION OF MIN, GAMMAS AND BETAS	A 39
	C		A 40
	C		A 41
		MIN=MD-OM2	A 42
		DELTA2=ACOS(((CAPRP1+RP2)*(CAPRP1+RP2)+R1+R1-R2-R2)/(2.*R1*(CAPRP1	A 43
45		1+RP2)))	A 44
		DELTA3=ACOS(((CAPRP2+RP3)*(CAPRP2+RP3)+R2+R2-R3-R3)/(2.*R2*(CAPRP2	A 45
		1+RP3)))	A 46
		GAMMA2=ACOS((R1+R1-R2-R2-(CAPRP1+RP2)*(CAPRP1+RP2))/(2.*R1+R2))	A 47
		GAMMA3P=ACOS((R2+R2-R3-R3-(CAPRP2+RP3)*(CAPRP2+RP3))/(2.*R2+R3))	A 48
		GAMMA3=GAMMA2+GAMMA3P	A 49
		BETA1=PI-DELTA2	A 50
50		BETA2=GAMMA2+PI-DELTA3	A 51
		BETA1D=BETA1/Z	A 52
		BETA2D=BETA2/Z	A 53

```

55 WRITE (6,45) MIN,MU,RPM,CAPRP1,CAPRP2,RP2,RP3,ACG1,ACG2,ACP1,ACP2
   WRITE (6,59) R1,R2,R3
   WRITE (6,46) RHOG1,RHOG2,RHOP1,RHOP2
   WRITE (6,47) TGI,IG2,TP1,TP2
   WRITE (6,48) NG1,NG2,NP2,NP3
   WRITE (6,62) M1,M2,M3
   WRITE (6,49) RH01,RH02,RH03,MO,K,PHOOT1
   WRITE (6,60) FPI,FP2
   WRITE (6,50) BETA10,BETA20

60

65 COMPUTATION OF OTHER PARAMETERS
   C
   C
   C
   DPHI1=360./NG1*Z
   DPSI1=360./NP2*Z
   DPHI2=360./NG2*Z
   DPSI2=360./NP3*Z
   L1=RHOG1+RHOP1
   L2=RHOG2+RHOP2
   Q1=M1*R1*OM2
   Q2=M2*R2*OM2
   Q3=M3*R3*OM2

70

75 PRELIMINARY COMPUTATIONS FOR MESH 1
   C
   C
   C
   C
   C
   DETERMINATION OF TRANSITION ANGLE OF MESH 1
   A1T=RHOG1*COS(BETA1+ALPH1)+FPI*SIN(BETA1+ALPH1)
   B1T=-RHOG1*SIN(BETA1+ALPH1)+FPI*COS(BETA1+ALPH1)
   C1T=(ACG1*ACG1-RHOG1*RHOG1-81*81-FPI*FPI)/(2.*81)
   ROOT11=A1T+A1T*B1T-B1T-C1T*C1T
   Y1T1=A1T+SORT(ROOT11)
   Y1T2=A1T-SORT(ROOT11)
   X1T=81T+C1T
   PS11T1=2.*ATAN2(Y1T1,X1T)
   PS11T2=2.*ATAN2(Y1T2,X1T)
   PS11E11=PS11T1
   PS11E12=PS11T2
   IF (PS11T1.GT.PI) PS11E11=PS11E11-2.*PI
   IF (PS11T1.LT.PI) PS11E11=PS11E11+2.*PI
   IF (PS11T2.GT.PI) PS11E12=PS11E12-2.*PI
   IF (PS11T2.LT.PI) PS11E12=PS11E12+2.*PI
   IF (PS11E11.GE.0.) TEST11=ABS(PI-BETA1+PS11E11-ALPH1)/Z
   IF (PS11E11.LT.0.) TEST11=ABS(PI+BETA1-(PS11E11+2.*PI-ALPH1))/Z
   IF (PS11E12.GE.0.) TEST12=ABS(PI-BETA1+PS11E12-ALPH1)/Z
   IF (PS11E12.LT.0.) TEST12=ABS(PI+BETA1-(PS11E12+2.*PI-ALPH1))/Z
   IF (PS11T1.LT.0.) PS11T1=PS11T1+2.*PI
   IF (PS11T2.LT.0.) PS11T2=PS11T2+2.*PI
   PS11I10=PS11T1/Z
   PS11I20=PS11T2/Z
   WRITE (6,31) PS11I10,TEST11
   WRITE (6,32) PS11I20,TEST12
   CALL TRANS1 (RHOG1,ALPH1,BETA1,FPI,ACG1,B1,DELGI,Z,PS11T1,PHI1T1,
100 1E11)
105

```

```

110 IF (G11.GT.FP1) GO TO 2
    PHI1T=PHI1T1
    PSI1T=PSI1T1
    GO TO 4
111 2 CALL TRANS1 (RHOG1,ALPH1,BETA1,FP1,ACG1,B1,DELGI,Z,PSI1T2,PHI1T2,
    1G12)
    IF (G12.LT.FP1) GO TO 3
    WRITE (6,51)
    STOP
115 3 PHI1T=PHI1T2
    PSI1T=PSI1T2
    4 IF (PHI1T.LT.0.) PHI1T=PHI1T+2.*PI
    IF (PSI1T.LT.0.) PSI1T=PSI1T+2.*PI
    PHI1TD=PHI1T/Z
    PSI1TD=PSI1T/Z
    WRITE (6,52) PHI1TD,PSI1TD
120
125 C
    C DETERMINATION OF CORRECT SIGN FOR ROUND ON FLAT REGIME OF MESH 1
    C
    A1F=ACG1-COS(PHI1T+DELGI+ALPH1)-B1-COS(BETA1+ALPH1)
    B1F=-ACG1+SIN(PHI1T+DELGI+ALPH1)+B1-5.*SIN(BETA1+ALPH1)
    C1F=RHOG1
    ROOT1F=A1F+A1F+B1F+B1F-C1F-C1F
    Y1F1=A1F+SQRT(ROOT1F)
    Y1F2=A1F-SQRT(ROOT1F)
    X1F=B1F+C1F
    PSI1F1=2.*ATAN2(Y1F1,X1F)
    PSI1F2=2.*ATAN2(Y1F2,X1F)
    IF (PSI1F1.LT.0.) PSI1F1=PSI1F1+2.*PI
    IF (PSI1F2.LT.0.) PSI1F2=PSI1F2+2.*PI
    IF (ABS(PSI1F1-PSI1T)-LT.ABS(PSI1F2-PSI1T)) GO TO 5
    SIGN1F=-1.
    GO TO 6
130
135 5 SIGN1F=1.
140
145 C
    C COMPUTATION OF FINAL AND INITIAL VALUES OF PHI AND PSI FOR MESH 1
    C
    6 DO 7 I=1,2000
        PHID1=PHI1TD-((I-1.)/100.
        PHI1=PHID1+Z
        A1F=ACG1-COS(PHI1+DELGI+ALPH1)-B1-COS(BETA1+ALPH1)
        B1F=-ACG1+SIN(PHI1+DELGI+ALPH1)+B1-SIN(BETA1+ALPH1)
        C1F=RHOG1
        ROOT1F=A1F+A1F+B1F+B1F-C1F-C1F
        Y1F=A1F+SQRT(ROOT1F)
        Y1F=B1F+C1F
        PSI1F=2.*ATAN2(Y1F,X1F)
        IF (PSI1F.LT.0.) PSI1F=PSI1F+2.*PI
        LX1=B1-COS(BETA1)+ACG1-COS(PSI1F-DPSI1+DELPI)-ACG1-COS(PHI1+DPHI1+
        1DELGI)
        LY1=B1-SIN(BETA1)+ACG1+SIN(PSI1F-DPSI1+DELPI)-ACG1+SIN(PHI1+DPHI1+
        1DELGI)
        LL1=SQRT(LX1+LY1+LY1)
150
155
159

```

```

160 DELEL1=LL1-L1
    IF (DELEL1.LE.0.) GO TO 8
7 CONTINUE
8 PH11F=PH11
  PSI1FF=PSI1F
  PH11F=PH11F+DPH11
  PSI1F=PSI1FF-DPSI1
  IF (PSI11.LT.0.) PSI11=PSI11+2.*PI
  PH11D=PH11/Z
  PSI1D=PSI11/Z
  PH11FD=PH11F/Z
  PSI1FD=PSI1FF/Z
  WRITE (6,53) PH11D,PSI1D,PH11FD,PSI1FD
C
C
175 DETERMINATION OF CORRECT SIGN FOR ROUND ON ROUND REGIME OF MESH 1
C
      A1R=ACG1*SIN(PH111+DELG1-DELP1)-B1*SIN(BETA1-DELP1)
      B1R=ACG1*COS(PH111+DELG1-DELP1)-B1*COS(BETA1-DELP1)
      C1R=(ACP1*ACP1+ACG1*ACG1+B1*B1-L1*L1-2.*ACG1*B1*COS(PH111+DELG1-DE
180      L11))/2.*ACP1
      ROOT1R=A1R*A1R+B1R*B1R-C1R*C1R
      Y1R=A1R+SORT(ROOT1R)
      Y1R2=A1R-SORT(ROOT1R)
      X1R=B1R+C1R
      PSI1R1=2.*ATAN2(Y1R1,X1R)
      PSI1R2=2.*ATAN2(Y1R2,X1R)
      IF (PSI1R1.LT.0.) PSI1R=PSI1R1+2.*PI
      IF (PSI1R2.LT.0.) PSI1R2=PSI1R2+2.*PI
      IF (ABS(PSI11-PSI1R1).LT.ABS(PSI11-PSI1R2)) GO TO 9
      SIGNR=-1.
      GO TO 10
9 SIGNR=1.
C
C
195 PRELIMINARY COMPUTATIONS FOR MESH 2
C
C
      DETERMINATION OF TRANSITION ANGLE OF MESH 2
C
10 A21=-RHOG2*COS(BETA2-ALPHP2)+FP2*SIN(BETA2-ALPHP2)
    B21=-RHOG2*SIN(BETA2-ALPHP2)+FP2*COS(BETA2-ALPHP2)
    C21=(ACG2*ACG2-RHOG2*RHOG2-B2*B2-FP2*FP2)/(2.*B2)
    ROOT21=A21+A21+B21*B21-C21*C21
    Y21=A21+SORT(ROOT21)
    Y212=A21-SORT(ROOT21)
    X21=B21+C21
    PSI211=2.*ATAN2(Y211,X21)
    PSI212=2.*ATAN2(Y212,X21)
    PSI2E1=PSI211
    PSI2E2=PSI212
    IF (PSI2T1.GT.PI) PSI2E1=PSI2E1-2.*PI
    IF (PSI2T1.LT.PI) PSI2E1=PSI2E1+2.*PI
    IF (PSI2T2.GT.PI) PSI2E2=PSI2E2-2.*PI
    IF (PSI2T2.LT.PI) PSI2E2=PSI2E2+2.*PI
    IF (PSI2E1-GE.0.) TEST21=ABS(PI-BETA2+PSI2E1+ALPHP2)/Z

```

```

215 IF (PSITE21-LT.0.) TEST21=ABS(PI+BETA2-(PSITE21+2.*PI+ALPHAP2))/Z
    IF (PSITE22-GE.0.) TEST22=ABS(PI-BETA2+PSITE22-ALPHAP2)/Z
    IF (PSITE22-LT.0.) TEST22=ABS(PI+BETA2-(PSITE22+2.*PI+ALPHAP2))/Z
    IF (PSI2T1-LT.0.) PSI2T1=PSI2T1+2.*PI
    IF (PSI2T2-LT.0.) PSI2T2=PSI2T2+2.*PI
    PSI2T1D=PSI2T1/Z
    PSI2T2D=PSI2T2/Z
    WRITE (6,33) PSI2T1D,TEST21
    WRITE (6,34) PSI2T2D,TEST22
    CALL TRANS2 (RHOG2,ALPHAP2,BETA2,FP2,ACG2,B2,DELG2,Z,PSI2T1,PHI2T1,
    1G21)
    IF (G21-GT.FP2) GO TO 11
    PHI2T=PHI2T1
    PSI2T=PSI2T1
    GO TO 13
11 CALL TRANS2 (RHOG2,ALPHAP2,BETA2,FP2,ACG2,B2,DELG2,Z,PSI2T2,PHI2T2,
    1G22)
    IF (G22-LT.FP2) GO TO 12
    WRITE (6,54)
    STOP
12 PHI2T=PHI2T2
    PSI2T=PSI2T2
13 IF (PHI2T-LT.0.) PHI2T=PHI2T+2.*PI
    IF (PSI2T-LT.0.) PSI2T=PSI2T+2.*PI
    PHI2TD=PHI2T/Z
    PSI2TD=PSI2T/Z
    WRITE (6,55) PHI2TD,PSI2TD
240 C
    C
    C
    DETERMINATION OF CORRECT SIGN FOR ROUND ON FLAT REGIME OF MESH 2
    A2F=ACG2-COS(PHI2T-DELG2-ALPHAP2)-B2*CGS(BETA2-ALPHAP2)
    B2F=-ACG2-SIN(PHI2T-DELG2-ALPHAP2)+B2*SIN(BETA2-ALPHAP2)
    C2F=-RHOG2
    ROOT2F=A2F+A2F+A2F+B2F-B2F-C2F-C2F
    Y2F1=A2F+SQRT(ROOT2F)
    Y2F2=A2F-SQRT(ROOT2F)
    X2F=B2F+C2F
    PSI2F1=2.*ATAN2(Y2F1,X2F)
    PSI2F2=2.*ATAN2(Y2F2,X2F)
    IF (PSI2F1-LT.0.) PSI2F1=PSI2F1+2.*PI
    IF (PSI2F2-LT.0.) PSI2F2=PSI2F2+2.*PI
    IF (ABS(PSI2F1-PSI2T)-LT.ABS(PSI2F2-PSI2T)) GO TO 14
    PSI2F1D=PSI2F1/Z
    PSI2F2D=PSI2F2/Z
    SIGN2F=-1.
    GO TO 15
14 SIGN2F=1.
250 C
    C
    C
    COMPUTATION OF FINAL AND INITIAL VALUES OF PHI AND PSI FOR MESH 2
255 DO 16 I=1,1000
    PHI2D=PHI2TD*(1-I.)/100.
    PHI2=PHI2D+Z
    A 213
    A 214
    A 215
    A 216
    A 217
    A 218
    A 219
    A 220
    A 221
    A 222
    A 223
    A 224
    A 225
    A 226
    A 227
    A 228
    A 229
    A 230
    A 231
    A 232
    A 233
    A 234
    A 235
    A 236
    A 237
    A 238
    A 239
    A 240
    A 241
    A 242
    A 243
    A 244
    A 245
    A 246
    A 247
    A 248
    A 249
    A 250
    A 251
    A 252
    A 253
    A 254
    A 255
    A 256
    A 257
    A 258
    A 259
    A 260
    A 261
    A 262
    A 263
    A 264
    A 265

```

11.35.22

07/31/79

FTN 4.6+420

PROGRAM CLOCK4 74/74 OPT=1

```

270      A2F=ACG2+COS(PHI2-DELG2-ALPHP2)-B2+COS(BETA2-ALPHP2)
          B2F=-ACG2+SIN(PHI2-DELG2-ALPHP2)+B2+SIN(BETA2-ALPHP2)
          C2F=-RHGG2
          ROOT2F=A2F+A2F+B2F+B2F-C2F+C2F
          Y2F=A2F+SIGN2F*SQRT(ROOT2F)
          X2F=B2F+C2F
          PSI2F=2.*ATAN2(Y2F,X2F)
          IF (PSI2F.LT.0.) PSI2F=PSI2F+2.*PI
          LX2=B2+COS(BETA2)+ACP2+COS(PSI2F+DPSI2-DEL2)-ACG2+COS(PHI2-DPHI2-
1DELG2)
          LY2=B2-SIN(BETA2)+ACP2+SIN(PSI2F+DPSI2-DEL2)-ACG2+SIN(PHI2-DPHI2-
1DELG2)
          LL2=SQRT(LX2*LX2+LY2*LY2)
          DELEL2=LL2-L2
          IF (DELEL2.LE.0.) GO TO 17
18 CONTINUE
17 PHI2F=PHI2
   PSI2FF=PSI2F
   PHI2I=PHI2F-DPHI2
   PSI2I=PSI2FF+DPSI2
   IF (PSI2I.GT.2.*PI) PSI2I=PSI2I-2.*PI
   PHI2ID=PHI2I/Z
   PSI2ID=PSI2I/Z
   PHI2FD=PHI2F/Z
   PSI2FD=PSI2FF/Z
   WRITE (6,56) PHI2ID,PSI2ID,PHI2FD,PSI2FD
290
295      C
295      C
          DETERMINATION OF CORRECT SIGN FOR ROUND ON ROUND REGIME OF MESH 2
          A2R=B2-SIN(BETA2+DEL2)-ACG2+SIN(PHI2I-DEL2+DEL2)
          R2R=B2+COS(BETA2+DEL2)-ACG2+COS(PHI2I-DEL2+DEL2)
          C2R=(L2-L2-B2-B2-ACG2+ACG2-ACP2+ACP2+2.*ACG2-B2+COS(PHI2I-DEL2-BE
1TA2))/(2.*ACP2)
          ROOT2R=A2R+A2R+B2R-B2R-C2R+C2R
          Y2R1=A2R+SQRT(ROOT2R)
          Y2R2=A2R-SQRT(ROOT2R)
          X2R=B2R+C2R
          PSI2R1=2.*ATAN2(Y2R1,X2R)
          PSI2R2=2.*ATAN2(Y2R2,X2R)
          IF (PSI2R1.LT.0.) PSI2R1=PSI2R1+2.*PI
          IF (PSI2R2.LT.0.) PSI2R2=PSI2R2+2.*PI
          IF (ABS(PSI2I-PSI2R1).LT.ABS(PSI2I-PSI2R2)) GO TO 18
          SIGN2R=-1.
          GO TO 19
310      18 SIGN2R=1.
315
315      C
315      C
          GEAR TRAIN MOTION MODEL, KINEMATICS
19 DDPHI1=NP2*(PHI2F-PHI2I)/((K*NG1)
   PHI1=PHI1+DDPHI1
   WRITE (6,35)
20 PHI1=PHI1-DDPHI1
   PHI1D=PHI1/Z

```

```

320 IF (PHI1.LE.PHI1F+DDPHI1) GO TO 30
C MESH: 1
C
325 IF (PHI1.LE.PHI1F) GO TO 21
AIR=ACG1*SIN(PHI1+DELGI-DELP1)-B1*SIN(BETA1-DELP1)
B1R=ACG1*COS(PHI1+DELGI-DELP1)-B1*COS(BETA1-DELP1)
C1R=(ACPI+ACPI+ACG1+ACG1+B1-L1+L1-2.*ACG1*B1-COS(PHI1+DELGI-BET
1A1))/(2.*ACPI)
ROOT1R=AIR+AIR+B1R+B1R-C1R+C1R
Y1R=A1R+SIGN1R*SQRT(ROOT1R)
X1R=B1R+C1R
PSI1=2.*ATAN2(Y1R,X1R)
IF (PSI1.LT.0.) PSI1=PSI1+2.*PI
IF (ABS(PHI1-PHI11).LT.0.0001) PSI11=PSI1
IF (ABS(PHI1-PHI11).LT.0.0001) PSI1P=PSI11
PSI1D=PSI1/Z
SLAM1=(B1*SIN(BETA1)+ACPI+SIN(PSI1+DELP1)-ACG1*SIN(PHI1+DELGI))/L1
CLAM1=(B1*COS(BETA1)+ACPI+COS(PSI1+DELP1)-ACG1*COS(PHI1+DELGI))/L1
LAMDA1=ATAN2(SLAM1,CLAM1)
IF (LAMDA1.LT.0.) LAMDA1=LAMDA1+2.*PI
PSDO11=PHOOT1+ACG1*(B1/ACPI+SIN(PHI1+DELGI-BETA1)+SIN(PHI1-PSI1+DE
1LG1-DELP1))/(A1R+COS(PSI1)-B1R+SIN(PSI1))
VST1R=PHOOT1*(ACG1+COS(PHI1+DELGI-LAMDA1)+RHOG1)-PSOOT1*(ACPI+COS(
1PSI1-DELP1-LAMDA1)-RHOP1)
STR=VST1R/ABE(VST1R)
GO TO 22
21 A1F=ACG1+COS(PHI1+DELGI+ALPH1)-B1+COS(BETA1+ALPH1)
B1F=-ACG1+SIN(PHI1+DELGI+ALPH1)+B1+SIN(BETA1+ALPH1)
C1F=RHOG1
ROOT1F=A1F+A1F+B1F+B1F-C1F+C1F
Y1F=A1F+SIGN1F*SQRT(ROOT1F)
X1F=B1F+C1F
PSI1=2.*ATAN2(Y1F,X1F)
IF (PSI1.LT.0.) PSI1=PSI1+2.*PI
PSI1D=PSI1/Z
G1=(ACG1*SIN(PHI1+DELGI)+RHOG1+COS(PSI1-ALPH1)-B1*SIN(BETA1))/SIN
1(PHI1-ALPH1)
PSDO11=PHOOT1*(ACG1+COS(PHI1-PSI1+DELGI+ALPH1))/(A1F+COS(PSI1)-B1
1F+SIN(PSI1))
VST1F=PHOOT1*(ACG1+SIN(PSI1-ALPH1-PSI1-DELP1)-RHOG1)
S1F=VST1F/ABS(VST1F)
C MESH 2
C
360 22 ODPHI2=PSI1-PSI1P
IF (ABS(PHI1-PHI11).LT.0.0001) PHI2=PHI2I
PHI2=PHI2+DDPHI2
PSI1P=PSI1
IF (PHI2.GT.PHI2F) PHI2=PHI2I
PHI2D=PHI2/Z
IF (PHI2.GE.PHI2T) GO TO 23
A2R=B2-SIN(BETA2+DELP2)-ACG2*SIN(PHI2-DELP2+DELP2)
A 319
A 320
A 321
A 322
A 323
A 324
A 325
A 326
A 327
A 328
A 329
A 330
A 331
A 332
A 333
A 334
A 335
A 336
A 337
A 338
A 339
A 340
A 341
A 342
A 343
A 344
A 345
A 346
A 347
A 348
A 349
A 350
A 351
A 352
A 353
A 354
A 355
A 356
A 357
A 358
A 359
A 360
A 361
A 362
A 363
A 364
A 365
A 366
A 367
A 368
A 369
A 370
A 371

```


07/31/79 11.35.22

FTN 4.6-420

PROGRAM CLOCK4 74/74 OPT=1

425 A22=ABS(((1.-MU*MU*S1F)*SIN(PSI1-ALPHP1)-MU*(1.+S1F)*COS(PSI1-ALPH
 1P1))/DN) A 425
 A23=ABS((MU*SIN(GAMMA2)+COS(GAMMA2))/DN) A 426
 A24=ABS(((1.-MU*MU*S2R)*SIN(LAMDA2)-MU*(1.-S2R)*COS(LAMDA2))/DN) A 427
 A25=ABS(((1.-MU*(1.+S1F)*SIN(PSI1-ALPHP1)+(MU*MU*S1F-1.)*COS(PSI1-ALP
 1HP1))/DN) A 428
 A26=ABS((-SIN(GAMMA2)+MU*COS(GAMMA2))/DN) A 429
 A27=ABS((-1.-MU*MU*S1F)*SIN(PSI1-ALPHP1)-MU*(S1F-1.)*COS(PSI1-ALP
 1HP1))/DN) A 430
 A28=ABS(1./DN) A 431
 A29=ABS((MU*(S1F-1.)+SIN(PSI1-ALPHP1))*((1.-MU*MU*S1F)*COS(PSI1-ALPH
 1P1))/DN) A 432
 A30=ABS(MU/DN) A 433
 A37=ABS(((1.-MU*MU*S2F)*SIN(PSI2+ALPHP2)+MU*(S2F-1.)*COS(PSI2+ALPH
 1P2))/DN) A 434
 A38=ABS(((1.-MU*MU*S1F)*SIN(PSI1-ALPHP1)-MU*(1.+S1F)*COS(PSI1-ALPH
 1P1))/DN) A 435
 A39=ABS((MU*SIN(GAMMA2)+COS(GAMMA2))/DN) A 436
 A40=ABS((MU*(S2F-1.)+SIN(PSI2+ALPHP2))-((1.-MU*MU*S2F)*COS(PSI2+ALPH
 1P2))/DN) A 437
 A41=ABS((-MU*(1.+S1F)*SIN(PSI1-ALPHP1)+(MU*MU*S1F-1.)*COS(PSI1-ALP
 1HP1))/DN) A 438
 A42=ABS((MU*COS(GAMMA2)-SIN(GAMMA2))/DN) A 439
 A43=ABS(((1.-MU*MU*S2F)*SIN(PSI2+ALPHP2)-MU*(1.-S2F)*COS(PSI2+ALPH
 1P2))/DN) A 440
 A44=ABS((MU*(S1R-1.)+SIN(LAMDA1)-((1.-MU*MU*S1R)*COS(LAMDA1))/DN) A 441
 A45=ABS((MU*SIN(GAMMA2)+COS(GAMMA2))/DN) A 442
 A46=ABS((MU*(S2F-1.)+SIN(PSI2+ALPHP2))-((1.-MU*MU*S2F)*COS(PSI2+ALPH
 1P2))/DN) A 443
 A47=ABS((-1.-MU*MU*S1R)*SIN(LAMDA1)+MU*(1.-S1R)*COS(LAMDA1))/DN) A 444
 A48=ABS((-SIN(GAMMA2)+MU*COS(GAMMA2))/DN) A 445
 A65=ABS((MU*(1.+S2R)*SIN(LAMDA2)+(MU*MU*S2R-1.)*COS(LAMDA2))/DN) A 446
 A66=ABS((MU*SIN(GAMMA3)-COS(GAMMA3))/DN) A 447
 A67=ABS((MU*MU*S2R-1.)+SIN(LAMDA2)-MU*(1.+S2R)*COS(LAMDA2))/DN) A 448
 A68=ABS((-SIN(GAMMA3)-MU*COS(GAMMA3))/DN) A 449
 A69=ABS(((MU*MU*S2F-1.)+SIN(PSI2+ALPHP2)-MU*(1.+S2F)*COS(PSI2+ALPH
 1P2))/DN) A 450
 A70=ABS((MU*SIN(GAMMA3)-COS(GAMMA3))/DN) A 451
 A71=ABS((-MU*(1.+S2F)*SIN(PSI2+ALPHP2)+(1.-MU*MU*S2F)*COS(PSI2+ALP
 1HP2))/DN) A 452
 A72=ABS((-SIN(GAMMA3)-MU*COS(GAMMA3))/DN) A 453
 C6=ACG2*(SIN(PHI2-DELG2-LAMDA2)-MU*S2R*COS(PHI2-DELG2-LAMDA2))-MU*
 1RH02*(A11+A14)-MU*RH02*S2R A 454
 C7=MU*RH02*(A13+A16) A 455
 C8=-1*ACPI*(SIN(PSI1+DELPI-LAMDA1)-MU*S1R*COS(PSI1+DELPI-LAMDA1))+M
 1U*RH02*(A12+A15)+MU*S1R*RH01 A 456
 C9=MU*RH01*(A18+A20) A 457
 C10=MU*RH01*(A17+A19)+ACG1*(SIN(PHI1+DELGI-LAMDA1)-MU*S1R*COS(PHI1
 1+DELGI-LAMDA1))-MU*S1R*RH01 A 458
 C11=ACG2*(SIN(PHI2-DELG2-LAMDA2)-MU*S2R*COS(PHI2-DELG2-LAMDA2))-MU
 1+PHC2*(A21+A24)-MU*RH02*S2R A 459
 C12=MU*RH02*(A23+A26) A 460
 C13=G1-MU*RH02*(A22+A25) A 461
 426 A 462
 427 A 463
 428 A 464
 429 A 465
 430 A 466
 431 A 467
 432 A 468
 433 A 469
 434 A 470
 435 A 471
 436 A 472
 437 A 473
 438 A 474
 439 A 475
 440 A 476
 441 A 477


```

GO TO 20
30 CYCLEFF=-BTOT*DDPHI1/(PHI1F-PHI1I)
WRITE (6,57) CYCLEFF
BTOT=0.
IF (ISTOP.NE.0) GO TO 1
STOP

C
C
535
540
545
550
555
560
565
570
575
580

31 FORMAT (6X,9#PSI11TD =,F9.4,3X,8#TEST11 =,F9.4)
32 FORMAT (6X,9#PSI112D =,F9.4,3X,8#TEST12 =,F9.4//)
33 FORMAT (6X,9#PSI212D =,F9.4,3X,8#TEST21 =,F9.4)
34 FORMAT (6X,9#PSI212D =,F9.4,3X,8#TEST22 =,F9.4//)
35 FORMAT (85H PHI1 PSI1 PSI2 PSI11 PSI12 PSI11 DPS12 SIR S2R S
11F G1 S2F G2 POINTEFF//)
36 FORMAT (6X,4(F4.0,2X),2(F5.0,2X),2(F3.0,2X),24X,F5.3)
37 FORMAT (6X,4(F4.0,2X),2(F5.0,2X),5X,F3.0,2X,F3.0,2X,F5.3,14X,F5.3)
38 FORMAT (6X,4(F4.0,2X),2(F5.0,2X),10X,2(F3.0,2X,F5.3,2X),F5.3)
39 FORMAT (6X,4(F4.0,2X),2(F5.0,2X),F3.0,19X,F3.0,2X,F5.3,2X,F5.3)
40 FORMAT (F10.3,F10.0/4F10.5/4F10.5//)
41 FORMAT (4F10.4)
42 FORMAT (4F10.4)
43 FORMAT (4F10.0)
44 FORMAT (3F10.4/F10.5/F10.4)
45 FORMAT (1H1,5X,5#MIN =,F8.4,3X,4#MU =,F6.3,3X,5#RPM =,F6.0//6X,8#C
1APRP1 =,F8.5,3X,8#CAPRP2 =,F8.5//6X,5#RPM =,F8.5,3X,5#RPM =,F8.5//
26X,6#ACG1 =,F8.5,3X,6#ACG2 =,F8.5,3X,6#ACP1 =,F8.5,3X,6#ACP2 =,F8.
35//)
46 FORMAT (6X,7#HMDG1 =,F8.5,3X,7#HMDG2 =,F8.5,3X,7#HMDP1 =,F8.5,3X,7
1#HMDP2 =,F8.5//)
47 FORMAT (6X,5#TG1 =,F8.5,3X,5#TG2 =,F8.5,3X,5#TP1 =,F8.5,3X,5#TP2 =
1,F3.5//)
48 FORMAT (6X,5#MG1 =,F5.0,3X,5#MG2 =,F5.0,3X,5#MP2 =,F5.0,3X,5#MP3 =
1,F5.0//)
49 FORMAT (6X,6#H01 =,F6.3,3X,6#H02 =,F6.3,3X,6#H03 =,F6.3//6X,4#H
1D =,F10.6//6X,3#K =,F6.1//6X,8#PH0T1 =,F5.1//)
50 FORMAT (6X,8#ETA1D =,F8.4,3X,8#ETA2D =,F8.4//)
51 FORMAT (6X,30#SOMETHING IS WRONG WITH MESH 1)
52 FORMAT (6X,8#PHI1TD =,F8.4,3X,8#PSI1TD =,F8.4)
53 FORMAT (6X,8#PHI1TD =,F8.4,3X,8#PSI1TD =,F8.4,3X,8#PHI1FD =,F8.4,3
1X,8#PSI1FD =,F8.4//)
54 FORMAT (6X,30#SOMETHING IS WRONG WITH MESH 2)
55 FORMAT (6X,8#PHI2TD =,F8.4,3X,8#PSI2TD =,F8.4)
56 FORMAT (6X,8#PHI2TD =,F8.4,3X,8#PSI2TD =,F8.4,3X,8#PHI2FD =,F8.4,3
1X,8#PSI2FD =,F8.4//)
57 FORMAT (1H0,5X,1#MCYCLE EFFICIENCY =,F5.3)
58 FORMAT (3F10.5)
59 FORMAT (6X,4#R1 =,F8.5,3X,4#R2 =,F8.5,3X,4#R3 =,F8.5//)
60 FORMAT (6X,5#F1 =,F8.5,3X,5#F2 =,F8.5//)
61 FORMAT (3E15.5)
62 FORMAT (6X,4#M1 =,E15.5,3X,4#M2 =,E15.5,3X,4#M3 =,E15.5//)
END

```

```

1  SUBROUTINE TRANS1 (RHOG,ALPH, BETA,FP,ACG,B,DELG,Z,PSIT,PHIT,G)
    PI=3.14159
    ST=(-RHOG+COS(PSIT-ALPH))+B*SIN(BETA)+FP*SIN(PSIT-ALPH))/ACG
    CT=(RHOG+SIN(PSIT-ALPH))+B*COS(BETA)+FP*COS(PSIT-ALPH))/ACG
    PHIT=ATAN2(ST,CT)-DELG
    PHINEXT=PHIT-.1+Z
    AF=ACG+COS(PHINEXT+DELG+ALPH)-B*COS(BETA+ALPH)
    BF=-ACG+SIN(PHINEXT+DELG+ALPH)+B*SIN(BETA+ALPH)
    CF=RHOG
    ROOT=AF+BF+CF+CF
    YF1=AF+SQRT(ROOT)
    YF2=BF-SQRT(ROOT)
    XF=BF+CF
    PSINEX1=2.*ATAN2(YF1,XF)
    PSINEX2=2.*ATAN2(YF2,XF)
    IF (PSINEX1.LT.0.) PSINEX1=PSINEX1+2.*PI
    IF (PSINEX2.LT.0.) PSINEX2=PSINEX2+2.*PI
    IF (ABS(PSINEX1-PSIT).LT.ABS(PSINEX2-PSIT)) GO TO 1
    PSINEX=PSINEX1
    GO TO 2
    1 PSINEX=PSINEX1
    2 G=(ACG+SIN(PHINEXT+DELG)+RHOG+COS(PSINEX-ALPH)-B*SIN(BETA))/SIN(
1PSINEX-ALPH)
    RETURN
    END

```

SUBROUTINE TRANS2 74/74 OPT=1

FTN 4.6+420 07/31/79 11.35.22

PAGE 1

```

1 SUBROUTINE TRANS2 (RHOG,ALPHP,BETA,FP,ACG,B,DELG,Z,PSIT,PHIT,G)
  PI=3.14159
  ST=(RHOG*COS(PSIT+ALPHP)+B*SIN(BETA)+FP*SIN(PSIT+ALPHP))/ACG
  CT=(-RHOG*SIN(PSIT+ALPHP)+B*COS(BETA)+FP*COS(PSIT+ALPHP))/ACG
  PHIT=ATAN2(ST,CT)+DELG
  PHINEXT=PHIT+.1*Z
  AF=ACG*COS(PHINEXT-DELG-ALPHP)-B*COS(BETA-ALPHP)
  BF=-ACG*SIN(PHINEXT-DELG-ALPHP)+B*SIN(BETA-ALPHP)
  CF=-RHOG
  ROOTF=AF+BF*BF-CF*CF
  YF1=AF+SQRT(ROOTF)
  YF2=AF-SQRT(ROOTF)
  XF=BF+CF
  PSINEX1=2.*ATAN2(YF1,XF)
  PSINEX2=2.*ATAN2(YF2,XF)
  IF (PSINEX1.LT.0.) PSINEX1=PSINEX1+2.*PI
  IF (PSINEX2.LT.0.) PSINEX2=PSINEX2+2.*PI
  IF (ABS(PSINEX1-PSIT).LT.ABS(PSINEX2-PSIT)) GO TO 1
  PSINEX1=PSINEX2
  GO TO 2
1 PSINEX1=PSINEX1
2 G=(ACG*SIN(PHINEXT-DELG)-RHOG*COS(PSINEX1+ALPHP)-B*SIN(BETA))/SIN(
  RETURN
  END

```

MIN = .1645 MJ = .200 RPM = 1000.
 CAPRP1 = .47725 CAPRP2 = .20670
 RP2 = .09085 RP3 = .06890
 ACG1 = .47725 ACG2 = .20670 ACP1 = .09085 ACP2 = .06890
 R1 = .75000 R2 = .75000 R3 = .75000
 RHOG1 = .03870 RHOG2 = .02070 RHOP1 = .01740 RHOP2 = .01040
 TG1 = .03480 TG2 = .02520 TP1 = .02800 TP2 = .02060
 NG1 = 42. MC2 = 27. NP2 = 8. NP3 = 9.
 M1 = .69514E-04 M2 = .97028E-05 M3 = .10780E-05
 RHO1 = .060 RHO2 = .030 RHO3 = .025
 MD = .000015
 K = 25.0
 PHOOT1 = -1.0
 FP1 = .08917 FP2 = .06811
 BETA10 = 112.2552 BETA20 = 145.0978
 PSI1T10 = 305.6017 TEST11 = 4.4495
 PSI1T20 = 343.6259 TEST12 = 42.4736
 PHI1T0 = 113.5016 PSI1T0 = 305.6017
 PHI1T0 = 115.9930 PSI1T0 = 292.4283 PHI1FD = 107.4216 PSI1FD = 337.4283
 PSI2T20 = 286.9442 TEST21 = 29.4719
 PSI2T20 = 312.0785 TEST22 = 4.3377
 PHI2T0 = 143.0461 PSI2T0 = 312.0785
 PHI2T0 = 136.7828 PSI2T0 = 330.9531 PHI2FD = 150.1161 PSI2FD = 290.9521
 PHI1 PHI2 PSI1 PSI2 DPSI1 DPSI2 S1R S2R S1F G1 S2F G2 POINTEF
 116. 137. 292. 331. 5. -16. 1. -1. .617
 116. 137. 293. 329. 5. -16. 1. -1. .626
 116. 138. 294. 328. 5. -16. 1. -1. .634
 116. 138. 294. 328. 5. -16. 1. -1. .642
 116. 139. 295. 324. 5. -16. 1. -1. .650
 116. 139. 295. 324. 5. -16. 1. -1. .657
 115. 140. 296. 321. 5. -16. 1. -1. .665
 115. 141. 296. 320. 5. -16. 1. -1. .672
 115. 141. 297. 318. 5. -16. 1. -1. .679
 115. 142. 297. 316. 5. -16. 1. -1. .686
 115. 142. 298. 315. 5. -16. 1. -1. .693
 115. 143. 298. 313. 5. -16. 1. -1. .689
 115. 143. 299. 312. 5. -16. 1. .068 .685

108.	150.	333.	291.	5.	-13.	1.	.083	1.	.067	.531
108.	137.	333.	331.	5.	-15.	-1.	.083	1.		.551
108.	137.	334.	329.	5.	-15.	-1.	.083	1.		.555
108.	138.	334.	328.	5.	-14.	-1.	.083	1.		.559
108.	138.	334.	327.	5.	-14.	-1.	.084	1.		.563
108.	139.	335.	325.	5.	-14.	-1.	.084	1.		.566
108.	139.	335.	324.	5.	-14.	-1.	.084	1.		.569
108.	140.	336.	322.	5.	-14.	-1.	.084	1.		.572
108.	140.	336.	321.	5.	-14.	-1.	.084	1.		.575
108.	141.	337.	320.	4.	-13.	-1.	.084	1.		.578

CYCLE EFFICIENCY = .620

DISTRIBUTION LIST

Commander
U.S. Army Armament Research and Development Command
ATTN: DRDAR-LCN, P. Tepper (30)
DRDAR-TSS (5)
Dover, NJ 07801

Commander
Harry Diamond Laboratories
ATTN: Library
DRXDO-DAB, D. Overman
Washington, DC 20418

Defense Technical Information Center (2)
Cameron Station
Alexandria, VA 22314

Weapon System Concept Team/CSL
ATTN: DRDAR-ACW
Aberdeen Proving Ground, MD 21010

Technical Library
ATTN: DRDAR-CLJ-L
Aberdeen Proving Ground, MD 21010

Director
U.S. Army Ballistic Research Laboratory
ARRADCOM
ATTN: DRDAR-TSB-S (STINFO)
Aberdeen Proving Ground, MD 21005

Benet Weapons Laboratory
Technical Library
ATTN: DRDAR-LCB-TL
Watervliet, NY 12189

Commander
U.S. Army Armament Materiel Readiness Command
ATTN: DRSAR-LEP-L
Rock Island, IL 61299

Director
U.S. Army TRADOC Systems Analysis Activity
ATTN: ATAA-SL (Tech Lib)
White Sands Missile Range, NM 88002

THIS REPORT HAS BEEN DELIMITED
AND CLEARED FOR PUBLIC RELEASE
UNDER DOD DIRECTIVE 5200.20 AND
NO RESTRICTIONS ARE IMPOSED UPON
ITS USE AND DISCLOSURE.

DISTRIBUTION STATEMENT A

APPROVED FOR PUBLIC RELEASE,
DISTRIBUTION UNLIMITED.